TECHNICAL REPORT STANDARD PAGE

1. Report No.	2. Government Accession No.	3. Recipient's Catalog No.
FHWA/LA-92/251		

4. Title and Subtitle	5. Report Date
Development of Engineering Design Procedures for Heat-Straightening Repair of Damaged Structural Steel in Bridges	December 1992
	6. Performing Organization Code
7. Author(s)	8. Performing Organization Report No.
Avent, Robinson, Madan, Shenoy	
9. Performing Organization Name and Address	10. Work Unit No.
Department of Civil Engineering Louisiana State University Baton Rouge, Louisiana 70803	11. Contract or Grant No. LA.HPR Study No. 90-2C
	13. Type of Report and Period Covered
12. Sponsoring Agency Name and Address	Final Comprehensive Report
Louisiana Transportation Research Center P.O. Box 94245 Baton Rouge, Louisiana 70804	14. Sponsoring Agency Code

15. Supplementary Notes

Conducted in cooperation with the U.S. Department of Transportation
Federal Highway Administration

16. Abstract

Reported here is a comprehensive experimental and analytical investigation of heat-straightening repair of damaged steel. The study summarizes over four years of research and development. A companion report, "Design Procedures for Heat-Straightening Repairs: An Engineering Guide," provides a summary of implementable procedures resulting from this research.

This research program began with the exhaustive study of simple plate elements in which the various factors affecting heat straightening were quantified. Testing and analytical development progressed from plates to small rolled shapes and, finally, to full size bridge elements. As a result, extensive experimental results are presented for plates, angles, channels and wide flange rolled shapes. Attention is also focused on composite and non-composite bridge girders and truss members. The experimental results are used as the basis for developing analytical procedures for predicting behavior. Many of these procedures are in the form of simple formulas suitable for hand computation. A computer program is also developed for application in design.

The most significant results and conclusions of the project are: (1) that heat-straightening can be effectively used for repair of damaged steel and the resulting behavior can be analytically predicted; (2) mechanical properties of the steel are unimpaired when proper quality control is used during heating; (3) a damage classification system is developed; (4) jacking forces can be used as part of the repair if the magnitude and location is controlled, however, cracking may result if not controlled; (5) repairs can be made on steel with damage up to 100 times the yield strain; and (6) if a repaired member is redamaged, heat-straightening repair can be repeated but should be limited to one repetition of repairs.

17. Key Words	18. Distribution Statement
Steel Bridges, Damage, Repair, Heat Straightening, Girders, Trusses	

19. Security Classif. (of this report)	20. Security Classif. (of this page)	21. No. of Pages	22. Price
Unclassified	Unclassified		

Form DOT F 1700.7 (8-69)

DEVELOPMENT OF ENGINEERING DESIGN PROCEDURES FOR HEAT-STRAIGHTENING REPAIR OF DAMAGED STRUCTURAL STEEL IN BRIDGES

FINAL REPORT

by

R. RICHARD AVENT
PROFESSOR AND CHAIRMAN OF CIVIL ENGINEERING

and

PAUL F. ROBINSON
ALOK MADAN
SUNIL SHENOY

DEPARTMENT OF CIVIL ENGINEERING
LOUISIANA STATE UNIVERSITY
BATON ROUGE, LA 70803

STATE PROJECT NO. 736-14-68
FEDERAL AID PROJECT NO. HPR-0010(13)
LSU PROJECT NO. 127-15-4161

CONDUCTED FOR

LOUISIANA DEPARTMENT OF TRANSPORTATION AND DEVELOPMENT
LOUISIANA TRANSPORTATION RESEARCH CENTER
in Cooperation with
U.S. Department of Transportation
FEDERAL HIGHWAY ADMINISTRATION

AUGUST, 1991

ABSTRACT

Reported here is a comprehensive experimental and analytical investigation of heat-straightening repair of damaged steel. The study summarizes over four years of research and development. A companion report, "Design Procedures for Heat-Straightening Repairs: An Engineering Guide," provides a summary of implementable procedures resulting from this research.

This research program began with the exhaustive study of simple plate elements in which the various factors affecting heat straightening were quantified. Testing and analytical development progressed from plates to small rolled shapes and, finally, to full size bridge elements. As a result, extensive experimental results are presented for plates, angles, channels and wide flange rolled shapes. Attention is also focused on composite and non-composite bridge girders and truss members. The experimental results are used as the basis for developing analytical procedures for predicting behavior. Many of these procedures are in the form of simple formulas suitable for hand computation. A computer program is also developed for application in design.

The most significant results and conclusions of the project are: (1) that heat-straightening can be effectively used for repair of damaged steel and the resulting behavior can be analytically predicted; (2) mechanical properties of the steel are unimpaired when proper quality control is used during heating; (3) a damage classification system is developed; (4) jacking forces can be used as part of the repair if the magnitude and location is controlled, however, cracking may result if not controlled; (5) repairs can be made on steel with damage up to 100 times the yield strain; and (6) if a repaired member is redamaged, heat-straightening repair can be repeated but should be limited to one repetition of repairs.

ACKNOWLEDGMENTS

As with any research project, the cooperation of the sponsoring agencies is essential. The authors wish to thank the Louisiana Transportation Research Center, the Federal Highway Administration, and the Louisiana Department of Transportation and Development for their support of the project. Special thanks are extended to Professor Peter Stopher, Director of LTRC, and Mr. Harold Paul, LTRC technical coordinator, for the helpful technical and managerial direction given to the project.

The authors would like to thank Mr. Joseph T. Smith, Structures and Facilities Maintenance Engineer, and Mr. Gil M. Gautraeu, Bridge Inventory and Inspection Engineer, for their assistance and guidance throughout the project.

The authors would also like to thank employees of the Maintenance Division of the Louisiana Department of Transportation and Development who assisted in the construction of the HEAT facility and in the placement of steel girders.

Dr. Luis de Bejar of the Department of Civil Engineering at LSU developed some statistically based predictions for damage repair. His contributions are gratefully acknowledged.

PROGRAM IMPLEMENTATION

For many years prior to the initiation of this research, heat-straightening repairs had been conducted on steel bridge structures. However, these repairs were not engineered and depended on the skill and knowledge of the contractor. While intuitive knowledge of the process was understood, a rational, quantitative definition of the method was lacking. This research has defined quantitatively, the behavior of the heat-straightening repair process.

There are two distinct categories of damage that are amenable to heat-straightening repair: Global damage identified by flexural bending or twisting of major structural components; and localized damage characterized by bulges, buckles, and crimps to local regions of the plate elements making up the cross-section of a structural component. Both types of damage usually occur simultaneously. However, the global damage is most often of primary concern for damaged structures. As a result, localized damage has not been addressed in either past or current research. The research results here apply to global damage only. Consequently, methodologies are not developed for the repair of localized damage and the repair methods developed here can only be implemented for global damage. This limitation represents a serious restriction to full implementation of heat-straightening repair by the LDOTD.

The research results developed in this investigation cover a wide range of global repair applications. A summary of the structural categories covered and their degree of readiness for implementation are summarized as follows by damage classification. Details on the classification system can be found in this report, but can be summarized as: strong axis, S, weak axis, W; and twisting, T.

Section Type	Damage Classification	Degree of Implementability
Plate	S	Full
Plate	W or T	Partial
Angle	S, W, or T	Partial
Channel	S, W	Full
Channel	T	Partial
Wide Flange	S, W, or T	Full
Composite Girders	W or S	None

Section Type	Damage Classification	Degree of Implementability
Composite Girders	T	Partial
Non-composite Girders	S or W	Full
Non-composite Girders	T	None
Axially Loaded Wide Flanges	S or W	Full
Axially Loaded Wide Flanges	T	None
Fatigue Sensitive Members	S, W, or T	None
Damage to Previously Straightened Members	S, W, or T	Full

Those categories listed as partially implementable will require more experimental data for complete verification. For the entries listed as having no implementability, these cases have not been studied in this or earlier research.

In summary, a significant number of categories of cross-sections and damage types are now either fully or partially implementable. This report details the research basis for implementing heat-straightening repairs. The companion report, "Design Procedures for Heat-Straightening Repairs: An Engineering Guide," provides a practical guide to implementation where applicable.

TABLE OF CONTENTS

LIST OF TABLES

LIST OF FIGURES

Chapter 1

INTRODUCTION

Scope of Investigation

Damage caused by vehicle impact, mishandling, or fire is a perennial problem associated with structural steel bridge members. For almost half a century, heat-straightening techniques have been applied to bends and distortions in order to restore the original shape of steel elements. A few craftsmen, who have years of experience with heat straightening, perform the technique in the field with varying degrees of success. Some of these experts have mastered heat straightening, but the process is still considered more of an art than a science.

The ability to repair bent structural steel members in place, often without even the need for temporary shoring, has generated interest in heat straightening from the engineering profession. However, engineers have had to rely primarily on their own judgment and the advice of experienced technicians in applying heat straightening techniques. Two key issues must be addressed: Do heat-straightening repair procedures exist which do not compromise the structural integrity of the steel? And if so, how can such repairs be engineered to ensure adequate safety of the repaired structure both during and after repair? The primary goal of this research project is to answer these two questions by experimentally evaluating various aspects of heat-straightening techniques and developing engineering analysis and design procedures for general applications. The project was initiated on June 10, 1985, with the sponsorship of the Louisiana Transportation Research Center (LTRC), the Louisiana Department of Transportation and Development (LADOTD), and the Federal Highway Administration (FHWA). The project was conducted in two phases. The first consisted of: (1) laboratory evaluation; (2) initial analytical development; and (3) limited field evaluation. The results have been reported (Avent 1989; Avent and Fadous 1989; Avent and Fadous 1987; Avent and Boudreaux 1987) and can be summarized as an exploratory investigation.

After a literature review at the beginning of the project, it appeared that the state-of-the-art could be summarized as follows:

1. The basic mechanisms of heat-straightening were well understood.
2. Fundamental parameters had been identified.
3. Vee heat behavior was fairly well documented for simple plate elements.

4. The effect of heat-straightening on material properties had been verified for a wide range of steels.
5. Actual field studies had verified basic behavior.
6. Practical applications depended primarily on the skill and knowledge of practitioner as opposed to rigorous engineering analysis.

The original research plan was based on these premises with the goal of supplementing laboratory studies and developing engineered procedures for field applications. However, as the research progressed, it became apparent that these original assumptions were too broad. First, the basic mechanism of heat-straightening was not well-understood in that the effects of both external restraints (jacking) and internal restraints (redundancy) were considered to be of minor concern rather than fundamental to the broad application of the process. Second, as a result of not identifying the importance of this parameter, there has been little documentation on the behavior of vee heated plates subjected to varying degrees of constraint and even less on rolled shapes. Third, while a fair amount of research indicates that most material properties are unaffected by heat-straightening, two important aspects have been overlooked: the influence of strain aging on ductility and residual stress distribution. Finally, the research information available was predicated almost entirely on laboratory studies of simple elements. The reported field investigations were qualitative rather than quantitative and thus could not serve as a building block for this research. Because of these voids in heat-straightening research, it was indeed true that the artesian practicing the trade was much more important than the engineer.

Several major accomplishments have occurred in the first phase of the project. First, the influence of external and internal constraints on plastic flow have been identified and documented experimentally. Without this understanding, the development of engineered heat-straightening repairs would not be possible. Second, all important parameters influencing heat-straightening have been systematically studied and evaluated for both plate elements and rolled shapes. More research data on this topic have been obtained during this project than in all previous projects combined. Third, the strength characteristics of damaged members subsequently repaired, both in the laboratory and the field, have been shown to be equal to their original strength. Until this project, such conclusions could only be surmised indirectly. Lack of such information has resulted in artificial restraints being placed on guidelines for heat-straightening repairs. Finally, for the first time, a detailed investigation of the behavior of damaged/repaired full-size bridge girders has been conducted.

It became obvious during phase I that additional experimental data would be needed and that certain aspects of the research needed to be refocused. The results were phase II of the project which consisted of: (1) Additional laboratory studies on plates and rolled shapes; (2) Full scale tests on composite and noncomposite girders and truss members; (3) Analytical modeling and computer analysis; and (4) A heat straightening training video.

The laboratory testing was focused on several areas in which experimental data was lacking. Tests were conducted on flat plates in two configurations. In one instance, the plates were heated in their original straight condition using identical procedures to that which would have been used had the plates been damaged in strong axis bending. These experiments are referred to as undeformed plate tests. They are important because practically all previous archival testing has been performed in this manner and the data is needed for comparison purposes. However, the more realistic approach is to induce damage and actually heat straighten the deformed plate. This study represents the first instance in which such deformed plate heat-straightening tests have been conducted.

The undeformed and deformed plate tests have been used to clarify some fundamental unanswered questions concerning heat straightening and to establish a baseline for studies on more complex shapes. Included have been tests to measure the distribution and magnitude of residual stresses. Heretofore, this issue has not been addressed. Material properties have also been measured. This study is particularly significant since little information is available on heat straightened deformed plates. As part of this investigation, a definition of degree of damage had to be developed which could be consistently applied to various levels of damage.

Since practically all prior rolled shape testing has been conducted on undamaged members, a major thrust of this project was to test damaged rolled shapes. Angles, channels, and wide flange beams (both undeformed and deformed) were heat straightened and measured for plastic rotations, residual stresses, and material properties. These tests formed the basis for the analytical development.

First, a formula for the plastic rotation per heat has been developed for a plate. This formula is rationally based and includes the effects of temperature, vee angle, and restraining force. The plate formula developed is extended to rolled shapes using modification factors to reflect the effect of location of the stiffening elements and the principal axis of the member.

The final objective has been to extend the laboratory testing to field applications in a simulated bridge facility. Addressed were the commonly occurring cases of impact to the bottom flange of composite or noncomposite girders and truss members bent about either axis. Both experimental and analytical results have been obtained.

The research results described here represent the most comprehensive study on heat straightening to date. A scientific basis is provided which will enable an engineering evaluation for heat-straightening repairs. A companion report, "Design Procedures for Heat-Straightening Repairs: An Engineering Guide," provides a summary of results for design, office use, and field implementation.

Heat Straightening Basics

The concept of heat straightening is relatively simple. Heat applied (usually by a torch) to damaged steel in a specific pattern will cause the steel to undergo permanent deformation in a desired direction. The heating process must be applied in various patterns and at various locations along a damaged member to produce straightening. Although heating alone may be used to straighten a bent member, loads may also be applied to increase the efficiency of the process. These loads are usually kept low enough to not cause hot mechanical straightening (Avent and Fadous 1989)

Many types of heating patterns exist, such as the spot, line, strip, and edge heats. These basic types are described as follows.

Vee Heat

The vee heat is the most basic pattern used to straighten strong axis bends in steel plate elements. As seen in Figure 1, a typical vee heat starts with a very small spot heat applied at the apex of the vee-shaped area using an oxyacetylene torch. When the desired temperature is reached (usually around 1200°F for A36 steel), the torch is advanced progressively in a serpentine motion toward the base of the vee. The cool material adjacent to the heated area resists the normal thermal expansion of the steel in the longitudinal direction. As a result, the heated material will expand through the thickness of the plate. At the completion of the heat, the entire heated area is at a high and relatively uniform temperature. As the steel cools, the material contracts longitudinally to a greater degree than the expansion during heating. Thus, a net contraction occurs which produces bending in an initially straight member, or straightening (if the plate is bent in the opposite direction to that of the movement) (Avent and Fadous 1988). The various heating parameters of a vee heat are simply defined. Applied loads are classified in terms of a load ratio (LR), the ratio of the moment present at the center of the vee, M, to the plastic moment capacity, M_p, of the cross-section in the direction of desired movement. Depth ratio (DR) is the ratio of the vee depth, d_v, to the plate width, w. The amount of permanent deformation experienced in the

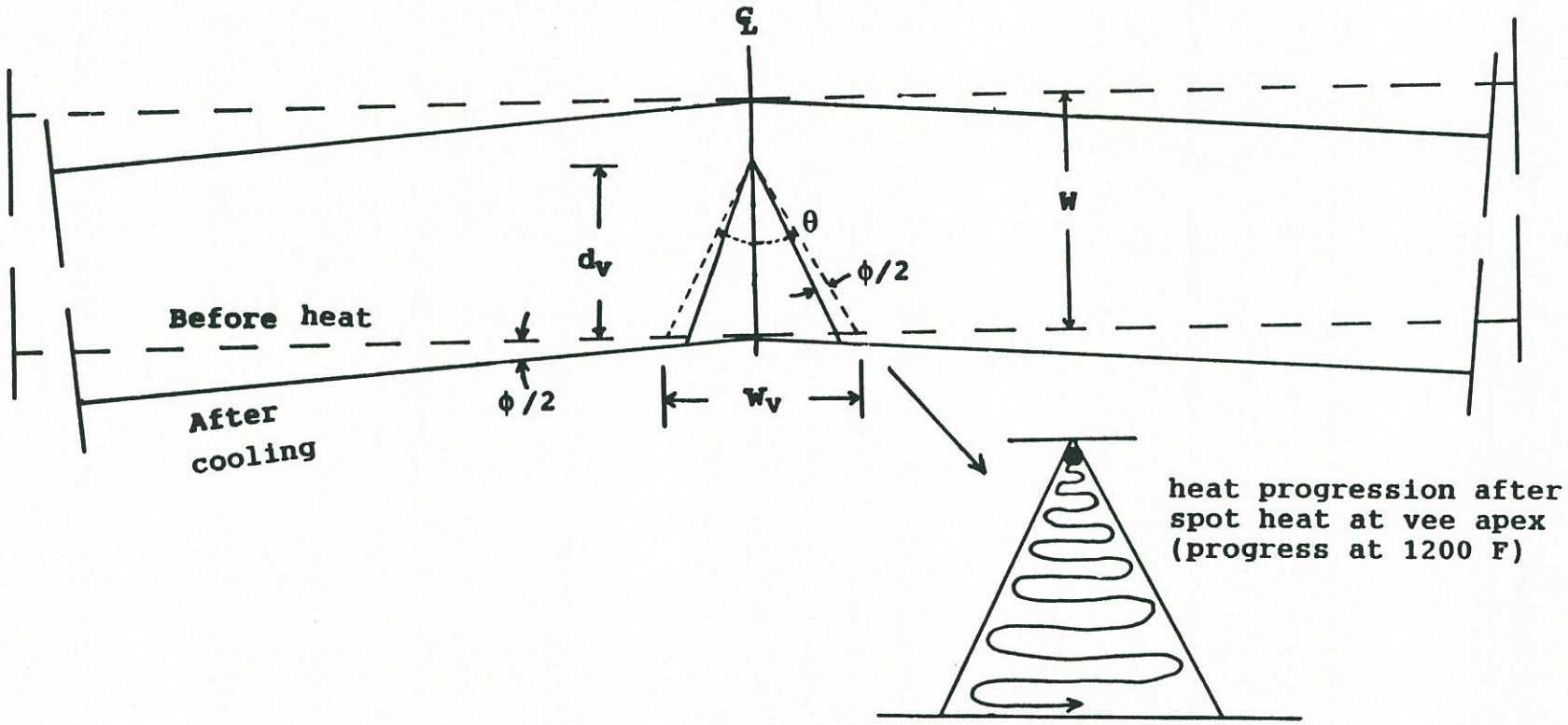

Figure 1. Illustration of vee heat.

plate element is classified as a plastic rotation, ϕ (Figure 1), determined from the plate geometry before and after each heating/cooling process.

Line Heats

Line heats are employed to repair a bend in a plate about its weak axis. A line heat consists of a single straight pass of a single orifice torch (Moberg 1979). The restraint in this case is provided by the surrounding cold metal in the element. The speed of the travel of the torch is critical as it determines the temperature attained. The ideal speed is that which produces a temperature of 1200°F at three-fourth thickness of the metal. If this condition is satisfied and the speed of the torch is uniform, a sharp bend can be expected with this heat pattern (R. Holt 1965, 1971).

Edge Heats

If a smooth gentle bend is desired, a strip of uniform width along the edge of the member is heated. A detailed study of stresses and strains, which result from edge heating a large I-beam, has been conducted by R. L. Brockenbrough (1970). A computer program was also developed to calculate stresses and strain. No formula was, however, derived to calculate the radius produced by a given width of heat or heating temperature.

Spot Heats

In a spot heat, a small round area of the metal is heated by moving the torch in a slow circular motion increasing the diameter until the entire area of the metal is heated. A spot heat causes upsetting of the metal into the thickness due to the restraint provided by the cool surrounding material. On cooling, a spot heat leaves tensile stresses in all the radial directions across the heated area. During a spot heat, the torch should not be held at a particular point for too long, as the spot may get too hot and buckling may occur due to greater thermal expansion on the heated side of the member (Moberg 1979). Spot heats are used to repair localized damage such as bulges, dents, bellies, or dishes in a plate element.

Strip Heats

Strip heats, also called the rectangular heats, are used to remove a one-directional bulge in a plate element. Strip heats are essentially elongated spot heats. They are accomplished by moving the torch back and forth in a serpentine fashion across a strip of desired length.

Various combinations of different heating patterns may be used depending on the structural configuration and damage pattern.

Rolled shapes consist essentially of plate elements. Therefore, the vee heat combined with other patterns can also be utilized to produce movement in these shapes. Figure 2a shows the basic heating pattern used to produce movement in the weak axis direction of a wide flange shape (referred to as Category W). First, the vee heats are applied to the flanges in the same manner as for plates, and then a strip heat is applied to allow for contraction in the web. Figure 2b shows the pattern used for strong axis bending (known as Category S). In this case, the vee heat is first applied to the web, and the strip heat is then applied to the flange at the open end of the vee. Similar patterns can be used for heating angles and channels.

Literature Review

The study of heat straightening has developed significantly over the past half-century. An early reference (J. Holt 1938) on the subject outlined the procedures necessary for straightening damaged steel of various configurations. These general procedures were used for many years, as evident in later references (J. Holt 1955; R. Holt 1965, 1971). Little scientific emphasis was placed on the heat straightening process or its effects.

Over the years, several studies were conducted to answer the many questions regarding the use of heat straightening, its effects, and its limitations. The culmination of these studies were two recent comprehensive reports regarding heat straightening. The first report (Shanafelt and Horn 1984) addressed the general damage assessment of structures with a rational approach to using heat straightening as one of many repair alternatives. The second report (Avent and Fadous 1988) was geared more toward optimizing the use of heat straightening, once the decision is made to use it.

Shanafelt and Horn's report was the first to discuss the subject of damage limitations regarding the use of heat straightening, although no evidence was presented to support their suggestions. Guidelines were given for damage inspection and measurement, along with the rationale behind choosing a repair procedure based on the measurements. General structural characteristics of steel (strength and fatigue) were incorporated into the decision-making process concerning proper locations at which heat straightening should be applied.

The report by Avent and Fadous (1989) focused on the behavior of steel when subjected to variations in heat straightening applications, i.e., temperature, load ratio, plate dimensions, etc. Conclusions were based on a number of experiments (approximately

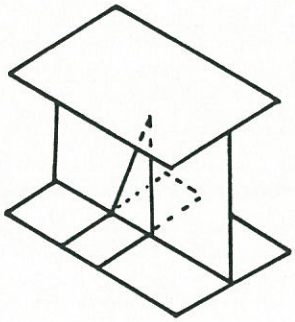

Figure 2a. Heating configuration for Category W wide flange.

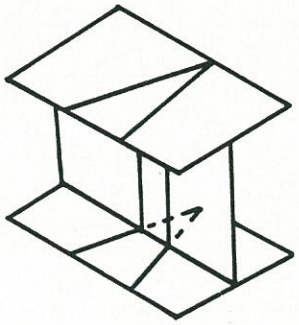

Figure 2b. Heating configuration for Category S wide flange.

483 heats were applied to various plates and rolled shapes). The theory regarding plastic rotations in plates from past studies (Holt 1971; Weerth 1971; Horton 1973) was expanded using the vast amount of experimental data.

Avent and Fadous also utilized experimental data obtained by Roeder (1985) where 68 plates were heated (using vee heats) as well as a few wide flange beam specimens of various sizes. Roeder also conducted actual strain measurements within the vee heated area, and formulated a finite element program to model residual strains and residual stresses resulting from a single vee heat on an undamaged plate element.

Roeder's plastic rotation data were highly influential in the development of the most recent equation to predict plastic rotations based on variations in vee heat applications. This equation, presented by Avent and Fadous (1988), was primarily the result of experiments conducted by Boudreaux (1987). For this reason, it is referred to by the author as Boudreaux's equation.

It should be noted that the earlier publications by Weerth and Horton provided the foundation for Roeder's work at the University of Washington, in terms of establishing methodology of heating and measuring the specimens. Thus, they were very important in establishing heat straightening techniques used by Boudreaux, Avent and Fadous, as well as the author. Moberg provided excellent summaries in the literature review of his masters thesis of all the important early work conducted (before 1980) in the field of heat straightening. For a logical and comprehensive presentation of the current state-of-the-art of heat straightening, the reader should refer to Avent (1990).

Only a minimal amount of damage repair on actual bridges has been conducted for which measurements were recorded, analyzed, and published. In fact, the only known example of such a study on an existing bridge was conducted by Moberg (1979) on the Bothell Bridge in the state of Washington. To provide a controlled atmosphere for studying full-scale bridge members, the Heat-Straightening Evaluation and Testing (HEAT) facility was constructed at Louisiana State University (Avent and Fadous 1989). This facility allows for the damage and repair of large wide flange sections resembling actual bridge girders (including composite members), without the hassle of traffic control.

Heat-straightening repair of a damaged steel member in the field proceeds under the influence of constraining forces which may be imposed externally (by jacking forces) and/or internally by the statical indeterminacy of the member. The literature review offered the following information on these two categories of straining forces.

External Restraints

External restraining forces are commonly used to expedite the heat-straightening process of the damaged member in the field. Considering a vee heated plate element, it may be visualized that a jacking force applied to the plate element in the direction of the desired movement produces a bending moment about the major axis, which tends to close the vee angle, thus causing greater confining stress to heated metal near the open end of the vee. The increased confinement impedes the reverse movement of the plate during the expansion phase, increases the upset and thus, produces more contraction during the cooling phase (Avent and Fadous 1988). Experimental studies conducted by Avent show that plastic rotations are directly related to the influence of jacking forces (Avent and Fadous 1987, 1989; Avent and Boudreaux 1987). In another investigation conducted by Nicholls and Weerth (1972), Weerth (1971), and Roeder (1986, 1987), behavior of vee heated plates was studied for various load ratios. Their results along with those obtained by Avent and Fadous (1988) in a similar study have been represented graphically (Figure 3). The curves show a near linear variation with respect to the vee angle and also reflect that the plastic rotation is proportional to the load ratio parameter. The load ratio, which is a measure of the external restraining force is calculated as the ratio of the externally applied moment at the vee heated section to its plastic moment capacity. Results of the experiments conducted by Avent and Fadous (1989) in a study of the heat-straightening behavior of composite girders show that the plastic rotations increase in a fairly linear manner with the load ratios until a certain level of the jacking forces beyond which the plastic rotations increase drastically. Thus, there is a distinct advantage to using an external constraining force during heat-straightening. However, it is recommended that the restraining force be used as a passive force rather than an active one during the heating process. Essentially, this means that the external jacking force should not be varied externally at any time during the heat-straightening of the member. The test data plotted by these researchers was thus based on a constant force during the entire heating and cooling cycle. The limit of the restraining force to be used during heat-straightening has been addressed in the literature only by these researchers. It seems that most practitioners set this limit by intuition. The primary limit of the jacking force recommended is the buckling capacity of the vee area during heating based on reduced yield stress. As the yield stress is typically reduced to one-half its original value at a temperature of 1200°F, the load ratio of 50% should be observed as the upper limit (Avent and Fadous 1988). Above this load ratio, hot mechanical straightening of the heated member might be experienced.

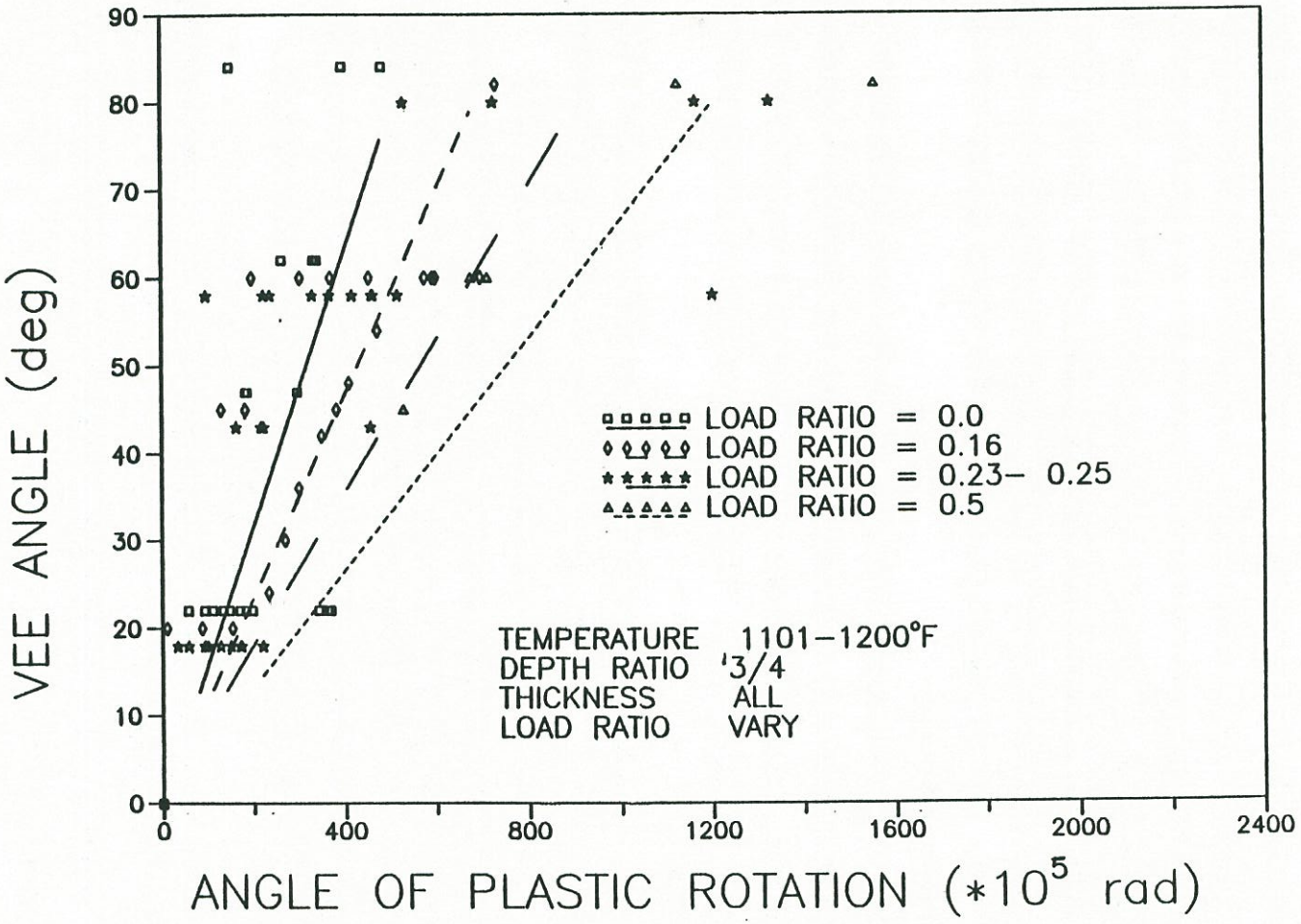

Figure 3. Vee angle versus angle of plastic rotation for vee heated plate elements.

Internal Constraints

Internal constraints play an equally important role in the heat-straightening process. These constraints may be caused by: (1) the presence of dead load during heating and/or (2) statical indeterminacy of the member. Depending on its direction, the dead load acting on the member may expedite or impede plastic rotations. In case the dead load on the member acts in the direction of the desired movement (in other words produces a bending moment compatible to the desired plastic rotation), the straightening effect is increased. On the other hand, a dead load in the other direction inhibits the straightening process. Roeder (1985, 1987) has shown that the process may even be reversed under these conditions and thus, may worsen the damage. A jacking force in the opposite sense may be required in this case to negate the effect of the dead load.

The internal constraint may also be imposed by the statical indeterminacy of the member. The damaged member may be restrained axially against longitudinal expansion, as in the case of compression members in trusses, or may be fabricated compositely with a deck slab, as in the case of a composite girder. The member may even be a component of an indeterminate framework.

In a large number of instances, the steel member to be repaired is a part of a truss structure and thus primarily a compression or tension member. An axially loaded member (in which the design strength is substantially influenced by axial loads on the member) is expected to behave differently in tension and compression. In an experimental study conducted by Roeder (1985), W6x25 sections were heated with a 1200°F vee heat on a single flange under axial loads of 40 and 80% of the AISC allowable service load. The columns supported this load with no indication of buckling. This suggested that the columns may be repaired by heat-straightening while they are supporting large service loads. However, additional study may be required with vee heats on both flanges to make a general conclusion. Roeder concluded that the P-Δ moments in these members (secondary moments due to the axial load and initial lateral deflection) have a two-fold effect. First, they reduce the column stiffness; and second, they impede the plastic rotations during heat-straightening by decreasing the compressive stresses at the open end of the vee and hence, increasing the heated deflection (see mechanism of heat-straightening). In view of the P-Δ effect, the addition of a small lateral load to the column which increases the compressive stresses in the heated area is recommended to enhance plastic rotations. In the heat-straightening repair of structural steel in the two hangers at the McChord Air Force Base (Engineering News Record 1959), supplemental forces were used on all compression members to avoid further distortion

while heating and thus assist in the straightening process. According to Holt (1971), if the centerline of a compression member falls outside the middle one-third of the member, these forces must be applied during heat-straightening of compression members. Members under tension will stretch rather than upset under axial loads. Hence, external forces must be employed to introduce compression in the heated area.

In summarizing the previous literature, it is evident that certain areas of research are lacking concerning the use of heat straightening. Some of the most important points are as follows:

1. Almost all studies have been conducted on initially straight specimens, with only one to four heat applications per specimen.
2. No experimentally measured residual stresses have been published for heat-straightened steel.
3. The few theoretical residual stresses in various references have been contradictory, even for the most simple plate elements.
4. Material properties of damaged steel repaired by heat straightening have never been studied, and there is no evidence to suggest that they would be the same as for undamaged steel subjected to the same process.
5. No experimental or theoretical rationale has been used to establish general damage limits on the use of heat straightening.
6. No one has adequately addressed the subject of repetitive damage to a heat-straightened member.
7. Little analytical work has been done to predict plastic rotations in a wide variety of rolled shapes and structural configurations.
8. Damage classification has been vague in past studies.
9. Field studies on heat straightening of composite and noncomposite girders have been very limited.
10. Little information is available on the behavior of compression members subjected to heat straightening.

Purpose and Objectives

The lack of adequate research in the area of actual damage repair using heat straightening has led to many questions concerning its use. The purpose of this research is to answer some of the most pressing questions, primarily in the areas of damage classification, damage limitations, residual stresses, behavioral characteristics, analytical

procedures, and changes in the material properties of damaged steel subjected to the process of heat straightening. Specifically, the following questions, frequently asked by those involved in heat straightening, are addressed:

1. How does the degree of member damage affect the heat straightening process?
2. How should damage be classified?
3. Is there an upper limit on the amount of damage that a steel member may undergo and still be heat-straightened?
4. How many times can a member be damaged and heat straightened?
5. What are the residual stresses resulting from heat straightening?
6. What changes in material properties are exhibited by steel that has been damaged and heat straightened?
7. Can analytical equations be developed to relate movements in heat straightened rolled shapes for all types to plate movements?
8. What results from heat curving studies can be applied to heat straightening?
9. Do compression members in trusses behave similarly to girders when heat straightened?
10. How do damaged composite and noncomposite girders respond to heat straightening?

Chapter 2

HEAT STRAIGHTENING OF PLATES

Several previous studies have been conducted on the behavior of initially straight plate elements subjected to the heat straightening process (actually heat curving), using the vee heat. These studies have included theoretical analyses of plastic rotations and residual stresses in undeformed steel plate elements (Weerth 1971; Roeder 1985). Actual experiments have also been completed (Weerth 1971; Roeder 1985; Avent and Fadous 1988), with geometric measurements being taken to determine plastic rotations. Material property tests have been conducted on heat curved steel plates (Nicholls and Weerth 1972). However, experimentally determined residual stresses have not been documented for vee heated plate elements nor has the behavior of deformed plates. The purpose of this chapter is to present a comprehensive experimental and analytical study of the heat straightening behavior of plates.

Undamaged Plates

In order to more clearly understand the residual stresses resulting from varying parameters in the heat straightening process, a number of experiments were conducted on a set of initially straight plates. The 4" x 1/4" x 24", A36 steel plates were simply-supported (using 5/8" bolts) on a stationary frame at a length of 22" (Figure 4). Each specimen was subjected to four heating/cooling cycles (alternating sides to prevent a net out-of-plane distortion). Each plate was assigned a specific vee angle, vee depth ratio, and load ratio for the four heating cycles.

The heating parameters for each of the plates are shown in Table 1. Each plate was heated using an oxyacetylene torch (#3 tip) to approximately 1200°F. The temperature was measured using an Omega high-temperature surface probe and thermometer. The load was applied by use of a hydraulic cylinder which produced the desired moment at the vee heat location (in this case, at the center line of the plate. The bolts used to hold the plate were loosely fastened to allow uninhibited plate movements. Slots in the frame allowed for any plate shortening that might occur.

Although residual stresses are often mentioned in literature on heat straightening, there has been little documented research in this area. Past research was conducted in the context of heat curving (not heat straightening), and thus is somewhat limited in its applicability to heat

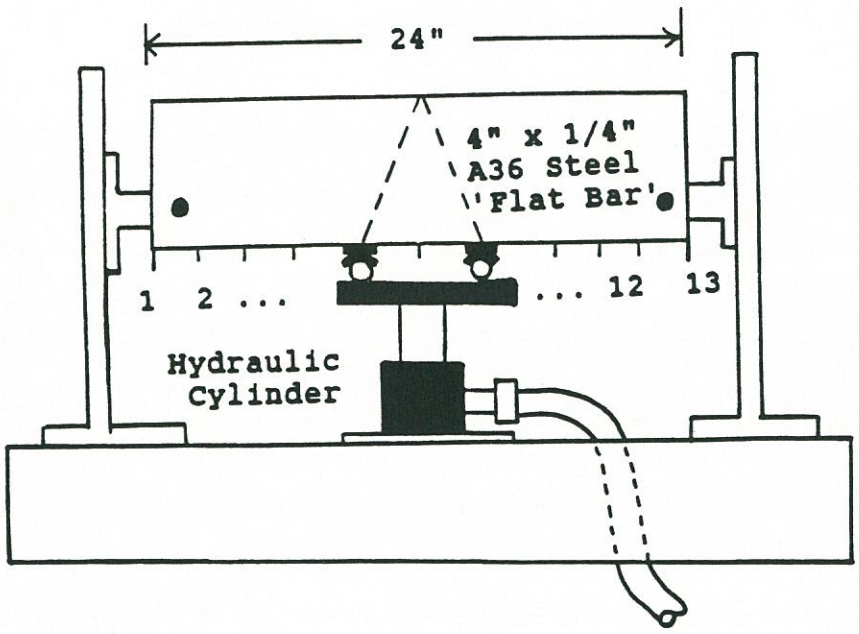

Figure 4. Experimental plate set-up.

Table 1. Heating parameters for undamaged plates.

Plate	Vee Angle	Load Ratio	Depth Ratio
I-1	20	0.00	1.00
I-2	45	0.00	1.00
I-3	60	0.00	1.00
II-1	20	0.00	1.00
VI-4	45	0.50	0.75
VI-6	45	0.00	0.75
VI-10	82	0.50	0.75
VI-12	82	0.00	0.75

straightening. Some of the most notable research was conducted at the University of Washington (Roeder 1985), where a finite element model was developed to predict the local behavior of a plate element subjected to a vee heat. Residual stresses were estimated using the model. An example of Roeder's residual stress distribution is shown in Figure 5.

Experimental research was conducted (Brockenbrough 1970b) to back up earlier theoretical residual stress studies (Brockenbrough 1970a) on heat-curved plate girders subjected to line heats. These stresses, determined by the "sectioning method" discussed below, were reasonably consistent with the theoretical values. Similar theoretical methods were used on vee-heated plate elements (Nicholls and Weerth 1972) and on wide flange beams (Horton 1973). However, the results were not supported by any experimental data.

The limited information regarding residual stresses in heat-straightened steel, necessitated the study of initially straight plates for two major reasons: (1) To experimentally verify Roeder's theoretical stresses from his finite element model, and (2) To provide a convenient and time saving way (compared to the use of damaged specimens) of checking changes in residual stresses resulting from variations in the parameters of the heat straightening process, i.e., vee angle, vee depth ratio, and load ratio. This type of parameter study was not possible for damaged specimens, due to the nature of the proposed experiments, in which the amounts of damage varied instead of the heating parameters.

Longitudinal residual stress patterns in all of the plates were determined using the "sectioning method", a well-established, but destructive method. This method is described as follows: A plate element may be marked in strips (Figure 6). Two gage holes (diameter = 0.0625", approx. depth = 0.20"), separated by a measured distance (in this case, approximately four 4 inches), are drilled along the center of each strip. The exact distance is measured to the nearest hundred thousandth of an inch, using an extensometer. Eight strips approximately one-half inch wide are cut from the 4-inch deep plate, and the distance between the two gage holes (along the center line of each strip) is remeasured.

The difference between the final and initial gage readings indicates that residual strains (and thus stresses) were present in the strip before cutting. A positive change indicates a compressive stress, and a negative change indicates a tensile stress. The stresses are computed by dividing the net change in length by the initial gage reading (to obtain strain) and multiplying by the modulus of elasticity of the material. Changes in temperature are taken into account by utilizing measurements of a standard gage length on a steel rod which changes depending on the temperatures during the initial and final strip measurements, respectively. The procedure was applied to both sides of the strip, and an average was taken. The

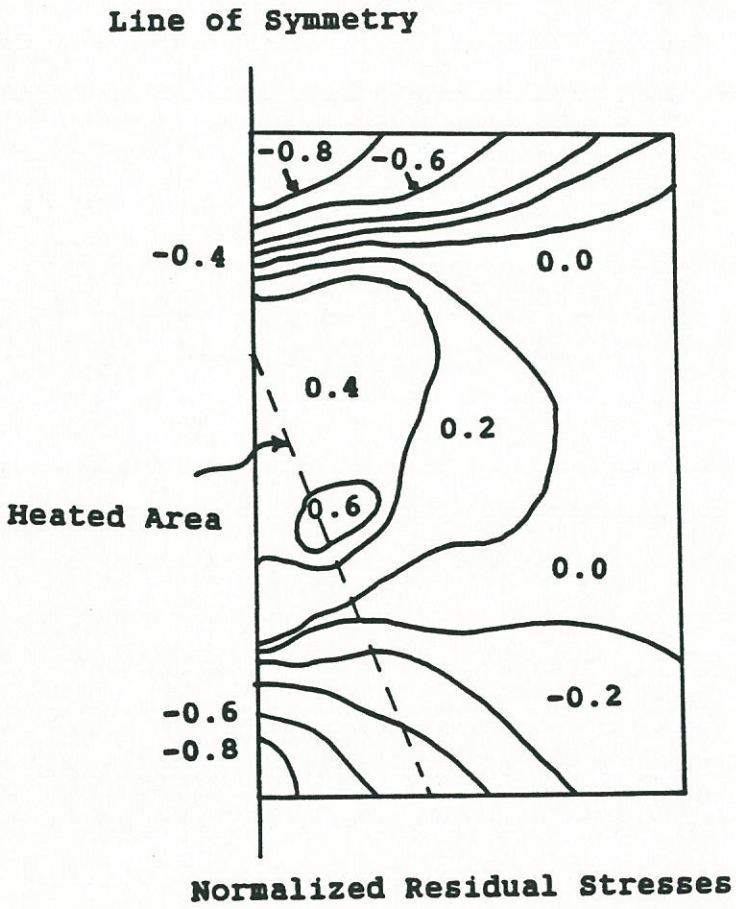

Figure 5. Residual stress distribution from finite element analysis (Roeder, 1985).

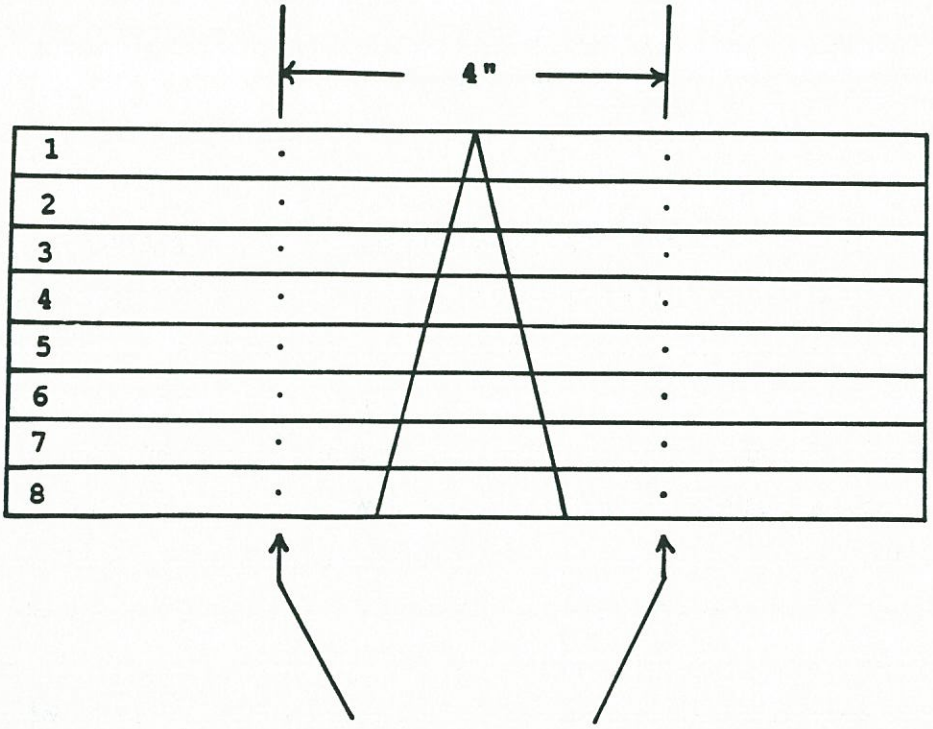

Figure 6. Strip configuration for sectioning method.

computed stress indicates the average residual stress present in the entire strip within the 4-inch gage length. Residual stresses have been shown to be relatively uniform throughout the thickness of thin plate elements (SSRC 1976).

First, an unheated plate (Plate UH) was tested for residual stresses to provide the basis for determining changes brought on by the vee heats. Stresses found in each strip are shown in Table 2 and plotted in Figure 7. The values are fairly low and the distribution compares reasonably well in shape with standard residual stress assumptions and previous experimental measurements (Avent and Wells 1982).

The residual stresses found for the heated undamaged plates are shown in Tables 2 and 3.

A distinction can be made by classifying "small vee angles" as those being less than or equal to 60 degrees, and "large vee angles" as those greater than 60 degrees. These two categories have significantly different magnitudes of residual stresses. The averages of all plates within each category are shown in Figure 8. The smaller vees exhibited considerably higher compressive stresses. Plots of these values are presented in Appendix A.

The residual stress patterns in all of the plates were similar in shape to Roeder's theoretical distribution (Figure 5), where normalized values were used. When comparing individual plates, it was found that the two parameters of load ratio and depth ratio, when considered separately, have no significant effect on the residual stress pattern. The stress patterns for the practical range of vees (20 to 60 degrees) consist of stresses which are approximately 100 percent larger than regularly assumed stresses in fabricated structural plate. The higher compressive stresses could be detrimental to column behavior associated with inelastic buckling at lower loads than normal.

Material property studies of undamaged steel plate elements subjected to the heat straightening process have been conducted in the past (Nicholls and Weerth 1972). A summary of all the studies (including rolled shapes and various heating patterns) is well documented (Avent 1989). Most researchers have stated that the process, when applied to undamaged specimens, has little effect on the material properties. These studies included a wide range of temperatures, types of heating patterns, and different types of steel. To avoid repeating past research, material property studies conducted by the author were limited to damaged specimens for which no previous material property information was available.

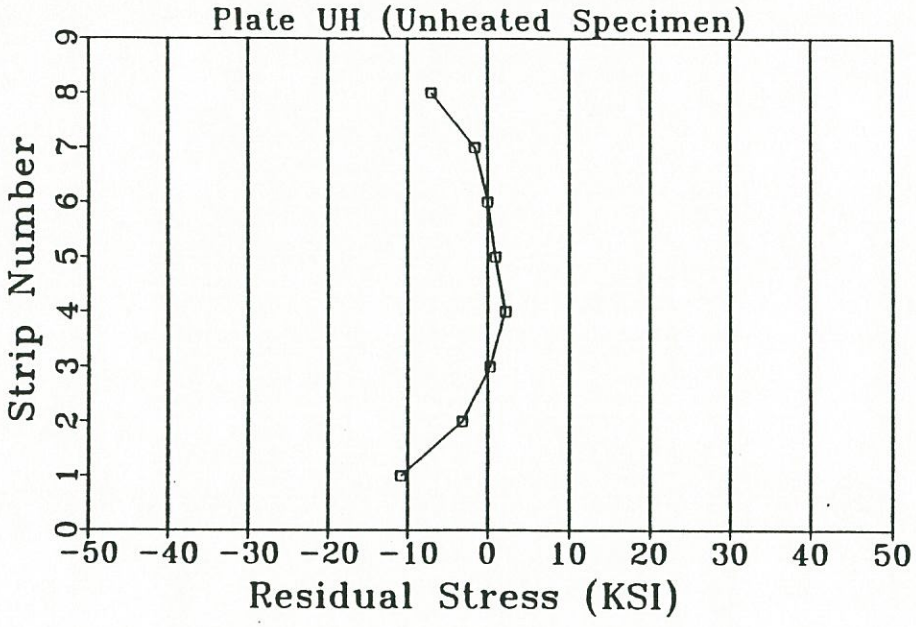

Figure 7. Residual stresses in unheated plate (Plate UH).

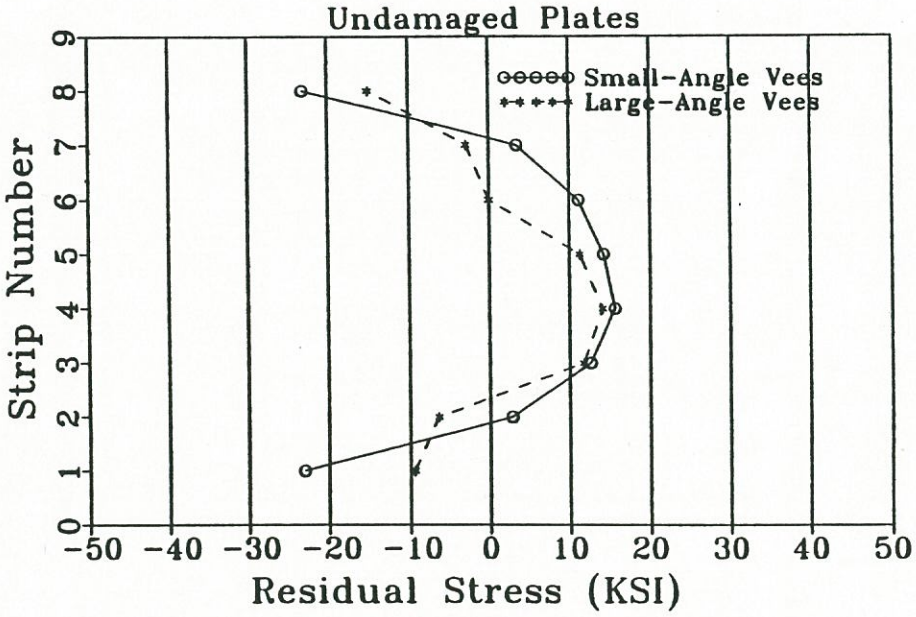

Figure 8. Average residual stresses resulting from vee heats.

Table 2. Experimentally determined residual stresses in undamaged plates: "large" vee angles (82°).

Strip	UH	Residual Stresses (ksi) in Plate #:		
		VI-12	VI-10	Avg.
1	-10.84	-9.43	NR*	-9.43
2	-3.08	-6.67	-6.16	-6.42
3	0.29	13.27	10.30	11.79
4	2.21	16.50	11.82	14.16
5	0.98	11.13	11.53	11.33
6	0.00	-1.38	1.41	0.02
7	-1.56	-3.63	-2.03	-2.83
8	-7.00	-11.85	-18.16	-15.00

*No reading was taken due to cutting error.

Table 3. Experimentally determined residual stresses in undamaged plates: "small" vee angles (20°, 45°, and 60°).

Strip	Residual Stresses (ksi) in Plate #:						
	I-1	II-1	I-2	VI-6	VI-4	I-3	Avg.
1	-24.47	-22.70	-23.96	-23.27	-16.68	-27.23	-23.05
2	0.11	11.75	4.84	5.98	-1.13	-4.79	2.79
3	13.23	17.61	7.56	16.17	7.18	19.15	12.56
4	16.11	16.59	15.23	17.29	19.66	16.31	15.68
5	16.24	12.62	14.29	14.28	11.13	17.18	14.29
6	9.24	NR*	8.59	9.64	9.97	18.63	11.21
7	8.20	NR*	0.15	2.00	7.03	0.07	3.49
8	-22.15	-24.36	-24.40	-23.89	-18.67	-25.19	-23.11

*No reading was taken due to cutting error.

Damaged Plates

Degree of Damage

A commonly posed question among those involved in heat straightening is the following: Is there an upper limit on the amount of damage that a steel member may undergo and still be heat straightened? To answer the question of damage limitation, one first must be able to define damage. Definitions of this type have been non-existent or, at best, extremely vague in previous literature concerning heat straightening.

In a comprehensive set of guidelines for the evaluation and repair of damaged steel bridge members, Shanafelt and Horn (1984) developed a method of quantifying damage in terms of strain. The following equation was used to determine the radius of curvature (R) along the edge of a damaged member:

$$R = \frac{(L_1 + L_2)^2}{(Y_1 - 2(Y_2) + Y_3)} \qquad (1)$$

The equation parameters are shown in Figure 9.

In the above reference, the radius of curvature in a damaged member, as calculated using Equation 1, was compared to the radius of curvature at the extreme fibers of particular cross-sections at the point of first yielding. The curvature was then expressed as a multiple of the yield strain value. Recommendations were made concerning upper limits on damage to members in which heat straightening should be applied. It was recommended that primary tension members having more than five percent nominal strain (about 42 times yield strain in A36 steel) should not be straightened unless the straightened elements were strengthened by additional splice material. Also, even if nominal strains were less than or equal to five percent, a limit of 15 times the yield strain (the strain at which strain hardening approximately begins) was placed on primary tension members for strains occurring at severe fatigue critical areas (AASHTO stress categories lower than C).

If severe fatigue critical details were present, according to the guidelines, the member would need to be strengthened with a minimum of 50 percent additional area. This minimum addition was based on the simple premise that if the member was initially designed for a working stress of about 0.5 F_y, the straightened member element could be neglected entirely and the maximum stress would not exceed F_y.

Using these guidelines, all primary tension member areas in severe fatigue critical areas with less than or equal to 15 times the yield point strain could be straightened. The

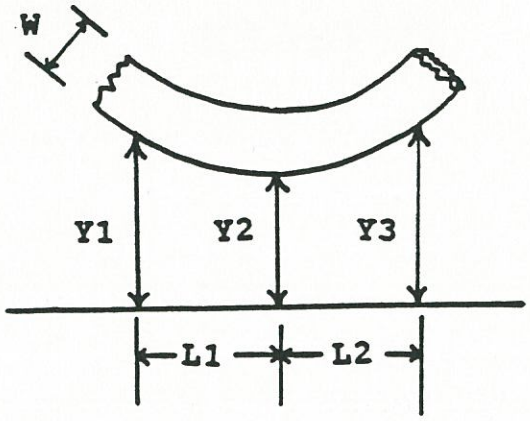

Figure 9. Method of establishing curvature from 3 points measurement (Shanafelt and Horn, 1984).

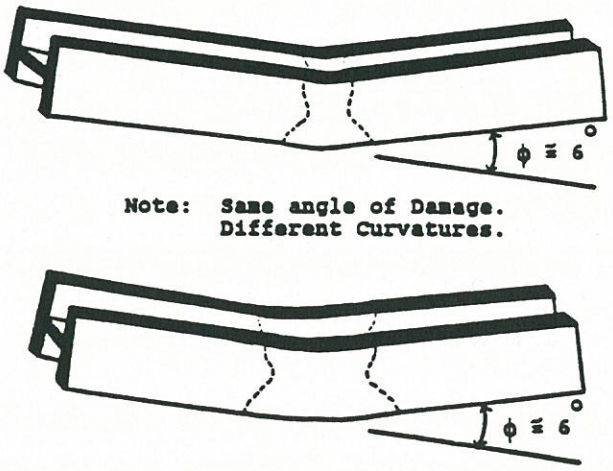

Figure 10. Variations in curvature for identical angles of damage.

preceding strain limitations were applied to primary tension members or primary members with tensile areas. No limitation on strain was placed on compression members or tension or compression secondary members.

Shanafelt and Horn suggested that measuring points for curvature be spaced at one-foot intervals. The validity of Equation 1 is based on the assumption of constant curvature in the region contained within the points (see Figure 9). However, in most actual damage situations, the damage is more localized, with the radius of curvature being highly variable throughout the damaged region. Therefore, in those cases, the one-foot spacing between measurements renders Equation 1 an inaccurate method of classifying damage. Also, the value of 15 times yield strain constitutes an extremely small bend in a plate element about its strong axis. The equation, as used, may not portray this fact in certain situations.

In the study of repetitively damaged, single curvature beams (as explained further in Chapter 3), it was discovered that the total "angle of damage" was a better definition of damage than curvature. This conclusion originated from the fact that approximately the same number of heats were required to straighten two beams damaged to the same angle, but with different curvature distributions (and different maximum curvatures) (see Figure 10). The angle of damage is simply the angle formed by the straight portions of the member which are on either side of the damaged region. This type of damage classification is similar to that used by Moberg (1979) during the actual repair of a damaged bridge. Of course, this definition does not nullify the importance of curvature. Curvature (or strain) is still the most logical characteristic for establishing damage limits, though not sufficient by itself for damage definition.

To help develop guidelines for damage limits, a number of deformed plate studies were conducted. Table 4 shows the deformed plates which were straightened. Shown are their damage classifications, maximum strains, and heating parameters used. Each plate had dimensions of 4" x 1/4" by 24". They were simply supported at 22" and were damaged with a center point loading to 4 different degrees of damage. Equation 1 was used, with much smaller intervals (one inch) between measuring points. This modification was to allow for a more uniform curvature over the span of measuring points to more accurately determine the maximum strain (in terms of yield) along the bottom edge of the plate.

It is obvious from Table 4, that small angles of damage represent quite large strains in terms of yield. It is also evident that strain does not directly vary with angle of damage (due to the spreading of the yield zone as the angle increases (see Figure 11).

Table 4. Heating conditions and angles of damage (deformed plates).

Plate	Angle of Damage (deg/millirad)	Max Strain (Multiple of Yield Str)	Vee Angle (deg)	Load Ratio (M/M_p)	Vee Depth Ratio
XXV-3	6.40/111.8	30	45	0.25	1.00
XXV-4	23.62/412.2	100	45	0.25	1.00
XXV-5	5.58/97.4	30	45	0.50	1.00
XXV-6	11.80/205.9	80	45	0.50	1.00
XXV-7	18.7/327.6	90	45	0.33	1.00
XXV-8	5.99/104.5	30	45	0.50	0.75
XXV-9*	21.12/368.6	80	20	0.50	0.75
XXV-10*	25.06/437.4	90	20	0.50	1.00
XXV-11*	18.21/317.8	100	60	0.50	0.75
XXV-12*	25.02/436.7	100	60	0.50	1.00

*The last four specimens were used just for plastic rotation data and were not straightened completely (20 heats were applied to each)

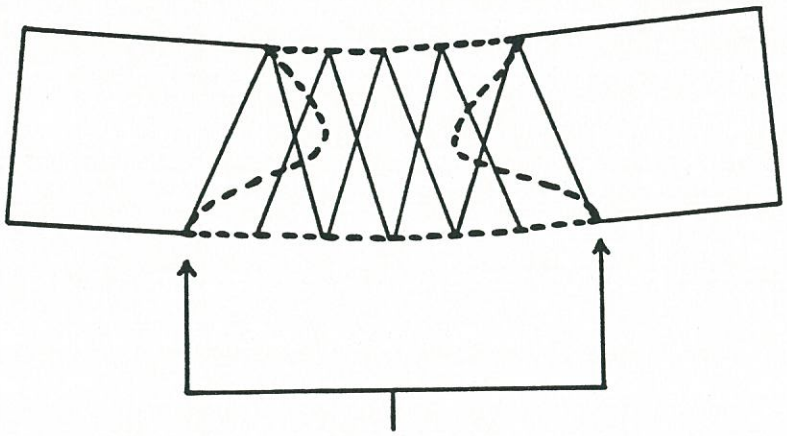

Figure 11. Vee locations to accommodate entire yield zone.

Each deformed plate was straightened, using the heating parameters shown in Table 4, in the same manner as the undeformed plates. The numbers of heating/cooling cycles required to straighten the plates ranged from 13 (for XXV-5) to 106 (for XXV-4) as seen in Table 5. The vee heat locations varied from heat to heat to insure that straightening was achieved throughout the yielded zone (see Figure 12).

Plastic Rotations

Almost all of the previous plastic rotation studies were associated with undamaged specimens, heated between one and four times each. In those studies (Roeder 1985; Avent and Fadous 1988), observations were made that the plastic rotations in undeformed plates exhibited widely scattered values under any given set of heating parameters. However, no conclusions could be drawn concerning any trends which might exist in the values of plastic rotations throughout a straightening process of a damaged plate involving more than four heats.

The plastic rotations resulting from each heat application on the damaged plates were determined in the following manner: A total of 17 points were established along the bottom edge of the plate. The plates were simply-supported (using 5/8" bolts) on a stationary frame at a length of 22" (Figure 4). Prior to the initial heating, the vertical distance from each point to a straight horizontal datum line was measured using dial calipers to the nearest ten-thousandth of an inch. After each heat, the distances were remeasured in the same manner.

From each set of measurements, linear regression was used to establish two straight lines (representing the bottom plate edge on each side of the center line of the plate, respectively). The plastic rotation, ϕ, is simply the change in the angle formed by these two lines, resulting from the heating process.

The damaged plate experiments contributed a great deal of information concerning plastic rotations. The plastic rotations for each individual plate are shown in Appendix B. As in previous research, the values exhibited a wide scatter. This scatter could be attributed to a number of things, e.g., relative location of heat to the previous heat, slight differences in temperature, changing residual stress patterns from heat to heat, etc. It is highly suspect, although great pains were taken to avoid it, that error in measurement also contributed to the scatter as a result of out-of-plane movement of the plates. However, despite the scatter, the large numbers of heats allow for statistically more meaningful average plastic rotations to be

Table 5. Summary of plastic rotation data (damaged plates).

Plate	Number of Heats	Mean Plastic Rotation (millirad)	Coefficient of Variation
XXV-3	23	4.63	0.46
XXV-4	106	3.82	0.70
XXV-5	13	6.94	0.17
XXV-6	35	5.60	0.58
XXV-7	58	5.56	0.45
XXV-8	21	4.69	0.40
XXV-9	20	3.81*	0.55
XXV-10	20	3.41*	0.44
XXV-11	20	6.43*	1.20
XXV-12	20	6.56*	0.53

*Values converted from actual 1100°F heating temperature to 1200°F using temperature relationship from previous heat straightening research

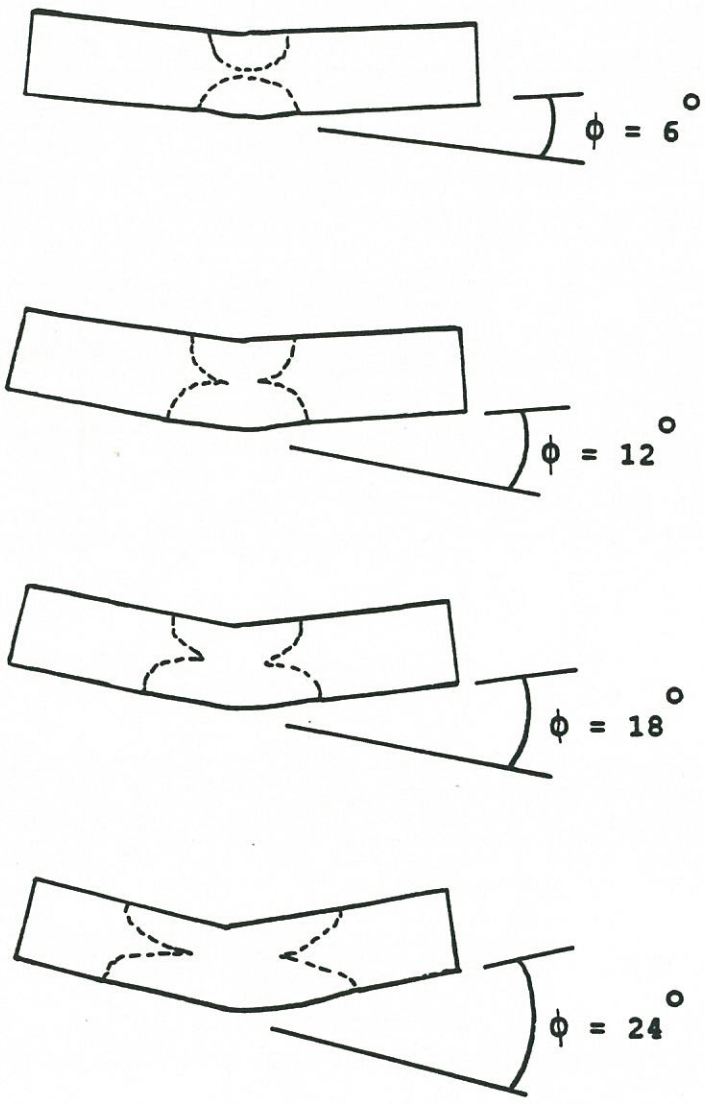

Figure 12. Spreading of yield zone with increasing angles of damage.

calculated as well as the observance of trends in these plastic rotations within an entire straightening process.

A summary of the plastic rotation data for each plate is shown in Table 5. The large number of heats on each plate reduces the uncertainty in predicting plastic rotations. Table 6 shows the average plastic rotations in specific heating sequences throughout the straightening process of each plate. In almost all cases, high plastic rotations resulted from the first three heats. However, past this point, only slight decreases occurred (most notably in plates XXV-9 through XXV-12). These findings were further supported in the study of damaged beams, where a statistical approach was used to determine that plastic rotations did not vary significantly from heat to heat after the first few heats (see Chapter 3).

Previous plastic rotation equations were based (theoretically and experimentally) on vee heats applied to straight plate elements only. Since the observation was made that in almost all of the damaged plates, lower plastic rotations occurred than predicted by these equations, an improved mathematical model is needed. The most recent comprehensive equation (Avent and Fadous 1988) based on Roeder's (1985) and Boudreaux's (1987) data is as follows:

$$\phi = F_t(T)\, F_l(M)\, \varepsilon_p(T) \sin \frac{\theta}{2} \tag{2a}$$

where ϕ is the plastic rotations in radians, θ is the vee angle and $F_t(T)$ is a temperature function which reflects the effect of heating temperature, T (in degrees Fahrenheit), and is given by

$$F_t(T) = 0.5 + 0.00125(T - 750) \tag{2b}$$

$F_l(M)$ is the load ratio function which reflects the effect of the external and internal constraining forces and is given by

$$F_l(M) = (0.9 + 3.4 \frac{M}{M_p}) \tag{2c}$$

where M is the moment at the heated section due to external constraining forces and M_p is the plastic moment capacity of the cross section. The confinement function, $\varepsilon_p(T)$, is the plastic strain when the steel is heated under conditions of perfect confinement to temperature, T, and is given by

Table 6. Plastic rotations in subsequent heating groups.

Plate	Average Plastic Rotation in Heat Numbers										
	1-3	1-10	11-20	21-30	31-40	41-50	51-60	61-70	71-80	81-90	91-100
XXV-3	3.62	4.21	4.91	----	----	----	----	----	----	----	----
XXV-4	2.72	3.88	3.97	5.51	4.24	4.13	2.76	3.92	3.59	3.69	2.73
XXV-5	7.55	6.71	----	----	----	----	----	----	----	----	----
XXV-6	12.67	8.31	5.62	3.84	----	----	----	----	----	----	----
XXV-7	7.65	6.34	6.46	3.86	5.45	6.02	5.12	----	----	----	----
XXV-8	5.57	5.56	4.02	----	----	----	----	----	----	----	----
XXV-9	6.15	4.20	3.43	----	----	----	----	----	----	----	----
XXV-10	4.29	3.95	2.86	----	----	----	----	----	----	----	----
XXV-11	8.22	6.85	6.00	----	----	----	----	----	----	----	----
XXV-12	8.11	6.98	6.14	----	----	----	----	----	----	----	----

$$\varepsilon_p(T) = (.001T^2 + 6.1T - 415)\ 10^{-6} - \left[\frac{(-720{,}000 + 4200T - 2.75T^2)}{806(500{,}000 + 1{,}333T - 1.111T^2)}\right] \quad (2d)$$

This equation assumed uniform strain throughout the vee width which linearly varied at the vee apex to the open end. $\varepsilon_p(T)$ is determined based on previous studies of the effects of temperature on the yield stress and modulus of elasticity of steel. Equation 2 reduces to the following at 1150°F and a load ratio of 0.323:

$$\phi = 2\varepsilon_p(T) \sin\left(\frac{\theta}{2}\right) \quad (3)$$

The load ratio of 0.323 was determined to be the value at which "perfect confinement" exists. Perfect confinement is the condition at which thermal expansion of the vee-heated area is zero. This is achieved by applying the maximum load ratio at which the permanent plastic strains are not assisted by any hot mechanical straightening (for a detailed derivation see Avent and Fadous 1988).

The experimental data obtained by Roeder and Boudreaux were well represented by Equation 2, when considered together. However, Boudreaux's data values were somewhat lower than Equation 2, and Roeder's where somewhat higher. It is not clear why the two researchers had significantly different plastic rotations.

An important aspect of Roeder's study was his experimental strain measurement. A number of pins were attached (in a rectangular grid) to various plate specimens in the region containing the vee heated area and its nearby proximity. By measuring the horizontal distances between the adjacent pins on each row before and after heating, a strain contour was established within this region. An example strain contour from Roeder is shown in Figure 13. The heating conditions for this plate were a 45° vee with depth ratio = 0.75, M/M_p = 0.13, and T = 1000°F.

A notable characteristic of Roeder's strain contour is that almost no strain occurred outside the vee heated area. This was expected and was part of the rationale behind past plastic rotation equations. However, the assumed uniform strain does not occur along any given horizontal line (for example, the lower edge of the plate). Since Roeder presented only one example strain distribution, it is difficult to draw many conclusions, especially in regards to the accuracy of the values themselves. It should be noted that the plastic rotation and strain values in this particular example were extremely high compared to the analytical equations

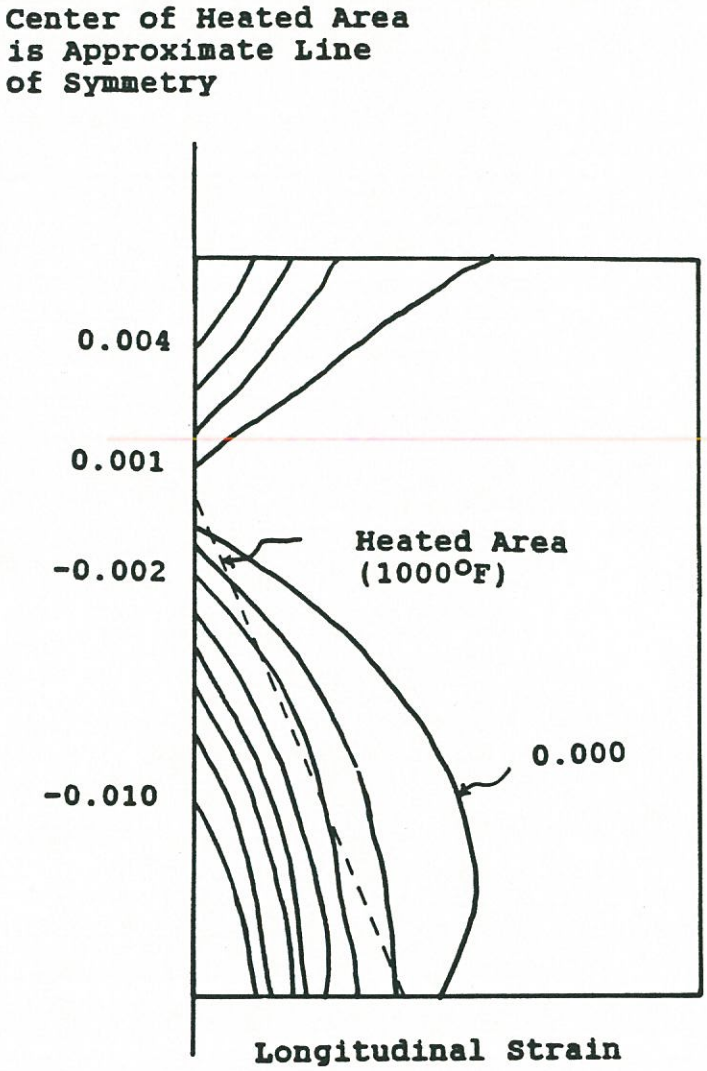

Figure 13. Experimental strain contour (from Roeder 1985).

used at that time. However, it can be concluded that the general shape of the contour is relatively representative of typical strains, assuming the measurements are accurate.

It can be seen in Figure 14 that the majority of the deformation in the open end of the vee occurs approximately within the inner two thirds of the heated region. Thus, it is reasoned that an "effective" vee angle ($\theta_e = 2/3$) should be used in Equation 2 to more accurately predict plastic rotations.

A least squares curve fit of the data represented by Figure 15 revealed the best effective angle to be approximately 30 degrees, when keeping the equation in the same form as Boudreaux's. This angle is 66 percent of the actual vee angle of 45 degrees. In other words, the effective angle would be 30/45 x θ, or 0.66 θ. The revised equation thus becomes

$$\phi = F_t(T)\ F_l(M)\ \varepsilon_p(T)\ \sin\frac{\theta_e}{2} \tag{4a}$$

which is simply

$$\phi = F_t(T)\ F_l(M)\ \varepsilon_p(T)\ \sin\frac{\theta}{3} \tag{4b}$$

or for T = 1200°, $\varepsilon_p = 0.00745$, $F_t(T) = 1.0625$

$$\phi = .00792\ (0.9 + 3.4\ \frac{M}{M_p})\ \sin\frac{\theta}{3} \tag{4c}$$

Equation 4b represents the experimental data in the current study very well. A comparison of experimental values and the theoretical curves from the previous equation (Equation 2) and the modified equation (Equation 4b) are shown in Figures 15 and 16 for two different load ratios. Clearly, the data closely match the newer equation better than the old one. Also shown are data from Boudreaux and Roeder. Boudreaux's data are also actually better represented by the modified equation than by the old one. Roeder's values are extremely high. Although few in number in these plots, Roeder's large number of heats at lower load ratios drastically affected Boudreaux's equation.

From Figure 17, for an angle up to about 20 degrees (which is the smallest practical vee angle), the Boudreaux equation would be sufficient to represent the data. However, within the more practical range between 20 and 60 degrees, the modified equation would be more applicable. This makes sense because the old equation, which is basically linear (within the practical range of vee angles), does not take into account the fact that the relationship between vee angle and plastic rotation in the range of large vee angles does not follow the

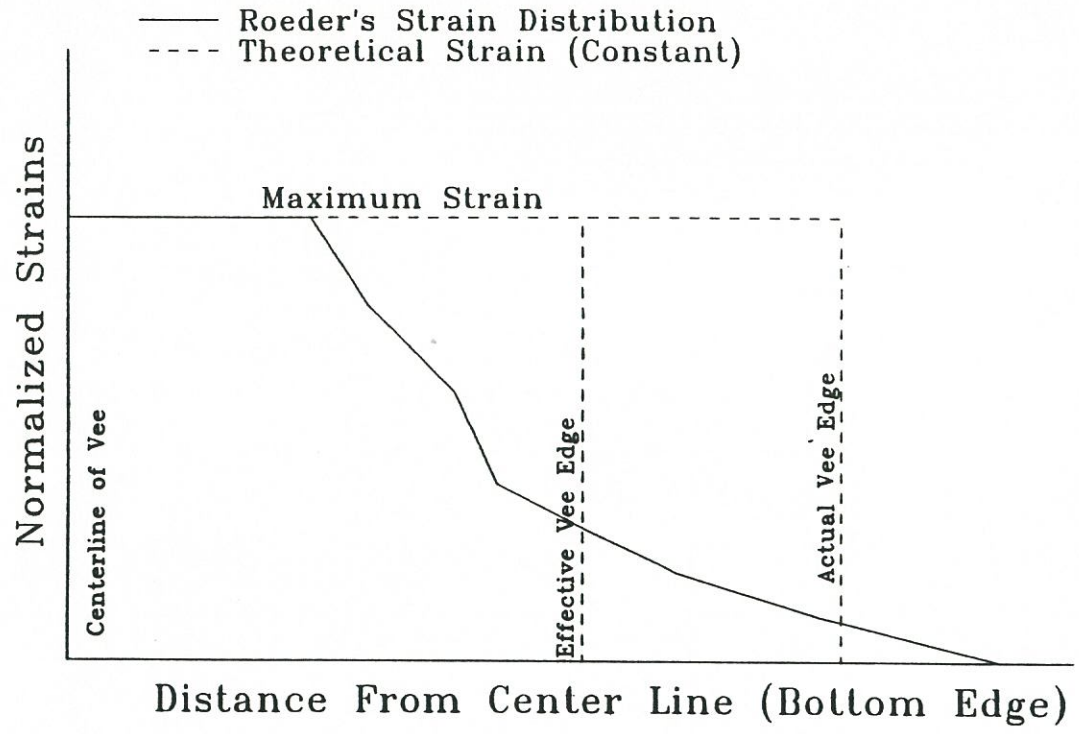

Figure 14. Strain at open end of vee (derived from Roeder 1985).

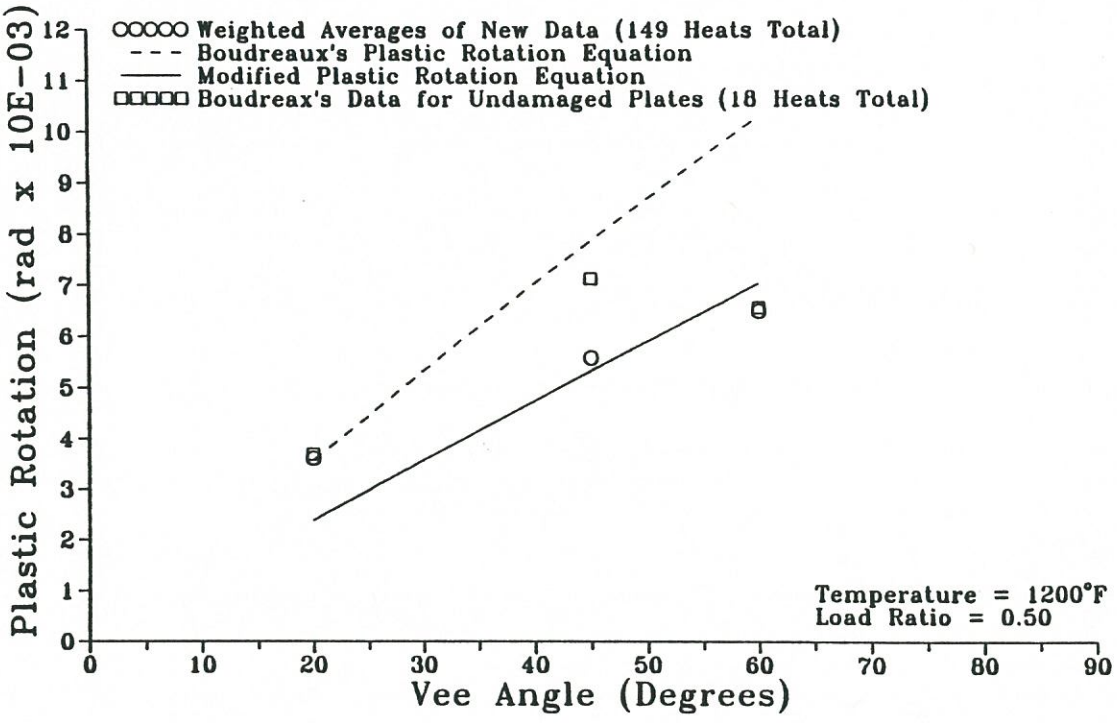

Figure 15. Comparison of old and new data with Boudreaux's equation and the modified equation (1200°F, $M/M_p = 0.5$).

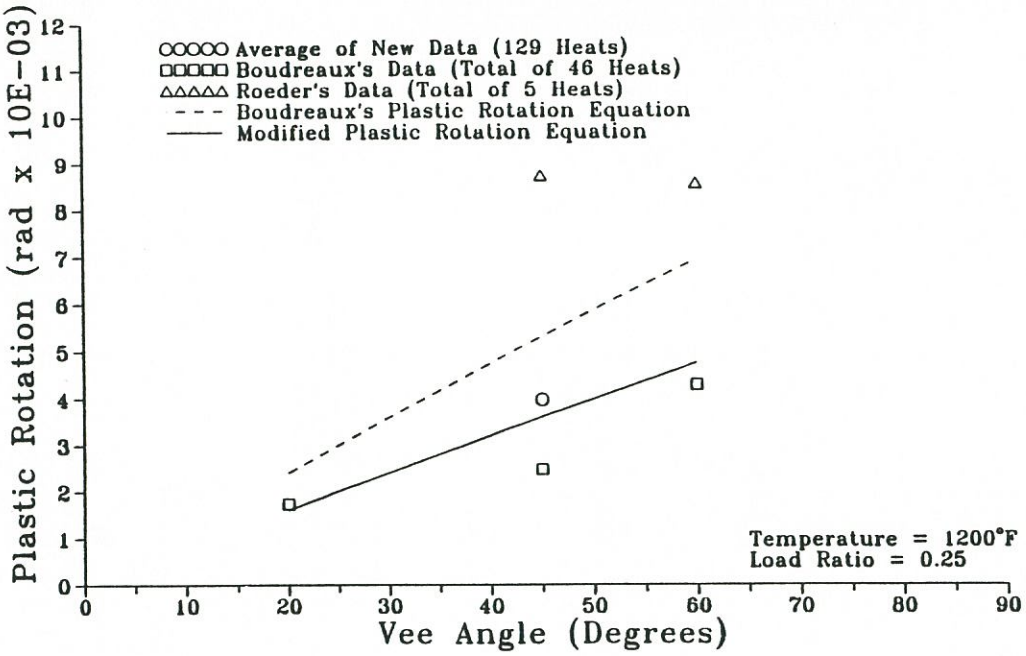

Figure 16. Comparison of old and new data with Boudreaux's equation and the modified equation (1200°F, $M/M_p = 0.25$).

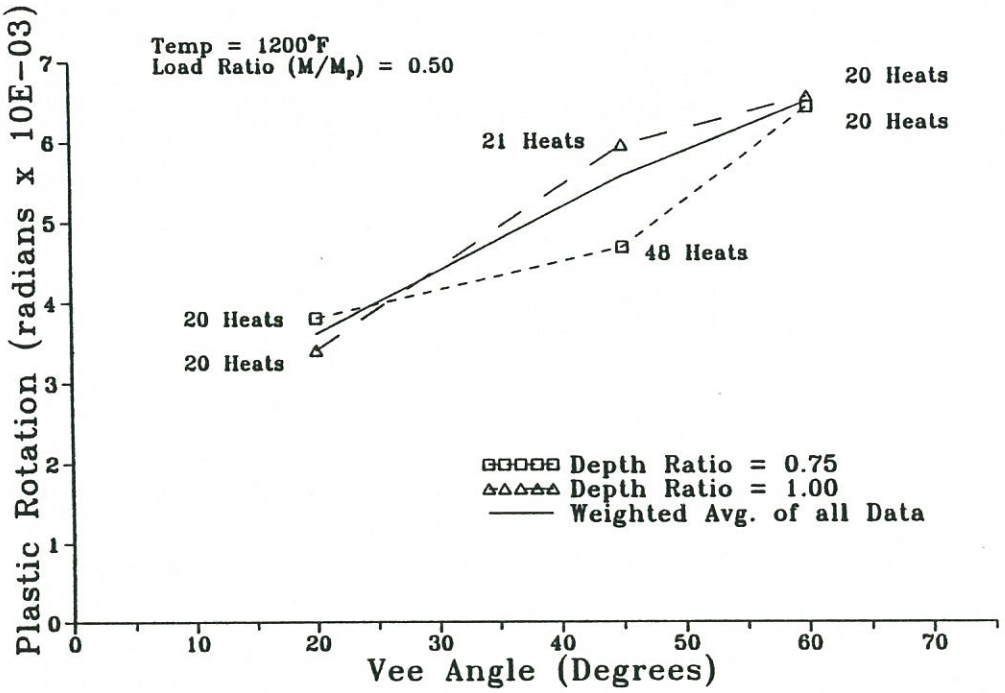

Figure 17. Comparing the effect of depth ration on plastic rotations for 20°, 45° and 60° vee heats on damaged plates.

same linear relationship. In fact, other research has indicated that the amount of increase in plastic rotation with vee angle, tends to decrease in the range of larger vee angles (Avent and Fadous 1988), although this fact was not specifically made apparent. This trend in plastic rotations at increasingly large vee angles is influenced by the nonuniform strains, exhibited by Roeder's strain contour. The nonuniformity is not as significant in the smaller angles, where the heating pattern is more concentrated.

Once the modified equation for plastic rotation was established, it was desirable to see how it compared to all of the data, previous and present. Table 7 shows Boudreaux's, Roeder's and the current data, along with computed values from Boudreaux's and the modified equations, for a wide range of heating conditions. Boudreaux's data averaged approximately 15% lower than the original equation, and the total average plastic rotations of the damaged plates are clearly better represented by the modified equation. From Table 7, the original plastic rotation equation was influenced greatly by Roeder's high values.

It is likely that the residual stress distribution has some influence on the fact that the plastic rotations are greater during the first three heats on a damaged specimen. In the study of residual stresses, it was found that the stress distribution in a straight plate heated four times was similar to that in a damaged plate, regardless of the number of heats that were applied to straighten it (see section on residual stresses in this chapter). Therefore, after, at most, four heats, the residual stresses "stabilize", as do the plastic rotations (when considering average values). It should be noted that the trend of higher plastic rotations in the initial three heats was also observed in the study of damaged wide flange beams and damaged full-scale simulated bridge girders.

While temperature, load ratio, and vee angle are included in Equation 4b, the depth ratio d_v/w is not. In previous research (Weerth 1971), statements have been made that depth ratio would significantly affect the plastic rotations, keeping all other parameters constant. However, not enough data was available to verify this statement. A study was undertaken here to obtain adequate data for two depth ratios, 1.00 and 0.75. The heating temperature was 1200°F and the load ratio was 0.5 in all cases. Only the vee angle was varied. Shown in Figure 17 are plastic rotations for 20-, 45-, and 60-degree vees for both 0.75 and 1.00 depth ratios. Vee depth ratios of 0.75 and 1.00 do not differ significantly. Thus, within this range of depth ratios, there is no need to account for vee depth in the equation. Weighted averages (with respect to the number of heats) of the data represented by Figure 17 are presented in Table 8.

Table 7. Comparison of plastic rotation data from various studies.

Vee	M/M_p	Plastic Rotations					
		Roeder*	Eqn. 3	Boudreaux	Damaged		Eqn. 4b
					1st	Avg.	
20	0	----	1.23	1.26	----	----	0.82
20	.25	----	2.41	1.74	----	----	1.61
20	.50	----	3.57	3.69	4.29	3.41	2.38
45	0	----	2.73	2.51	----	----	1.84
45	.25	8.72	5.30	2.47	2.88	3.96	3.58
45	.50	----	7.87	7.13	11.28	5.58	5.32
60	0	6.98	3.56	2.53	----	----	2.44
60	.25	8.55	6.93	4.28	----	----	4.74
60	.50	----	10.30	6.57	8.10	6.56	7.03
82	0	----	4.67	3.43	----	----	3.27
82	.25	10.47	9.08	6.25	----	----	6.36
82	.50	----	13.50	12.68	----	----	9.45

*Note: All of Roeder's vee heats had depth ratios of either 0.67 or 0.75, and all of his values were extremely high. Some of Roeder's values are for temperatures lower than 1200°F. For example, the average value of 8.72 milliradians for the 45 degree vee (M/M_p = 0.25) includes one values of 8.20 obtained at 975°F and a depth ratio of 0.67.

Table 8. Effect of depth ratio on plastic rotations.*

Vee Angle (degrees)	Plastic Rotation 3/4-depth vee (millirad)	Plastic Rotation full-depth vee (millirad)	Weight Average (millirad)
20	3.81 (20)	3.41 (20)	3.61
45	4.69 (21)	5.96 (48)	5.58
60	6.43 (20)	6.56 (20)	6.50

*Note: All values are for 0.5 load ratio at 1200°F (the number of heats are shown in parentheses)

Statistical Study of Plastic Rotations

The primary purpose of predicting plastic rotations is to determine the number of heats required to straighten a given damaged specimen. If the total damage were divided by the average plastic rotation, an estimate of number of heats would be obtained. However, it is more desirable to know the reliability behind such predictions. Because of the random nature of plastic rotation as a variable, using the simple average does not indicate reliability.

To achieve statistically reliable predictions, a detailed study of the experimental plastic rotations was conducted (de Bejar, et. al 1991) using the author's data. Simple engineering predictors based on the linearized theory of reliability were derived using the uniform value of a preselected target reliability index. Two different forms of the predictor were formulated based on whether or not the principal statistics of the process for the subject specimen are known. These models were theoretically verified by a separate model using spectral analysis in the frequency domain.

The reliability model, using the principal statistics of a sample specimen, is

$$N = k_i + R \cdot V_i \sqrt{k_i} \tag{5}$$

where N is the number of heats required, R is the target reliability index, $k_i = \phi_D/m_i$ (ϕ_D is the angle of damage in milliradians), and $V_i = \sigma_i/m_i$ is the coefficient of variation of the plastic rotations in the sample.

For a case where no data is available, a simple engineering predictor for N was formulated:

$$N = \frac{\alpha \cdot X}{5} \cdot \left[K_1 + \frac{0.77X}{\sqrt{\alpha}} \right] \cdot K_2 \tag{6}$$

where $X = \sqrt{\phi_D}$, (ϕ_D in milliradians), $K_1 = 1 + 1/\alpha$, and $K_2 = \sqrt{1 + \alpha/\gamma}$, if $1 \leq \gamma/2 \leq \text{int}(\alpha)$; or $K_1 = K_2 = 1$, otherwise; $\alpha = 0.5\ M_p/M_e$ is one-half of the reciprocal of the load ratio; γ is the closest integer representing the number of times that 6-degrees (104.72 milliradians) is contained in specified damage angle, ϕ_D; and int is an operator returning the integer part of a real number.

Equation 6 was slightly modified for plate XXV-8 (due to its 0.75 depth ratio), although it has been shown above that, in general, there is no significant difference in the plastic

rotations for this depth when compared to full depth vees. The modification yielded the following equation:

$$N = \frac{\delta X}{2} \cdot (1 + 0.77\delta X) \qquad (7)$$

where $\delta = 0.75$ is the vee depth ratio.

Table 9 shows the results of the study when compared to the actual number of heats required to straighten the plates. It should be noted that numbers are slightly greater than the actual number of heats applied to the experimental plates because in all cases, the plates would have required about two more heats to be completely straightened. Shown in Table 9, the values for each of the analytical models were close to each other and with the actual number of heats. Also shown is the number of heats required if every heat produced the exact value computed by the most recently modified plastic rotation equation (Equation 4b). In all but one case (XXV-7), the newly modified plastic rotation equation has excellent agreement with de Bejar's values. It should be noted that the data for plate XXV-7 seemed to be out of step with the rest of the plates, possibly due to faulty readings on the pressure gauge on the hydraulic cylinder.

Residual Stresses

Average residual stresses were determined by the sectioning method for three different regions on the damaged plates: Regions A, B, and C (see Figure 18).

By classifying the plates in groups of small degree of damage (angle of damage = 6 degrees) and large degree of damage (angle of damage = 12 to 24 degrees), these two groups experienced slightly different residual stress patterns. These classifications are logical when considering strains, with the small degree of damage classification exhibiting approximately 30 times yield strain, and the larger degrees of damage 80 to 100 times yield strain. The less damaged plates experienced larger stresses in region B, and lower stresses in regions A and C, when compared to the more damaged plates, where the stresses were relatively uniform (for each strip) in all three regions (see Figures 19 through 21). This is probably a result of a more uniform strain distribution caused by the spreading of the yield zone. Values for the two separate categories are shown in Tables 10 through 13. The stresses were computed at using (1) the commonly assumed value of E = 29,000 ksi for modulus of elasticity (at Regions A, B, and C), and (2) the measured values obtained from the tensile tests (at Region B only) (see section on material properties). It should be noted that some of

Table 9. Comparison of de Bejar's results with modified equation.

Plate	Number of Heats Required to Straighten the Specimen				
	Reliability Theory		Spectral Analysis	Modified Eqn. 4b	Actual No. of Heats*
	Eqn. 6	Eqn. 5			
XXV-3	29	29	30	33	25
XXV-4	125	123	124	122	108
XXV-5	17	15	16	19	15
XXV-6	46	44	45	41	38
XXV-7	67	66	65	84	60
XVV-8	27**	26	27	21	23

*Adjusted for complete straightening using average of all plastic rotations for that specimen

**Eqn. 7 was used instead of Eqn. 6

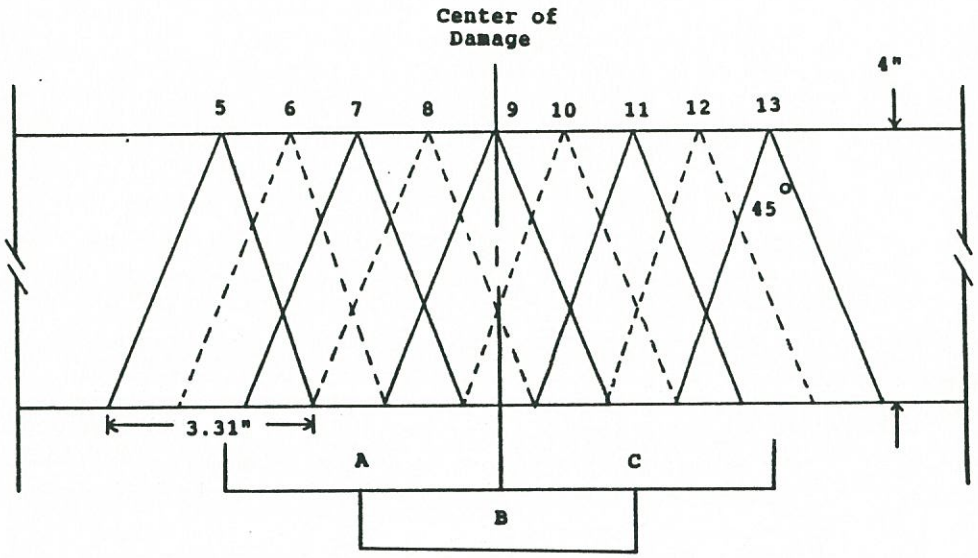

Figure 18. Regions A, B and C for residual stress measurements.

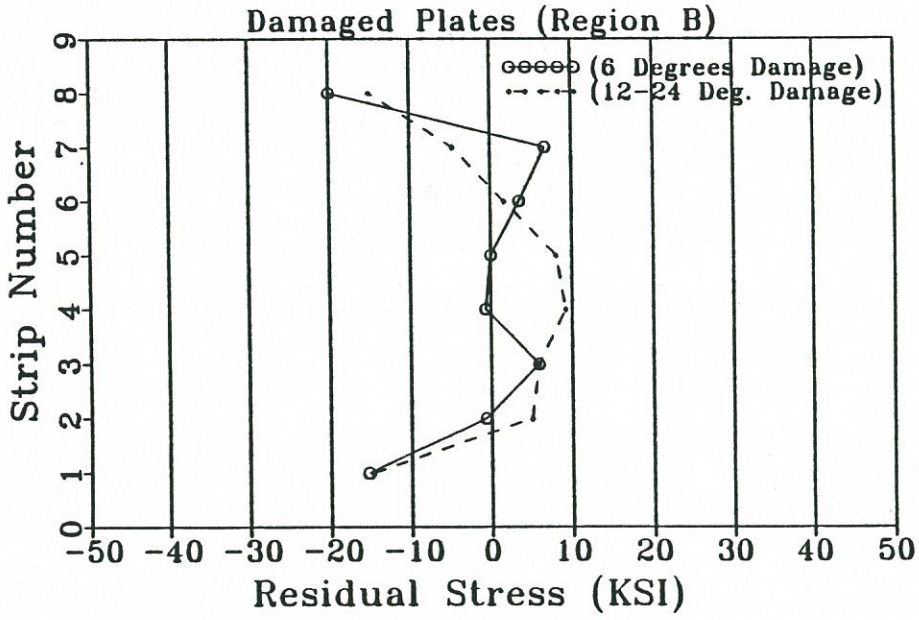

Figure 19. Residual stress distribution for Region B (estimated modulus of elasticity of 29,000 ksi).

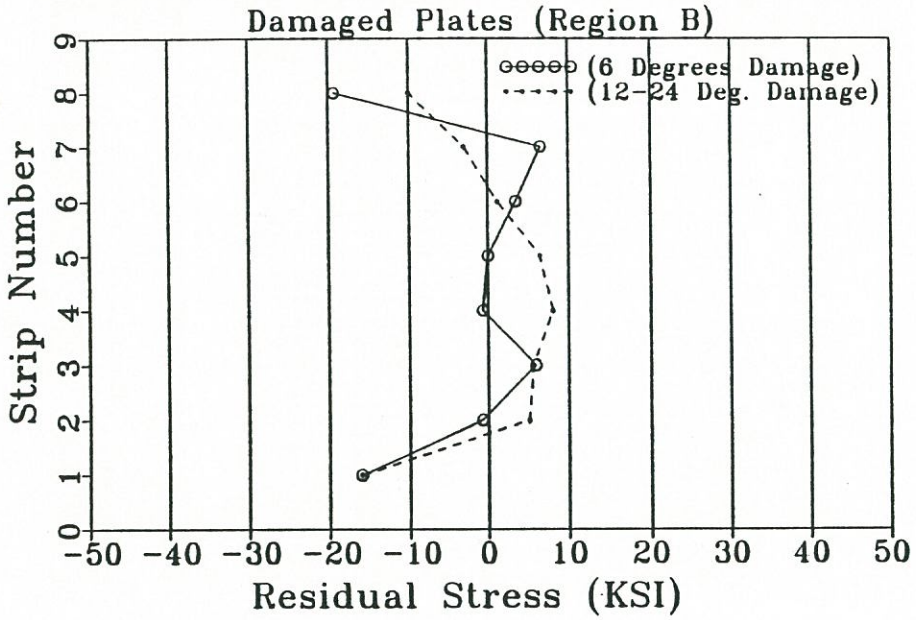

Figure 20. Residual stress distribution for Region B (moduli of elasticity from tensile test results.

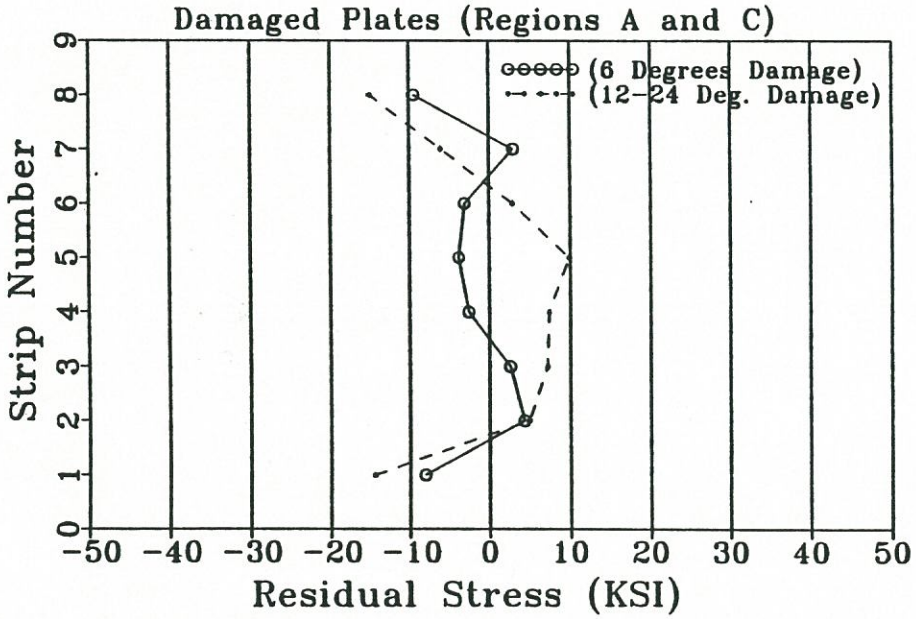

Figure 21. Residual stress distributions for Regions A and C (estimated modulus of elasticity of 29,000 ksi).

Table 10. Experimentally determined residual stresses in damaged plates: "small" angles of damage (approx. 6°) using assumed value of E = 29,000 ksi.

Strip No.	Residual Stresses (ksi) in Plate #		Average
	XXV-3	XXV-5	
A1	-2.29	-8.16	-5.23
A2	8.02	4.97	6.50
A3	0.51	4.21	2.36
A4	-1.96	-6.31	-4.14
A5	1.02	-5.58	-2.28
A6	-2.18	-1.56	-1.87
A4	2.76	6.13	4.45
A8	-11.75	-4.10	-7.93
B1	NR	-15.30	-15.30
B2	-5.91	4.57	-0.67
B3	6.97	4.86	5.92
B4	3.95	-5.22	-0.64
B5	3.88	-3.81	0.04
B6	4.68	2.40	3.54
B7	6.01	7.47	6.74
B8	-25.99	-13.93	-19.96
C1	-13.23	-8.70	-10.97
C2	0.36	3.81	2.09
C3	1.86	3.59	2.73
C4	-1.13	-0.80	-0.97
C5	-9.25	-1.42	-5.34
C6	-7.47	-1.02	-4.24
C7	-0.04	3.08	1.42
C8	-11.68	-10.04	-10.86

NR = No reading due to cutting error

Table 11. Experimentally determined residual stresses in deformed plates: "small" angles of damage (approx. 6°) using measured E values from tensile tests.

Strip No.	Residual Stresses (ksi) in Plate #		Average
	XXV-3	XXV-5	
B1	NR	-16.72	-16.01
B2	-6.05	4.68	-0.69
B3	7.31	4.62	5.92
B4	4.22	-4.61	-0.62
B5	4.24	-3.27	0.04
B6	5.15	2.01	3.48
B7	6.65	6.08	6.58
B8	-28.95	-11.00	-19.27

NR = No reading due to cutting error

Table 12. Experimentally determined residual stresses in deformed plates: "large" angles of damage (12° to 24°) using assumed value of E = 29,000 ksi.

Strip No.	Residual Stresses (ksi)			Avg.
	XXV-4	XXV-6	XXV-7	
A1	-18.41	-7.14	-22.23	-15.93
A2	3.30	8.23	4.79	5.44
A3	7.03	4.10	10.73	7.29
A4	8.52	1.67	14.54	8.24
A5	12.00	0.69	23.96	12.22
A6	7.83	-1.63	8.88	5.03
A7	NR	NR	NR	NR
A8	NR	NR	NR	NR
B1	-11.71	-17.47	-15.19	-14.79
B	3.59	7.36	4.03	4.99
B3	4.06	3.01	10.66	5.91
B4	5.58	12.15	10.00	9.24
B5	9.21	6.41	8.63	8.08
B6	4.13	NR	-1.41	1.71
B7	-4.68	NR	NR	-4.68
B8	NR	NR	NR	NR
C1	-14.29	-9.28	-15.41	-12.99
C2	4.10	3.19	5.66	4.32
C3	6.09	1.31	13.77	7.06
C4	7.40	1.60	10.66	6.55
C5	10.12	3.26	9.28	7.55
C6	6.45	-3.34	-0.87	0.75
C7	NR	NR	NR	NR
C8	NR	NR	NR	NR

NR = No reading due to cutting error

Table 13. Experimentally determined residual stresses in deformed plates: "large" angles of damage (12° to 24°) using E values from tensile tests.

Strip No.	Residual Stresses (ksi) in Plate #:			Avg.
	XXV-4	XXV-6	XXV-7	
B1	-12.96	-13.33	-21.58	-15.96
B2	3.75	5.66	5.04	5.09
B3	3.99	2.34	11.54	5.60
B4	5.14	9.51	9.17	8.06
B5	7.91	5.06	6.45	6.47
B6	3.07	NR	-0.99	1.21
B7	-2.94	NR	NR	-2.94
B8	NR	NR	NR	NR

NR = No reading due to cutting error

the gage holes were destroyed in the stripping process, thus rendering the strips unreadable. Stress distributions for each individual plate are shown in Appendix C.

As in the undamaged plates, load ratio and depth ratio individually have no apparent effect on the residual stress patterns. It is likely that the same effects of vee angle on residual stresses found for the undamaged plates can be applied to the damaged plates. In that case, larger vee angles would reduce the magnitudes of the residual stresses.

The basic shape of the residual stress pattern in each plate was similar to that of the undamaged plates. The stress distribution resembles very closely (in value and shape) the commonly assumed parabolic distribution for plates and flanges of wide flange beams. Thus, vee heats on a single plate element would not significantly affect its "column behavior".

Shortening

In past literature, the subject of member shortening due to heat straightening has been mentioned, but never fully discussed. One researcher stated that using smaller vee depth ratios should result in less member shortening, given any particular damage situation (Moberg 1979). However, it could be argued that less shortening would occur when using full-depth vee heats, since the top fibers have been heated and are subjected to a tensile stress. As shown below, the amount of shortening in a member can be quite significant, regardless of the vee depth ratio used.

Figure 22 shows the basic concept of the shortening phenomenon. First, one has a plate of given length. If the plate is damaged about its strong axis with a midpoint loading as shown, the top edge of the plate experiences compressive yielding (shortening) and the bottom edge of the plate experiences tensile yielding (stretching). As the plate is subjected to the heat straightening process, the top edge experiences some "restretching" in the longitudinal direction (as evidenced by Roeder's strain distribution). However, these positive strains are small in comparison to the simultaneous shortening of the bottom edge of the plate.

To quantify the amount of shortening experienced for a given amount of damage, measurements were made on some of the deformed plates. Initial plate lengths (before damage) and final measurements (after straightening) were taken, and the amounts of shortening are shown in Table 14. Regardless of initial and final lengths, all of the shortening occurs only within the damaged region (meaning shortening should not be expressed as a percentage of total length, but simply as a length itself).

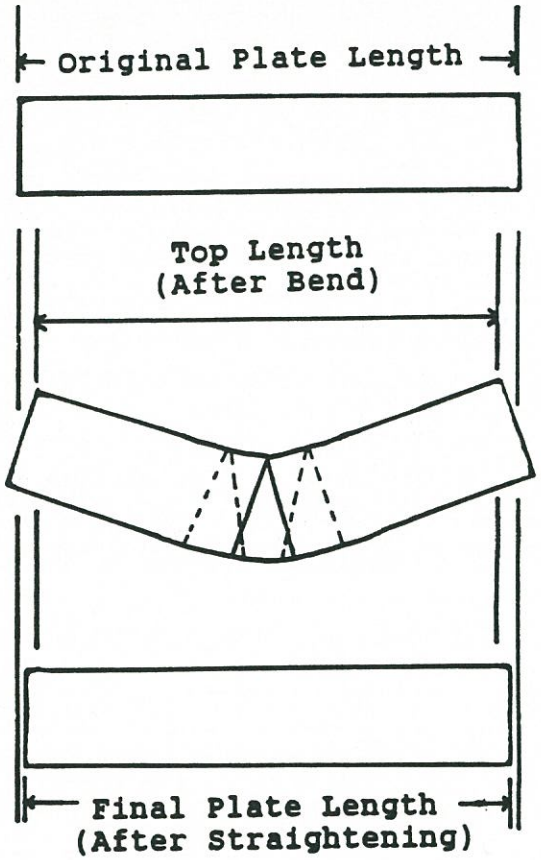

Figure 22. Representation of shortening resulting from a damage/repair cycle.

Table 14. Shortening of plates as a result of heat straightening.

Plate No.	Damage (rad)	Damage (deg)	Shortening (in.)
XXV-8	0.1045	5.99	0.080
XXV-6	0.2059	11.80	0.175
XXV-7	0.3276	18.77	0.310
XXV-4	0.4122	23.62	0.550

A plot of shortening vs. degree of damage is shown in Figure 23 for the plates with a depth of 4 inches. As seen in the plot, shortening varies quite directly with degree of damage, up to a certain point (somewhere between 18 and 24 degrees), for the specimens studied. With only 4 specimens, conclusions concerning the shortening phenomenon are tentative. However, shortening appears to be a function of plate depth (since strain will vary with plate depth for a given angle of damage). The shortening is also affected by the angle of damage itself, but does not vary with vee depth ratio, at least in the 0.75 to 1.00 range. The amount of shortening in Plate XXV-8 was about the same as for all of the deformed beams (see Chapter 6), in which the same amount of damage was experienced and 3/4-depth vees were also used. All of the specimens with 3/4-depth vees seemed to follow the same trend of shortening exhibited by those heated with full-depth vees. A preliminary formula for estimating shortening (based only on the four plates in Table 14) is

$$S = W \cdot (0.02\ \phi_D) \quad \text{for} \quad 0 < A < 24° \tag{8}$$

where S = shortening in inches, ϕ_D = angle of damage in degrees, and W = plate depth (width).

Redistribution of Material

As a result of shortening, the heated portions of the deformed plates thickened upon straightening. This fact becomes especially important in influencing future damage (if any) of the plate, as discovered in the study of deformed beams (see Chapter III). After the residual stress strips were cut from each plate, it became very easy to measure thicknesses at various locations along each strip. Thicknesses at a total of five points (see Figure 24) on each of the eight strips were measured to the 1/1000" using dial calipers. The measured thicknesses at the various points are presented in Appendix D.

Thickening was greatest for the plates damaged to the largest degrees. For example, in Plate XXV-4, the specimen with the greatest amount of damage (23.62°), the thicknesses (measured for each strip) along the center of damage averaged 0.655 inches. When compared to the average thickness of the plate before damage (0.495 inches), the thickening results in a 32 percent increase in cross-sectional area. At points further away from the center of damage, thickening is less pronounced, but nevertheless, some thickening occurs within all of the yield zone. With a thicker cross-section meaning a stronger member, it is likely that little significance should be placed on the thickening experienced.

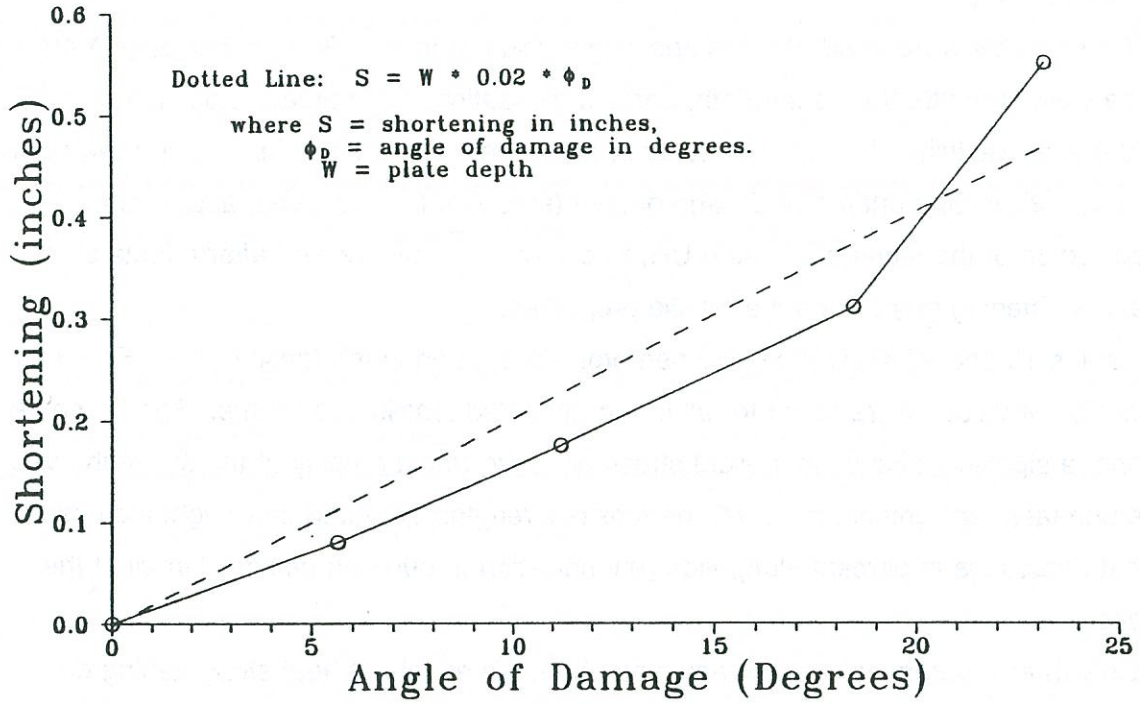

Figure 23. Shortening versus angle of damage in plate elements.

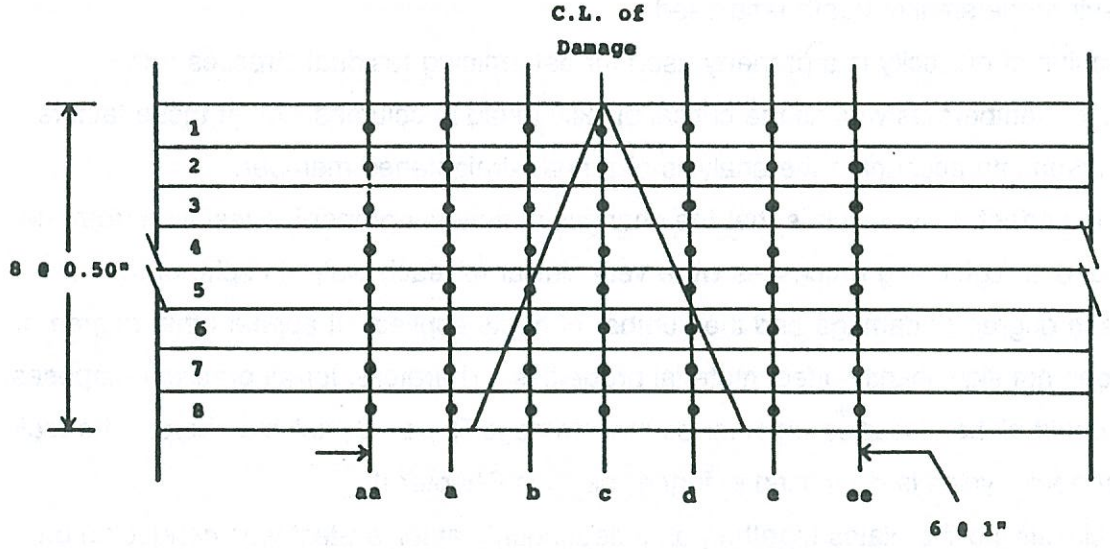

Figure 24. Points used in measure thickening in plates repaired by heat straightening.

Material Properties

Tensile tests were conducted on specimens taken from plates XXV-3 through XXV-8 to determine yield strength, tensile strength, percent elongation, and percent reduction in area and modulus of elasticity. For each plate, specimens were taken from the heated area at the top (strip 1 or 2), middle (strip 4 or 5), and bottom (strip 7 or 8) of the vee, and from an unheated region of the same plate (strip UH) to compare the before and after effects of the damage/straightening process on the tensile properties.

Tables 15 and 16 show the specimen properties found in the tensile tests. For each plate, consistent values were found for all of the unheated tensile specimens. For the heated specimens, a significant increase in yield stress occurred (most notably at the top of the vee) over the unheated specimens, although the tensile strengths exhibited only slight increases. Significant reductions in percent elongation (an indication of ductility) occurred in all of the specimens.

Only three references mention anything about the effects of heat straightening on modulus of elasticity (Weerth 1971; Nicholls and Weerth 1972; Horton 1973), and these references implied that single vee heat applications on mild steel did not effect modulus of elasticity. The values in Table 16 indicate that modulus of elasticity is significantly affected by one damage/repair cycle. A significant decrease in E occurred at the open end of the vee in most cases (with the exceptions of XXV-3 and XXV-8). The high values in Plate XXV-8 are likely a result of the smaller depth ratio used.

Modulus of elasticity is a property used for determining residual stresses and deflections in members as well as the critical buckling load in columns. All of these factors should be taken into account in the analysis of a heat-straightened member.

An important observation is that the changes in material properties resulting from the damaging and straightening processes were very similar for each plate, in spite of the vast differences in degree of damage and the number of heats applied. It appears that degree of damage does not significantly affect material properties. Therefore, for all practical purposes, the plates could all be classified together as "1st Damage/Repair Cycle" members. The topic of damage/repair cycles is discussed in further detail in Chapter III.

By classifying the plates together, an independent samples t-test was conducted on each of the properties in Table 15 to attach a statistical significance to the effects of one damage/straightening process on these properties. This test (which is discussed in detail in Chapter VI) is an excellent method for determining the confidence level at which one can predict changes resulting from some process or event, even with a small number of samples.

Table 15. Material properties of damaged plates.

Specimen/ Strip		Yield Stress (ksi)	Maximum Stress (ksi)	Percent* Elong.	Percent Red. in Area
XXV-3	(UH)	46.8	68.7	45	58
XXV-3	1	51.7	70.5	33	46
XXV-3	5	49.8	70.6	38	60
XXV-3	7	50.0	70.3	39	60
XXV-4	(UH)	48.7	71.7	41	56
XXV-4	2	52.3	71.2	30	62
XXV-4	5	51.9	71.9	31	60
XXV-4	7	51.7	69.7	34	64
XXV-5	(UH)	45.1	72.4	42	57
XXV-5	1	55.4	73.6	30	60
XXV-5	4	51.1	72.6	41	58
XXV-5	8	48.3	71.2	36	57
XXV-6	(UH)	43.9	66.5	46	60
XXV-6	2	52.0	68.4	34	63
XXV-6	5	48.3	68.8	36	60
XXV-6	7	47.0	69.0	36	60
XXV-7	(UH)	46.9	69.6	43	59
XXV-7	2	50.0	70.7	32	57
XXV-7	5	46.0	67.9	--	--
XXV-7	8	43.7	67.6	35	65
XXV-8	(UH)	42.3	69.0	41	58
XXV-8	2	60.1	75.6	28	51
XXV-8	4	48.6	71.7	35	59
XXV-8	8	50.9	70.7	34	56

Rates of strain = 0.4545 in/in per minute up to yield
= 1.0714 in/in per minute up to failure

*1-inch gage length

Table 16. Moduli of elasticity of damage plate specimens.

Specimen/ Strip		Modulus of Elasticity (ksi x 10^3)
XXV-3	(UH)	28.9
XXV-3	1	----
XXV-3	5	31.7
XXV-3	7	32.3
XXV-4	(UH)	32.3
XXV-4	2	30.3
XXV-4	5	24.9
XXV-4	7	18.2
XXV-5	(UH)	31.2
XXV-5	1	31.7
XXV-5	4	25.6
XXV-5	8	22.9
XXV-6	(UH)	24.2
XXV-6	2	22.3
XXV-6	5	22.9
XXV-6	7	17.0
XXV-7	(UH)	28.6
XXV-7	2	36.3
XXV-7	5	21.7
XXV-7	8	18.3
XXV-8	(UH)	27.8
XXV-8	2	43.6
XXV-8	4	35.5
XXV-8	8	28.9

Table 17 shows the confidence levels of one damage/repair cycle causing an increase (or decrease) in the particular tensile properties of a steel plate specimen. A high level of confidence exists that yield strength will increase, and that percent elongation will decrease (at all positions within the heated region). However, the confidence level of increased tensile stress and decreased reduction of area are very low (values under 95 to 97.5 percent are often rejected in hypothesis testing (Hicks 1982).

Considering only the high confidence levels for yield stress increase and ductility reduction, the respective percentages of these properties (for each specimen) in relation to those in the unheated specimens as well as to the ASTM standards are listed in Table 18. For yield stress, the ASTM standard value is 36 ksi, and the standard for percent elongation is 34.

It should be noted that the highest value for yield stress (60.1 ksi) was obtained in strip #2 of plate XXV-8. This plate was the only plate on which tensile tests were conducted which had a depth ratio of 0.75. It is suspected that, because strip #2 is in a region that has undergone compressive deformation, but has not been directly heated, it retains more of a strain hardening effect than it would if it were contained within the vee heated area (as strip #2 is for full-depth vees). As mentioned earlier, the minor restretching effect in the upper portions of the plate (addressed by Roeder) possibly causes a cyclic hardening effect not experienced if the material is heated. This specimen alone (among the plates) experienced a significant increase in tensile strength over the unheated specimen for that plate (10 percent). It should also be noted that similar high yield and tensile stresses were experienced (near the vee apex) after the first bend in the study of repetitively damaged wide flange beams, where a depth ratio of 0.75 was also used.

A summary of tensile test results of past research is shown in Table 19 for A36 steel heated at various temperatures and configurations. A more complete summary comprising of many different steel types is shown in a previous report (Avent 1986). All of the specimens in Table 19 were initially straight (plates, wide flange sections, and plate girders). Yield stresses in the heated specimens were only slightly higher (1-3%) than unheated specimens in the same studies, although the loss of ductility ranged from 13 to 25 percent (approximately the same range as the damaged plates in the current study). The lower yield stress increase in the undamaged specimens was probably a result of the fact that these specimens were never subjected to any cold bending (and thus strain hardening). It is difficult to draw any conclusions from Brockenbrough's study (using line heats), because the properties of the steel before heating are not known. As in the current study, all of the specimens listed in Table 19

Table 17. T-test results (for material property comparison).

Strip No.	Yield* Stress	Maximum* Stress	Percent** Elong.	Percent** Red. in Area
1 and 2	99.9	92.0	99.9	69.8
4 and 5	99.2	78.0	99.6	3.7
7 and 8	96.2	53.9	99.9	8.9

*Confidence level that heat straightening a deformed plate once will cause an increase in the property shown over that of the same specimen before the damage/ straightening cycle

**Confidence level that heat straightening a deformed plate once will cause an decrease in the property shown over that of the same specimen before the damage/straightening cycle

Table 18. Comparison of material properties in heat straightened steel with unheated specimens and ASTM standard values (current research).

Plate/ Strip		Yield Stress		Percent Elongation	
		% of UH Specimen	% of ASTM Standard	% of UH Specimen	% of ASTM Standard
XXV-3	1	110	144	74	97
XXV-3	5	106	138	84	112
XXV-3	7	107	139	87	115
XXV-4	2	107	145	73	88
XXV-4	5	107	144	76	91
XXV-4	7	106	144	83	100
XXV-5	1	123	154	71	88
XXV-5	4	113	134	98	121
XXV-5	8	107	131	86	106
XXV-6	2	118	144	74	100
XXV-6	5	110	134	78	106
XXV-6	7	107	131	78	106
XXV-6	2	107	139	74	94
XXV-6	5	110	128	--	--
XXV-6	7	107	121	81	103
XXV-8	2	142*	167*	68	82*
XXV-8	4	115	135	85	103
XXV-8	8	120	141	83	100

*Plate XXV-8 was the only plate tested that had a depth ratio of 0.75. The high yield stress values and low % elongation values are probably related to this fact (see text)

Table 19. Comparison of material properties of steel subjected to the heat straightening process with unheated specimens and ASTM standard values (past research).

Temp/ Heat Type	Yield Stress		Percent Elongation	
	% of UH Specimen	% of ASTM Standard	% of UH Specimen	% of ASTM Standard
1200*/vee+	103	--	75	--
1200*/vee++	100	--	87	--
1100-1200/vee+	100	--	87	--
1000/line**	--	118	--	96
1000/line**	--	108	--	94
1000/line**	--	106	--	93
1000/line**	--	90	--	96
1000/line**	--	97	--	96
1000/line**	--	105	--	96
1000/line**	--	101	--	100
1000/line**	--	97	--	100
1000/line**	--	100	--	100

*Average of unspecified number of values

+Nicholls and Weerth 1972; Weerth 1971 (average of unspecified number of specimens of heat-curved plates)

++Horton 1973 (heat-curved wide flange sections)

**Brockenbrough and Ives 1970 (heat-curved girders)

experienced only slight increases in tensile strength (a property not significantly affected by strain hardening).

Tensile Properties and Fatigue

The importance of increased yield stress and tensile strength and decreased ductility in the specimens lies in the areas of stress concentrations and fatigue. Stress concentrations often occur around discontinuities in structural members such as holes, fillets, notches, and the like (Barsom and Rolfe 1987). Structural designers usually rely on the ductility of the material to redistribute the load around a mild stress concentration, hence ignoring the effects of the stress concentration. However, a decrease in ductility allows for less stress redistribution, thus causing the higher stresses to remain concentrated.

Fatigue life is the total number of cycles (load fluctuations) required at a certain stress level to cause the initiation and propagation of cracks to a critical size. Regardless of how the cycles are classified, once above the "fatigue limit", an increase in stress means a lower fatigue life for any given material with a given geometry, i.e., presence of notches, holes, etc. The fatigue limit is the stress at which an infinite number of cycles can theoretically be applied without fatigue.

Studies have shown that the fatigue-crack-initiation threshold in various steels is related to the yield strength as well as tensile strength (Barsom and Rolfe 1987). This threshold basically establishes an upper stress for a given notch geometry at which an infinite number of cycles can be applied without crack initiation. Equations basing the threshold on both tensile strength and yield strength have been formulated and agree well with each other for most structural steels (where the ratios of tensile to yield strengths are fairly consistent). However, the tensile to yield strength ratio was severely altered in the heat straightened plates.

In general, the fatigue-crack-initiation threshold increases with tensile as well as yield strength. However, tensile strength increases were slight in the heat straightened plates, when compared to ductility losses (9.5% vs. 32% in the "worst case" specimen 2 on Plate XXV-8). Thus, the fatigue-crack-initiation threshold, based solely on tensile strength, could possibly be exceeded by increased stress caused by the ductility loss, resulting in failure.

Like ductility, fracture toughness (a value proportional to the energy consumed during plastic deformation) decreases as yield strength increases. The ability of a particular flaw, or stress concentrator, to cause catastrophic damage depends on the fracture toughness of the material (Flinn and Trojan 1986). It can be assumed that a 42 percent increase in yield

strength (and a 32 percent loss in ductility), as in the example specimen above, would constitute a severe reduction in the ability of a member (under a given set of conditions) to resist brittle fracture.

Because the subject of stress concentrations and brittle fracture depends on specific conditions, it is difficult to make recommendations without detailed analyses of these specific situations. It cannot be overemphasized that heat straightening areas of high stress concentration should be avoided when possible and only done after a sufficient analysis by a qualified engineer. However, since varying degrees of damage seemed to have similar material properties, degree of damage would not be the deciding factor on whether or not a member should be straightened in a fatigue critical area. Therefore, the suggestions made by Shanafelt and Horn for strain limitation in severe fatigue critical areas (where strain hardening was the basis) are considered only as a precautionary limits with no scientific rationale. Further study should be conducted to determine if heat straightening should be allowed for any degree of damage in the severe fatigue critical areas.

Since the effects of heat straightening on material properties, did not seem to relate to the degree of damage of plates (at least past the initial strain hardening point), Shanafelt and Horn's suggested limit of five percent nominal strain in tension members (41.67 times yield strain, if assumed yield strain is 0.0012) has no basis (recall that this constitutes a fairly small angle of damage in a plate element bent about its weak axis, especially with a large plate width). It was found that a strain of at least 100 times yield can be heat straightened with little or no difference in material property changes than for much smaller strains. Thus, in areas other than fatigue critical areas, the amount of shortening that will be experienced should be the determining factor when contemplating the use of heat straightening.

Conclusions

The study of damaged plates shows that results from previous undamaged plate studies cannot necessarily be applied to damaged plates, especially for residual stresses and material properties. However, the relative effects of individual heating parameters on plastic rotations and residual stresses are similar in undamaged and damaged specimens. For the first time, residual stress patterns in damaged specimens are determined and compare closely with patterns commonly assumed in practice for as-rolled plate specimens. The large numbers of heats applied to the damaged plates reduce the uncertainty in plate behavior resulting from vee heats. Both deterministic and probabilistic models have been presented to

predict the effects of plastic rotations. Thus, the ability to make reliable predictions concerning repair time has now been enhanced.

Yield stress, modulus of elasticity, and percent elongation were all found to be quite variable, even within a given plate, and should be considered before heat straightening operations begin. Some conclusions and suggestions from past research concerning damage limits on the use of heat straightening have now been experimentally verified (and modified in some cases). The results of this research allow engineers a more scientific approach to establishing a repair procedure for a given damage situation.

With plates being the fundamental element of structural shapes, the results of the damaged plate studies answer the basic questions concerning the straightening of more complex shapes. The following chapter is devoted to the study of heat straightening effects on rolled shapes.

Chapter 3

HEAT STRAIGHTENING OF ROLLED SHAPES

Damage Classifications

This chapter is devoted to quantifying the behavior of various rolled shapes (angles, channels, and wide flange beams). Since these shapes consist of multiple plate elements, the plate equation for plastic rotation forms the basis for the extension to rolled shapes. Included are experimental data from past research on undamaged specimens (Boudreaux 1987), and current data from damaged specimens. These data will be used to verify the mathematical models. The focus will be first on plastic rotations, followed by a discussion on residual stresses.

With a single plate, the only damage considered is bending about the strong axis. However, with rolled shapes, bending may occur about either the strong or weak axis and still result in the individual plate elements being bent primarily about their strong axes. A distinction must be made between the various types of damage. Three categories are defined and addressed in this research:

1. Category S: Denotes primary bending about the major, or "strong" axis.
2. Category W: Denotes primary bending about the minor, or "weak" axis.
3. Category T: Denotes unsymmetrical bending that results in torsion, or "twisting" about the longitudinal axis of the member.

In cases where the moment of inertia is the same for either axis, the member will be classified as a Category S member. A distinction is also made between the bending elements and stiffening elements of a cross-section. The bending elements are the plate elements of the cross-section subjected to strong axis bending about their own local axes. The stiffening elements are perpendicular to the bending elements and are bent about their own local weak axes. In most cases associated with major distortion of the entire member, yielding occurs in the bending plate elements but not in the stiffening elements. When yielding occurs in the stiffening elements, it is usually associated with localized bulges, crimps and buckles about the element's minor axis. This type of damage is not addressed here.

Angles and Channels

Undamaged Specimens

In the previous studies conducted by Boudreaux, a number of angles and channels were subjected to the heat straightening process. These shapes are essentially the most simple rolled shapes, as they can be considered as a single plate which is in a "folded" form. The heats presented below were applied to produce Category W bending in channels and Category S bending in equal leg angles with the "stiffening element" located at the open end of the vee (see Figure 25). The stiffening element is the leg of the angle that is not being vee heated. In the case of the channel, the stiffening element is the web.

In Boudreaux's study, it was found that when using the same heating parameters on these shapes as for the plates, much greater plastic rotations resulted. An equation to predict plastic rotations for these shapes was briefly addressed, with no in-depth look at the reasons for the larger rotations. Part of the current research involved a study of the plastic rotations of the angles and channels. The plastic rotations are shown below in Table 20 and 21 (Avent and Fadous 1988). All were heated at approximately 1200°F, and had a depth ratio of 1.00.

Geometric Considerations

An understanding of the basic behavior of a heat-straightened angle or channel can be obtained by considering them as folded plates. First, the angle's shape can be related to that of the plate when considering plastic rotations. For illustrative purposes, an L4x4x1/4 angle is chosen. Assume that if the angle is unfolded, the same heat could still be applied, though now on a single plate with approximately an 8-inch depth (see Figure 26a).

As shown in Figure 26a, the deformation at the open end of the vee heat (at the center of the plate) is given and assumed value of x_v. If the rotation of the entire plate were governed by this value, and assuming a linear strain distribution throughout the plate, the amount of deformation at the bottom of the plate would be $2x_v$. Since a rectangle rather than a vee extends over the lower portion of the section, this assumption may not be as exact as in the case of a fully extended vee. However, for discussion purposes it will be assumed to be exact.

With the conditions as shown in Figure 26a, the average deformation in the lower half of the plate is 1.5 x_v. If this deformation were to be experienced in the stiffening element of the angle, then the amount of plastic rotation would be 1.5 times the plastic rotation of a 4-inch plate heated with the same vee. The fold in the plate element results in a magnified

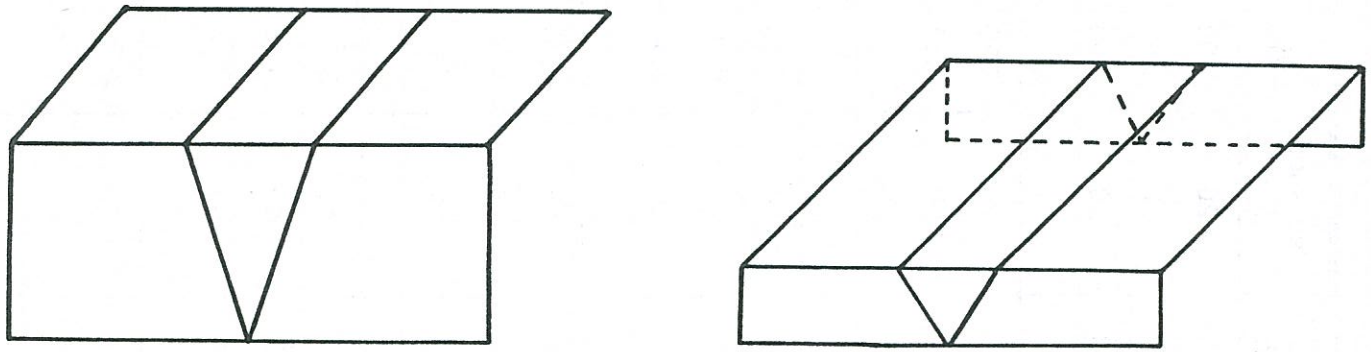

Figure 25. Heating patterns (Category S for equal leg angle and Category W for channel) with stiffening element at open end of vee.

Table 20. Plastic rotations for L4x4x1/4 angles.

Specimen	Heat No.	Vee Angle (deg)	M/M_p	Plastic Rotation (millirad)
VI-1	1	20	0.00	1.74
	2	20	0.00	1.50
	3	20	0.00	0.98
				Avg 1.41
VI-2	1	20	0.25	6.21
	2	20	0.25	4.87
	3	20	0.25	5.82
				Avg 5.63
VI-3	1	20	0.50	11.03
	2	20	0.50	8.92
	3	20	0.50	13.36
				Avg 11.10
VI-4	1	45	0.00	3.08
	2	45	0.00	3.58
	3	45	0.00	2.38
				Avg 3.16
VI-5	1	45	0.25	7.88
	2	45	0.25	11.28
	3	45	0.25	8.93
				Avg 9.36
VI-6	1	45	0.50	15.71
	2	45	0.50	15.96
	3	45	0.50	16.20
				Avg 15.96

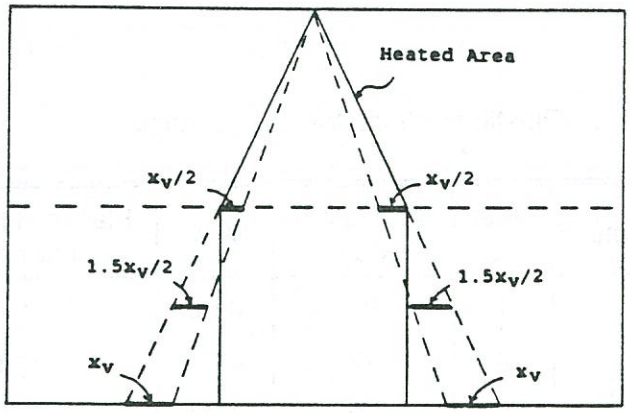

(a) equal leg angle

d_s is the distance from the "apex" end of the vee heated leg to the stiffening element, and is not dependent on vee depth. The value of d_s varies from zero to w, depending on vee orientation ($d_s \cong w$ in this figure).

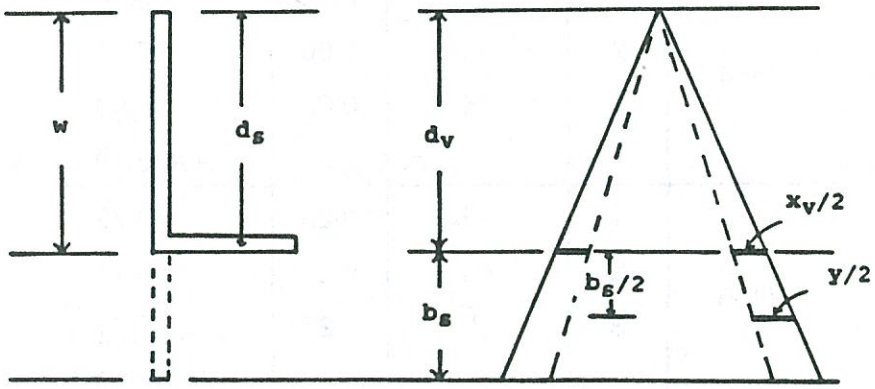

(b) general angle

Figure 26. "Unfolded" angle with vee and rectangular heating patterns shown.

Table 21. Plastic rotations for C6x8.2 angles.

Specimen	Heat No.	Vee Angle (deg)	M/M_p	Plastic Rotation (millirad)
VIII-1	1	20	0.00	2.40
	2	20	0.00	5.89
	3	20	0.00	2.52
				Avg 3.60
VIII-2	1	20	0.25	9.32
	2	20	0.25	7.92
	3	20	0.25	6.30
				Avg 7.85
VIII-3	1	20	0.50	14.63
	2	20	0.50	9.14
	3	20	0.50	10.98
				Avg 11.58
VIII-4	1	45	0.00	3.82
	2	45	0.00	7.13
	3	45	0.00	4.63
				Avg 5.19
VIII-5	1	45	0.25	9.79
	2	45	0.25	6.15
	3	45	0.25	6.24
				Avg 7.39
VIII-6	1	45	0.50	17.99
	2	45	0.50	15.75
	3	45	0.50	9.55
				Avg 14.43

plastic rotation. It should also be noted that the varying strains experienced at different points in the stiffening element will produce some out-of-plane distortion (discussed in detail below).

The channel can also be "unfolded" to establish a relationship between its plastic rotations and those of a plate. Figure 27 shows the channel (C6x8.2) in its unfolded position with the heating pattern used. As shown, the channel can be considered as two angles with the vees being heated simultaneously.

Consider one half of the channel. The vee depth is 1.92 inches. A comparison can be made to a vee-heated 1.92-inch plate, where the assumed deformation is again designated a value, x_v, at the open end of the vee. If this deformation governed the relative movement with a linear strain distribution throughout the half of the web considered (to the original web centerline), then the deformation at the centerline of the web would be equal to 2.56 x_v, with the average deformation for the half of the web being 1.78 x_v. With the same considerations for the other half of the channel (because of the other vee heat), the average deformation in the entire web would also be 1.78 x_v. Thus, to an even greater degree than the case of the angle, plastic rotations will be magnified over those of plates by the channel's folded geometry. For both the angle and channel, the experimental data will be used to determine the degree of this magnification.

Load Ratio and Stress Considerations

If a load ratio is applied during the heating process, one must consider that the stress distribution throughout the vee heat differs in an angle than it does for a plate. Figure 28 shows the cross-section of an angle, along with its major, minor, and principal axes. Since the cross-section is not symmetrical, a vertical load will produce vertical bending only if some type of lateral restraint is used. With the neutral axis being located relatively close to the stiffening element, the case of vertical bending results in a greater percentage of a given vee heat in compression than for plates.

If no lateral restraint is provided, a vertical load will not produce just vertical bending. The simple bending formula, My/I, cannot be used to calculate stresses in the vee heated area resulting from the load. Instead, the unsymmetrical bending formula must be utilized. The stresses at Point B (Figure 28) are shown in Table 22, for load ratios of 0.25 and 0.50. When considering no lateral restraint, as opposed to using My/I, the stresses are quite large.

The stress present in the channel is simply calculated by My/I due to its symmetrical shape (when considering weak axis bending). Because of the short distance from the neutral

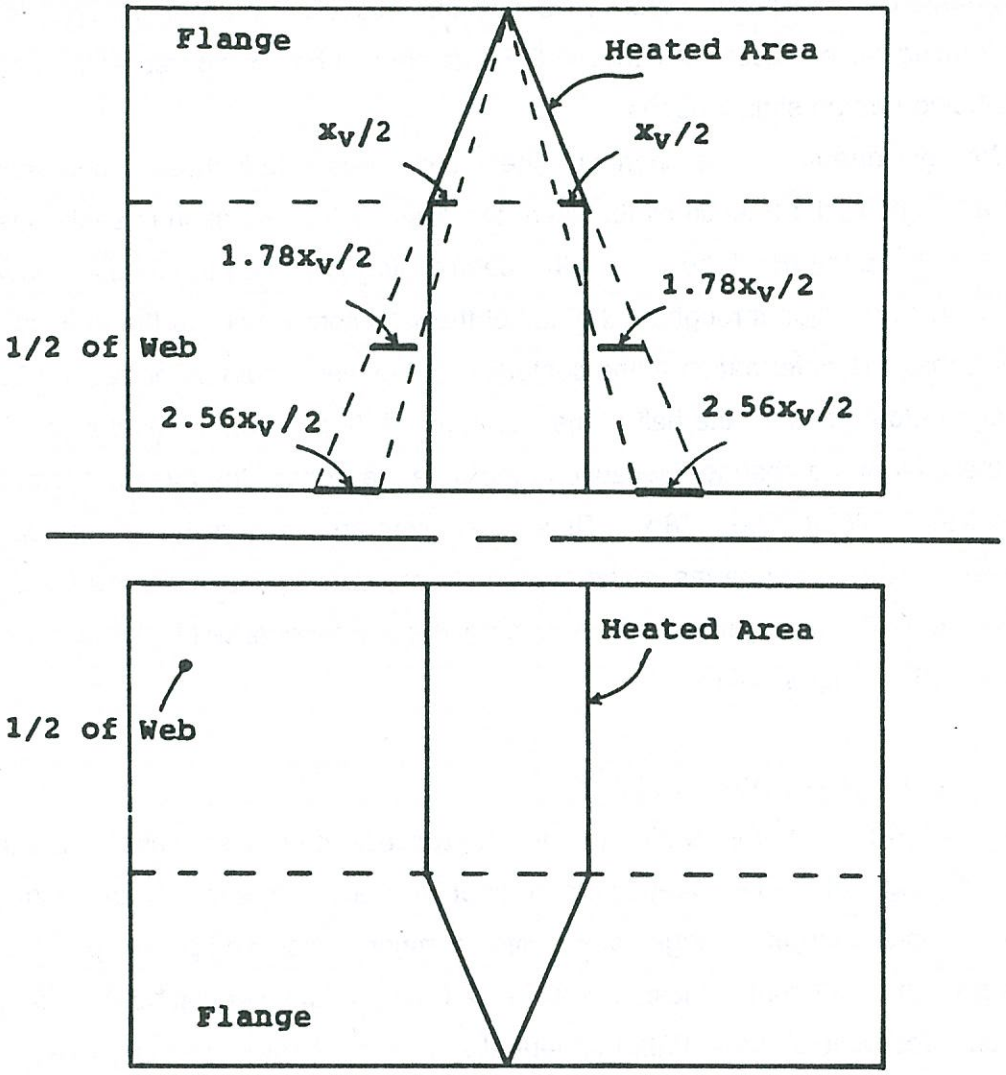

Figure 27. "Unfolded" channel with vee and rectangular heating patterns shown.

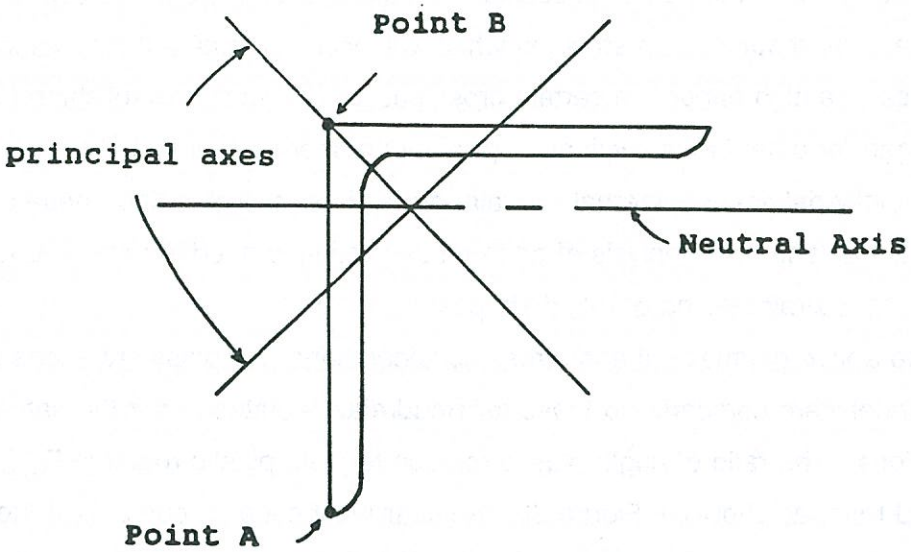

Figure 28. Cross-section of a typical angle.

Table 22. Stresses at Point B (at open end of vee) of an L4x4x1/4 angle.

M/M_p*	Stress (ksi)	
	With Lateral Restraint	Without Lateral Restraint
0.25	6.10	14.36
0.50	12.19	28.71

*Note: Boudreaux calculated load ratio based on the use of lateral restraint, but did not use lateral restraint in the actual experiments

axis to the stiffening element (see Figure 29), the value for y (and thus stress) at any point in the stiffening element is small (only 13.18 ksi for $M/M_p = 0.50$).

It is apparent from the above discussion that load ratio (expressed as M/M_p) in itself does not indicate the magnitude of stresses which will occur for different cross-sections. In fact, stresses can be high enough in certain cross-sections to justify establishing lower limits on load ratio than for other cross-sections to prevent hot mechanical straightening. Since the stress level partially defines the internal restraint during heat straightening, these stresses will affect the plastic rotation. An analysis of each cross-section is needed to decide load ratios to be used in the heat straightening of rolled shapes.

With the above geometrical and stress considerations, the plastic rotations for each angle and channel were compared to those for Boudreaux's plates under the same respective heating conditions. The ratio of angle plastic rotation to plate plastic rotation, $R_{a/p}$, was plotted vs. load ratio, as shown in Figure 30. A linear least squares curve fit of the data reveals that $R_{a/p}$ was close to the estimated value of 1.5 at zero load ratio, and that an increase in load ratio caused a significant increase in $R_{a/p}$. This data reinforces the hypothesis of dual effects of the geometric and stress considerations.

A similar plot is shown (Figure 31) for the ratio of channel plastic rotation to plate plastic rotation, $R_{c/p}$. Here again the value of $R_{c/p}$ at zero load ratio seemed to correspond with the geometrical considerations. As expected, because stresses are relatively low in the channel, when compared to the stresses in a plate under the same conditions, an increase in load ratio did not result in a significant increase in $R_{c/p}$. Again, the above hypothesis is verified.

The geometric magnification associated with angles or channels can be rationally derived with the following assumptions based on geometric considerations: (1) The folded plate can be unfolded and considered as a deeper plate with the longitudinal strain constant with respect to depth; (2) the plastic rotation is magnified by the average displacement of the stiffening element in the unfolded position acting over the vee depth in the folded position; and (3) the plastic rotations are small, i.e., $\tan \phi = \phi$. Referring to the angle represented by Figure 27b, these assumptions imply that the plastic rotation of the angle, ϕ_a, is

$$\phi_a = \frac{y}{d_v}$$

with the y value obtained from the linear geometry in Figure 28b to be

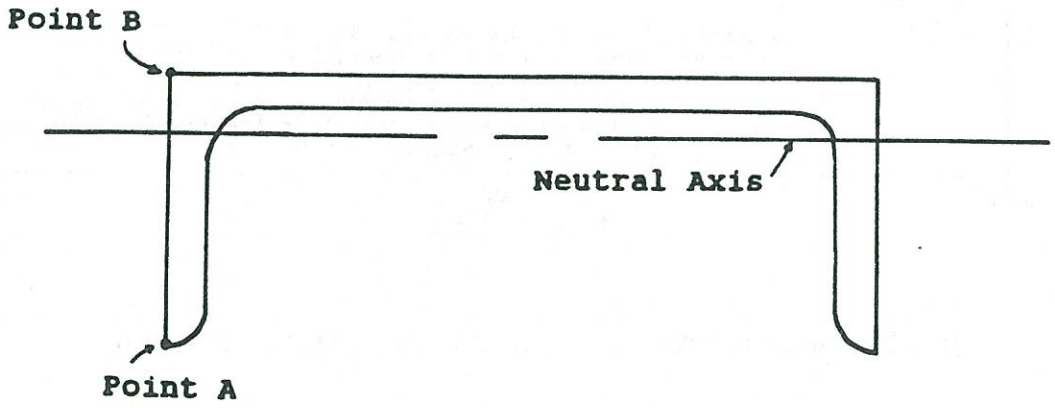

Figure 29. Cross-section of a typical channel.

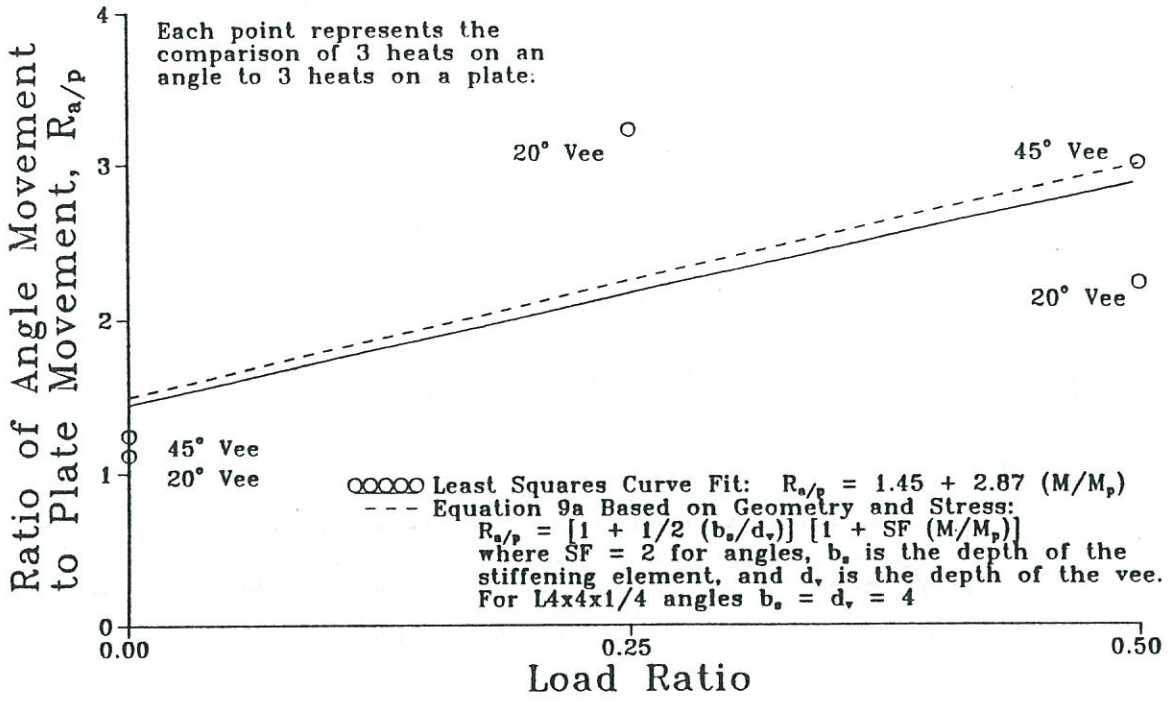

Figure 30. Angle-to-plate movement ratio (R_a/p) versus load ratio.

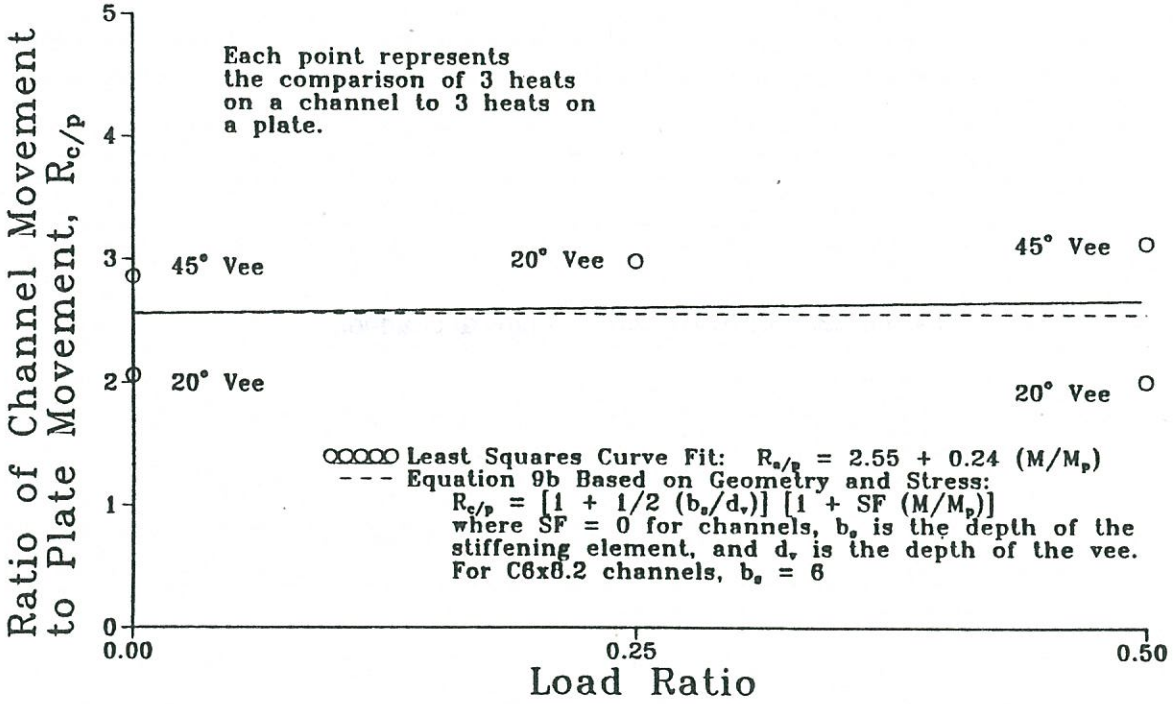

Figure 31. Channel-to-plate movement ratio (R_c/p) versus load ratio.

$$y = \frac{\frac{(d_v + b_s)}{2} x_v}{d_v}$$

The plastic rotation of the equivalent unfolded plate, ϕ_p, is

$$\phi_p = \frac{x_v}{d_v}$$

Thus, the ratio of the plastic rotation of the angle to that of the equivalent unfolded plate is

$$R_{a/p} = \frac{\phi_a}{\phi_p} = \frac{y}{x_v}$$

or

$$R_{a/p} = 1 + \frac{1}{2} \frac{b_s}{d_v} \tag{9}$$

where d_v = the depth of the vee, and b_s = the width of the stiffening element.

The data for the channel closely matched Equation 9. The use of geometric assumption (2) above would not predict this fact, because the web (and thus b_s) was divided by two. Therefore, it is assumed that the plastic rotations in channels are governed by the displacement at the center of the web, as opposed to a quarter point, as would be the case if using assumption (2) for one half of the channel being considered as an angle. The greater magnification is likely a result of contributions from both vees being heated at the flanges. Thus,

$$y = \frac{(d_v + b'_s) x_v}{d_v}$$

where $b'_s = b_s/2$, leading again to Equation 9 for use in channels (b_s is the total width of the stiffening element or web).

The stress amplification of plastic rotation to the unsymmetrical shape of the angle can be rationally derived on the basis of the following assumptions: (1) The variation of $R_{a/p}$ is linear with respect to the load ratio, and (2) a load ratio of 50% increases $R_{a/p}$ by a stress

factor, $S_f = 2$. These assumptions are based on the results of the least squares curve fit of the available data for angles (Figure 30). Using these assumptions, Equation 9 is further modified as

$$R_{a/p} = [1 + \frac{1}{2}\frac{b_s}{d_v}][1 + S_f \frac{M}{M_p}] \quad (9a)$$

where $S_f = 2$.

For a channel, which is a symmetrical section when considering Category W heating patterns, the data indicates a negligible effect of the stress factor. Thus, for channels

$$R_{c/p} = [1 + \frac{1}{2}\frac{b_s}{d_v}][1 + S_f \frac{M}{M_p}] \quad (9b)$$

where $S_f = 0$.

The plastic rotation equations for angles and channels are simply modified versions of the plate equation by factors of $R_{a/p}$ and $R_{c/p}$, respectively:

$$\phi_a = \phi_p [1 + \frac{1}{2}\frac{d_s}{d_v}][1 + 2 \frac{M}{M_p}] \quad (10a)$$

$$\phi_c = \phi_p [1 + \frac{1}{2}\frac{d_s}{d_v}] \quad (10b)$$

where ϕ_c is the plastic rotation of a channel. It should be noted that the equations above are based on a relatively small amount of data, and more research is needed to verify this model for angles and channels of various sizes. However, these equations do agree well with the available data, as seen in Figures 30 and 31. The angle formula should be applicable for either Category S or W damage, while the channel formula applies for only Category W. The formula developed for Category S wide flange beams in the following sections can also be used for Category S channels.

Out-of-Plane Movement

In order for the geometric considerations illustrated above to be valid, an out-of-plane movement (in the direction perpendicular to the desired direction of movement) would

obviously have to occur. With the linear continuous strain concept, even though the stiffening element is heated with a rectangle, its strain behavior resembles that of a vee heat and thus the stiffening element would shorten more on one edge (opposite the vee in the case of the angle) than the other. According to the theory, the out-of-plane movements should be fairly large (especially when using a load ratio, in which case, the entire rectangular heat is in compression).

In the angles listed above, the average out-of-plane plastic rotations were computed and compared to the plastic rotations in the desired direction. These values and comparisons are shown in Table 23.

As can be seen from Table 23, the out-of-plane movements are quite large in all cases, and they increase significantly with load ratio (note the very large value for VI-6). However, when compared to the plastic rotations in the desired direction, the zero load ratio cases exhibited more relative movement. In fact, the out-of-plane movements were greater than the in-plane ones. The large out-of-plane movements are more than likely larger than the desired movement because the vee heated leg of the angle has already been heated, offering less resistance to rotation. The lower out-of-plane to in-plane movement ratios encountered at larger load ratios are probably due to restraint caused by the larger forces.

Depending on whether or not the out-of-plane movements are beneficial to the overall repair of the given specimen, alternative heating patterns may be necessary to prevent them. The vee heat would be applied as normal, and the stiffening element would still need to be heated to allow rotation in the desired direction. However, instead of a rectangular heating pattern, it is likely a reverse vee heat (continuing from the open end of the original vee, and tapering down to a point) would allow desired rotation, while reducing the out-of-plane movement. In its "unfolded" position, the heating pattern would resemble a diamond shape, a pattern used by pipe welders to straighten pipe distortions. Heating in the proper fashion is essential for obtaining movement.

Damaged Specimens

A number of channels and angles were damaged and straightened in the current study, as indicated in Table 24. The average plastic rotations are shown for each different combination of heating parameters used (different combinations were used on some specimens). All of the damaged specimens had the vee apex applied at the stiffening element (Figure 32).

Table 23. Comparison of out-of-plane plastic rotations to plastic rotations in the in-plane direction of movement.

Specimen	Out-of-Plane Plastic Rotations (millirad)	Ratio of Out-of-Plane to In-Plane Movement
VI-1	2.93	2.07
VI-2	4.03	0.72
VI-3	6.59	0.59
VI-4	4.55	1.44
VI-5	7.85	0.84
VI-6	10.76	0.67

Table 24. Damaged angle and channel specimens.

Specimen/ Category	M/M_p	Depth Ratio	No. of Heats	Avg. PR (milliradians)
L6x4x5/16 (S)*	0.22	1.00	3	4.66
L6x4x5/16 (S)	0.50	1.00	16	9.10
L6x4x5/16 (W)	0.50	1.00	3	11.11
L4x4x1/4	0.33	0.75	2	5.57
L4x4x1/4	0.33	1.00	5	6.75
C6x8.w (W)	0.50	1.00	14	5.78

*S means strong-axis bending, W means weak-axis bending. Note: All vee heats were 45°, and all had the stiffening element at the vee apex

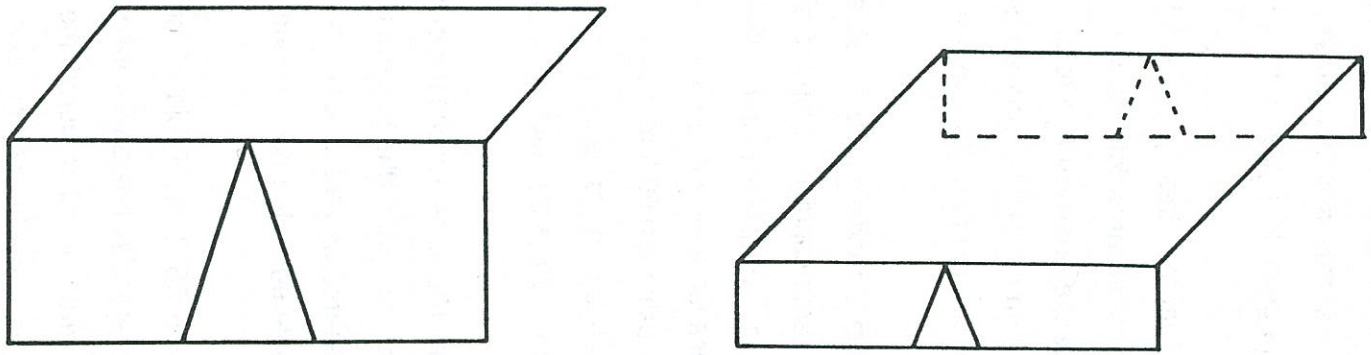

Figure 32. Heating patterns for angles and channels stiffening element vee apex.

A notable fact from Table 24 is that very large plastic rotations occurred for all of the angles (when compared to plates under the same conditions). With the stiffening element at the vee apex (and thus heated only with a line heat), the only explanation deals with stress. Larger stresses (than for plates) occur in the angles. These large stresses are compressive over most of the vee (because the neutral axis is shifted toward the stiffening element). The stresses at the open end of the vee are given in Table 25 for the various cases of angles (point A in Figure 28).

From Table 25, it can be seen that the stresses are significantly higher in the angles than for the plates. It is suggested that load ratios for this type of bending should be kept below 0.33 to prevent yielding (even before heating!) and to prevent buckling at the open end of the vee. The load ratio is still based on the plastic moment considering vertical bending only, i.e., by use of the plastic modulus about the horizontal axis, to be consistent with current practice.

In each case above, the stress in the extreme fiber was about 1.4 times the stress in the extreme fiber of a plate under the same conditions. Due to similar neutral axis positions in each shape, it seems likely that the plastic rotations in each angle should differ from plate plastic rotations by similar factors. Because a very large amount of hot mechanical straightening obviously occurred when using a 0.50 load ratio, it is more practical to compare only the cases of 0.22 and 0.33 load ratios with plates under similar conditions (see Table 26). This will allow a proper modification of the plate equation for angles damaged in this fashion, using reasonable load ratios.

Table 26 indicates that Equation 10a is an excellent indicator of plastic rotations in angles with the stiffening element at the vee apex (the b_s term is considered equal to zero because the stiffening element is not heated as part of an extended vee). It should be noted that the value of 2 for SF applies for both equal leg and unequal leg angles (for the two cases shown).

The plastic rotations for specimen C6x8.2 in Table 24 indicate that Equation 10b closely predicts plastic rotations for Category W heats with the stiffening element at the vee apex (again b_s is considered equal to zero). In other words, the plastic rotations should be equal to those for plates subjected to the same heating conditions. Recall from Table 24, that the average plastic rotation for specimen C6x8.2 was 5.78 milliradians for 14 heats with a 45° vee angle and a 0.5 load ratio. This average value is close to the average plastic rotation of 5.32 milliradians found in plates when using the same heating parameters.

Table 25. Stresses at open end of vee for various cases of heats on angles (stiffening element at vee apex).

Shape/ Category	Load Ratio	Stress (ksi)	Equivalent Plate Stress (ksi)
L6x4x5/16 (S)	0.22	16.08	11.88
	0.50	36.55*	27.00
L6x4x5/16 (W)	0.50	37.90*	27.00
L4x4x1/4	0.33	25.78	17.82

*These values assume yielding does not occur

Table 26. Comparison of actual to theoretical plastic rotations in angles.

Shape	Load Ratio	Actual ϕ_a (millirad)	Theoretical ϕ_p of Plate (millirad)	Eqn. 10a ϕ_a (millirad)	R_a/p**
L6x4x5/16 (S)	0.22	4.66	3.37	4.85	1.38
L4x4x1/4	0.33	6.75*	4.16	6.91	1.62

*These values represent the heats with depth ratio = 1

**Ratio of angle plastic rotation to plate rotation

From the above observations, Equations 10a and 10b predict very well the plastic rotations in angles and Category W channels, regardless of the vee orientation. These equations are based on the influences of both the stiffening element and the stresses present during the heating process. However, these equations should be written in a form which accounts for the location of the stiffening element:

$$\phi_a = \phi_p \left[1 + \frac{1}{2} \frac{d_s}{w} \frac{b_s}{d_v}\right] \left[1 + 2 \frac{M}{M_p}\right] \tag{10c}$$

$$\phi_c = \phi_p \left[1 + \frac{1}{2} \frac{d_s}{w} \frac{b_s}{d_v}\right] \tag{10d}$$

where d_s is the distance from the edge of the vee heated plate element closest to the vee apex (Figure 26b) to the stiffening element, and w is the width of the vee heated element. The term d_s/w is zero when the stiffening element is at the vee apex and one when the stiffening element is at the open end of the vee. The d_s/w term simply indicates of the effect of the stiffening element based on its location.

It is apparent that vee depth is inversely proportional to plastic rotation in Equations 10c and 10d. If these equations were used, then very low depth ratios would indicate very high plastic rotations. This does not occur in actuality. Instead, only full-depth vees were used to formulate Equations 10c and 10d $d_v = w$. Evidence from plate tests indicate that depth ratios between 0.75 and 1.00 will produce similar magnitudes of plastic rotations. Thus, assuming the $d_v = w$, then

$$\phi_a = \phi_p \left[1 + \frac{1}{2} \frac{d_s b_s}{w^2}\right] \left[1 + 2 \frac{M}{M_p}\right] \tag{11a}$$

$$\phi_c = \phi_p \left[1 + \frac{1}{2} \frac{d_s b_s}{w^2}\right] \tag{11b}$$

Equations 11a and 11b are considered valid for depth ratios ranging from 0.75 to 1.00. Figures 33, 34 and 35 show the comparisons of various shapes to their respective plastic rotation equations.

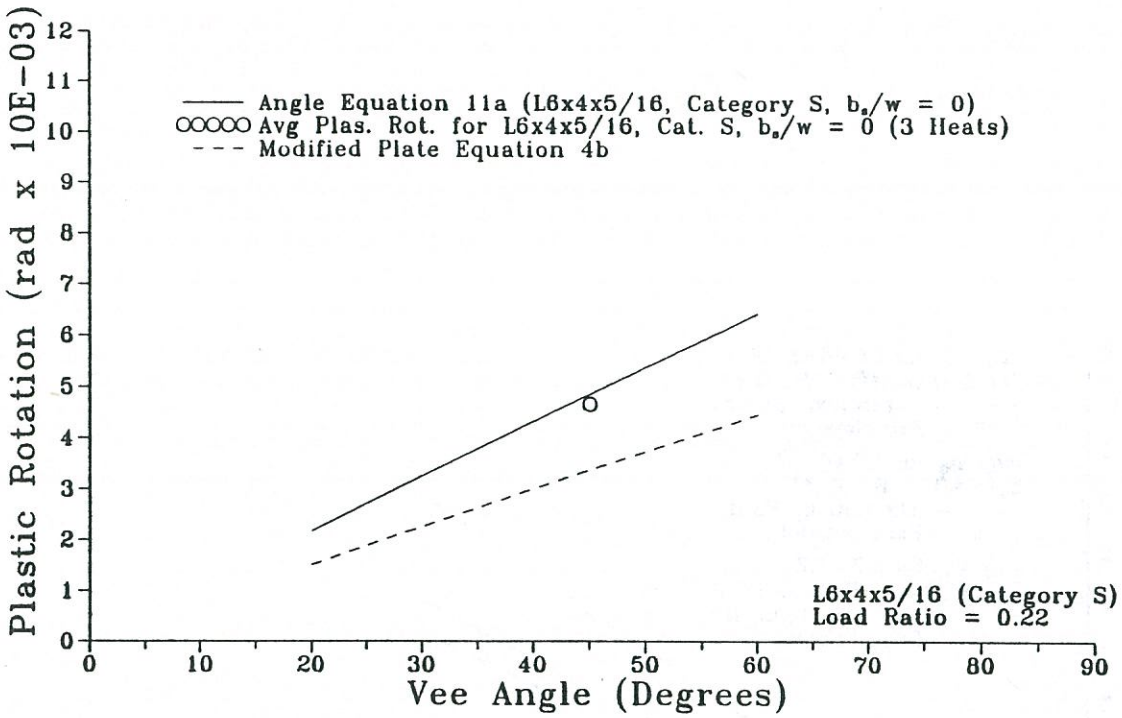

Figure 33. Comparison of plastic rotations in L6x4x5/16 specimen with Equations 11a and 4b.

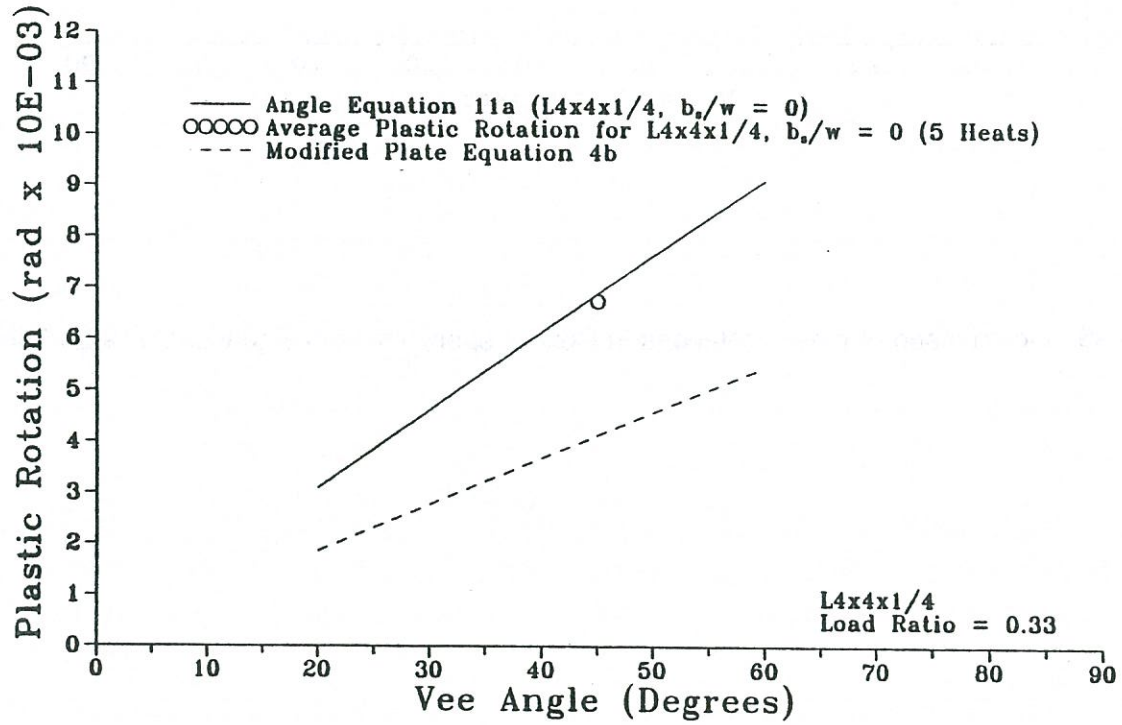

Figure 34. Comparison of plastic rotations in L4x4x1/4 specimen with Equations 11a and 4b.

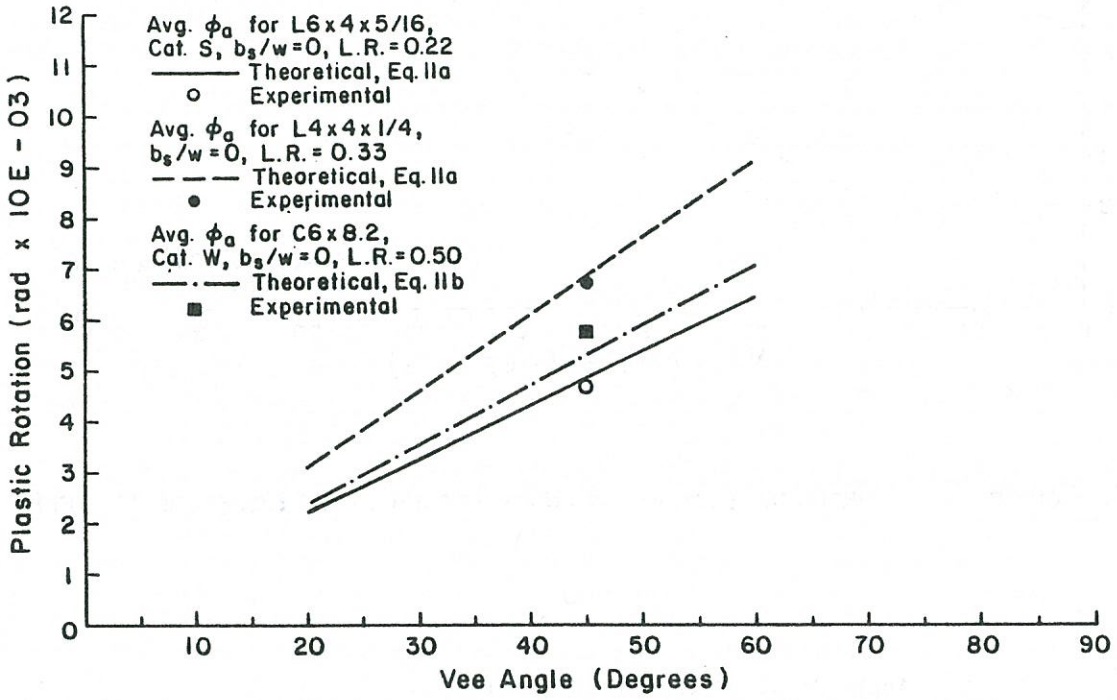

Figure 35. Comparison of plastic rotations in C6x8.2 specimen with Equations 11a and 4b.

Residual Stresses

Residual stress patterns were experimentally determined for some representative samples of angles and channels. The geometry of the shapes prevented measurements with the extensometer on both sides of certain strips. However, the continuity and consistency of the plots indicate that by just measuring one side, sufficient results were obtained. The residual stress values are given in Tables 27 through 29, and shown in Figures 36 through 40). The strip number locations are shown in the figures. These values should be fairly representative of the respective heating configurations on the various shapes.

In the two undamaged angles (VI-1 and VI-4), the residual stress patterns were quite similar (slightly higher compressive stresses were found at the leg ends of specimen VI-4). The only difference in these two specimens is the vee angle used (20° and 45°, respectively). Until further study, it can be assumed that the type of pattern shown for these two specimens (compression on edges and where the two legs meet) is representative of angles.

An interesting fact is that the damaged angle specimen, L4x4x1/4, exhibited the same type of residual stress pattern as the undamaged angles. It should be noted that two different heating patterns were used for the damaged and undamaged specimens. It is apparent that the heating/cooling process in the angles results in quite high (around 40 ksi) compressive stresses near the end of the legs, regardless of the location of the vee apex, relative to the stiffening element. It is suggested that further research be conducted on the subject of residual stress patterns in channels and other sizes of angles subjected to the heat straightening process.

Undamaged Wide Flange Beams

Many steel bridge members do not consist of either a single plate or even channels and angles. More commonly, bridges are constructed using plate girders and wide flange shapes. Often these members are damaged as a result of accidents.

Plastic rotation studies have been conducted in the past (Horton 1973; Avent and Fadous 1988), on a few undeformed wide flange beams. Some material properties resulting from heat curving have been investigated, with theoretical studies used to predict residual stresses (Horton 1973). However, no experimental residual stress measurements were made. In the current study, a number of undeformed wide flange beams were subjected to the heat straightening process in a laboratory environment. Plastic rotations were investigated to add to previous data, and residual stresses were experimentally determined.

Table 27. Residual stresses in undamaged angles.

Specimen	Strip	Residual Stress (ksi) in Vee Heated Leg	Residual Stress (ksi) in Rectangular Heated Leg
VI-1	1	-22.04	-19.69
	2	3.09	-7.40
	3	9.17	6.42
	4	11.46	9.79
	5	10.04	15.37
	6*	7.03	15.73
	7*	-5.29	13.92
	8*	-20.16	-17.40
VI-4	1	-26.10	-27.08
	2	-10.19	-2.76
	3	3.87	6.16
	4	15.48	0.33
	5	21.90	9.54
	6*	8.48	12.91
	7*	5.44	12.04
	8*	-43.07	-31.83

*Only one side measured

Table 28. Residual stresses in undamaged channel (IX-6).

Strip No.	Stress (ksi) in Top Flange	Stress (ksi) in Web	Stress (ksi) in Bottom Flange
1*	-24.43	-30.67	2.54
2*	-9.79	0.36	4.06
3*	15.59	2.32	-2.83
4	5.37	9.65	-12.51
5	---	13.85	---
6	---	17.98	---
7	---	17.37	---
8	---	17.44	---
9*	---	12.69	---
10*	---	11.67	---
11*	---	-34.80	---

*Only one side measured

Table 29. Residual stresses in damaged angles.

Specimen/Strip		Residual Stress (ksi) in Vee Heated Leg**	Residual Stress (ksi) in Rectangular Heated Leg
L4x4x1/4	1*	-47.49	-53.65
	2*	17.91	-9.57
	3*	33.57	2.10
	4	34.06	16.32
	5	27.55	21.90
	6	19.87	22.84
	7	-10.30	-9.72
	8	-35.74	-22.70
L6x4x5/16	1*	12.25	----
	2*	-4.71	-2.61
	3*	14.65	12.33
	4	27.55	14.36
	5	43.86	21.57
	6	31.50	26.90
	7	29.69	43.21
	8	18.27	31.54
	9	10.19	----
	10	-7.87	----
	11	-25.34	----
	12	-35.38	----

*Only one side measured

**Some vee heats were also applied to both legs due to some bending occurring in horizontal direction (from vertical loading) during damage

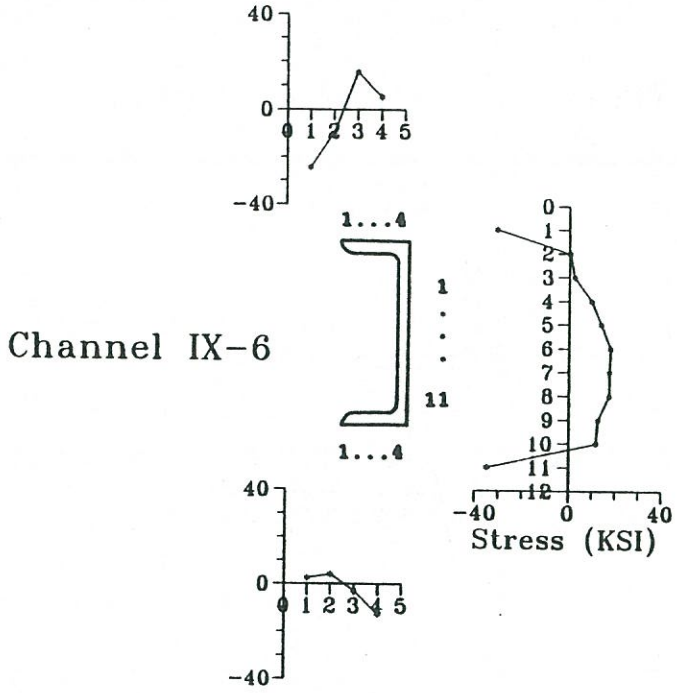

Figure 36. Stresses in channel IX-6 (45° vee, M/M_p = 0.50, depth ratio = 1.00).

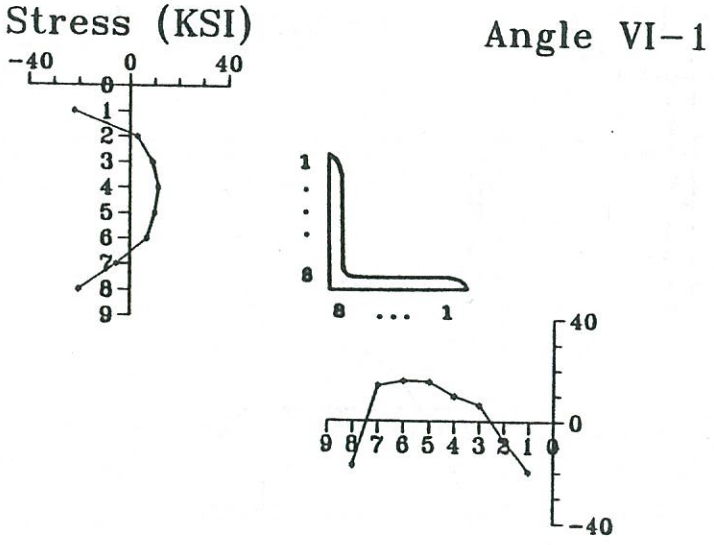

Figure 37. Stresses in angle VI-1 (20° vee, M/M_p = 0.00, depth ratio = 1.00).

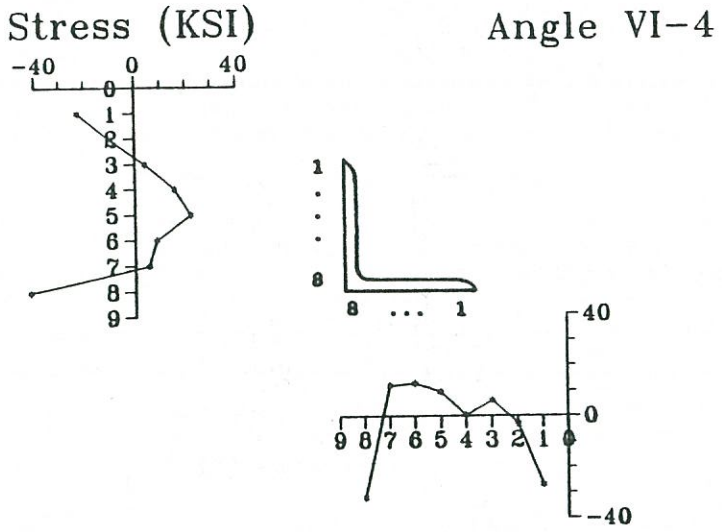

Figure 38. Stresses in angle VI-4 (45° vee, M/M_p = 0.00, depth ratio = 1.00).

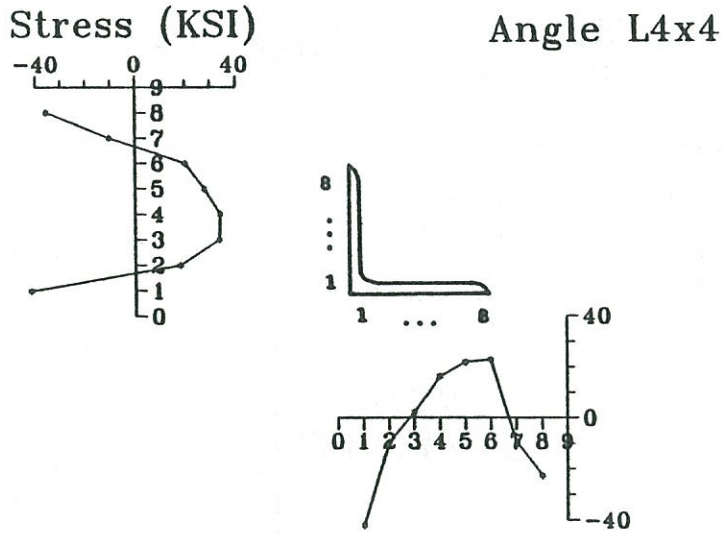

Figure 39. Stresses in angle L4x4 (45° vee, M/M_p = 0.50, depth ratio = 1.00).

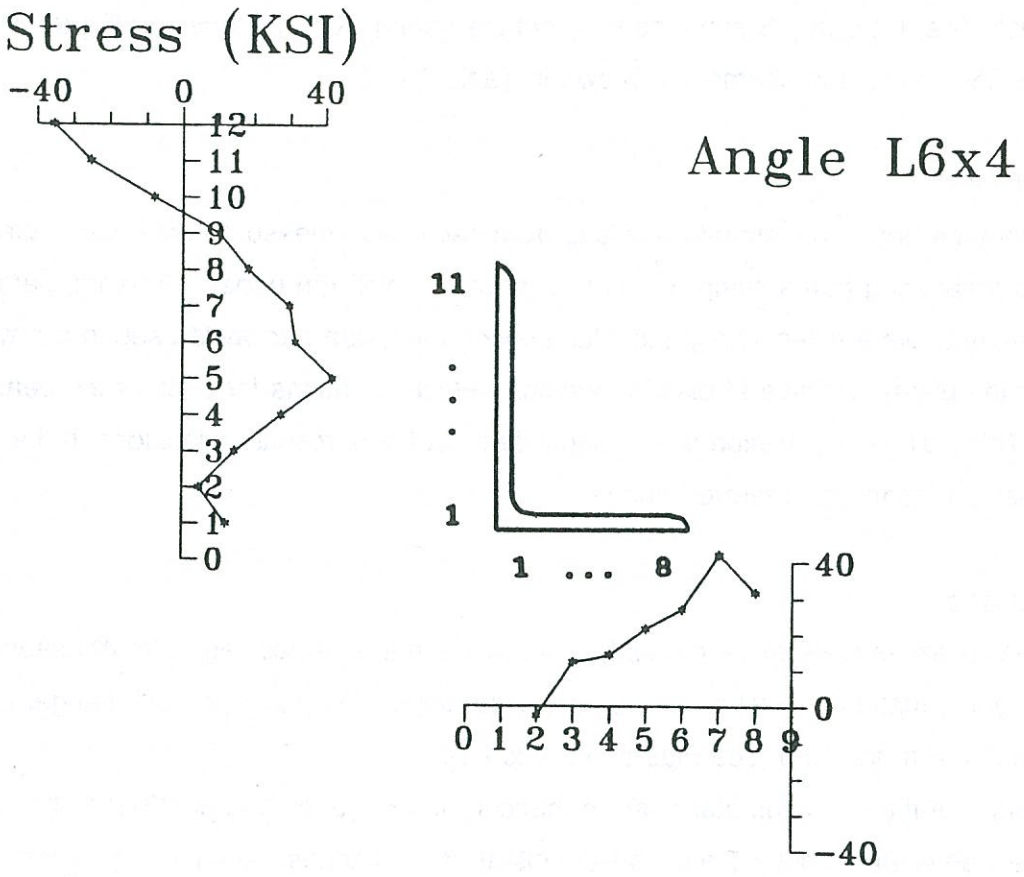

Figure 40. Stresses in angle L6x4 (45° vee, M/M_p = 0.33, depth ratio = 1.00).

Test Setup

The studies were similar to those of the undeformed plates; in this case, using 5-foot long specimens of W6x9 rolled shapes (A36 steel), the beams were bolted to a stationary frame in cantilever fashion, and loads and heat were applied accordingly. Each initially straight beam was subjected to four heating/cooling cycles to produce Category W movement (about the weak axis) Category S movement (about the strong axis) as shown in Figure 41. The heating conditions for the beams are shown in Table 30.

Plastic Rotations

To determine beam movements resulting from each heat, measurements were taken using a sliding measuring frame along a set of guide rails, which ran under the beam, parallel to it. Measurements were taken at eight locations along the beam and were used in a similar manner as for the plates to arrive at plastic rotations. Plastic rotations for each of the beams are shown in Table 31. A discussion of the significance of these results is included in the section on plastic rotations in deformed beams.

Residual Stresses

Residual stresses were experimentally determined in the heated region of the beams using the sectioning method. In all of the beams, eight strips were cut from each flange, and six strips were cut from the web (see Figures 42 and 43).

The shape of the extensometer used to measure the gage lengths prohibited obtaining stresses in the web within about 1.5 inches from either of the flanges, thus limiting stress readings to six strips. Also, for the same reason, only in strips 1 and 8 in the flanges were both sides of the strip measured. Although only one side was measured for strips 2 through 7, the results from strips 1 and 8 have shown that one side of the strip can be used to estimate the residual stress fairly well.

An unheated specimen (Beam UH) was tested for residual stresses (Table 32 and Figure 44), to compare with the heated specimens. These stresses matched very closely with a plot of the residual stresses in a roller straightened W6x20 shape shown in the Structural Stability Research Council Guide to Stability Design Criteria for Metal Structures (1976). Roller straightening (or rotorizing) is a common mill practice for straightening small wide flange shapes to meet sweep and camber tolerances. The process redistributes and greatly reduces the initial residual stresses in the flanges (a characteristic evident in Beam UH, where these stresses are quite low) (SSRC 1976).

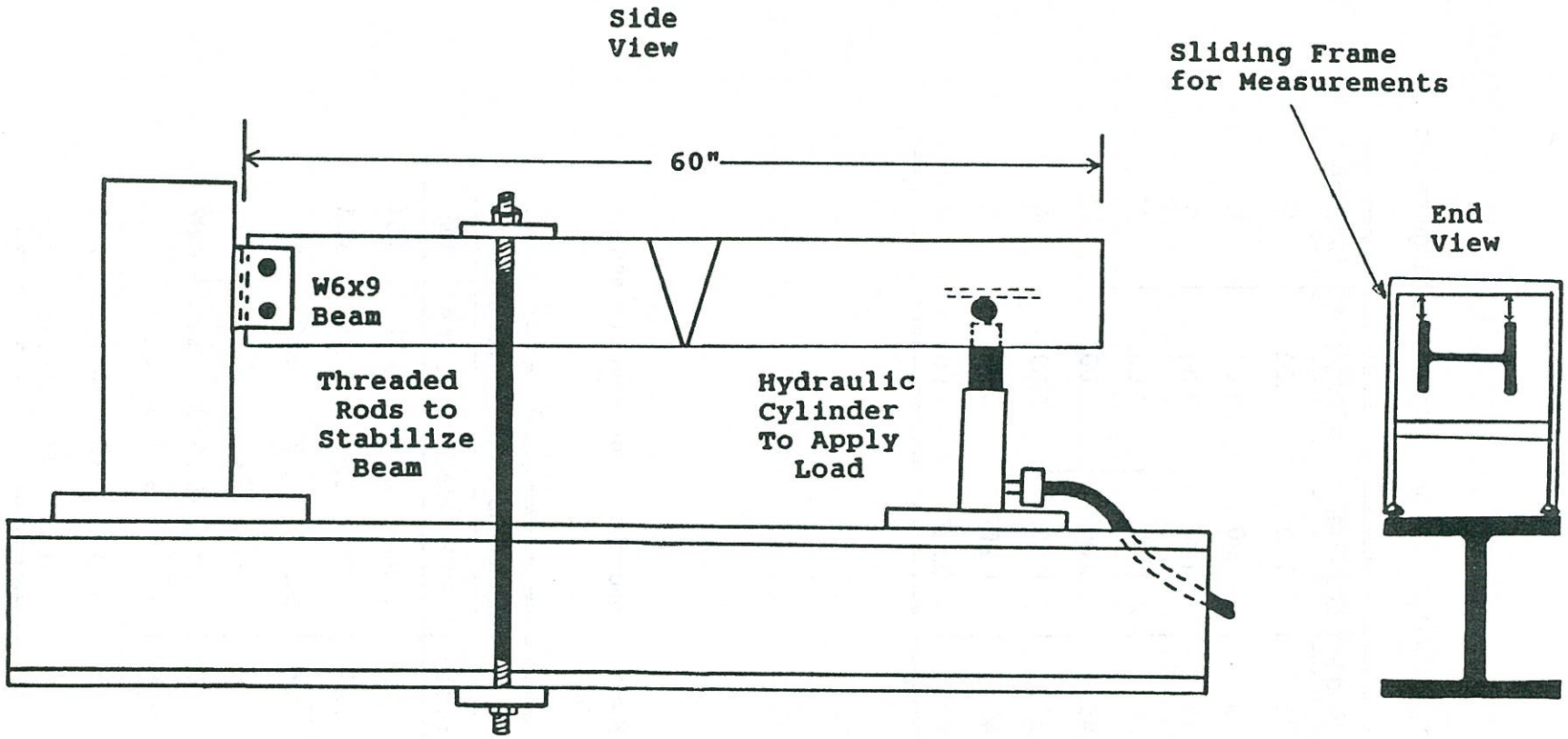

Figure 41. Beam heating set-up

Table 30. Heating conditions for undamaged wide flange beams.

Beam	Vee Angle	Load Ratio	Depth Ratio	Category
I-1	20	0.00	1.00	S
I-2	45	0.00	1.00	S
I-4	30	0.00	1.00	S
II-1	20	0.00	1.00	W
II-3	45	0.00	1.00	W
III-2	20	0.50	1.00	W
IV-5	45	0.25	1.00	S
IV-6	45	0.50	1.00	S

Table 31. Plastic rotations in undamaged wide flange beams.

Beam	Plastic Rotation (milliradians)				
	Heat 1	Heat 2	Heat 3	Heat 4	Avg.
I-1	2.25	3.58	2.85	3.48	3.04
I-2	3.77	6.43	5.51	5.70	5.35
I-4	3.94	2.54	4.96	5.33	4.19
II-1	1.87	1.62	0.21	1.06	1.19
II-3	2.90	2.69	0.70	-3.00	0.82
III-2	7.57	6.77	6.93	5.28	6.64
IV-6	8.94	6.40	6.50	No heat	7.31
IV-6	6.83	7.00	7.67	No heat	7.17

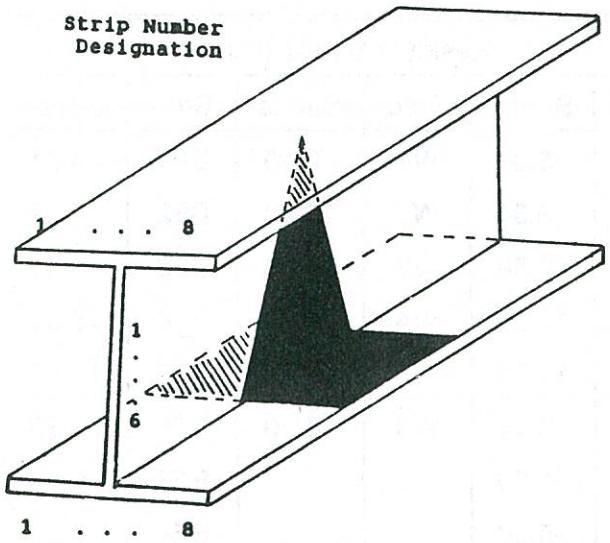

Figure 42. Residual stress strip locations (Category S heat).

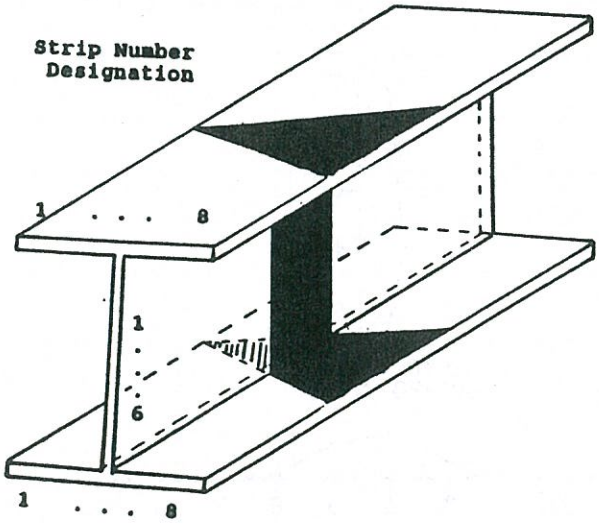

Figure 43. Residual stress strip locations (Category W heat).

Table 32. Experimentally determined residual stresses in an unheated W6x9 specimen (Beam UH).

Residual Stress (ksi)					
Strip	Stress	Strip	Stress	Strip	Stress
TF1	5.08	W1	-9.46	BF1	-4.61
TF2	-3.34	W2	-12.22	BF2	-6.09
TF3	0.58	W3	-13.60	BF3	6.31
TF4	10.51	W4	-14.97	BF4	15.30
TF5	11.23	W5	-11.64	BF5	11.75
TF6	3.12	W6	-4.20	BF6	1.23
TF7	-1.60			BF7	-0.44
TF8	-5.08			BF8	0.61

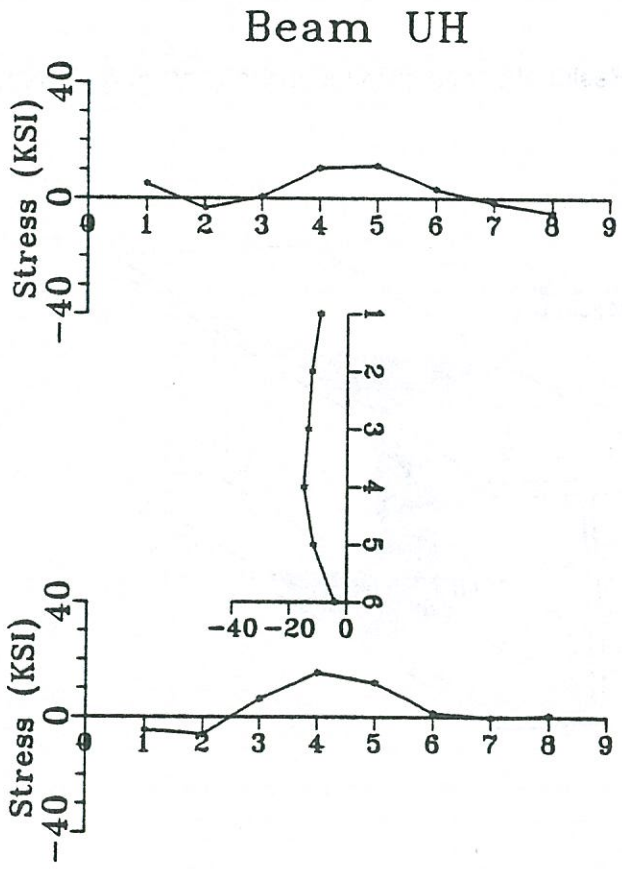

Figure 44. Residual stresses in unheated wide flange beam "UH".

Values for the Category W, small vee angle Category S, and large vee angle Category S specimens are shown in Tables 33 through 35. Average residual stress distributions for the three categories are shown in Figure 45. Individual residual stress distributions for each beam are shown in Appendix E. From the residual stress patterns in the heated undamaged beams, the following observations are made:

1. The patterns were significantly different in the Category S and Category W specimens.

2. Load ratio and depth ratio were again found to not significantly change the stress patterns, when all other parameters were held constant.

3. By classifying the 20- and 30-degree vee angles as small and 45-degree vee angles as large, there were significant pattern differences in the two classifications in the Category S specimens (no significant difference in Category W specimens).

4. The residual stresses are greatly increased when vee heats are applied to undamaged beams. With most (or all) of both flanges experiencing compressive stresses (in sweep and camber heats), column strength would be affected.

Damaged Wide Flange Beams

With the exception of a few recent specimens (Avent and Fadous 1988), information regarding the heat straightening of damaged wide flange beams has been previously unavailable. For this reason, a number of experiments were designed to: (1) study the total heat straightening process of a damaged member and, (2) answer questions concerning the feasibility and effects of repeatedly damaging/repairing a given member. This second point stemmed from the fact that once a member encounters damage and is heat straightened, the possibility exists that the same member will undergo damage again during its lifetime.

The primary focus of this research was to determine the variation in material properties of steel subjected to the repetitive damage/straightening process, as well as to find the change in residual stresses in the member. Heating parameters were the same for all specimens. Practical information is also provided herein concerning plastic rotations in the context of an entire repair process, which consists of many heats. Two types of beams were studied, weak axis bending (Category W) and strong axis bending (Category S). Weak axis damage is more conducive to pure heat straightening research, because local buckling (which requires hot mechanical straightening) can easily be prevented. Also, weak axis damage is similar to the type of damage often encountered in bridge girders from over-height vehicles (usually only one flange is damaged).

Table 33. Experimentally determined residual stresses in undamaged, Category W wide flange beams.

Strip	Residual Stress (ksi) in Beam #:			Avg.
	II-1	II-3	III-2	
TF1	-14.86	-14.39	-16.68	-15.31
TF2	-8.99	-8.12	-11.09	-9.40
TF3	-4.50	-12.62	-8.99	-8.70
TF4	-11.96	-21.90	-10.37	-14.74
TF5	-16.82	-21.46	-14.07	-17.45
TF6	-12.69	-15.66	-7.18	-11.84
TF7	-9.72	-9.57	-7.25	-8.85
TF8	-14.03	-16.25	-17.01	-15.76
W1	13.27	21.55	30.42	21.75
W2	14.07	22.51	30.38	22.32
W3	15.08	23.39	29.33	2.60
W4	17.01	24.25	28.64	23.30
W5	18.38	23.96	22.77	21.70
W6	20.12	23.06	18.63	20.60
BF1	-22.27	-24.76	-13.99	-20.34
BF2	-6.16	-14.43	-11.89	-10.83
BF3	-5.00	-18.34	-8.70	-10.68
BF4	-7.83	-10.37	-16.82	-11.67
BF5	-9.57	-16.24	-15.73	-13.85
BF6	-11.38	-13.05	-7.61	-10.68
BF7	-16.02	-16.24	-3.34	-11.87
BF8	-19.83	-24.18	-14.14	-19.38

Table 34. Experimentally determined residual stresses in undamaged, Category S wide flange beams ("large" vee angles).*

Strip	Residual Stress (ksi) in Beam #:			Avg.
	I-2	IV-5	IV-6	
TF1	-23.13	-23.97	-16.32	-21.14
TF2	-0.65	-1.60	-4.71	-2.32
TF3	0.94	2.54	3.05	2.18
TF4	2.76	5.08	4.06	3.97
TF5	1.23	0.94	3.63	1.93
TF6	-2.76	6.89	-0.58	1.18
TF7	-3.99	5.15	3.26	1.47
TF8	-16.32	-17.59	-5.99	-13.30
W1	28.53	34.77	16.32	26.54
W2	23.35	33.64	13.60	23.53
W3	25.16	29.62	12.15	22.31
W4	27.55	29.62	12.15	20.58
W5	23.17	18.09	-0.76	13.50
W6	20.88	6.46	-12.47	4.96
BF1	-44.01	-42.02	-22.55	-36.19
BF2	-44.15	-25.23	0.07	-23.10
BF3	-31.25	6.09	7.32	-5.95
BF4	-25.67	12.91	-2.83	-5.20
BF5	-8.05	16.39	3.19	3.84
BF6	-13.92	12.18	5.73	1.33
BF7	-24.29	7.47	05.95	-7.59
BF8	-38.57	-41.62	-39.12	-39.77

*45° vees

Table 35. Experimentally determined residual stresses in undamaged, Category S wide flange beams ("small" vee angles).*

Strip	Residual Stress (ksi) in Beam #:		Avg.
	I-1	I-4	
TF1	--24.15	-22.59	-23.37
TF2	-22.62	-12.04	-17.33
TF3	-28.93	-8.56	-18.75
TF4	-18.85	-7.83	-13.34
TF5	-22.40	-12.47	-17.44
TF6	-21.17	-12.91	-17.04
TF7	-19.00	-11.46	-15.03
TF8	-19.87	-11.96	-15.91
W1	33.82	43.11	38.47
W2	34.66	41.84	38.25
W3	33.53	38.39	35.96
W4	34.73	29.97	32.35
W5	28.53	24.69	26.61
W6	19.91	11.20	15.56
BF1	-36.11	-30.31	-33.21
BF2	-12.11	-3.91	-8.01
BF3	-9.57	-3.92	-6.75
BF4	-1.09	-4.57	-2.83
BF5	-6.16	-6.16	-6.16
BF6	-9.64	-5.08	-7.36
BF7	-14.07	-16.17	-15.12
BF8	-34.44	-33.07	-33.76

*Small angles = 20 and 30 degrees

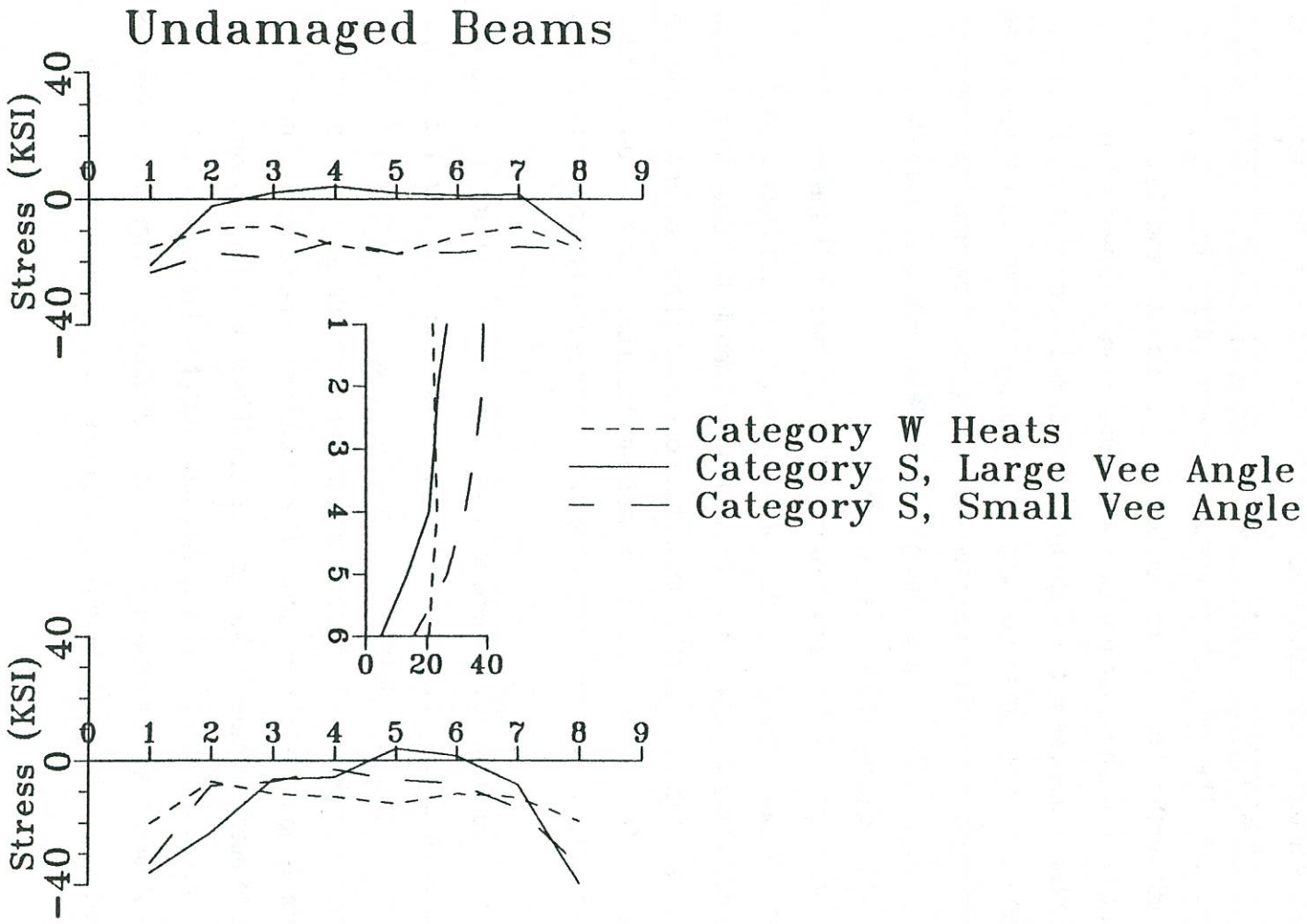

Figure 45. Average residual stresses in undamaged wide flange beams after Category W (sweep) and Category B (camber) heats.

Weak Axis Damage

Four beams (W6x9's) were used in the study. Each beam was damaged about its weak axis to an angle of about seven degrees (approximately the same as the least damaged of the deformed plates). Each beam was repaired using a 45 degree vee with a depth ratio of 0.75 and a load ratio of 0.5. The vee angle and depth ratio were initially chosen for two reasons: (1) To investigate the shortening caused by such a depth ratio, and (2) because a 45 degree vee provides maximum movement without creating too large a heating area (a factor significant in causing local flange buckling during the straightening process). Further precautions were taken against buckling by placing one C-clamp around the two flanges at the center of the open end of the vees. This prevented the buckling, but it did not hinder plastic rotation. Without such precautions, flange buckling is inevitable, as was concluded by studying various size members in preliminary experiments.

The number of damage/repair cycles varied for each of the beams (Table 36). Each repair cycle consisted of approximately 20 heats, with the average plastic rotation shown for each repair cycle (individual plastic rotations are presented in Appendix F). Each time a beam was damaged and straightened, a net shortening of about one-tenth of an inch occurred in the heated region (Table 37). These values match very well with the plate shortening equation in Chapter III. It is therefore recommended that Equation 10 be applied to wide flange beams as well as plates.

With the shortening, a thickening developed in the middle region, causing a spreading of the yield zone in each subsequent bend as seen in Figure 46 (values shown in Table 38). The thickening resulted in a smoother distribution of curvature (due to thinner portions further from the centerline tending to yield earlier than before), although the total angle of damage was kept as consistent as possible for each bend. Due to the larger yield zone, the heat locations were added to accommodate the spread. Additional locations used are shown in Figure 47. With the number of heats required to straighten each bend remaining fairly consistent, classification of damage became based on angle of damage rather than curvature, a factor of more importance in the study of damaged plates where damage amounts varied significantly more.

Plastic Rotations

The individual plastic rotation values for each heat are presented in Appendix F. With most of the plastic rotation data in the past being restricted to a few values per member, there was no evidence that plastic rotations experience any changes as a particular straightening

Table 36. Summary of damaged beam data.

Beam/RC#**	Angle of Damage		No. of Heats	Avg. P.R. (millirad)	Coefficient of Variation
	(degree)	(millirad)			
XXI-1/1	7.34	128.1	20	6.85	0.28
XXI-2/1	7.67	133.9	20	6.65	0.30
XXI-2/2	8.22	143.5	23	6.70	0.26
XXI-3/1	7.15	124.8	18	6.64	0.16
XXI-3/2	7.21	125.8	22	5.93	0.26
XXI-3/3	7.14	124.7	19	6.19	0.28
XXI-3/4	7.17	125.2	21	6.30	0.29
XXI-4/1	7.06	123.2	18	6.42	0.28
XXI-4/2	6.56	114.4	17	6.52	0.17
XXI-4/3	7.50	131.0	21	5.91	0.33
XXI-4/4	7.20	125.7	20	6.12	0.39
XXI-4/5	6.87	119.9	21	5.68	0.39
XXI-4/6	6.42	112.0	13*		
XXI-4/7	7.16	125.0	16*		
XXI-4/8	7.27	126.9	14*		

*Some heats included two vees due to time constraints

**Repair cycle number

Table 37. Shortening resulting from each damage/repair cycle (initial measurement length = 22", average damage = 7.20°).

Beam	Measurement of Beams after Damage/Repair Cycle #:							
	1	2	3	4	5	6	7	8
1	21.93							
2	----	21.79						
3	21.92	21.79	21.70	21.60				
4	----	21.78	21.65	21.51	21.47	21.35	21.23	21.12
Average	21.92	21.79	21.68	21.56	21.47	21.35	21.23	21.12
Average Shortening per Cycle	0.08	0.13	0.11	0.12	0.09	0.12	0.12	0.12
Total average shortening for all cycles = 0.11"								

Table 38. Increasing yield zone after each damage/repair cycle (see Figure 48).

Beam	Length of yield zone (in inches) after Bend #: (Top row = top fiber, bottom row - bottom fiber)							
	1	2	3	4	5	6	7	8
1	---- ----							
2	---- ----	8.20 8.40						
3	5.90 6.00	8.05 8.65	9.75 10.40	10.30 11.65				
4	5.50 5.80	8.15 8.40	9.50 10.20	10.50 12.00	10.70 13.20	10.70 13.30	11.50 15.25	11.50 15.25
Averages	5.70 5.90	8.13 8.48	9.63 10.30	10.40 11.83	10.70 13.20	10.70 13.20	11.50 15.25	11.50 15.25

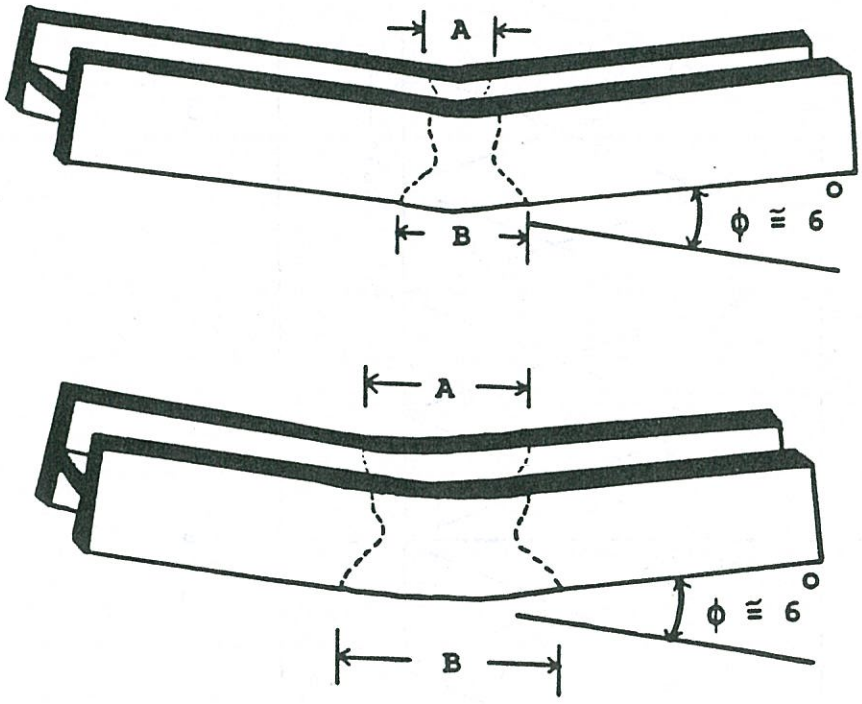

Figure 46. Spreading of yield zone in subsequent bends of damaged wide flange beam specimens.

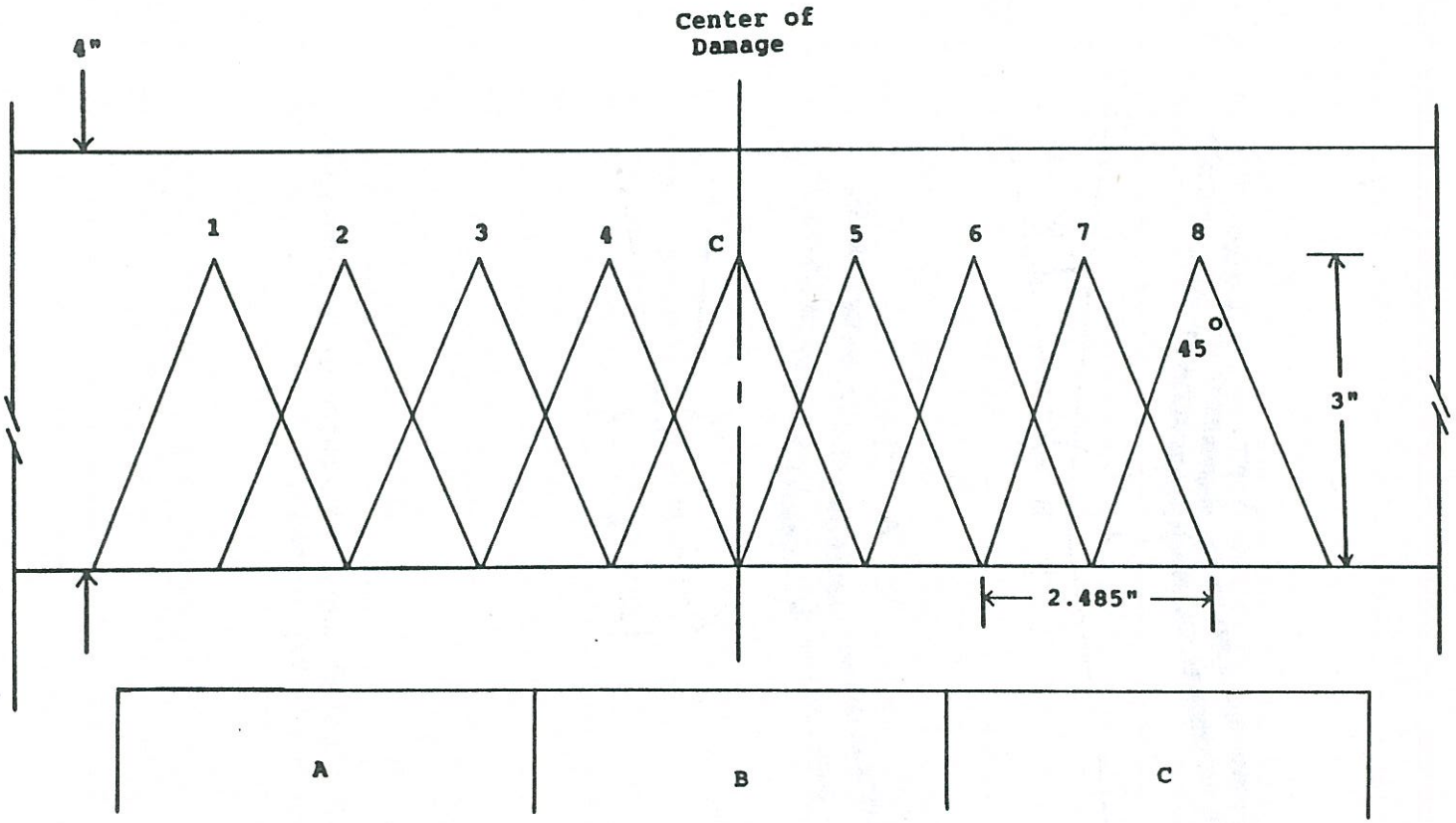

Figure 47. Heat locations used for damaged beams, with Regions A, B and C for residual stress measurements shown.

process progressed, especially when a great number of heats were required. Therefore, data from the four damaged beams were used to investigate any changes (of statistical significance) in the plastic rotations throughout a straightening process, even with all heating parameters remaining constant. The primary goals were: (1) to compare the plastic rotations resulting from any given heat to another within a given straightening process; (2) to determine any differences in plastic rotations from one repair cycle to the next; and (3) to point out any relevant trends in the plastic rotation values.

The initial investigation was twofold. First, only the 1st bends of each of the four specimens were considered (using a dependent samples test) to investigate any trends concerning plastic rotation values within a given process. Second, the first bend of one specimen was compared with the 2nd, 3rd, 4th, and 5th bends, respectively, of all the other specimens combined (using an independent samples test on means), to investigate differences, if any, between the plastic rotations in different repair cycles.

Comparison of Heats Within a Given Repair Cycle

Since each beam was damaged at least once, plastic rotation data from all of the specimens were considered. The method used is known as a dependent samples t-test (Hicks 1982). This method is used when one has the same sample "before and after" some treatment has been applied. The usual procedure is to take differences between the first and second observations (in this case, two plastic rotations at different heat numbers) on the same specimen, and test the hypothesis that the "mean difference" (using all four beams), μ_D, between the two plastic rotations in question is zero (This would actually mean that there is no significant difference). This reduces the problem to a test on a single mean:

Hypothesis "zero": $H_0: \mu_D = 0$

Hypothesis "one" : $H_1: \mu_D = 0 \quad (\mu_D > 0)$

with 'n' differences, α. The test statistic, t, is as follows:

$$t = \frac{\bar{d}}{s_d/n} \tag{12}$$

(with n-1 degrees of freedom). Reject if $t \geq t_{1-\alpha/2}$ (or $t \geq t_{1-\alpha}$).

A sample of n is chosen (with all four beams considered, n = 4). Two sets of measurements are taken (for example plastic rotations for heat number 1 on all beams and plastic rotations for heat number 2 on all beams). Differences are computed for each beam. The mean of these differences, $\bar{d}$, is computed, along with their standard deviation, s_d. From

the above equation, t is found and from this value, a decision regarding the hypothesis H_1 is made. To illustrate the method, the plastic rotations (shown in milliradians) for the first two heat numbers are compared:

Beam:	XXI-1	XXI-2	XXI-3	XXI-4
P.R. for Ht #1:	10.97	12.16	6.14	10.39
P.R. for Ht #2:	4.94	5.52	7.61	10.06
Difference, d:	6.03	6.64	-1.47	0.33

Mean difference, $\bar{d} = 2.88$

Std. dev., sd = 4.06

n = 4

degrees of freedom, df = n - 1 = 3

From the Student's t-distribution table (Benjamin and Cornell 1970), the following "P-value" was found for the above conditions:

$$P = 87.5\%$$

This P-value indicates that there is an 87.5% confidence level, given the four plates studied, that the plastic rotation resulting from heat number 1 would be greater than the plastic rotation resulting from heat number 2. Here it becomes obvious that the number of samples used will drastically affect the results. For example if the same mean difference and standard deviation were found, using 16 beams instead of 4, the resulting P-value would be over 99%. However, with that many samples, it is unlikely that these values would be even remotely similar.

The value of 87.5% is not considered high (hypotheses are often tested in the 95% to 97.5% range). The hypothesis H_1, which suggests that plastic rotations will be greater for the first heat than for the second heat, should be rejected.

P-values were found, comparing each heat number with each other. These values are shown in Table 39. The numbers in the table represent the confidence level that the heat on the horizontal axis will cause less plastic rotation than the heat on the vertical axis.

High P-values were common when comparing various heats to heat #1. This results from the relatively high plastic rotations experienced from the first heat (a characteristic observed in many damaged specimens, including plates and full-scale, simulated bridge girders). It is suspected that the higher rotations in the first heats are the result of residual stresses resulting from the damaging process.

From Table 39, the probability is high that the heats toward the end of the heating process will produce slightly lower plastic rotations. This could have resulted from the fact that toward the end of the heating process, heats are more localized (because most of the

Table 39. P-values for comparing plastic rotations at different heat numbers within a straightening process.

Heat No.	1	2	3	4	5	6	7	8	9	10	11	12	13	14	15	16	17
1	----	87.2	96.3	95.2	93.0	92.3	97.9	91.5	78.2	93.7	94.2	92.3	96.3	96.6	98.2	97.3	96.9
2		----	84.2	82.4	67.4	50.0	57.2	50.0	24.1	46.3	70.5	50.0	64.2	73.3	91.5	87.2	84.2
3			----	60.8	42.7	21.7	39.2	21.7	8.5	17.6	29.5	21.7	50.0	60.8	92.3	84.2	78.3
4				----	32.6	6.3	32.6	10.4	4.8	5.8	2.3	7.6	39.2	53.7	93.7	88.5	80.4
5					----	21.7	42.7	11.5	4.8	26.7	46.3	29.5	53.7	64.2	84.2	96.9	92.3
6						----	60.8	46.3	3.7	39.2	78.3	42.7	80.5	90.6	96.0	99.9	98.2
7							----	39.2	6.3	29.5	53.7	64.2	70.5	73.3	88.5	87.2	89.6
8								----	3.4	42.7	73.3	53.7	75.9	84.2	93.7	99.9	98.9
9									----	91.5	91.5	93.7	96.0	96.3	96.9	99.6	99.9
10										----	84.2	60.8	93.7	99.0	99.0	97.7	95.6
11											----	78.3	57.3	78.3	97.9	93.0	87.2
12												----	92.3	98.4	98.0	97.5	96.0
13													----	78.3	92.3	84.2	85.8
14														----	96.3	80.5	78.3
15															----	42.7	46.3
16																----	64.2
17																	---

The P-values shown indicate the confidence level that the heat represented by the number on the horizontal axis will produce less plastic rotation than the heat represented by the number on the vertical axis.

plate has already been straightened). However, when examining these P-values (for the heats toward the end of the process), the "high" values (over 95%) are found only when comparing with heats 6, 8, 9, 10, and 12. This indicates that heats 6, 8, 9, 10, and 12 exhibited unusually high plastic rotations (obviously a matter of chance, not statistical significance).

Most of the other P-values were found to be far below 95%, and the few that are above 95% do not exhibit any noticeable pattern or trend in the amount of plastic rotation experienced throughout the straightening process. Therefore, after the first heat, it seems that at any point during the straightening process, one should expect similar plastic rotations.

Average Plastic Rotations in Different Repair Cycles

After the above discovery, a relatively simple check was made to determine if the number of damage/repair cycles that a member has been through affects plastic rotation. As mentioned previously, beams damaged more than once exhibit different curvature and experience thickening resulting from previous repairs (and, as seen below, have different material properties). It is assumed that for these beams, just as in those damaged only once, the plastic rotation values within the given repair cycle will exhibit no significant trends.

However, to compare plastic rotations in different repair cycles, independent sample t-tests (Issa 1978, Hicks 1982) were utilized. Since beam XXI-1 only experienced 1 damage/repair cycle, its plastic rotation values were chosen to be compared with the plastic rotation values from all the beams that experienced 2, 3, 4, and 5 bends, respectively. In this way, the maximum number of samples could be utilized, while still insuring independence.

First, the means and standard deviations of the plastic rotations were grouped by repair cycle (see Table 40). The following equations were used to determine the test statistic, t', and the degrees of freedom, df:

$$t' = \frac{\bar{Y}_1 - \bar{Y}_2}{\sqrt{\frac{s_1^2}{n_1} + \frac{s_2^2}{n_2}}} \qquad (13)$$

Table 40. Statistical data for independent samples t-test.

Category	Beams in Category	Plastic Rotations (millirad)		
		Mean (x)	Std Dev (s)	No. of Samples (n)
1st Bend	XXI-2	6.60	2.38	19
2nd Bend	XXI-2 XXI-3 XXI-4	6.18	1.60	60
3rd Bend	XXI-3 XXI-4	6.01	1.90	40
4th Bend	XXI-3 XXI-4	6.20	2.14	40
5th Bead	XXI-4	5.68	2.25	21

$$df = \frac{[\frac{s_1^2}{n_1} + \frac{s_2^2}{n_2}]^2}{\frac{[\frac{s_1^2}{n1}]^2}{n_1 + 1} + \frac{[\frac{s_2^2}{n_2}]^2}{n_2 + 1}} - 2 \qquad (14)$$

The Student's t distribution table was again utilized, yielding the P-values shown in Table 41. The P-values were quite low. This indicates that no matter how many times a member has been damaged, plastic rotations will be close in value to those experienced during the first repair cycle, despite any material property differences or plate thickening.

Plastic Rotation Prediction Equation (Category W)

As in angles and channels, it is desirable to predict plastic rotations in wide flange sections, based on variations in heating parameters. In a past study (Avent and Fadous 1988), a preliminary equation was developed to predict movements in rolled shapes (including wide flanges) based upon the location of the stiffening element with respect to the vee apex and relative to the vee depth (in the case of Category W wide flange sections, the stiffening element is the web). It was concluded, based on limited and quite scattered data, that in undamaged Category W wide flange specimens, the stiffening element (web) has no apparent effect on the plastic rotations.

Boudreaux concluded that, for this type of heating pattern, the plate equation was valid. However, it has already been pointed out that Boudreaux's plate equation was influenced by Roeder's extremely high experimental plastic rotations. Also, many of Boudreaux's plastic rotations in the Category W wide flange specimens were higher than even his plate equation would suggest.

The complex heating pattern for this type of damage does not immediately lend itself to a simple "folded plate" approach used for angles and channels to relate plastic rotations. However, it is reasonable to assume that the web (stiffening element) would have less effect on plastic rotations in this type of heating than it would, for example, on channels or angles with the stiffening element at the open end of the vee. In fact, the wide flange beam could actually be considered as a channel with its web shifted to the center of the two flanges. Recall equation 11b:

Table 41. P-values for varying repair cycle numbers.

Repair Cycle	P-value*
2	70.6%
3	78.1%
4	67.8%
5	86.5%

*P-values represent the confidence level that the average plastic rotations in the repair cycle shown will be less than in the 1st repair cycle

$$\phi_c = \phi_p \left[1 + \frac{1}{2} \frac{d_s\, b_s}{w^2}\right] \qquad (11b)$$

In the case of a Category W wide flange heat, the value for d_s/w is always 1/2. For a W6x9 specimen, b_s = 6" and w = 4", thus Equation 11b indicates 37.5 percent larger movements in Category W wide flanges than in plates.

In the repetitively damaged beams, the average plastic rotation (for 215 heats) was 6.30 milliradians. The modified plate equation (Eqn. 4b) for the same heating conditions (45° vee and 0.50 load ratio) yields a value of 5.32 milliradians (the actual average for the damaged plates was 5.58 milliradians). It is apparent from these data alone, that an increase of only 18% over the modified plate equation exists for plastic rotations in Category W wide flange specimens.

When examining experimental data for the damaged beams, their relationship to plate plastic rotations seem to possess the same magnification characteristic that was initially assumed for both angles and channels (see discussion of geometric considerations for angles and channels). In other words, the magnification would be 1/4 instead of 1/2 to accurately represent the geometric effects on plastic rotations, because only 1/2 of the section is considered due to symmetry. Plastic rotations for Category W wide flanges heat may be rationally estimated using the following equation:

$$\phi_w = \phi_p \left[1 + \frac{1}{4} \left(\frac{d_s\, b_s}{w^2}\right)\right] \qquad (15)$$

Equation 15 represented the data well (Figure 48) and should be valid for the estimation of plastic rotations in damaged Category W wide flanges with depth ratios between 0.75 and 1.00. Regardless of the depth ratio, for Category W beams, the load ratio should not affect the beam-to-plate movement ratio, at least in damaged specimens. Three undamaged Category W specimens in the current study were heated with full depth vees. Of the three, two agreed well with Equation 15. The other exhibited rather high values, as were found in some of Boudreaux's specimens. As shown later in this chapter, residual stresses in the damaged beams are entirely different than in the undamaged specimens, and this fact could be a major reason why the plastic rotations also differ in some cases. For damaged specimens, conclusions should not be made from a few heats on undamaged specimens.

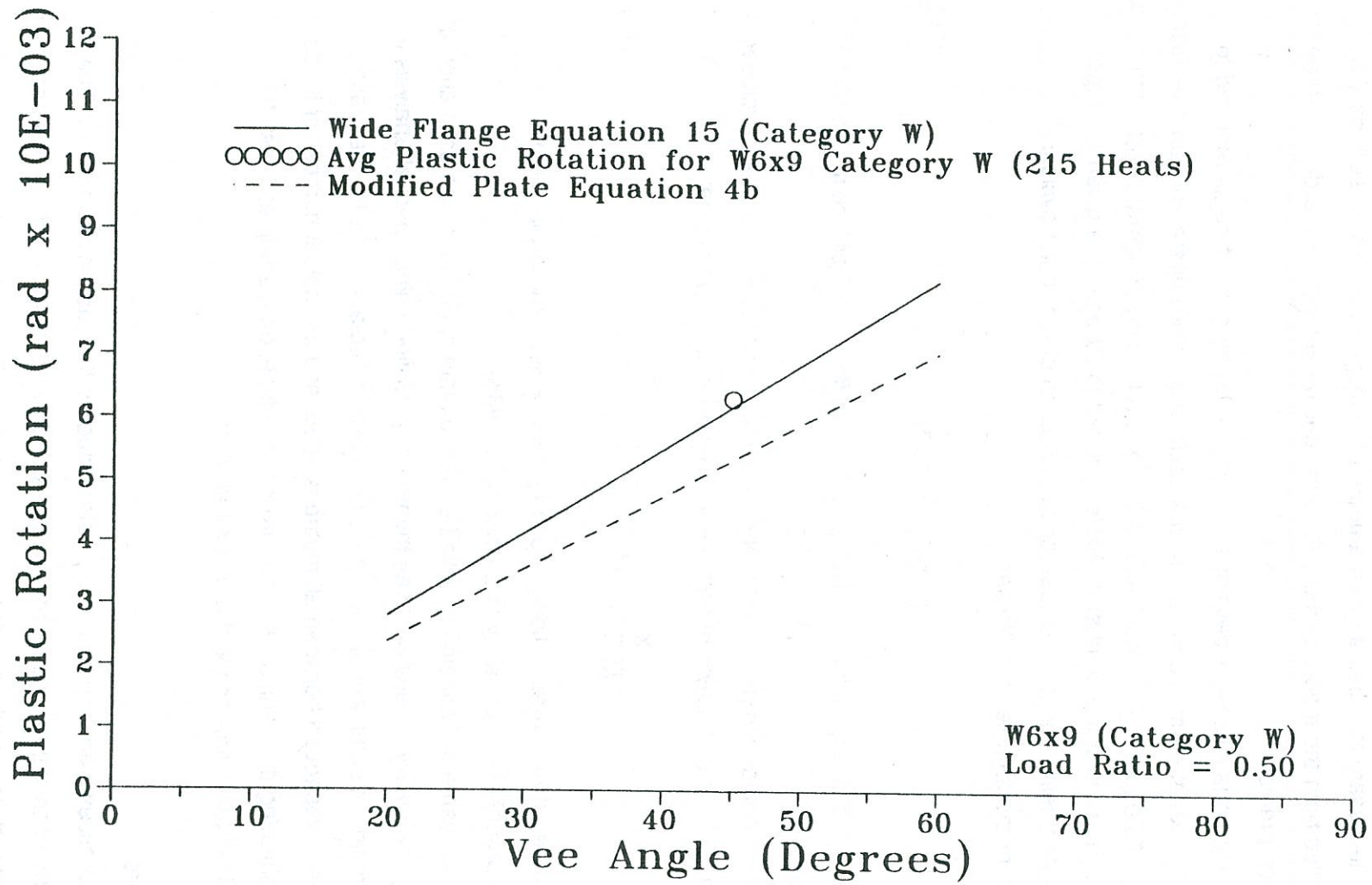

Figure 48. Comparison of plastic rotations in repetitively damaged, Category W wide flange beams with Equations 15 and 4b.

Statistically Based Predictions for Damage Repair

As for plates, it is important to be able to predict, with a given amount of certainty, the number of heats necessary to repair a given amount of damage. For this reason, de Bejar (1991) again applied both the theory of reliability and spectral analysis to the damaged beam data to obtain such predictions.

The following equations were developed to predict the number of heats required to repair a wide flange beam damaged about its weak axis to a known degree of damage, using a 45° vee angle, 0.75 depth ratio, a load ratio of 0.5, and a heating temperature of 1200°F. A general expression to predict the number of heats required to straighten a given damage angle was formulated using one sample test (beam) for each of the repair cycles. Using the principal statistics of the sample, one obtains

$$N = k_i + R \cdot V_i \cdot \sqrt{k_i} \tag{16}$$

where R is the target reliability index, $k_i = \phi_D/m_i$, and $V_i = \sigma_i/m_i$ is the coefficient of variation of the plastic rotations.

An excellent engineering predictor for N (with target reliability R = 2) was developed, independent of the principal statistics of any given sample for any repair cycle:

$$N = \frac{X}{(6 - r)} \cdot [1 + 0.11X \cdot (8 - r)] \tag{17}$$

where r is the number of the corresponding repair cycle, $X = \sqrt{\phi_D}$, and ϕ_D is given in milliradians. The probability of certainty is approximately 98%.

Following the same methodology applied earlier to plate specimens, the estimation of N, as provided by the theory of reliability was theoretically verified using spectral analysis in the frequency domain. A summary of the results is shown in Table 42. As for the plates, excellent agreement was found between all methods used, and the actual number of heats required for straightening the beams. As seen from the independent samples t-test, the number of heats is virtually independent of the repair cycle.

Residual Stresses

Residual stresses were experimentally determined by the sectioning method. The stresses were fairly consistent in the beams with one and two damage/repair cycles and fairly consistent in those with four and eight damage/repair cycles. This indicates that the number

Table 42. Comparison of different estimates of the number of heats required for damage repair (from de Bejar, et al., 1991).

Sample*/ Repair Cycle	Reliability Theory (R = 2)		Spectral Analysis	N** (Tests)
	Eqn. 16	Eqn. 17		
XXI-2/1	23	25	25	23
XXI-3/2	22	24	26	23
XXI-3/3	23	23	24	21
XXI-3/4	23	22	23	21
XXI-4/5	26	25	26	22

*One representative sample was chosen for each repair cycle

**The actual number of heats required for complete straightening

of bends might affect the distribution. No conclusions can be made concerning heating parameter variations in the repetitively damaged specimens, due to the fact that vee angle, depth ratio, and load ratio were consistent for all the specimens. Values of all residual stresses computed for the damaged beams are given in Tables 43 through 47. Values are shown, using an estimated modulus of elasticity of 29,000 ksi as well as the actual values of E obtained from tensile tests on specimens taken from the central damage region (see section on material properties). Stresses in Beams XXI-3 and XXI-4 were also found in 4-inch regions whose centers were four inches to the left and right of the center of damage, respectively to determine how the residual stresses changed depending on their location with respect to the damaged area (Figure 46). Individual residual stress distributions for all of the damaged beams are shown in Appendix G.

Figures 49 (using assumed E) and 50 (using measured E's) show the average residual stresses in the flanges of the specimens for the different categories and locations (the shortening of the beams prevented the measurement of residual stresses in the webs, except for XXI-1). The numerical values of these averages are shown in Tables 43 through 47. Residual stress plots for each individual beam are presented in Appendix G.

It is interesting to note that the residual stress patterns in all of these beams were exactly opposite in nature than in the undamaged beams, i.e., tension in the flanges and compression in the web. This is probably a result of the closing action of the vees in the flanges compressing the web (as was obvious by severe web buckling after a number of damage/repair cycles. The residual stress distribution is ideal for column members, and thus, it is likely that sweep-type heat straightening using vee heats is viable for column repair. However the web buckling, if not controlled could definitely limit the number of times a given column could be sufficiently repaired.

Material Properties

Tensile tests were conducted on the damaged beams, to determine the same properties as for the deformed plates. Table 48 shows the results of the tensile tests. The values for the unheated specimens were very consistent in all four categories of material properties given. The largest yield and tensile stresses in the heated specimens were observed in the vee apex region (recall the same characteristic in the damaged plates), although the stresses were also fairly large in the mid-vee region and at the open end of the vee. Changes in ductility also followed the same pattern as in the plates. In fact, all of the property changes in beam XXI-1 resembled those for plate XXV-8 (recall that this was the only

Table 43. Residual stresses in damaged beams (1 and 2 damage/repair cycles, assumed E = 29,000 ksi).

Strip No.	Residual Stress (ksi) in Beam		Avg. of all Flanges
	XXI-1	XXI-2	
TF1	4.72	-0.76	
TF2	5.58	6.02	
TF3	12.69	6.96	
TF4	15.15	7.90	
TF5	18.13	10.66	
TF6	21.75	17.62	
TF7	19.94	15.88	
TF8	-7.76	8.23	
W1	-14.32	NA	
W2	-9.90	NA	
W3	-6.50	NA	
W4	-5.58	NA	
W5	-7.14	NA	
W6	-13.85	NA	
BF1	4.46	-5.22	0.80
BF2	10.30	4.42	6.58
BF3	10.65	6.09	9.10
BF4	8.19	3.77	8.75
BF5	16.45	4.57	12.45
BF6	16.39	11.60	16.84
BF7	23.42	17.76	19.25
BF8	12.44	3.95	4.22

NA = Not available because of web distortion due to shortening

Table 44. Residual stresses in damaged beams (1 and 2 damage/repair cycles, measured E values used).

Strip No.	Residual Stress (ksi) in Beam		Avg. of all Flanges
	XXI-1	XXI-2	
TF1	4.72	-0.74	
TF2	6.52	5.12	
TF3	12.69	5.11	
TF4	12.59	4.88	
TF5	16.25	7.65	
TF6	20.93	14.40	
TF7	20.42	14.51	
TF8	-8.46	8.34	
BF1	4.46	-5.06	0.79
BF2	12.04	3.76	6.65
BF3	10.65	4.47	7.91
BF4	6.81	2.33	6.34
BF5	14.75	3.28	10.05
BF6	15.77	9.48	14.98
BF7	23.99	16.23	18.65
BF8	13.56	4.00	4.44

NA = Not available because of web distortion due to shortening

Table 45. Residual stresses in damaged beams (4 and 8 damage/repair cycles) at Region B (assumed E = 29,000 ksi).

Strip No.	Residual Stress (ksi) in Beam		Avg. of all Flanges (Location B)
	XXI-3	XXI-4	
TF1	1.41	-20.08	
TF2	15.52	-12.40	
TF3	24.51	16.02	
TF4	19.29	21.61	
TF5	29.94	32.41	
TF6	34.51	25.01	
TF7	12.73*	12.98	
TF8	-8.05	-13.20	
BF1	-13.63	-1.52	-8.46
BF2	17.91	-7.76	3.32
BF3	23.64	2.90	16.77
BF4	16.60	2.83	15.08
BF5	27.19	-2.18	21.84
BF6	39.01	7.90	26.61
BF7	35.02	10.59	19.53
BF8	-10.42	-8.12	-9.94

NA = Not available because of web distortion due to shortening

*Reading unavailable, so the average of strips 6 and 8 was used

Table 46. Residual stresses in damaged beams (4 and 8 damage/repair cycles) at Region B (measured E values used).

Strip No.	Residual Stress (ksi) in Beam		Avg. of all Flanges (Location B)
	XXI-3	XXI-4	
TF1	1.76	-26.66	
TF2	18.04	-16.55	
TF3	18.00	22.04	
TF4	19.16	29.21	
TF5	32.31	44.14	
TF6	40.22	34.22	
TF7	14.74*	17.90	
TF8	-10.74	-19.12	
BF1	-17.01	-2.02	-10.88
BF2	20.81	-10.36	4.14
BF3	25.51	3.89	20.30
BF4	16.49	3.83	17.68
BF5	29.35	-2.97	26.81
BF6	45.47	10.79	34.13
BF7	43.71	14.61	26.13
BF8	-13.86	-11.76	-13.22

NA = Not available because of web distortion due to shortening

*Reading unavailable, so the average of strips 6 and 8 was used

Table 47. Residual stresses in damaged beams (4 and 8 damage/ repair cycles) at Regions A and C (assumed E = 29,000 ksi).

Strip No.	Residual Stress (ksi) in Beam				Avg. of all Flanges
	XXI-1		XXI-1		
	Loc. A	Loc. C	Loc. A	Loc. C	
TF1	-9.14	13.70	36.07	14.90	
TF2	6.96	13.63	14.65	23.93	
TF3	5.37	8.63	19.43	19.14	
TF4	0.87	-8.27	3.84	5.58	
TF5	8.34	-15.30	10.15	-8.99	
TF6	12.18	10.29	13.20	6.96	
TF7	8.27	6.24	8.56	7.25	
TF8	-6.13	6.33	2.07	10.84	
BF1	3.62	-9.61	11.38	2.61	7.94
BF2	7.69	8.04	12.69	13.56	12.64
BF3	3.34	2.39	16.46	13.49	11.03
BF4	-8.41	1.74	9.57	7.25	1.52
BF5	-6.45	9.14	5.87	5.73	1.06
BF6	7.98	12.62	15.66	16.17	11.88
BF7	17.33	9.28	20.01	8.70	10.71
BF8	12.22	-6.31	15.62	6.09	4.97

Note: web stresses not available because of web distortion due to shortening

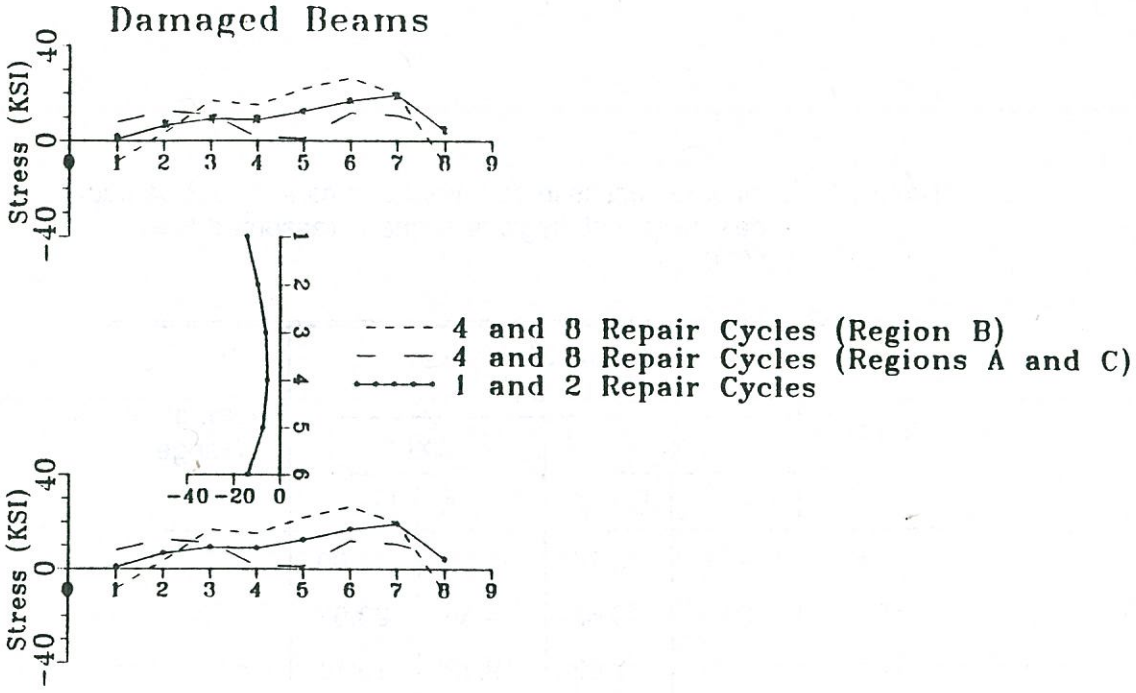

Figure 49. Residual stress distributions in damaged, Category W wide flange beams (estimated E = 29,000 ksi).

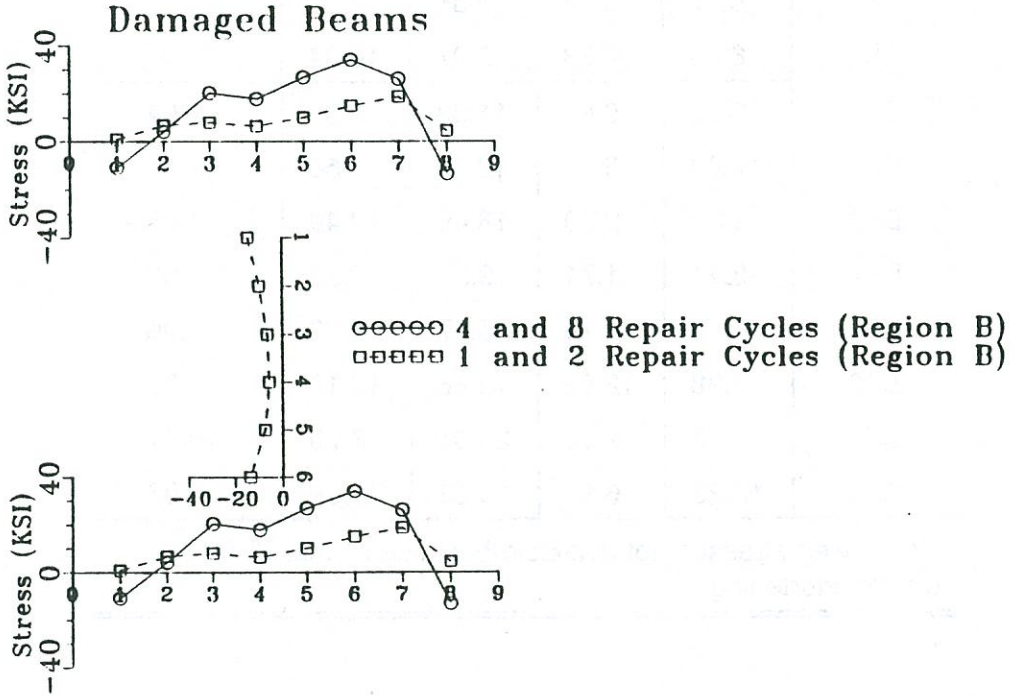

Figure 50. Redisual stress distributions in damaged, Category W wide flange beams (measured E values used from tensile tests).

Table 48. Material properties of damaged plates.

Specimen/ Strip		Yield Stress (ksi)	Maximum Stress (ksi)	Percent* Elong.	Percent Red. in Area
XXI-1	(UH)	45.4	67.4	43	63
XXI-1	2	57.7	73.6	30	62
XXI-1	4	53.9	73.4	36	64
XXI-1	8	49.4	70.2	29	64
XXI-2	(UH)	47.6	68.3	42	66
XXI-2	2	63.5	78.0	31	60
XXI-2	4	51.3	75.4	32	61
XXI-2	8	52.2	71.0	31	65
XXI-3	(UH)	45.08	68.0	43	65
XXI-3	2	70.9	82.5	22	59
XXI-3	4	56.6	75.3	26	57
XXI-3	8	52.7	75.9	27	42
XXI-4	(UH)	46.8	68.1	45	66
XXI-4	2	88.1	99.1	15	41
XXI-4	4	51.3	76.3	24	52
XXI-4	8	49.8	71.5	23	61

Rates of strain = 0.2206 in/in per minute up to yield
= 0.8824 in/in per minute up to failure

*All values have been converted to represent an ASTM standard sized specimen (see ASTM A370 section 11.6.1). A 1-inch gage length was used

plate heated with a 0.75 depth vee). This was to be expected, since the heating parameters were identical for these two members.

Table 49 shows the moduli of elasticity for all of the tensile specimens. The values differ from the damaged plate values in that they were not as low in general, and the lowest values were found in the middle region of the flanges rather than at the open end of the vee. It seems possible that, from the results of the damaged plates and the damaged beams, one can assume that original E values for a given specimen (before damage) will be more closely maintained when 3/4-depth vees are used.

Changes in all the material properties became more evident with the increasing number of damage/repair cycles. Table 50 shows the percentages of individual properties in relation to unheated specimens taken from each beam and in relation to the ASTM standard values (yield stress = 36 ksi, tensile stress = 67 ksi, and percent elongation = 34). Although, after two damage/repair cycles, the property changes still compared well with plate XXV-8, after four bends, the increase in yield and tensile stress, and the loss in ductility were sharp. This trend continued until, after eight cycles, the yield stress was a significantly high 88.1 ksi, with a ductility loss of 67 percent. Figures 51 through 53 illustrate the trends in stress increase and ductility loss as a function of repair cycle number.

As mentioned previously, the point at which loss in ductility becomes dangerous is case specific. However, the extreme losses encountered in the repetitively damaged beams show that there is probably a limit to the number of times that any given member should be repaired. It seems that after two cycles, the properties resemble those after one cycle. Thus, whatever is safe to straighten once could be safely straightened twice under the same conditions.

The ductility losses are significantly greater after 4 and 8 damage/repair cycles, respectively. These findings are further substantiated by the fact that during the study of full-scale simulated bridge girders, one girder exhibited brittle behavior by cracking during a heat in its third repair cycle. It is concluded that until further research is conducted, members damaged more than twice should not be subjected to heat straightening.

Strong Axis Damage

Beam XX-1 was subjected to strong axis damage to determine plastic rotations and residual stresses resulting from heat straightening a damaged Category S specimen. Fifteen heats (full-depth,45° vee, 0.5 LR) were necessary to straighten the beam, which was damaged to an angle of approximately 6.5°. It should be noted that some local buckling

Table 49. Moduli of elasticity of damaged beam specimens.

Specimen/ Strip		Modulus of Elasticity (ksi x 10^3)
XXV-1	(UH)	32.3
XXV-1	1	33.9
XXV-1	5	24.1
XXV-1	7	31.6
XXV-2	(UH)	29.4
XXV-2	2	24.7
XXV-2	4	17.9
XXV-2	8	29.4
XXV-3	(UH)	26.9
XXV-3	2	33.7
XXV-3	4	28.8
XXV-3	8	38.7
XXV-4	(UH)	38.7
XXV-4	2	39.2
XXV-4	4	----
XXV-4	8	----

Table 50. Comparison of material properties in heat-straightened steel beams with unheated specimens and ASTM standard values.

Beam/Strip	Yield Stress		Tensile Stress		% Elongation	
	% UH	% ASTM	% UH	% ASTM	% UH	% ASTM*
XXI-1/2	127	160	109	110	69	88
XXI-1/4	119	150	109	110	85	106
XXI-1/8	109	137	104	105	69	85
XXI-2/2	133	176	114	116	74	91
XXI-2/4	108	143	110	113	79	94
XXI-2/8	110	145	104	106	74	91
XXI-3/2	155	197	121	123	51	65
XXI-3/4	124	157	111	112	62	76
XXI-3/8	115	146	112	113	64	79
XXI-4/2	188	244	146	148	33	44
XXI-4/4	110	143	112	114	54	71
XXI-4/8	106	138	105	107	51	68

*Converted values for ASTM standard size specimens were used

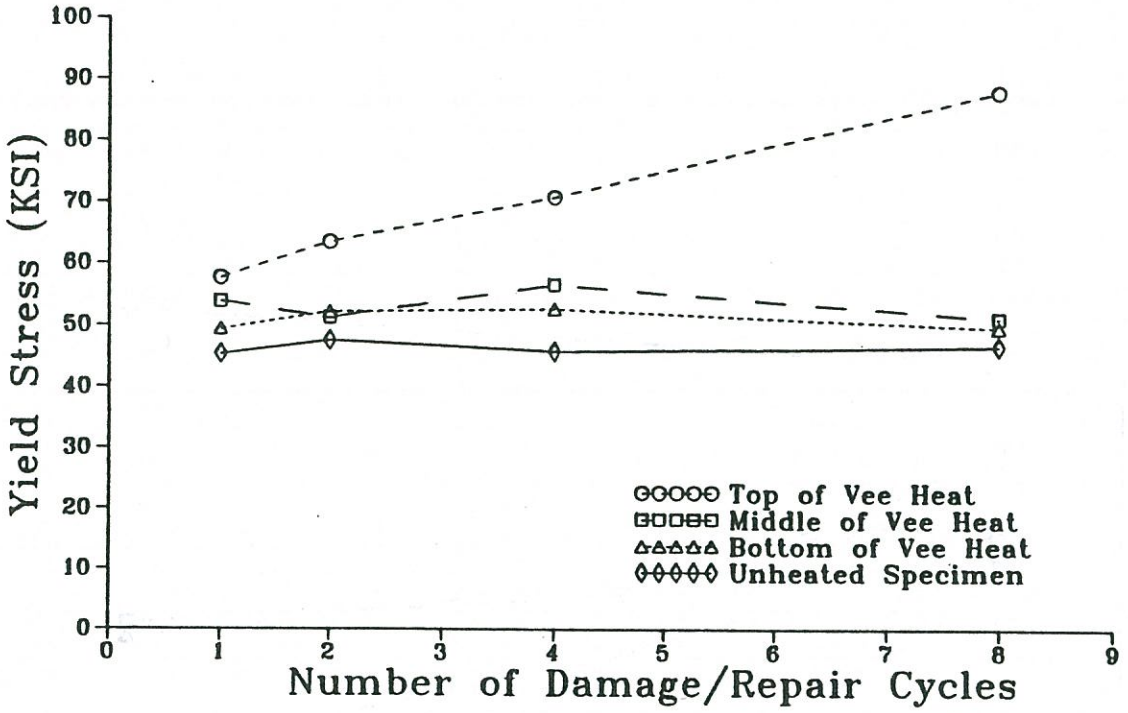

Figure 51. Yield stress versus number of repair cycles.

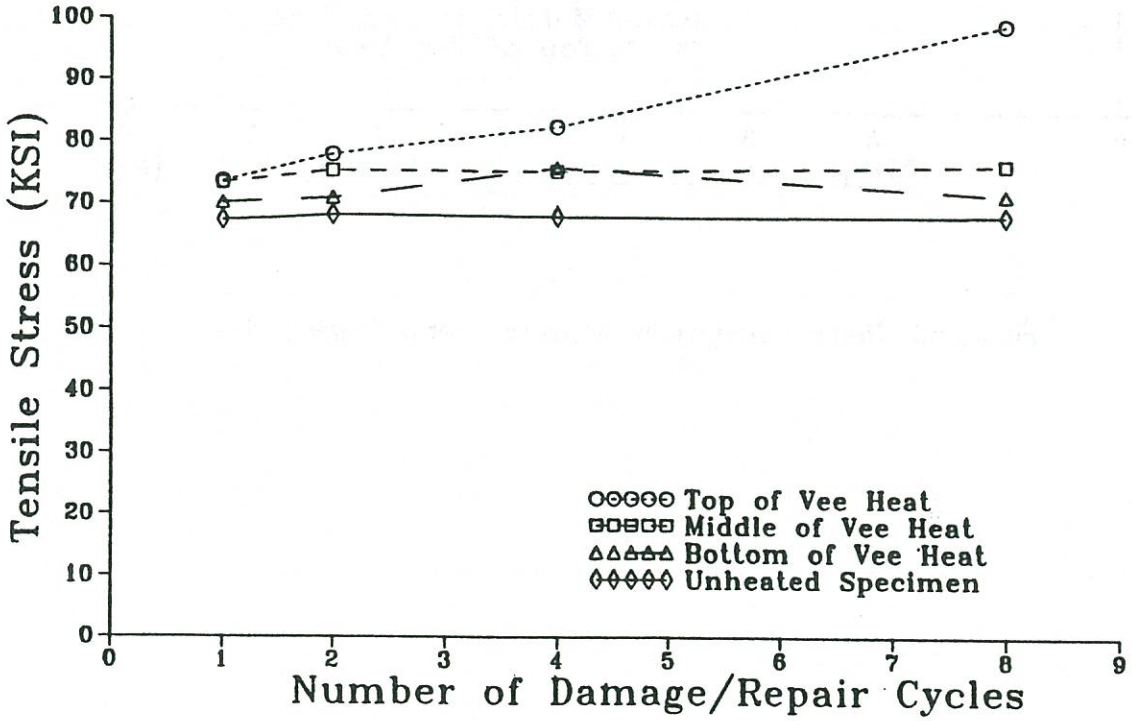

Figure 52. Tensile stress versus number of repair cycles.

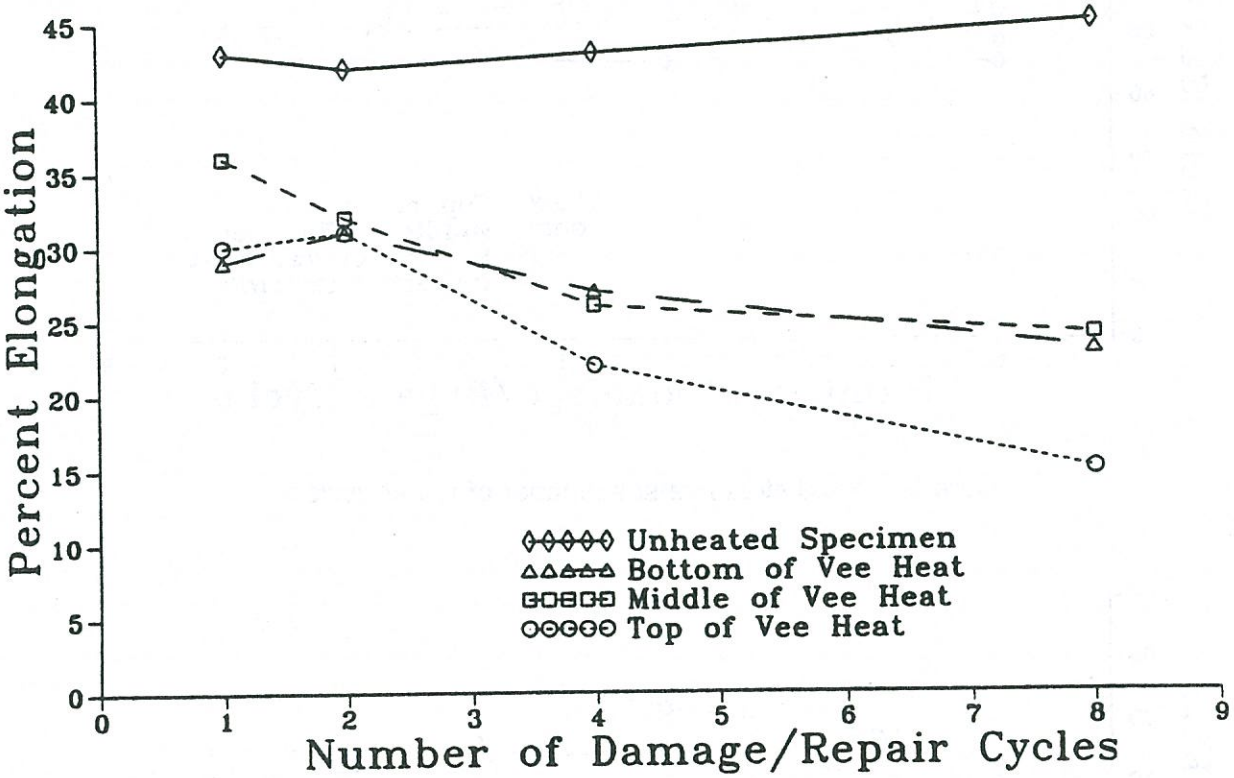

Figure 53. Percent elongation versus number of repair cycles.

occurred in the top flange during the damaging process, resulting from the compression it experienced. This local buckling was removed by hot mechanical straightening before heat straightening was applied.

Plastic Rotations (Category S)

As in the other shapes studied, the plastic rotations in the Category S wide flanges were related to those of the plates. To illustrate the geometric relationship, consider the wide flange shape in Figure 54a. Two flange legs are folded (Figure 54b) to become a "continuation" of the web (Figure 54c). The shape then resembles a plate with a partial depth vee applied along with a rectangular heat (Top flanges not considered).

The geometric considerations appear very similar to those used for angles. However, it is likely that load ratio does not have the significant affect that it had on the angles, because the stresses are lower in the stiffening element of the wide flange shape. In fact, for a load ratio of 0.5, the stresses are 20.2 ksi as compared to the value of 28.71 ksi calculated for the laterally unsupported angle in (Table 22).

With the load ratio not considered as a multiple factor in comparing with the plate equation, the form of Equation 11b may be used to predict plastic rotations for the Category S beams:

$$\phi_s = \phi_p \left[1 + \frac{1}{2} \frac{d_s\, b_s}{w^2}\right] \qquad (18)$$

For all Category S wide flanges, $d_s/w = 1$. For W6x9 shapes, $b_s = 4"$, and $w = 6"$ (in this case w is the depth of the web and b_s is the width of the flange). With these values, the Equation 18 yields the following:

$$\phi_s = \phi_p \left[1 + \left(\frac{1}{2}\right) (1) \left(\frac{4}{6}\right)\right] = 1.33\, \phi_p$$

The individual plastic rotations for the Category S beams are presented in Table 51. As for the Category W beams, higher plastic rotations were experienced than for plates under the same heating conditions. The average actual plastic rotation was 7.57 milliradians, as compared to the value of 5.32 milliradians from the plate equation 4b. The predicted value is 7.08 or 93% of the actual. Equation 18 well represents the plastic rotations in the damaged Category S wide flange specimen (Figure 55).

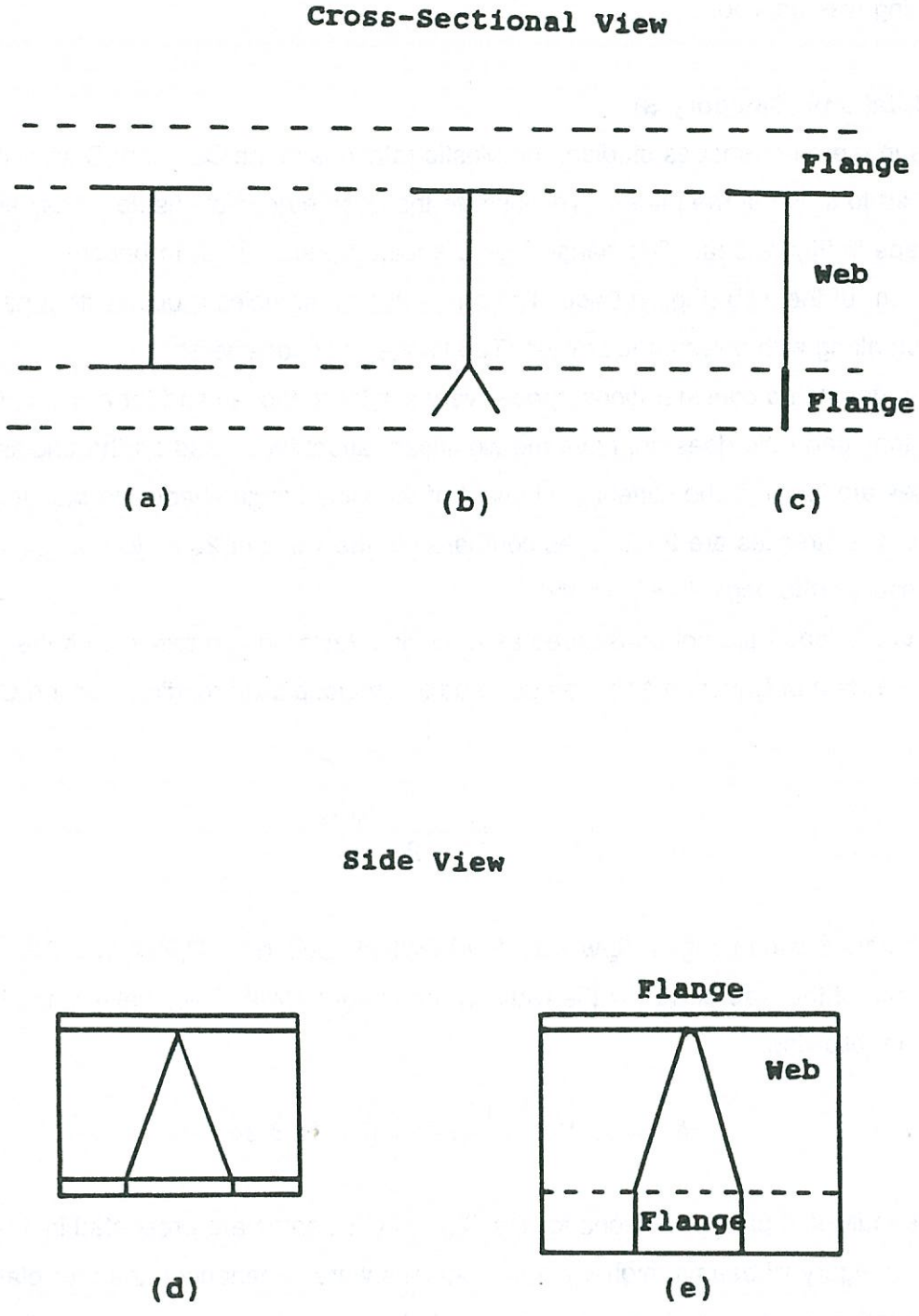

Figure 54. Geometric relationship between Category S wide flanges and plates.

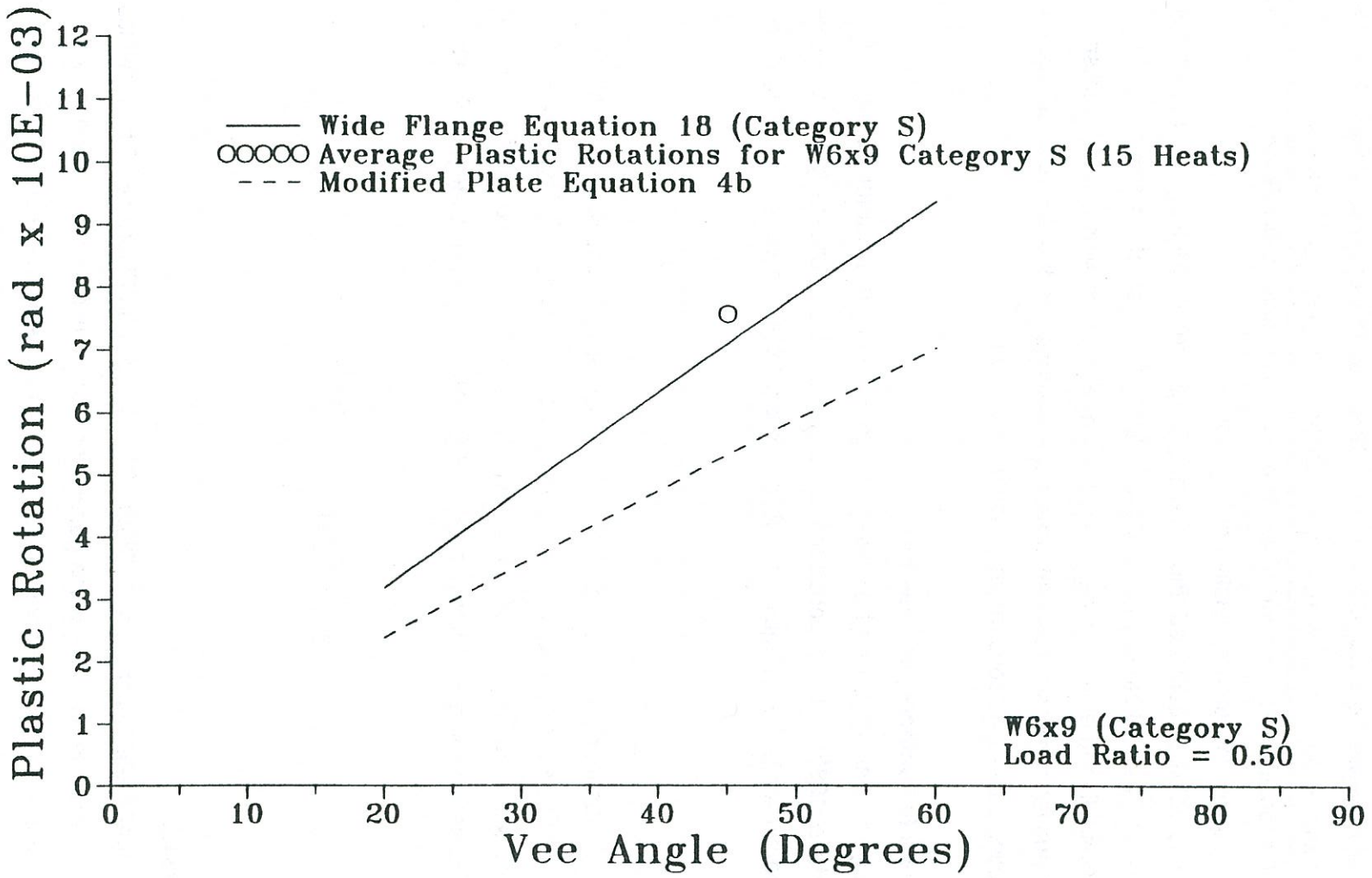

Figure 55. Comparison of data from beam XX-1 with Equations 18 and 4b.

Plastic rotations were also found for five undamaged Category S beams (Table 51). Most of these values were significantly higher than those determined by Equation 18 (although specimen IV-6 matched the Equation 18 almost exactly). Comparisons are shown in Table 52. Similar results were obtained by Boudreaux, where beams with lower load ratios experienced the largest movements relative to Equation 18.

Differences between damaged and undamaged specimens are likely a result of their significantly different residual stress patterns (see below). Because of the relatively low number of heats applied to each undamaged specimen, along with wide scatter in plastic rotation values and differences in residual stresses, it is suggested that they not be used as a basis for predicting plastic rotations for undamaged specimens.

Plastic Rotations for Category S Channels

Relatively few channels were heat straightened for bending about the strong axis (Avent and Fadous, 1989). The response of this sample of C6x8.2 undamaged specimens was found to be similar to that of equivalent plates. If Eq. 18 is applied to the Category S C6x8.2, then

$$\phi_c = 1.16\ \theta_p$$

indicating close correspondence to the plate equation. Since the cross section configuration of channels and wide flange beams are quite similar when considering Category S heat straightening, the same rational as used to develop the wide flange formula can be applied to the channel. Consequently, it is recommended that Eq. 18 be used for Category S channels, that is;

$$\phi_{cs} = \phi_p \left[1 + \frac{1}{2}\ \frac{d_s b_s}{w^2}\right] \qquad (19)$$

Residual Stresses

The residual stress distribution for Beam XX-1 is shown in Figure 56. The individual values are shown in Table 53. The stress pattern resembles those of the undamaged specimens, with compression throughout both flanges and tension in the center portion of the web. However the compressive stresses are much higher than in the undamaged specimens, especially near the junctions of the flanges and the web (some undamaged specimens

Table 51. Individual plastic rotations for a damaged, Category S wide flange beam (specimen XX-1).

Heat Number	Plastic Rotation (milliradians)
1	3.83
2	11.63
3	8.60
4	8.33
5	8.34
6	6.19
7	7.87
8	6.72
9	9.03
10	7.41
11	9.97
12	3.11
13	3.85
14	8.15
15	10.49
Average	7.57

Table 52. Comparison of plastic rotation in undamaged, Category S wide flanges to Equation 18.

Beam	Vee	M/M_p	Plastic Rotations (milliradians)		Ratio of Equation/ Actual
			Actual	Eqn. 18	
I-1	20	0.00	3.04	1.09	2.78
I-2	45	0.00	5.35	2.45	2.18
I-4	30	0.00	4.19	1.63	2.56
IV-5	45	0.25	7.31	4.76	1.53
IV-6	45	0.50	7.17	7.08	1.01

Table 53. Residual stresses in a damaged, Category S wide flange beam (specimen XX-1).

Strip No.	Residual Stress (ksi)		
	Top Flange	Web	Bottom Flange
1	-25.34	25.70	-33.10
2	-19.07	23.04	-19.58
3	-14.72	22.15	-19.87
4	-37.77	24.90	-31.68
5	-44.44	24.75	-18.05
6	-13.41	26.83	-14.50
7	-11.93	----	-33.57
8	-10.44	----	-46.62

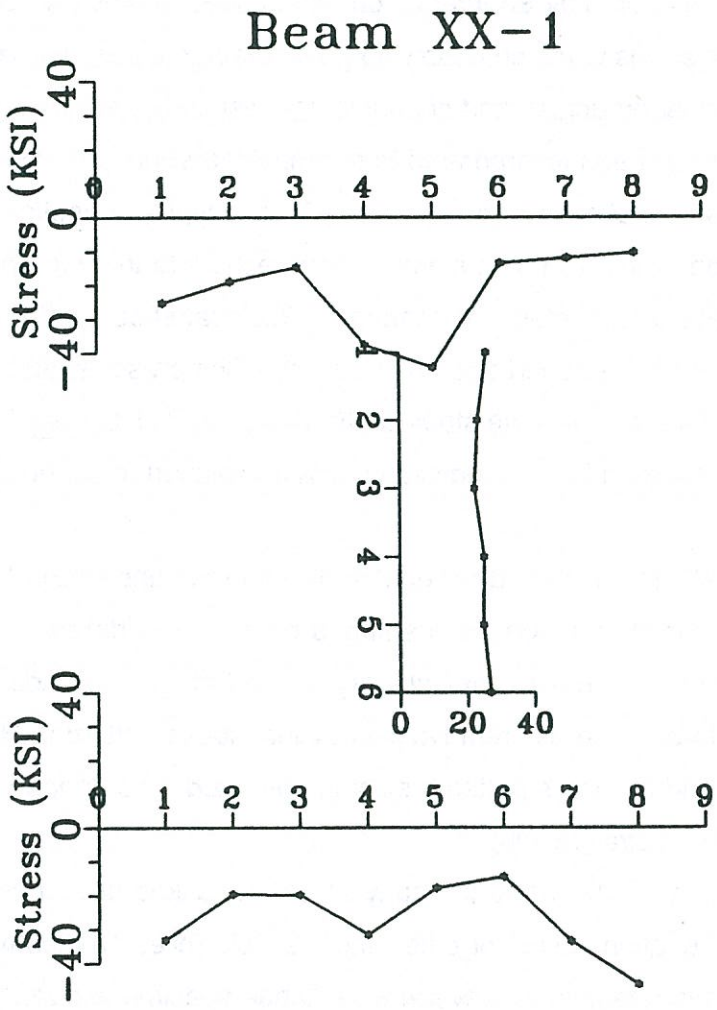

Figure 56. Stresses in beam XX-1 (45° vee, M/M_p = 0.50, depth ratio = 1.00).

actually had low tensile stresses in this region). Compressive stresses are greatest near the flange tips, as in most of the other types of specimens studied, and these stresses are much higher than commonly assumed residual stresses in wide flange shapes.

Conclusions

The past study conducted by Boudreaux on undamaged angles and channels indicated extremely high plastic rotations when compared to plates heated under the same conditions. The current study on damaged angles and channels has resulted in similar findings. Cross-section geometry has been incorporated into a modified equation (based on the plate equation) to predict plastic rotations for these shapes for two types of heating patterns. Stresses and the location of the stiffening element, with respect to the vee apex, both have an effect on the plastic rotations in angles and channels. Residual stress patterns were found for a few of the specimens (both damaged and undamaged). Compressive stresses near the leg tips were quite high in some cases. The study of the angles and channels illustrates the fact that more variables are involved in the prediction of plastic rotation in shapes other than simple plates.

The study of plastic rotations and residual stresses in the undamaged wide flange beams provides a basis for comparison with damaged beams. The different heating configurations necessary for the heating of Category S and Category W wide flange sections, respectively, are found to produce different typical residual stress patterns. However, it is yet unknown what kind of residual stress patterns exist in damaged wide flange sections that have been repaired by heat straightening.

The damaged beam study answered many previously asked questions about heat straightening. General equations used for other, more simple rolled shapes were found to be useful for predicting plastic rotations for several wide flange specimens damaged about their weak axes or strong axis. The plastic rotations were quite consistent (with the exception of the first heat of each repair cycle), regardless of the number of heats previously applied within a given repair cycle or the number of damage/repair cycles previously experienced.

Residual stress patterns were also consistent for various categories of beams: (1) Category W, 1 and 2 damage/repair cycles; (2) Category W, 4 and 8 damage/repair cycles; and (3) Category S. The stresses were found to be quite different than those in undamaged specimens heated with the same heating patterns. It is likely that these stresses are responsible for differences in plastic rotations experienced in damaged and undamaged specimens.

Material properties were affected by each damage/repair cycle experienced. Most significantly, yield stress increased greatly at some locations and percent elongation was drastically reduced after, at most, four damage/repair cycles (possibly three). An upper limit of 2 damage/repair cycles on heat straightening is recommended. Properties after 1 and 2 damage/repair cycles were similar to each other and resembled those of a plate which was damaged once and subjected to the same heating parameters (3/4-depth vee).

It is likely that using full depth vees will reduce the detrimental effect of loss in ductility experienced most noticeably above the vee apex of a 3/4-depth vee. It has been concluded from the damaged beams as well as the damaged plates that full-depth vees do not cause any more shortening than 3/4-depth vees. Shortening in Category W beams can be predicted using the same equation used to predict shortening in plates. The shortening in the flanges caused severe web buckling, and the buckling increased with each damage/repair cycle.

Chapter 4

HEAT-STRAIGHTENING DAMAGED BRIDGE GIRDERS

The development of engineered heat-straightening technology begins with the study of simple plates and rolled shapes. However, field applications are much more complex. The most typical type of damage occurs in bridge overpasses where a supporting steel bridge girder may be hit by an over-height vehicle. The purpose of this chapter is to describe the investigation of bridge girder damage associated with both composite and noncomposite behavior.

The objectives of this phase of the study can be summarized as follows:

1. To conduct a detailed experimental investigation of the field behavior of damaged prototype structural steel composite and noncomposite bridge girders subjected to heat-straightening by:
   (i) Inducing controlled deformation in a prototype composite bridge girder to simulate the typical damage pattern caused in the field by impact loads from over-height vehicles;
   (ii) Developing computer aided techniques for processing raw data from field measurements to assess the induced damage and decide the course of repair;
   (iii) Measuring and documenting the important parameters involved in the study; and,
   (iv) Evaluating the relationship between the average plastic rotation, load ratio and the depth of the girder for a given vee angle, vee depth and heating temperature.
2. To develop an analytical model based on a deterministic approach for quantifying the heat-straightening response of damaged structural steel bridge girders in the presence of internal redundancy associated with the composite girder/deck construction. The analytical model will be used to derive a simple formula, which takes into account the load ratio and the depth of the girder as the important variables, to predict the average plastic rotations achieved per heating cycle.
3. To verify the theoretical model or formula with the experimental results available.

4. To extend the analytical model to include the effects of statical indeterminacy in the bridge girder due to lateral bracing along the span of the girder.

Composite Girders

Scope of the Testing Program

The available literature shows little quantitative research evidence on the heat-straightening repair of full-scale structural steel elements. Moberg (1979) accomplished a detailed field investigation of the heat-straightening behavior of damaged bridge girders. The field repair conducted by him on the Bothell Bridge in Washington State is the earliest documented source of experimental data on the subject. The only later contribution is the experimental study of the field behavior of damaged prototype composite bridge girders, conducted by Avent and Fadous (1987, 1989a, 1989b). The other reported experiments on bridge girders have been mostly qualitative in nature. As a result, the existing research evidence on heat-straightening was predicated almost entirely on the laboratory evaluation of simple elements. The laboratory studies have furnished adequate data for evaluating most of the parameters that influence the heat-straightening response of full-scale steel members. However, one fundamental parameter has been overlooked in these studies, which is the internal redundancy of the member. Often, the damaged steel member in the field displays an inherent redundancy due to its structural configuration, which imposes an internal constraint on the heat-straightening mechanism of the member. The importance of these constraints in affecting the heat-straightening performance of the member cannot be over-emphasized. A structural steel girder used in composite bridge construction, with one of its flanges compositely connected to the deck slab of the bridge, is a popular example of such an internally redundant member.

A detailed and controlled set of field experiments was designed to provide a more comprehensive data-base on the field behavior of damaged composite bridge girders. The objective was to quantify the heat-straightening behavior of composite bridge girders. Emphasis was placed on studying the interaction of the internal redundancy with both the external restraining forces and heat patterns in relation to heat-straightening process in composite bridge girders. A number of heat-straightening tests were conducted on damaged prototype composite bridge girders. Two 20 ft long, A-36 steel girders of different geometries (W10x39 and W24x76) were tested. Each girder was damaged and repaired using the

heat-straightening method. The level of jacking forces was varied in the course of repair in order to evaluate the effect of external restraining forces on each girder.

The experimental study on the W10x39 composite girder (Cases SB-1 and SB-2) was completed previously, and the results have already been reported by Avent (1988). A part of the testing program proposed for the W24x76 girder (Cases SB-3 and SB-4) were also completed prior to the preparation of the report and are documented therein. The remaining tests on the W24x76 girder were completed subsequently. Reported here are the test results and procedures with an evaluation of the factors affecting girder behavior.

Test Set-up

The heat-straightening tests (included in this chapter) were conducted in the HEAT (Heat Straightening Evaluation and Testing) facility. The facility was fabricated to simulate the damage and repair of full-scale bridge girder systems with the opportunity for controlling and monitoring the involved parameters. A 20 ft long, A36 steel, W24x76 girder was installed on the HEAT facility with each end of the bottom flange bolted to a cross beam (on the HEAT frame) using 4 1/2" diameter bolts. The bolt holes on the beam were made round at one end and slotted at the other to allow free longitudinal movement of the girder. The bottom flange of the girder was connected to simulate a pinned joint at one end and a roller joint at the other end. The diaphragms were placed at the ends only. Two diaphragms were connected at each end of the girder on either face of the web. A 19'x4'x12" concrete slab was connected to the top flange for simulating composite action by the use of eighteen 1" bolts placed in rows of two at 2 ft intervals along the length of the beam. The normal weight concrete slab imposed a dead load of 600 lbs per linear foot. The composite construction with the top slab eliminates all the degrees of freedom in the entire top flange.

Damage Inducement and Measurements

The damage encountered in composite girders in the field is typically caused by an impact load on the bottom flange from an over-height vehicle. The damage inducement operation was designed to simulate this typical mode of damage. Damage was induced in the originally undeformed W24x76 girder by applying a midspan static load applied transversely to the bottom flange in its own plane. The load was applied using a 25 ton capacity hydraulic cylinder controlled by a 15,000 psi capacity hydraulic pump. The load was applied gradually and was monitored by a 10,000 psi capacity pressure dial gage. A dial gauge was used to monitor the lateral displacements on the bottom flange at the point of damage. The girder

was damaged to achieve a plastic deformation of around 4.5 inches in the bottom flange in the direction of the applied load. The maximum applied load was 41 kips. The damaged girder is shown in Figure 57.

Measurements were taken at nineteen cross-sections. These cross-sections were selected so as to adequately define the damaged shape of the girder. Since larger curvatures existed near the center of damage, closer spacings were used in that proximity. As the curvatures diminished on moving away from the center, the spacings between the cross-sections were increased. The measured cross-sections had a symmetrical layout about the center of damage (Figure 57). Eight points were measured on the boundary of the girder at each of these cross-sections (Figure 58). The arrows indicate the lines along which the measurements were taken for various points.

Subsequent to measuring the damaged configuration of the W24x76 composite girder, the damage was assessed. The individual plate elements of the girder were graphically analyzed for the identification of the yield zones. Both the bottom flange and the web were plotted at appropriate intervals to determine flexural characteristics. The radii of curvatures at various locations on the plot were evaluated and compared to the limiting values prescribed for yielding by Shanafelt and Horn (1984). Damage assessment of the girder revealed that the bottom flange had yielded as a long flat plate in bending about its strong axis. Measurements on the web showed that the web had plastically deformed as a flat plate in bending about its weak axis, thus producing a well defined yield line. For instance, after the third damage cycle on the W24X76 composite girder, the yield zone in the bottom flange was confined within a distance of 1 ft, between the points 8 and 12 (Figure 57). The yield line in the web occurred 1.75 to 2.00 inches below the top flange, extending over a span of 15 ft from point 2 to point 18 (Figure 57). The dashed areas of the flange and web correspond to the zones in which plastic yielding had occurred. The yield zones in the flange and web extended to a variable distance on either side of the center of damage, depending upon the degree of the damage to each of them. In addition, the web exhibited a dish-like depression towards the bottom flange at the center of damage. The depression somewhat resembled a folding of the web about its centerline with its concave surface towards the load. Due to its composite construction with the concrete slab, no deformations occurred in the top flange. Visual examination of the girder did not disclose any cracks or tears. However, a localized dent was detected on the bottom flange at the point of load contact.

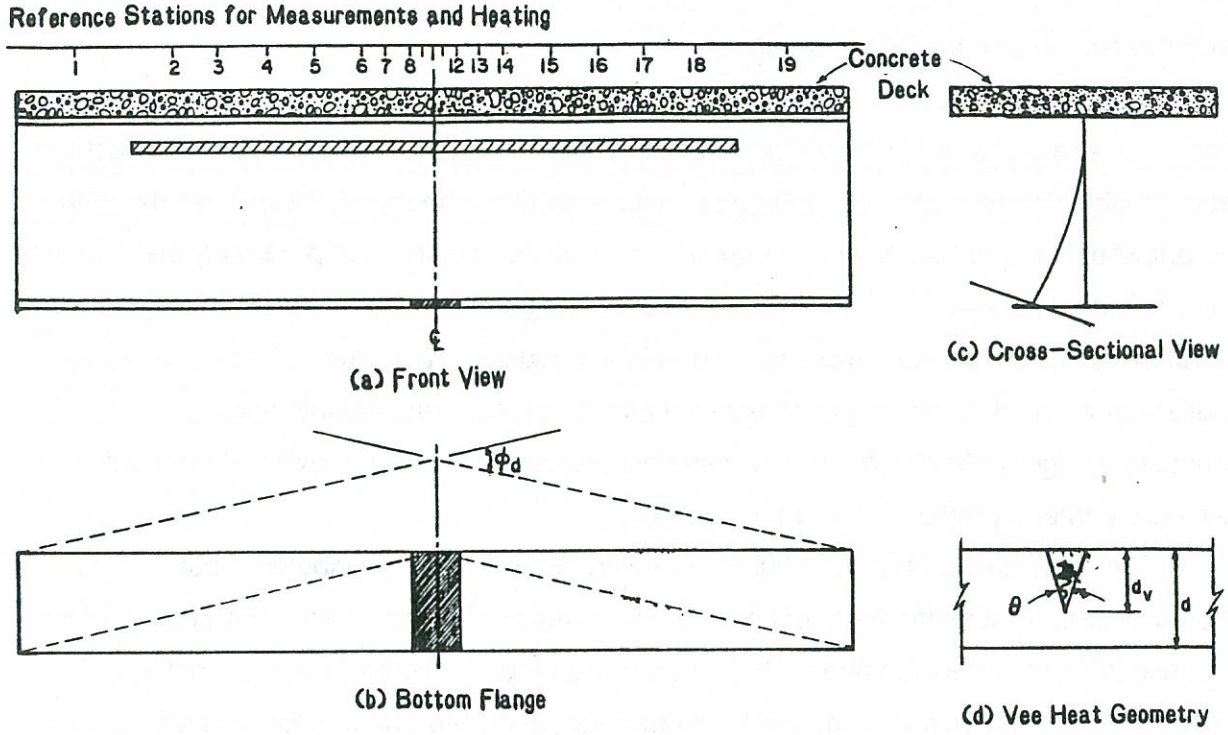

Figure 57. Deformed shape, yield zones and measuring location for the W24x76 composite girder.

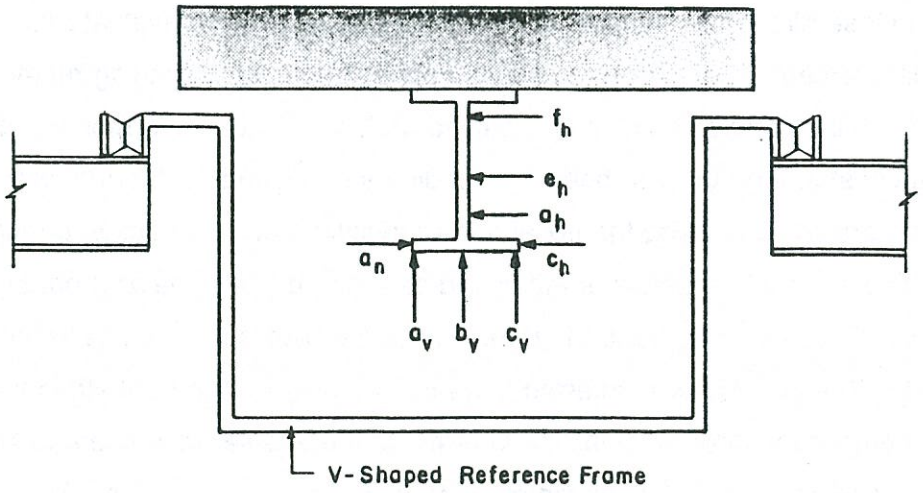

Figure 58. Cross-section of slab-girder syste measurement reference frame and measured points.

Identification of the Variables involved

It is apparent from the available research evidence that the heating temperature, vee depth, vee angle and the constraining forces are the fundamental parameters that affect the heat-straightening response of damaged structural steel members. Sufficient experimental and analytical information have been presented in earlier chapters for predicting the influence of the heating temperature, vee depth and the vee angle on the heat-straightening process. Therefore, these parameters were not varied in the course of this study. The study was focused on evaluating the role of constraining forces in the heat-straightening repair of composite bridge girders. The term 'constraining forces' refers to the external restraints, as well as, the internal redundancy of the member.

The laboratory studies on plates and rolled shapes have contributed a substantial amount of data to quantify the effect of external restraining forces on the heat-straightening response of such simple elements. However, because of the complicated geometry and boundary conditions involved, the analytical models developed on the basis of these data show serious limitations when used to forecast the response of full scale composite girders. It has been conjectured that the indeterminacy associated with the structural configuration of these members affects their heat-straightening response. When external restraining forces are applied, the internal redundancy influences the transmission of these forces to the heated areas within. A comparative study of the heat-straightening behavior of two composite girders of different geometries was conducted (W10x39 and W24x76) for assessing the role of indeterminacy in these girders. A variable jacking force was applied to evaluate the effect of external restraining forces. The jacking force was applied to create a bending moment in the bottom flange about its strong axis in the vee heated region. The bending moment acts as a positive external constraint on the vee heat by impeding the longitudinal thermal expansion during the heating phase, increasing the upset and producing more contraction during the cooling phase. The external constraint is measured as a non-dimensionalized parameter, which is a ratio of the bending moment, M, at the vee to the plastic moment capacity of the bottom flange, M_p. The parameter is referred to as the load ratio. The heat-straightening response of the composite girder is quantified in terms of the angular movement of the bottom flange at the center of damage. This movement is termed the plastic rotation. These tests were designed to evaluate the relationship between the load ratio (as the independent variable) and the plastic rotation (as the dependent variable) for the given geometry of the girder.

Case SB-5: Third damage and repair of W24x76 composite girder. The same W24x76 girder, which was damaged and heat-straightened twice previously for test cases SB-3 and SB-4, was redamaged. Damaged was induced by statically loading the girder to obtain a lateral plastic deformation of 5 inches at the midspan. A maximum concentrated load of 40 kips was applied. The damage pattern observed was similar to the characteristic pattern described in Figure 57. The failure mechanism consisted of yield zones in the web as well as the bottom flange. The yield zone in the bottom flange was observed over a span of 1 ft. The yield line in the web occurred 2 inches below the top flange and extended over a distance of 15 ft. Both the yield zones were located symmetrically about the center of damage.

A total of thirty heating cycles were conducted. The progressive movement of the bottom flange in the course of these cycles is shown in Figure 59. In all the heating cycles a 30 degree vee angle, three-quarters depth vee, and a heating temperature of 1200°F was maintained. The temperature was regulated using a contact pyrometer. The heating cycles were classified into heating sequences on the basis of the load ratio/heat pattern combination applied. The heat patterns generally consisted of vee heat in the plastically deformed portion of the bottom flange accompanied by a line heat applied to the yield line in the web. This heat pattern was established as one of the most effective based on the past heat-straightening experiments on composite girders. Two single orifice oxyacetylene torches were used for heating. A sufficient number of heating cycles were conducted in each sequence to establish a pattern of behavior.

In the first heat sequence eleven heating cycles were performed with zero load ratio. No jacking forces were used for this sequence. The vee heats were confined to the middle 6 inches of span between the measuring points 10 and 12. The location of the vee heats was varied in this zone to minimize the effect of residual stresses developed in the previous heating cycle. The vee heat were applied on the lower face of the bottom flange. The line heats were applied on the convex surface of the web between the measuring points 2 and 18 for the first eight heating cycles. The heating was conducted by two trained operators. The yield line on the web was heated first with the two operators moving the torch from each end towards the center. A small distance away from the center, one of the operators discontinued the line heat and started the vee heat on the bottom flange. The other operator continued the line heat, with the result that both the vee and the line heats were completed simultaneously. After eight heating cycles, the minor axis curvatures in the web were again computed at various points along the length to determine the remaining extent of the yield line. The length of the line heat was adjusted in the subsequent heats to ensure that only those portions of the

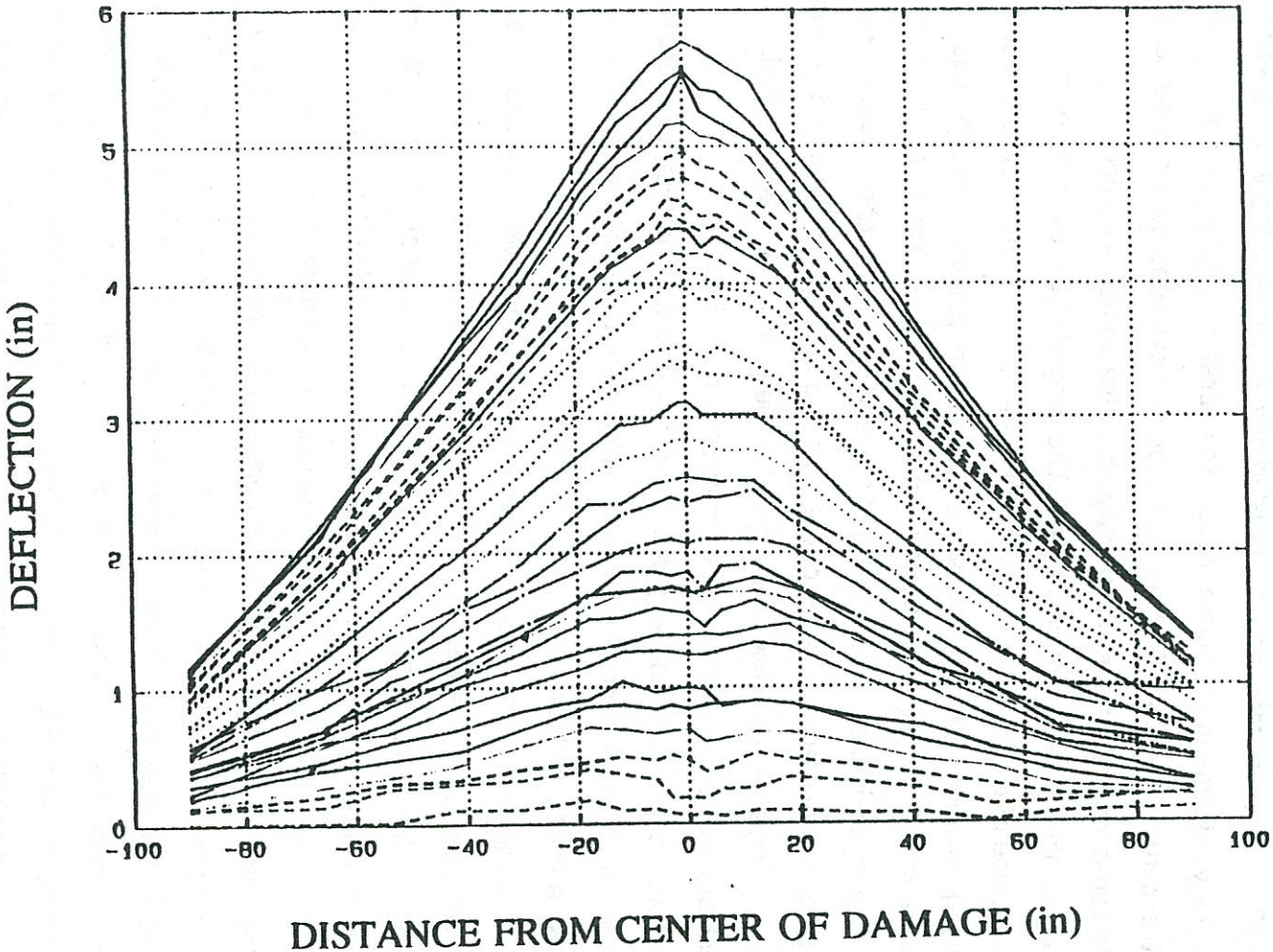

Figure 59. Plot of bottom flange movement for thirty heating cycles on SB-5 girder specimen.

web were heated which still showed plastic curvatures. For the remaining heating cycles, therefore, the line heat was applied between measuring points 4 and 16. An average plastic rotation of 3.550 millirads was observed for the eleven heating cycles conducted in the first sequence. The plastic rotations observed for the individual cycles are recorded in Table 54.

The second heat sequence was performed with a load ratio of 0.50. In order to avoid interference with the vee heat, the jack was installed one foot away from the center of damage and the pressure was adjusted accordingly to obtain the correct load ratio at the center of damage. Nine heating cycles were conducted in this sequence. The reading on the pressure gauge was recorded at the end of the cooling phase for each heating cycle. The heat pattern used in the previous sequence was repeated. The line heat was applied to the reduced yield line on the web, identified at the end of the eighth heating cycle of the previous sequence. The plastic rotations for each cycle of the second sequence are also shown in Table 54. An average plastic rotation of 4.005 millirads was observed per heating cycle. The pressure gauge reading registered an increase just after the heating was completed. However, a net decrease was recorded after the cooling phase. This was expected and is explained in terms of the reverse movements of the bottom flange during the restrained expansion stage and the subsequent larger positive movements during the unrestrained contraction stage.

At the end of nine heats of this sequence, it was observed that the web had developed considerable bulging about the vertical minor axis, in the lower half of its depth, extending over a central span of 18 inches. It was suspected that the incompatible longitudinal contraction in the bottom flange and the web, at the location of the vee, had caused the buckling. The buckling in the web raised a cautionary concern about the possible impedance to the straightening effect offered by the consequent residual stresses. It was decided to apply half-depth strip heats on the web at the location of the vee heat. The width of the strip heat was kept equal to the width of the vee at the flange fillet. All the subsequent heating cycles with 0.5 load ratio included the rectangular heats. These were categorized as heat sequence 3. Nine heating cycles were conducted in this sequence. The length of the yield line was evaluated again and the line heat was curtailed further. The average plastic rotation achieved per cycle was 3.75 millirads, which is six percent less than that for sequence 2. The individual plastic rotations are recorded in Table 54. The application of the rectangular heats did not improve the plastic rotations. However, they were effective in relieving the buckling in the web. At the end of ten cycles of sequence 3, the girder was practically restored to its original configuration, as can be seen from the plot of the movement of the bottom flange during the first three sequences (Figure 59). The plastic curvatures in the bottom flange as

Table 54. Summary of experimental results for Girder SB-5 under influence of each heating cycle.

Heating Sequence (1)	Heating Cycle (2)	Vee Heat Location (point number) (3)	Line Heat Location (point number) (4)	Load ratio (M/M_p) (5)	Plastic Rotation/Vee radx10^3 (6)
1	1	10	2-18	0.0	9.221
1	2	11	2-18	0.0	3.740
1	3	10/11	2-18	0.0	3.158
1	4	10	2-18	0.0	4.240
1	5	9/10	2-18	0.0	2.328
1	6	9	2-18	0.0	2.827
1	7	10	2-18	0.0	4.658
1	8	11	2-18	0.0	-0.582
1	9	10/11	4-16	0.0	4.242
1	10	11	4-16	0.0	1.331
1	11	10	4-16	0.0	3.910
				Average	3.552
2	1	9	4-16	0.50	7.490
2	2	11	4-16	0.50	-2.164
2	3	9/10	4-16	0.50	8.823
2	4	10/11	4-16	0.50	3.830
2	5	9	4-16	0.50	5.579
2	6	10	4-16	0.50	5.247
2	7	9	4-16	0.50	2.998
2	8	11	4-16	0.50	5.331
2	9	9	4-16	0.50	1.499
				Average	4.005
3	1^R	10	5-15	0.50	4.415
3	2^R	9	5-15	0.50	1.999
3	3^R	9/10	5-15	0.50	2.999
3	4^R	10/11	5-15	0.50	5.582
3	5^R	10	5-15	0.50	9.165
3	6^R	9/10	5-15	0.50	-1.583
3	7^R	10/11	5-15	0.50	2.666
3	8^R	10/11	5-15	0.50	6.666
3	9^R	9	5-15	0.50	0.917
3	10^R	9/10	5-15	0.50	5.333
				Average	3.750

R - Rectangular heat applied to the web
x/y - Vee heat applied between pointe x & y

well as the web were corrected. Only a minor local kink remained in the bottom flange at the center of damage. A local bulge was also discernible in the web due to the buckling encountered in sequence 2.

Case SB-6: Fourth damage and repair of W24x76 composite girder. The same W24x76 girder was redamaged statically by a midspan jacking load using the procedure previously described. The maximum load required was 40 kips. A permanent lateral deflection, 4.5 inches in magnitude, was obtained at the center of damage. The resulting damage pattern was similar to the previous case (Figure 57). The heating patterns and repair procedures were identical to those used in sequence 2 of case SB-5. The rectangular heats were not included in the heat pattern, as the damage had stretched the web to its unbuckled configuration. The damage was assessed for the identification of the yield zones and the location of the vee and line heats decided accordingly. A load ratio of 33 percent was selected for evaluation. The decision to use this particular load ratio was made for two reasons: (1) To establish a pattern of variation in the heat-straightening response of the girder with the load ratio and, (2) To compare the results with those obtained from the heat-straightening tests performed previously in the project by different operators under same load ratio. The purpose was to check for inconsistencies due to the human factor involved. Nine heating cycles were performed in this sequence. The progression of the bottom flange movement with each cycle is illustrated in Figure 60. In the course of the ninth heating cycle, a loud snapping sound was heard. When the girder was inspected on completing the cycle, a distinct longitudinal crack was noted in the web at the location of the yield line. The crack was formed on the convex side (which was not line heated), extending over a length of 5 inches with a maximum opening 1/16 inch wide. The crack is shown in Figure 61. The beam was replaced by a new W24X76 girder. The results from the ninth heating cycle were discarded. Since sufficient number of heating cycles had already been completed for evaluating the response of the girder under 33 percent load ratio, it was decided to terminate the sequence. The plastic rotations obtained as a result of the first 8 heating cycles are represented in Table 55. The average plastic rotation for the sequence was 4.817 millirads.

Case SB-7: Damage and repair of the new W24x76 girder. The newly installed W24X76 composite girder was damaged by a midspan static load to obtain the characteristic damage pattern. The resulting deformations were analyzed to determine the extent of the yield zones in the web and the bottom flange. The repair was conducted using the same

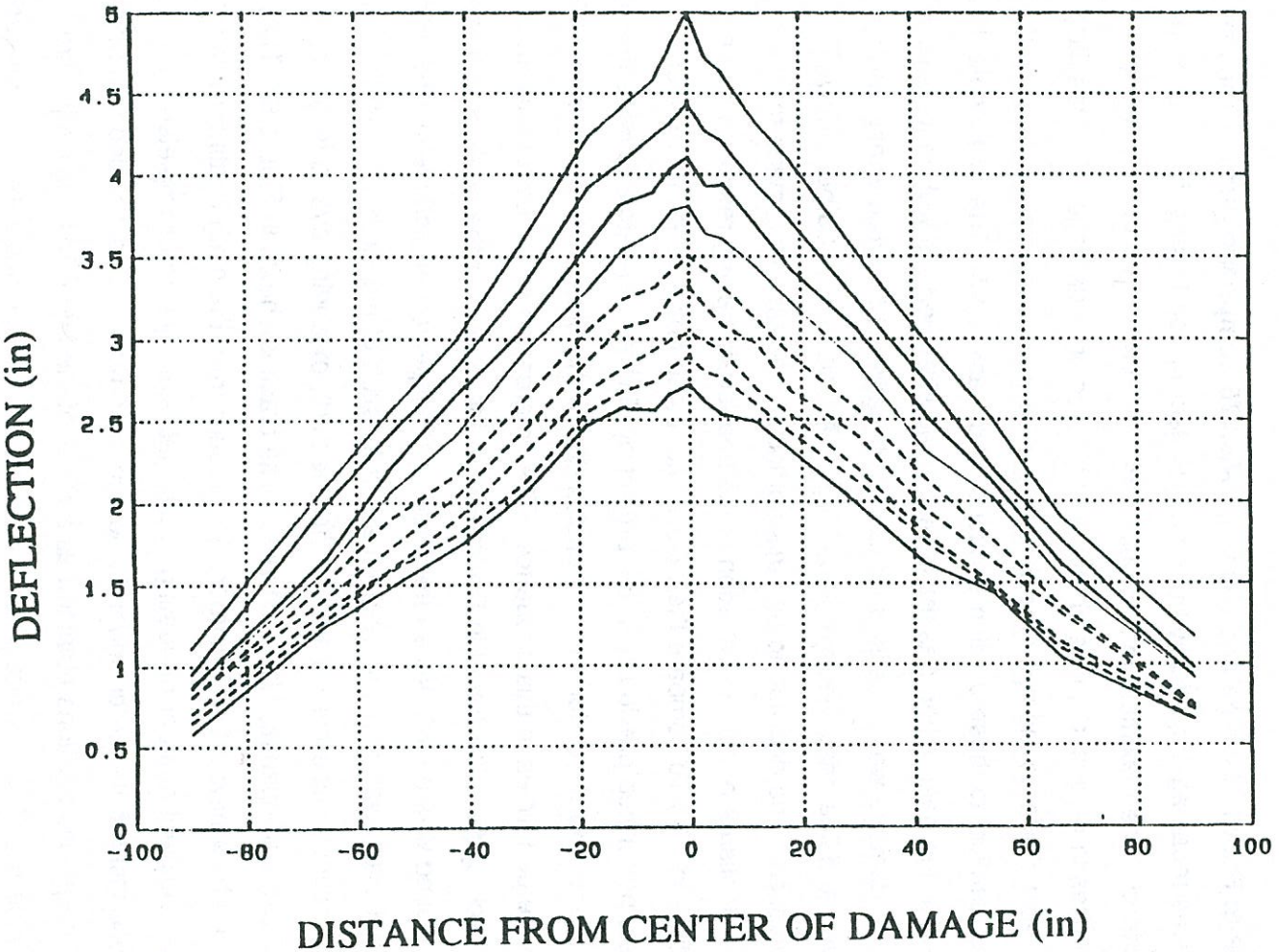

Figure 60. Plot of bottom flange movement for nine heating cycles on SB-6 girder specimen.

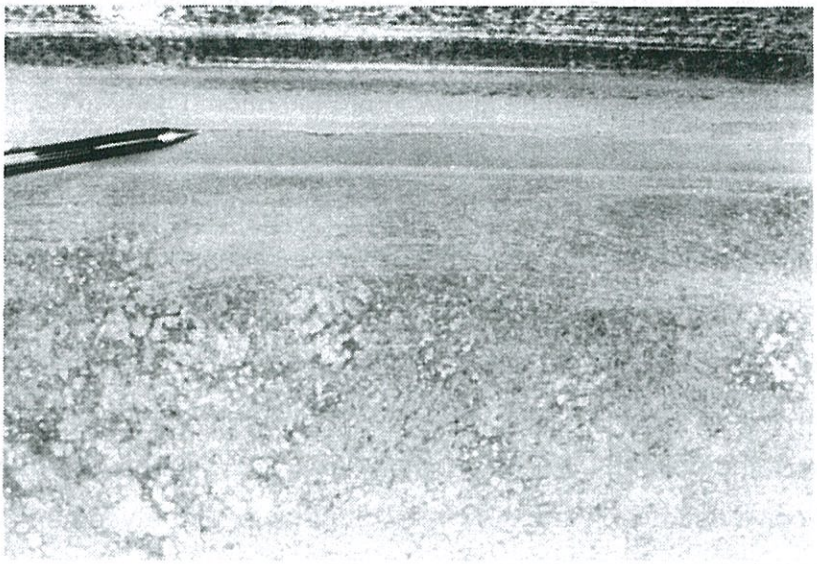

Figure 61. View of the crack of SB-6.

Table 55. Summary of Experimental Results for SB-6 under the influence of each heating cycle.

Heating Sequence	Heating Cycle	Vee Heat Location (point numbers)	Line Heat Location (point numbers)	Load Ratio (M/M_p)	Plastic Rotation/Vee radx10^3
(1)	(2)	(3)	(4)	(5)	(6)
4	1	10	2-18	0.33	8.235
4	2	9	2-18	0.33	4.243
4	3	10	2-18	0.33	6.075
4	4	10	2-18	0.33	6.659
4	5	11	2-18	0.33	4.829
4	6	10	2-18	0.33	2.082
4	7	9	2-18	0.33	4.164
4	8	11	2-18	0.33	2.248
				Average	4.817

method. The applied load ratio was increased to 75 percent. This load ratio was rather high, as it had seldom been used in laboratory studies. It was applied in an attempt to find the limiting load ratio, that would replicate the 'hot mechanical straightening' phenomenon encountered in the past studies on W10X39 composite girder. The sequence consisted of eight heating cycles. The progressive straightening of the bottom flange in each of these cycles is shown in Figure 62. The plastic rotations achieved in the individual cycles are tabulated in Table 56. As expected, the plastic rotations encountered in these sequences were abnormally high. The average plastic rotation for the sequence was calculated to be 11.474 millirads. Thus, the average plastic rotation increased by 124 percent on raising the load ratio from 50 to 75 percent. During the eighth heating cycle, the bottom flange suddenly fractured in the early part of the vee heat. The crack initiated on the convex longitudinal edge of the bottom flange at the point of application of the vee heat. It had a maximum opening 1/16 inch wide and continued over a length of 1" from the apex of the vee perpendicular to the flange edge. The crack is shown in Figure 63.

Case FLD-1: Field Repair of Crowley Bridge. In the course of the research project, a field repair of a damaged bridge girder was conducted. The damaged girder was one of the four primary supporting girders in a 75 ft. span bridge on highway La 91 near Crowley in Louisiana. The girders, which ran parallel to the 75 ft span of the bridge, were simply supported on end piers with their top flanges compositely connected to the deck slab of the bridge. Lateral bracing was provided by diaphragms located at the ends and quarter points along the span (See Figure 64a for beam layout). The diaphragms were connected between the webs of the adjacent girders. The damaged girder, which was the west outside girder over the eastbound lane, was hit on its lower flange by an over-height vehicle moving east in the right lane of the underpass beneath (Figure 65).

A traffic control plan was designed to ensure the convenience and safety of the commuters. A lift was used to gain access to the damaged area. Damage appraisal of the W33x241 girder showed that the bottom flange had suffered a lateral plastic displacement of 2.95 in. towards the adjoining girder (Figure 65). The center of damage was located 22.75 ft. from the south end pier. The damage assessment also revealed that the first intermediate diaphragm (d_1) from the south end pier was severely distorted. A large local bulge had also formed in the web at the location of the damaged diaphragm. The bulge started 6 inches below the top flange, extending over a depth of 17 inches and a length of 18 inches. The damaged diaphragm was removed prior to starting the repair because of two reasons:

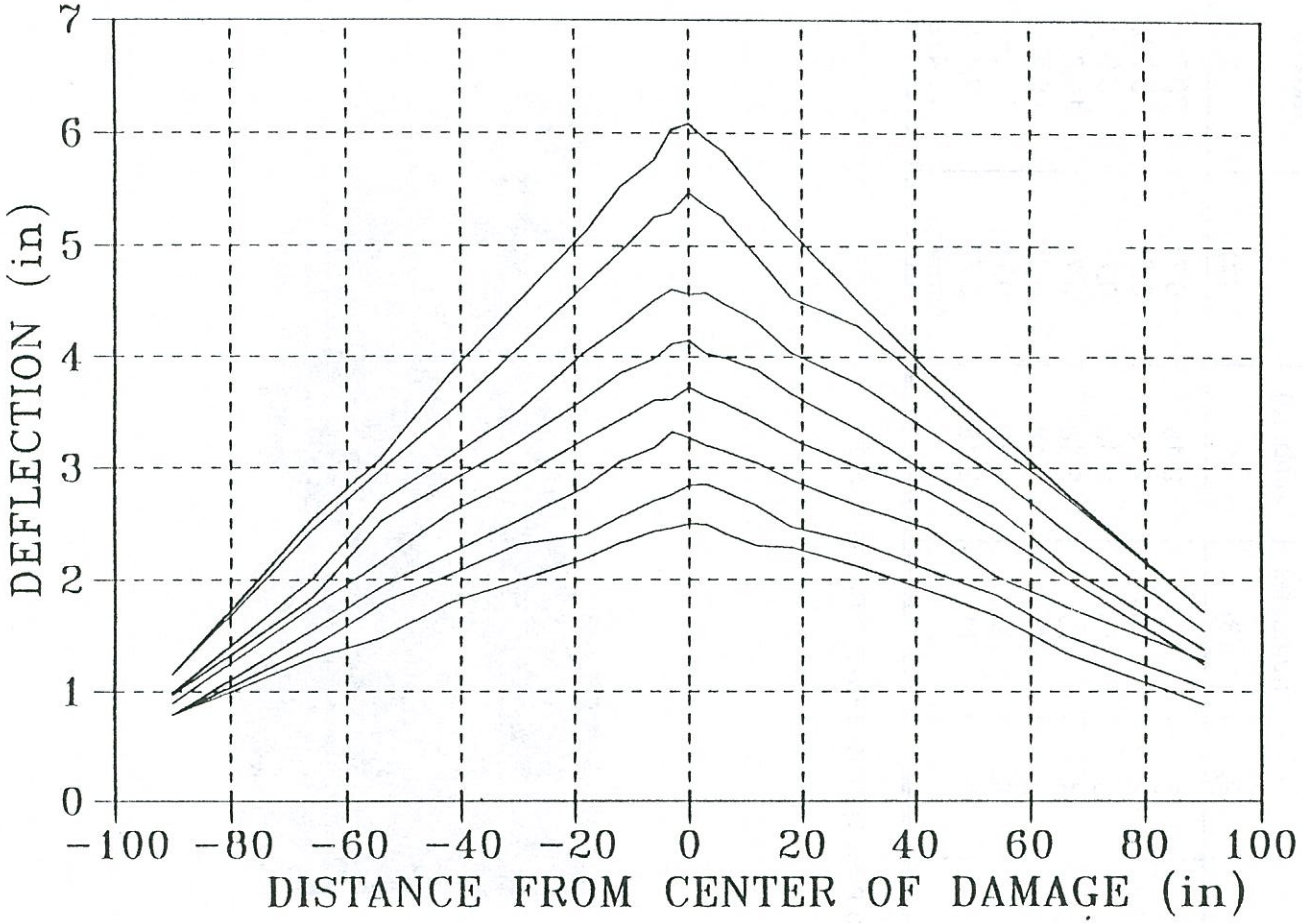

Figure 62. Plot of bottom flange movement for nine heating cycles on SB-7 girder specimen.

Table 56. Summary of Experimental Results for SB-7 under the influence of each heating cycle

Heating Sequence (1)	Heating Cycle (2)	Vee Heat Location (point numbers) (3)	Line Heat Location (point numbers) (4)	Load Ratio (M/M_p) (5)	Plastic Rotation/Vee radx10^3 (6)
5	1	10	2-18	0.75	20.367
5	2	10	2-18	0.75	8.736
5	3	10	2-18	0.75	8.904
5	4	10	2-18	0.75	10.823
5	5	9/10	2-18	0.75	6.412
5	6	9	2-18	0.75	11.661
5	7	11	2-18	0.75	13.413
				Average	11.474

x/y - Vee heat applied between points x and y

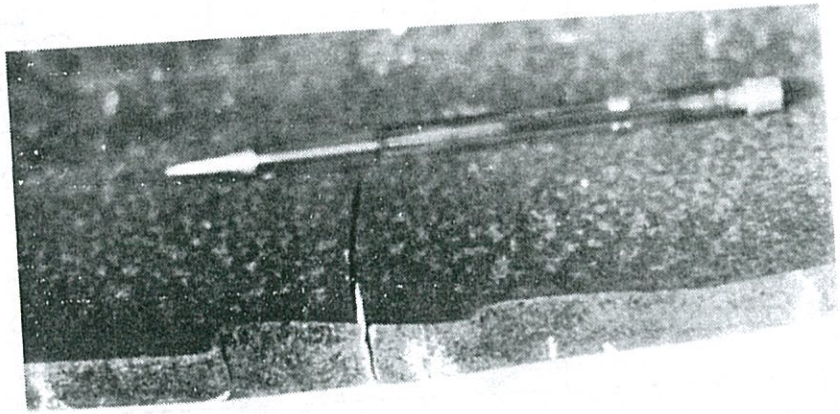

Figure 63. View of the crack in SB-7.

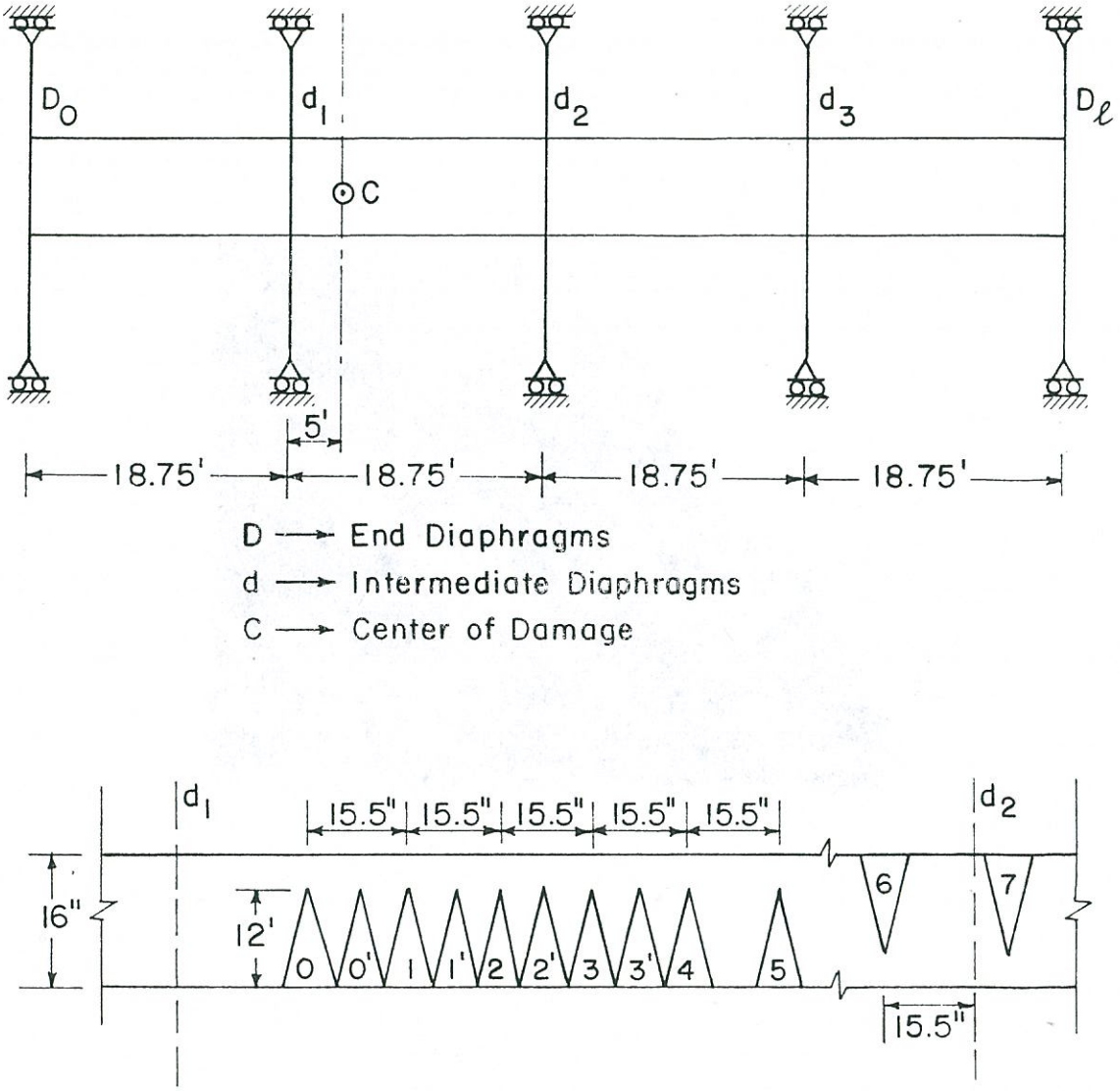

Figure 64. Layout of the damage W33x241 composite girder on Crowley bridge showing the location of the center of damage and vee heats.

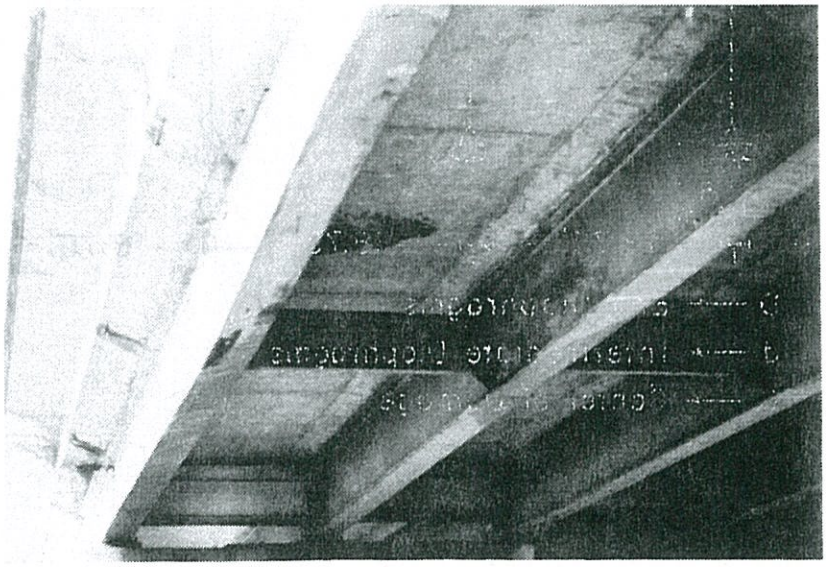

Figure 65. Photographic view of the damaged composite girder in Crowley Bridge.

(1) Since the diaphragm was too seriously damaged to be repaired, it was decided to replace the diaphragm. (2) After the removal of the diaphragm, the girder exhibited an unbraced span of 37.50 ft. A longer unbraced span was desirable for the repair, as it reduced the counter-productive redundant forces associated with the lateral bracings. The other diaphragms were still functional. The girder was laterally braced at the mid-point (d_2) and only one quarter point (d_3) at the time of repair. The deflected shape of the bottom flange resembled that of a continuous beam supported at the location of the diaphragms. The bottom flange in the adjacent unbraced spans was curved in the opposite direction. However, plastic curvatures were observed only near the center of damage in the larger unbraced span. The bottom flange in the other spans showed compatible elastic deformations.

A jacking force of 12,900 lbs was applied 2 ft away from the center of damage. Based on the unbraced span of the girder, this force corresponded to a load ratio of 0.25 on the damaged girder. The bottom flange was mostly heated at two locations, about one foot apart, in the plastically deformed regions (Figure 64b). Ten heating cycles were conducted on the damaged girder. For the first eight heating cycles, vees of three-quarters flange depth and 30 degree angle were used. In the last two cycles, the vee angle was varied to 45 degree. Both the top and bottom of the flange were heated to ensure uniform temperature distribution through the thickness. The line heats were not performed, since no yield line could be observed on the web. The plastic movements achieved were measured carefully at the center of damage with reference to a string stretched between the end piers. The measurements were taken at the end of each heating cycle. Good plastic movements were observed for the first three heating cycles, after which they started diminishing. After the fifth heating cycle the bottom flange did not move, regardless of the number of heating cycles applied. It was surmised that the redundant forces associated with the lateral bracing were imposing a negative constraint on the straightening effect. Therefore, it was decided to revise the heating pattern at the end of the eighth heating cycle. Two reverse vee heats (vees numbered 6 and 7 in Figure 64b) were added, one on each side of the adjoining intermediate diaphragm. The reverse vee heats were predicted to relieve the counter-productive redundant moments at the braced cross-section. However, no further plastic rotation was obtained in the next two heating cycles. The final deflection of the bottom flange at the end of the tenth heating cycle was measured as 1.83 in. An average movement of only 0.1 inch per cycle was obtained. The straightening achieved in the individual heating cycles is presented in Table 57. The progressive movement of the bottom flange is illustrated in Figure 66.

Table 57. Summary of Experimental Results for SB-8 under the influence of each heating cycle

Heating Sequence (1)	Heating Cycle (2)	Vee Heat Location (point numbers) (3)	Line Heat Location (point numbers) (4)	Load Ratio (M/M_p) (5)	Plastic Rotation (inch) (6)
1	1	1	-	0.25	0.11
1	2	1,3	-	0.25	0.34
1	3	1,3	-	0.25	0.58
1	4	0,2	-	0.25	0.10
1	5	1	-	0.25	0.0
1	6	2,3	-	0.25	0.15
1	7	0',1',2'	-	0.25	0.10
1	8	4,5 6,7 0',1'	-	0.25	0.0
1	9*	6,7 1,3	-	0.25	0.0
1	10*	2,5	-	0.25	-0.28
				Average	0.11

*45° 3/4 depth vee

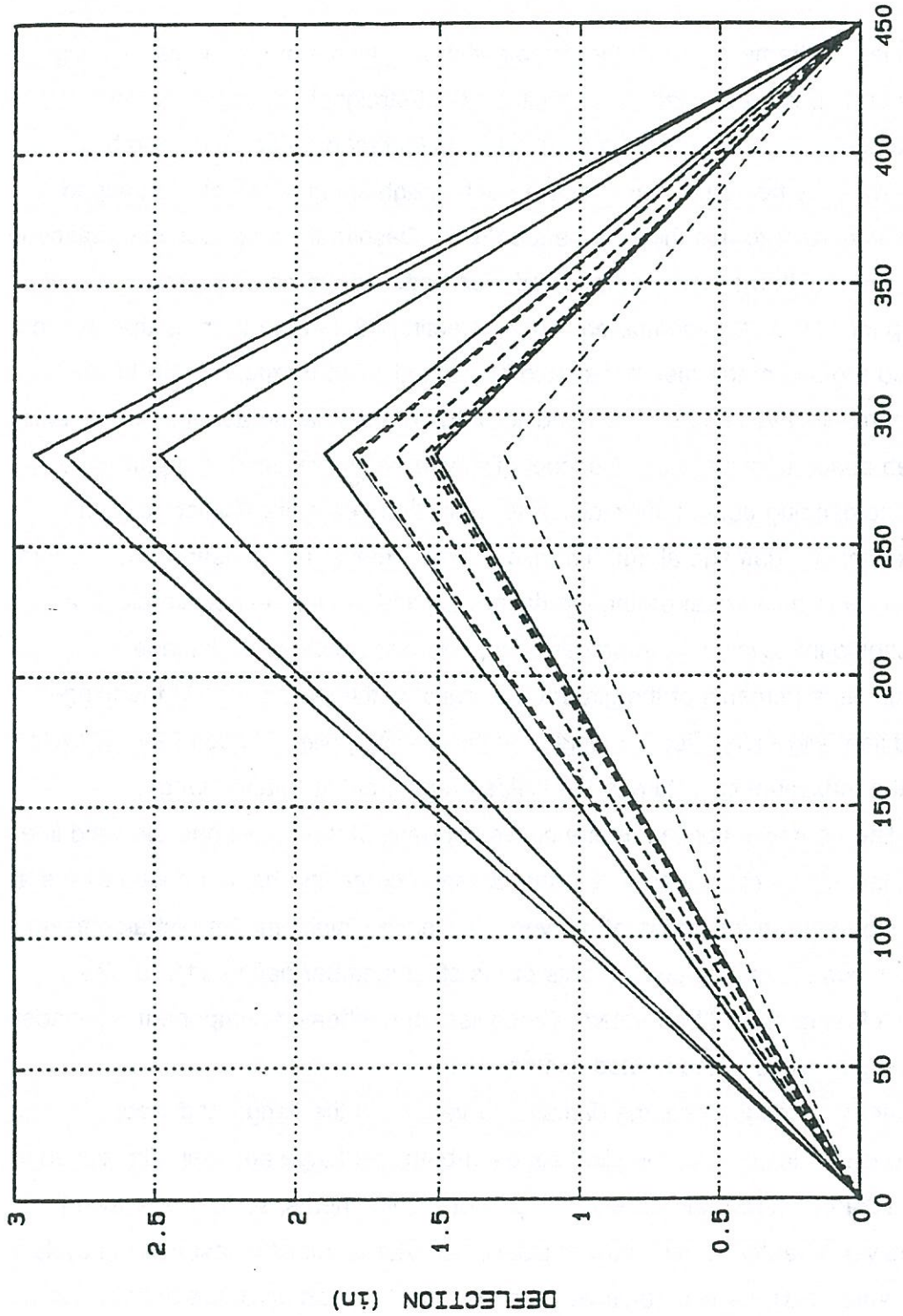

Figure 66. Bottom flange movement for ten heating cycles for FLD-1 girder specimen.

Evaluation of Factors Affecting Heat-Straightening Behavior of Composite Girders

Heat Patterns

The term 'Heat Patterns' refers to the combination and layout of vee heats, rectangular heats, edge heats and spot heats used to conduct the heat-straightening repair of the damaged steel member. Depending on the damaged configuration of the steel member, different heat patterns may be used. For effective heat-straightening repair of a damaged steel member, it is important to use the right heat pattern. Despite their obvious importance in heat-straightening, heat patterns have not received much attention in past research.

The basic principle to be remembered, when selecting the heat pattern, is that all the plastically deformed regions of the member should be heated. The damage to the W24x76 composite girder primarily involved inelastic bending of the bottom flange about its major axis and that of the web about its minor axis. Conceptually, vee heats are used to repair plate elements with plastic bending about their major axis, while line heats are applied to repair plate elements with flexural damage about their minor axis. Hence, a vee heat on the bottom flange in conjunction with a line heat on the top flange, applied to their respective plastically yielded portions, should intuitively be the proper heat pattern to repair such damage.

After careful measurements of the girder deformations, the yield zones in the flange and the web (yield line) were identified. A single vee heat was applied in each heating cycle, at the location of the maximum curvature in the yielded region of the bottom flange. Simultaneously, a line heat was applied on the convex surface of the web along the yield line. From the past studies, it was concluded that in the absence of the line heat, the web exerts a negative constraining force on the action of the vee and hence inhibits the heat-straightening repair. In general, if two interacting components of the steel member have suffered plastic deformations, both of them should be heated. Otherwise, the unheated component will hinder the heat-straightening process of the heated component.

As the girder was straightened, the damage curvatures in the flange and web decreased. With each heating cycle, the yield zones in both the flange and web diminished in length. Care was taken to continually adjust the span of the line heats, so that only those portions of the web were heated which showed plastic curvatures after the last heating cycle. Similarly, it was ensured that the vee heats were confined to that portion of the bottom flange which remained yielded. As indicated by past studies, application of heat to elastic curvature areas can produce some reverse curvature in these areas. Some important facts about heat

pattern, that were established in previous studies (Avent and Fadous, 1987, 1988, 1989; Fadous, 1987) on composite girders were used and verified in the present study:

(1) All the plastically deformed regions of the composite girder should be heated.

(2) A line heat along the yield line on the web mitigates the negative constraining effect imposed by the web on the bottom flange vee heat and hence expedites the straightening process. An effective heat pattern in the heat-straightening repair of a composite girder comprises vee heats and line heats applied to the plastically deformed regions of the flange and web respectively.

(3) Heat should be applied to only those regions which suffer plastic deformations.

The only change of heat patterns introduced in this study was the inclusion of a half-depth web strip heat during one sequence. The purpose of this heat was to reduce the differential shortening between web and flange. It has been shown by Robinson (1991) that significant shortening occurs during the heat-straightening of rolled shapes. It has also been shown by Robinson that the amount of shortening is similar for both the three-fourth and full depth vee across the flange. In either case, as the flange shortens, compressive stresses are induced in the web. Web buckling eventually results as observed in test specimen SB-5. By heating the web with a half-depth strip, the web can deform and relieve some of these stresses. The application of strip heats on the web in sequence 3 did not influence the average plastic rotations appreciably. However, they did tend to reduce the buckling of the web near the center of damage due to the unequal straightening of the bottom flange and web. More research data is required to evaluate the precise role of rectangular heats in the heat-straightening of composite girders.

Restraining Forces

Restraining forces play a significant role in affecting the heat-straightening process. Depending on the external loading and the structural configuration of the member, constraints are induced in the heated area of the member. The term 'restraining force' is used to refer to these constraints which interact with the heating pattern to have a positive or negative effect on the heat-straightening mechanism. Accordingly, the restraining forces may act to expedite or impede the heat-straightening repair of the member. The simplest way of providing this constraint is to allow the unheated metal within the member to restrict thermal expansion, by using a suitable heat pattern (as in the case of a vee heated plate). This is a form of an internal constraint. Internal constraint may also be imposed by the self-weight, axial loading or the statical indeterminacy of the member. These internal constraints may be conducive or

counter-productive to the heat-straightening mechanism of the member. Frequently, external restraining forces are used to complement or even substitute for the internal constraints required for the heat-straightening phenomenon. In any case, given the same magnitude and direction of the constraint, the resulting mechanism is identical and theoretically yields the same plastic rotations or movements.

The importance of restraining forces in the heat-straightening process has been recognized in the field for many years. Hence, jacking forces have frequently been used to enhance the heat-straightening repair of a wide range of damaged structural steel members. It can be seen that sufficient experimental and analytical information is presently available to predict the heat-straightening response of plates in the presence of external restraining forces. More often than not, the damaged steel member exhibits an internal redundancy due to its geometry and boundary conditions. Constraint is imposed on the heat-straightening mechanism due to this redundancy in the member. A composite structural steel girder is a common example of such a member. These tests were designed to evaluate the effect of external restraining forces on the heat-straightening behavior of such members.

The tests conducted on the W 24x76 composite girders have been classified into five heat sequences according to the load ratio/heat pattern applied during heating. The five heat sequences included apparent load ratios of 0.0, 0.5, 0.75 and 0.33 in that order. Subsequent to the completion of these tests, samples from the test girders were submitted for strength analysis to verify the yield strength of the material. The report of strength analysis ascertained that the actual yield strength of the material differed from the nominal value prescribed for the girders (36 ksi). The applied load ratios were re-evaluated taking into account the actual values of the yield stress. Figure 67 shows the plots of the applied load ratios (based on actual yield stress) versus average plastic rotations for various heat sequences conducted on the W24x76 as well as W10x39 composite girders. The average values for each load ratio were connected with a straight line. From a previous study (Boudreaux, 1987), the relation between the load ratio and the average plastic rotation was found to be fairly linear for plates. The test results obtained for composite girders in this study follow the same pattern with one important difference. While the data points corresponding to 0.0, 0.255 and 0.386 load ratios, for the W24x76 composite girder, conform to the linear pattern, the data point for 0.654 load ratio is divergent. A significant increase in the observed average plastic rotation occurred on increasing the apparent load ratio from 0.5 in sequence 2 and 3 to 0.75 in sequence 4. As shown in Figure 67, the load ratio versus plastic rotation curve exhibits a sharp discontinuity at 0.386 load ratio. It can be seen that beyond this point

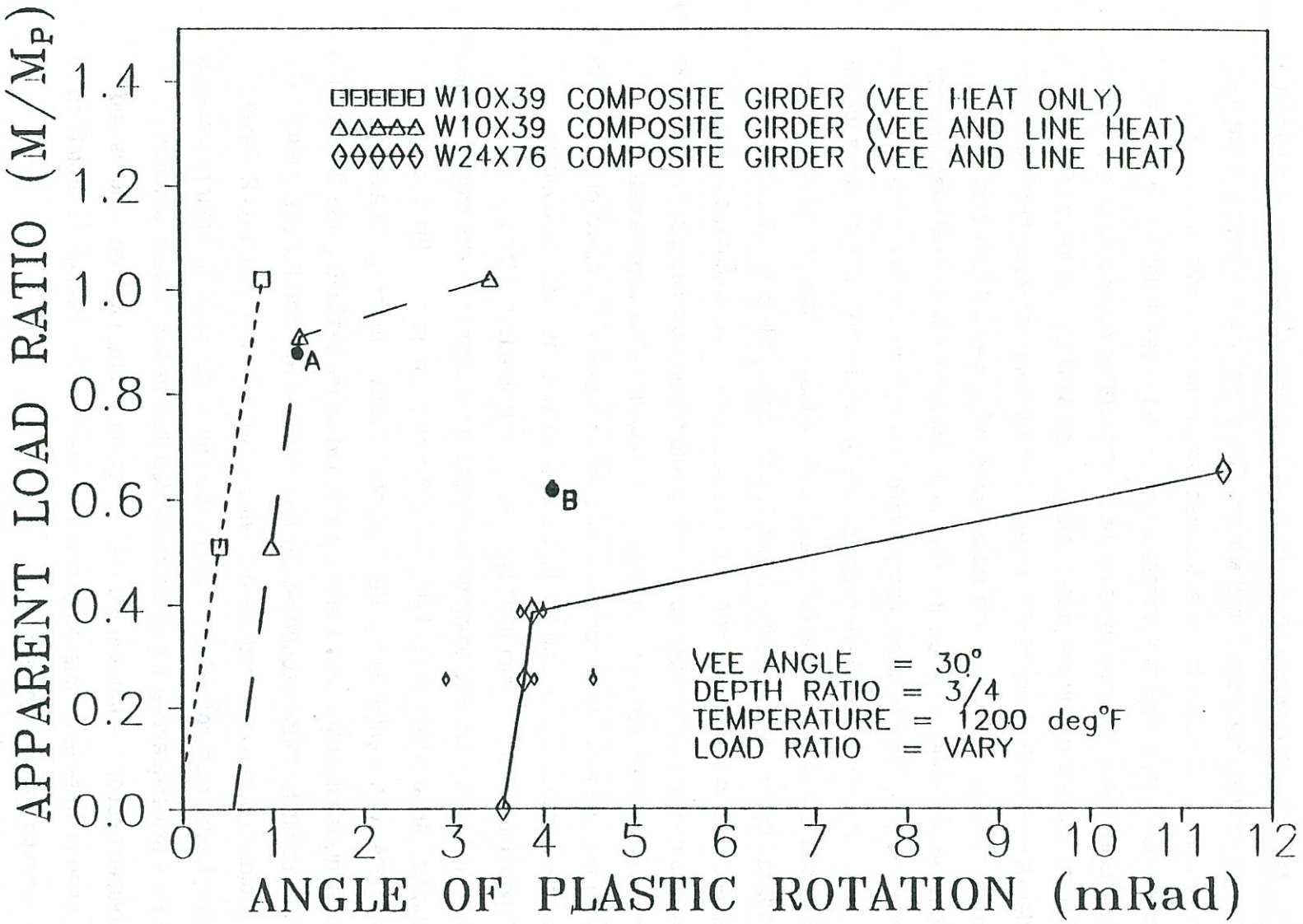

Figure 67. Apparent load ratio vs. angle of plastic rotation on the tested specimens.

of discontinuity, dramatically large plastic rotations are encountered. A similar pattern is observed for the W10x39 composite girder (with the web line heat).

The other factor which primarily affects the heat-straightening response of a composite girder is the internal redundancy caused by the interaction of the bottom flange and the web. The interaction produces redundant forces at the web-flange interface which impede the plastic rotations by acting as a negative internal constraint to the vee action in the bottom flange. A comparison of the load ratio vs. average plastic rotation curve (Figure 67) obtained for the W 24x76 composite girder in the present study to the similar curve for the W 10x39 composite girder (Avent and Fadous, 1987), reveals that the lower slopes of both the curves were almost equal. This implies that for the same increment in the load ratio, both the shallow and deep beams exhibit an equal increase in the plastic rotation. However, for zero or any given load ratio, significantly large plastic rotations were encountered in the case of the deeper beam. Thus, the two curves were nearly parallel to each other, with the curve for the deep girder displaced forward on the plastic rotation axis. It may be argued that the redundant forces produced by the web-flange interaction in composite girders, inhibit the straightening effect more in a shallow beam than in a deep beam. As discussed in the previous section of this chapter, the damage to the composite girder produces plastic curvatures in the web about its minor axis along the yield line. This plastic deformation resists any elastic bending of the web about its minor axis during the straightening process of the bottom flange. Hence, the presence of the yield line in the web tends to magnify the counter-productive redundant forces and further inhibits the straightening effect of the bottom flange vee. By using a line heat on the web along the vee heat in the bottom flange, these inhibiting forces are mitigated. An appraisal of the influence of the web line heat (on the heat-straightening response of the composite girder) was obtained by comparing the average plastic rotations achieved in sequences 1 and 4 performed on the W10x39 girder (Case SB-1). The experimental results for these sequences are reported by Avent and Fadous (1988). The average plastic rotation observed in sequence 4, which involved a line heat, was 2.4 times that for sequence 1, which did not include a line heat on the web. Since all other parameters are common for the two sequences, it may be concluded that the line heat, in practice, increased the plastic rotation 2.4 times in the W10x39 girder. Thus, the heat patterns and jacking forces, used in these tests, interact to minimize the negative internal constraints so as to achieve the optimum straightening effect.

When applying a lateral load to the bottom flange near the center of the composite girder, the moment produced is transferred to the end reactions by two mechanisms: (1) The

bottom flange acts as a flexural beam supported at the ends and, (2) the web acts as a flexural plate (and at large deformations, a membrane plate) supported by the deck and end diaphragms. It seems intuitive that the shallower girder would have more stiffness and thus transfer a larger share of the applied load from the bottom flange than the deeper girder. The data tends to verify this observation since the load ratio has less effect on the shallow girder. By adopting a load ratio definition with the plastic moment of the bottom flange by itself in the denominator, the implication is that most of the load transfer is through the bottom flange. With the W10x39 composite girder showing relatively small plastic rotations at load ratios greater than 100%, it is obvious that the web carries a significant portion of the jacking load. A primary question then becomes: How is the distribution of jacking forces between the flange and web to be determined?

Stiffening Effect of the Web

The heat-straightening repair of a composite bridge girder (damaged by a midpoint impact load on the bottom flange) is typically conducted in the presence of an external jacking force applied on the bottom flange in the direction of the desired movement. In the past research on composite girders (Avent and Fadous, 1978, 1988, 1989), a convenient definition of the load ratio was to express the moment produced by the jacking force in terms of the plastic moment capacity of the bottom flange. This definition is misleading if the web effects are significant. The web interacts with the bottom flange in a complex or indeterminate manner and hence, the applied moments are distributed among both the bottom flange and web. In other words, the web stiffens the response of the bottom flange to the jacking force. It may be argued that only that fraction of the total bending moment which is distributed to the bottom flange provides external restraint to the vee heat. Hence, the load ratio as defined earlier for a composite girder does not reflect the moment in the bottom flange and may be considered only as an 'apparent' load ratio. It would, therefore, be more relevant to calculate the load ratio using this fractional bending moment. The load ratio, thus calculated, shall be termed as the 'effective load ratio'.

In order to evaluate the stiffening of the bottom flange due to the web in a composite girder, the load versus deflection curves for the W 10x39 and W 24x76 girders (Figure 68) were compared to the corresponding theoretical curve for an isolated plate identical to the bottom flange. The load was represented as a non-dimensionalized parameter, given as the ratio of the bending moment at the center of the damage to the stiffness of the bottom flange. The deflection was similarly represented as the ratio of the lateral displacement at the same

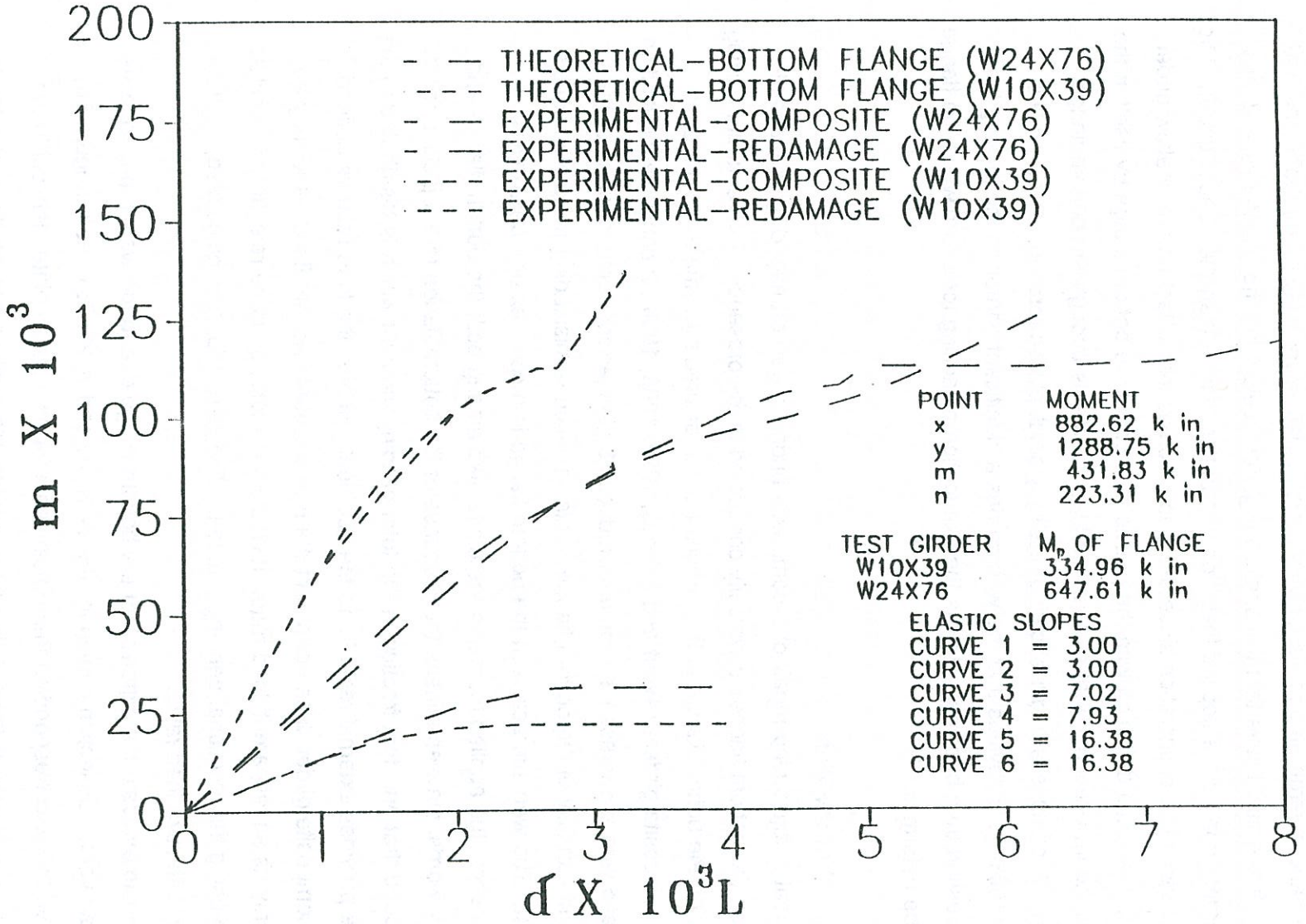

Figure 68. Non-dimensional plots of moment m vs. deflection δ.

point to the length of the member. From the plots (Figure 68), it can be seen that the deep girder exhibits greater deflections for the same load. Also, the bottom flange in the absence of the web would exhibit even higher deflections. This behavior is consistent with the precept that the stiffening effect of the web on the bottom flange should be less for deeper beams.

Hot Mechanical Straightening

A large increase in plastic rotations was observed using sequence 5, when a 65 percent load ratio was applied to the W24x76 composite girder. The average plastic rotation obtained for this load ratio was 275 percent of the value extrapolated from the straight line fit through the data points for the lower load ratios. Similar observations were made in the previous study (Avent and Fadous, 1989) for the W 10x39 composite girder. However, the shallow girder that was studied, exhibited this digression at a comparatively much higher apparent load ratio of 135 percent. These deviations were addressed by Fadous in his thesis (1987) and were attributed to a phenomenon called 'Hot mechanical straightening'. The past studies on the temperature characteristics of steel have shown that the yield stress of steel decreases with increasing the temperature. It is known from these studies that a heating temperature of 1200°F reduces the yield stress in an A-36 steel member to approximately 36% of its original value. Thus, the elevated temperatures associated with heat-straightening enable the yielding of the member at the relatively low stresses produced by the external jacking forces. In effect, during hot mechanical straightening of a steel member, the jacking forces are merely pushing the member mechanically due to the reduced yield stress.

From the non-dimensional plot of midspan moment versus deflection (Figure 68) obtained from the damage inducement process, the initial yield for the W 24x76 composite girder was encountered at an applied jacking force of 22,030 lbs. The force corresponds to a moment as high as 199% of the plastic moment capacity of the bottom flange. In other words, a load ratio of 199% is required to plastically deform the girder at room temperature. Since the yield stress of steel at 1200°F is 36% to that at room temperature, a load ratio of 0.36 times 199% should cause hot mechanical straightening, provided all the yield zones are heated. Based on these figures, a load ratio of 71% is required to produce hot mechanical straightening in the W24x76 composite girder. Experimentally, this limiting load ratio was found to be somewhat under 65% (Figure 67). An explanation along similar lines was given for the W10x39 composite girder by Avent and Fadous in their research (1988). While not a rigorous proof, this analysis provides strong evidence that hot mechanical straightening occurs if the yield strength of the girder diminishes to a value less than the external restraining force.

It is recommended that the jacking forces be measured and controlled during heat-straightening. Means of analyzing the appropriate level of jacking forces are given in later sections.

Cracking

An unusual phenomenon that was observed in the course of these experiments was the cracking in the girders subjected to heat-straightening. On the basis of the available evidence, it is premature to accurately define the mechanism of crack-formation during heat-straightening. However, some speculation may be made regarding the possible reasons that led to the formation of the cracks during these experiments. The crack that appeared in beam SB-6 occurred during the fourth damage and repair cycle. It occurred in the web parallel and adjacent to the line heat. The crack also corresponded to the tension side of the web with respect to the application of the jacking force. Robinson (1991) determined two characteristics that may explain this type of cracking. Robinson measured ductility and yield stress on repetitively damaged plates. He found that the yield stress increased and ductility decreased rather dramatically after more than two damage/repair cycles. The implication is that the stress-strain characteristics become quite similar to brittle materials. Second, Robinson's residual stress measurements indicated high residual stresses in areas of concentrated heats such as the apex of the vee. Line heats are similarly concentrated. It is therefore concluded that repetitive damage combined with high residual stresses led to a brittle failure. The behavior further verifies Robinson's conclusion that the number of damage/repair cycles on a steel member should be limited to two.

The crack in SB-7 occurred under quite different circumstances. The beam cracked during the first damage/repair cycle with the crack occurring on the tension side of the bottom flange (as defined by the applied jacking force). An unusually high jacking force was used (75% load ratio). Similar fractures have also been reported during field repairs. The most likely cause was the high jacking force combined with the somewhat reduced ductility due to the heating. This behavior reinforces the concept that the jacking forces should be evaluated analytically and never applied without a gauge to control the magnitude.

Statical Indeterminacy Due to Intermediate Diaphragms

The field repair of the composite bridge on highway La 91 offered significant research evidence about the heat-straightening behavior of composite bridge girders with lateral bracing along the span. An important hypothesis derived from this study was that the indeterminacy

associated with these bracings produces redundant forces/moments at the braced sections which provide negative internal constraints to the vee action. The idea is illustrated by considering an example of a heat-straightened composite girder with diaphragms at the ends and third points. Figure 69(a) shows the bottom flange of such a girder. The response of the bottom flange, to a vee heat applied at the center O of span BC, is analyzed by idealizing the member as a continuous beam. The beam is assumed to be supported at the location of the diaphragms in the composite girder Figure 69(b). The idealized beam is statically indeterminate to the second degree with the reactions R_b and R_c acting as the statical redundants. The redundant reactions are released to obtain a statically determinate beam (Figure 70). The released beam is analogous to a simple-span composite girder (with end diaphragms only). The effect of a vee heat at point O in the simple-span composite girder can be represented as an applied plastic rotation in the released beam (Figure 70). A rotation ϕ at point O will be accompanied by corresponding displacements bb' and cc' at points b and c respectively. The reactions and displacements are assumed to be positive in the direction shown. However, compatibility conditions in the indeterminate beam restrict the translational displacements at points b and c of the released structure. Thus, the kinematics of the problem requires that:

$$\Delta_b = \Delta_c = 0 \tag{19}$$

Intuitively, for compatibility conditions to be satisfied at these points, the redundant reactions at B and C act in a sense, so as to produce displacements in a direction opposite to that caused by the vee heat in the released structure. The indeterminate forces impose a negative internal constraint on the vee action in the form of a bending moment at the point of the vee. The bending moment acts in a direction tending to open the vee and thus works against the applied load ratio. This moment shall be referred to as the residual moment. The progressive movement of the bottom flange, due to heat-straightening, results in an accumulation of the residual moments which impede further plastic rotations. Continued heat-straightening would lead to a stage, when the residual moments balance the positive effect of both the load ratio and internal restraint. The decreased plastic rotations in the composite girder on the Crowley Bridge may be explained in terms of its indeterminate behavior. The residual moments in the bottom flange accumulated to such an extent that a resultant negative load ratio was created at the point of the vee heat which deterred further straightening.

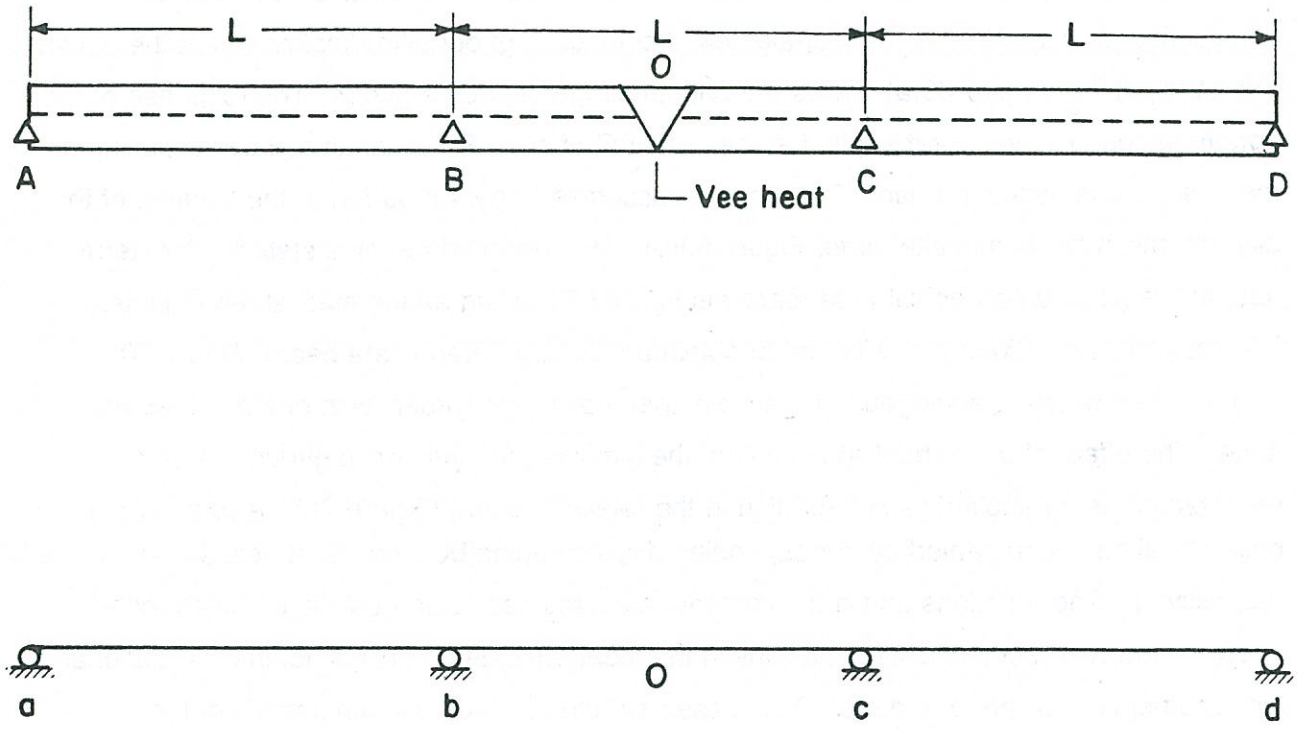

Figure 69. Bottom view of the generalized composite girder with intermediate diaphragm and the idealized continuous beam.

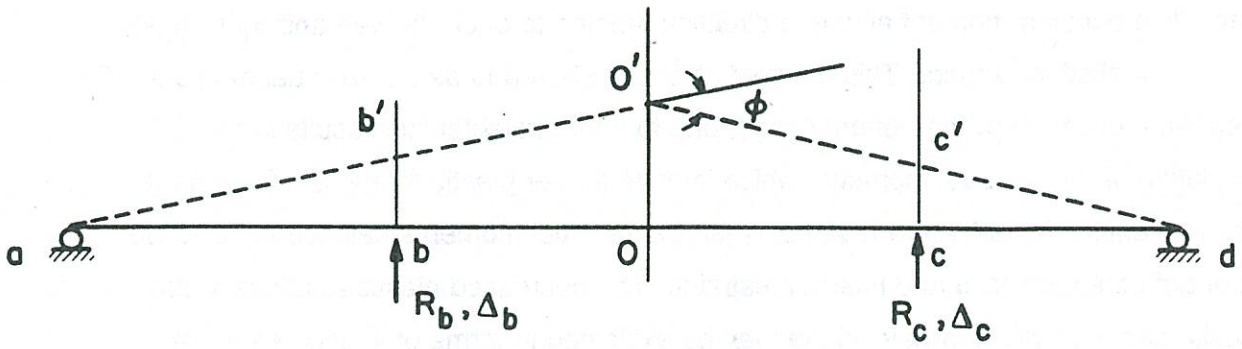

Figure 70. Released structure shown with redundant reactions and applied displacements.

Analytical Development

Theoretical Model for Heat-Straightening Response

Distribution of External Restraining Forces in Composite Girders. A W-shaped girder may be considered as an assemblage of rectangular plate elements mutually connected by rigid longitudinal joints. The components of the assembly are the web and the flanges connected to it on either edge. The boundary conditions of a simple span W shaped composite girder (with only end diaphragms) restrict the deformations in the top flange completely while restraining the transverse movements in the bottom flange and the web at the ends. The indeterminacy associated with the geometry and the boundary conditions of the composite girder produces complex interactions between the elements of the idealized plate assembly. Thus, when an external jacking force is applied to the bottom flange, the redundant forces acting at the web-flange interface stiffen the response of the bottom flange. As a result, the bending moments produced by the applied force are distributed between the bottom flange and web. Only that fraction of the applied moment which is transmitted to the bottom flange is effective in providing external constraint to the vee. For computing the effective load ratio, it is necessary to evaluate the percentage of moment that is resisted by the bottom flange. Exact analysis of the problem based on a continuum mechanics approach is rather complex, as the basic element of the system, a flat plate is cumbersome to analyze. The intricacy of the problem suggests a recourse to numerical techniques such as the finite elements or finite difference methods. Although a fair degree of accuracy may be achieved with these techniques, the lengthy computations involved make them unsuitable for adaptation to microcomputers. Alternatively, the moment distributed to the bottom flange may be determined simply by measuring the actual strains in the field. This approach limits the scope for developing predictive analysis for broad applications in design offices.

A simplistic approach was adopted to model the distribution of external restraining forces in a generalized composite girder. The indeterminate response of the bottom flange was modeled using the analogy of an equivalent plate element. Some simplifying assumptions that have been used are:

(1) The bottom flange acts as a stiffened plate element in bending about its major axis. The modification in stiffness is uniform along the length of the girder.

(2) The deflections in the bottom flange due to the applied load ratio are small, i.e, tan $\theta \sim \theta$ where θ is the angle subtended by the bottom flange to the horizontal plane.

(3) The bottom flange resists the in-plane component of the jacking force by membrane actions only. The membrane actions are decoupled from the slab or out-of-plane actions in the bottom flange.

(4) The cross-sectional dimensions of the bottom flange are very small compared to its length. Hence, normal strains along the width are negligible.

(5) No shear deformations exist in the bottom flange.

(6) The Poisson's ratio of the material is negligible.

In short, these assumptions imply that the bottom flange acts as a stiffened beam element in pure bending about its major axis. The validity of these assumptions will be examined later by exact analysis of the problem. A stiffness modification factor was evaluated for the bottom flange in the W10x39 and W24x76 composite girders that were tested. The factor, thus obtained, was used to estimate the partial bending moment distributed to the bottom flange. The underlying analytical development is as follows.

Consider a long rectangular plate element of length L, thickness t and width b, subjected to a concentrated transverse in-plane load P applied at the midspan. Assuming that the plate undergoes pure bending about its major axis (no shear deformations), the midspan deflection Δ is given as:

$$\Delta = \frac{PL^3}{\frac{48EI}{(1-\nu^2)}} \qquad (20)$$

in which, E = modulus of elasticity of the material, I = Moment of Inertia of the plate in major axis bending, and ν = Poisson's ratio. As ν is small, the quantity $(1-\nu^2)$ is almost equal to unity. Hence Equation 20 may be written as:

$$\Delta = \frac{PL^3}{48EI} \qquad (21)$$

Equation 21 may be non-dimensionalized by rearranging as:

$$\frac{\frac{PL}{4}}{\frac{4EI}{L}} = 3\left(\frac{\Delta}{L}\right) \tag{22}$$

The function (PL/4) equals the midspan bending moment M about the major axis of the plate. Defining the quantity (4EI/L) as the corresponding flexural stiffness K of the plate element, Equation 22 may be rewritten as:

$$\frac{M}{K} = 3\left(\frac{\Delta}{L}\right) \tag{23}$$

Representing the non-dimensional ratios M/K and Δ/L by m and δ respectively, Equation 23 may be expressed as:

$$m = 3\delta \tag{24}$$

From the load-deflection measurements made during the damage inducement process of the W10x39 (Avent and Fadous, 1989) and W24x76 composite girders (present study), a plot of m vs δ for the bottom flanges of each girder was obtained (Figure 68). Superimposed on these plots is the theoretical relationship given by Equation 24 for an isolated plate element. Since Equation 24 is non-dimensional, the slope of the elastic portion of the theoretical curve will be 3, regardless of the dimensions and the material properties of the flange plate. In the case of composite girders, the slope of the linear portion was evaluated to be greater than 3. The slope was represented by the variable S. Thus the linear portion of the plot for the bottom flange in a composite girder can be mathematically represented as:

$$m_{comp} = S\delta \tag{25}$$

where the subscript 'comp' stands for the bottom flange in the composite girder. From equations 24 and 25, it follows that,

$$\frac{m_{comp}}{S} = \frac{m}{S} = \delta \tag{26}$$

Using the definitions of m and δ, Equation 26 may be written as,

$$\frac{M_{comp}}{SK} = \frac{M}{3K} = \frac{\Delta}{L} \tag{27}$$

in which M_{comp} denotes the midspan moment applied to the bottom flange in a composite girder. The moment required to produce a given elastic deflection at midspan of the bottom flange in a composite girder is greater than that for a dimensionally identical isolated plate element. Equation 27 may be rewritten to express the relationship as follows:

$$\frac{M_{comp}}{(\frac{S}{3} K)} = \frac{M}{K} = e\ (\frac{\Delta}{L}) \tag{28}$$

The quantity in the parenthesis is S/3 times the stiffness K of the plate element. It represents the effective stiffness of the bottom flange in a composite girder and shall be denoted as K_{comp}. Thus,

$$K_{comp} = \frac{S}{3} K \tag{29}$$

The stiffness of the bottom flange plate is modified due to its assembly with the web in the composite girder. The term S/3 is the stiffness modification factor, and shall be denoted as γ. It is calculated as one-third the slope of the elastic portion of the m_{comp} vs. δ curve for the bottom flange in the composite girder. If K_f is the flexural stiffness of the bottom flange, considered as a hypothetical plate element in bending about its major axis, then its effective stiffness in the composite girder is given as:

$$K_{comp} = \gamma K_f \tag{30}$$

The restraining moment in the bottom flange was estimated by assuming that the total external moment is distributed to the flange in proportion to its stiffness. Therefore, for a total external restraining moment M_{comp} in a simple span composite girder, the restraining moment in the bottom flange M_f may be approximated as:

$$\frac{M_f}{M_{comp}} = \frac{K_f}{K_{comp}} \tag{31}$$

From Equations 30 and 31,

$$\frac{M_f}{M_{comp}} = \frac{1}{\gamma}$$

or,

$$M_f = \frac{1}{\gamma} M_{comp} \qquad (32)$$

Thus, $1/\gamma$ is a multiplier for the externally applied moment to obtain the restraining moment in the bottom flange. The parameter $1/\gamma$ will be termed as the moment distribution factor ξ for the composite girder. Proceeding further to evaluate the values of γ and ξ for the W10x39 and W24x76 composite girders, the slope of the linear portion of the m vs.δ plot of each girder is calculated. The calculations are based on the curves corresponding to the initial damage of the girders.

For the W10x39 girder,

Slope S_1 = 16.382, which gives the stiffness modification factor as:

$$\gamma_1 = \frac{S}{3} = 5.461$$

and the moment distribution factor as,

$$\xi_1 = \frac{1}{\gamma} = 0.183$$

For the W24x76 girder,

Slope S_2 = 7.021, and the stiffness modification factor is calculated as:

$$\gamma_2 = \frac{S_2}{3} = 2.340$$

which gives the moment distribution factor as:

$$\xi_2 = \frac{1}{\gamma_2} = 0.427$$

For the purpose of design, it was desirable to develop a simple criteria for evaluating the stiffness modification factor for the bottom flange in any arbitrary W-shaped composite girder. A final assumption was made for this purpose. The stiffening effect of the web was assumed to vary linearly with the ratio of its depth to thickness. Figure 71 shows a plot of the

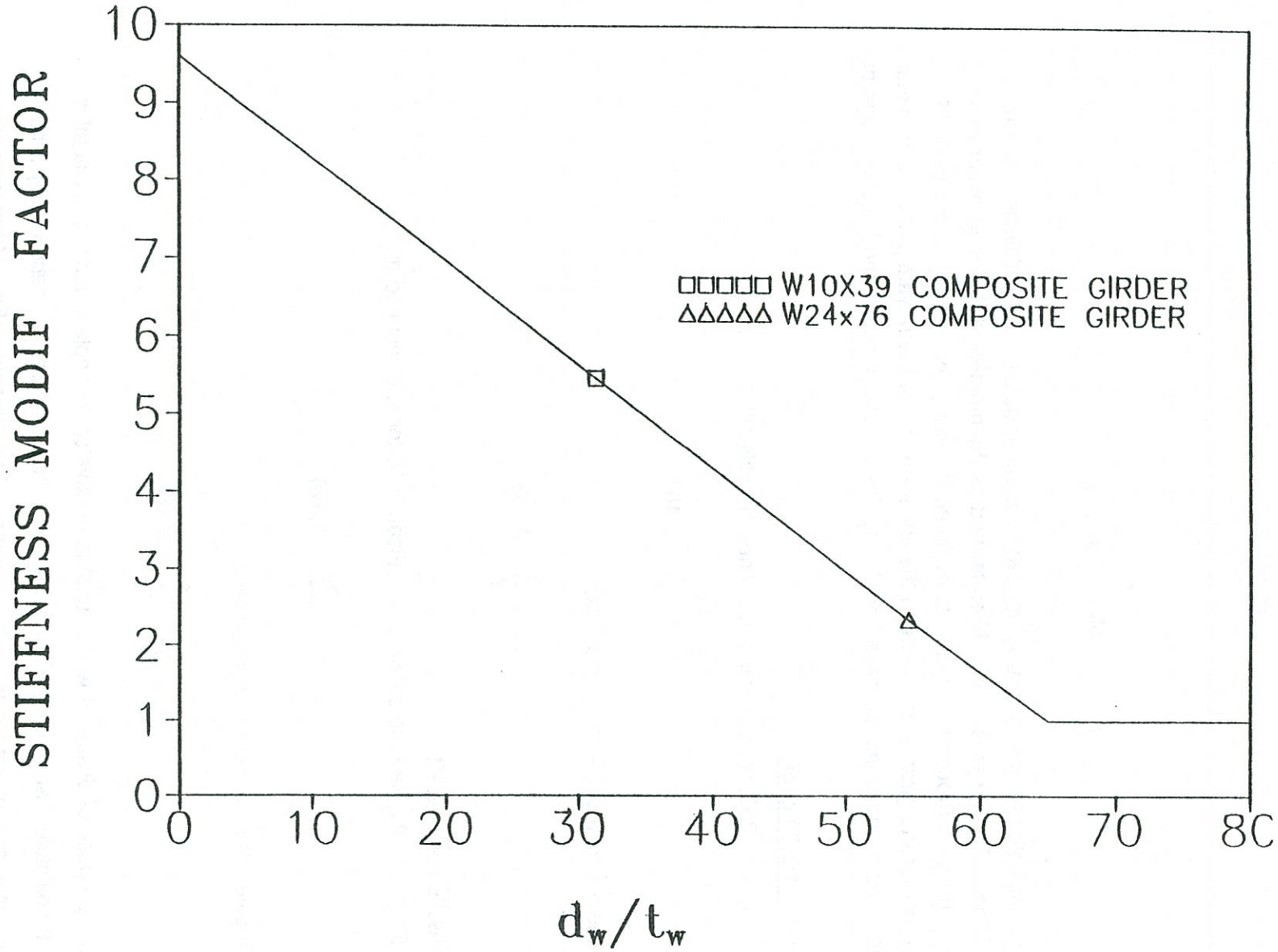

Figure 71. Stiffness modification factor γ vs. d/t ratio of the web in a composite girder.

stiffness modification factor γ versus the depth (d_w) to thickness (t_w) ratio of the web. Two data points corresponding to the W10x39 and W24x76 girders were available from the previous analysis. From theoretical considerations, the upper bound for the stiffness modification factor is infinity, which corresponds to a girder of zero depth. Also, the lower bound value of the factor is 1.0 , which corresponds to a free plate. Based on these premises a straight line plot was drawn. The plot provides convenient and direct means to determine approximately the stiffness modification factor for the bottom flange in the composite girder. Knowing the (d/t) value of the web, one can conveniently read the corresponding value of γ from the plot.

A check was obtained on the validity of these values by examining the non-dimensional moment versus deflection curves for the damage inducement of the two girders (Figure 68). Based on the initial yield, the yield moments for composite girders (M_{yc}) were determined from the experimental curves. The theoretical moments required for initial yield of the hypothetical bottom flange plate (M_{yf}) of each girder were also evaluated. The points m and n identify the initial yielding on the theoretical curves 1 and 2 for the bottom flange plates. The ratio to the yield moment for the composite girder (M_{yc}) of yield moment of the bottom flange (M_{yf}) was computed for each girder. The resulting quantity shall be termed as the initial yield ratio of the composite girder. The experimental yield moments are calculated at the point which marks the linear and non-linear portions of the curve and signifies the beginning of yielding (points x and y on curves 5 and 3 respectively). Since the deflections in the bottom flange were measured for plotting these curves, the yield points on the curves represent the yielding of the bottom flange about the major axis. It is reasonable to assume that the bending moment acting about the major axis of the bottom flange equals its initial yield moment at the yield point. Based on the foregoing logic, the reciprocal of the initial yield ratio approximates the fraction of the total bending moment that is resisted by the bottom flange. In other words, the quantity M_{yf}/M_{yc} should equal the Moment Distribution Factor ξ, defined previously for the bottom flange, at the yield point. The quantity M_{yf}/M_{yc} was calculated to be 0.253 for the W10x39 girder and 0.335 for the W24x76 girder. These values show fairly good agreement with the theoretical values.

Exact Solution of the Bottom Flange Response. A W-shaped girder is structurally classified as a multiple folded plate system. The term 'multiple' is used to describe the inter-connection of more than two plates at the fold line (Figure 72a). The fold lines frame into the transverse diaphragms, which may be at the ends (end diaphragms) or at several

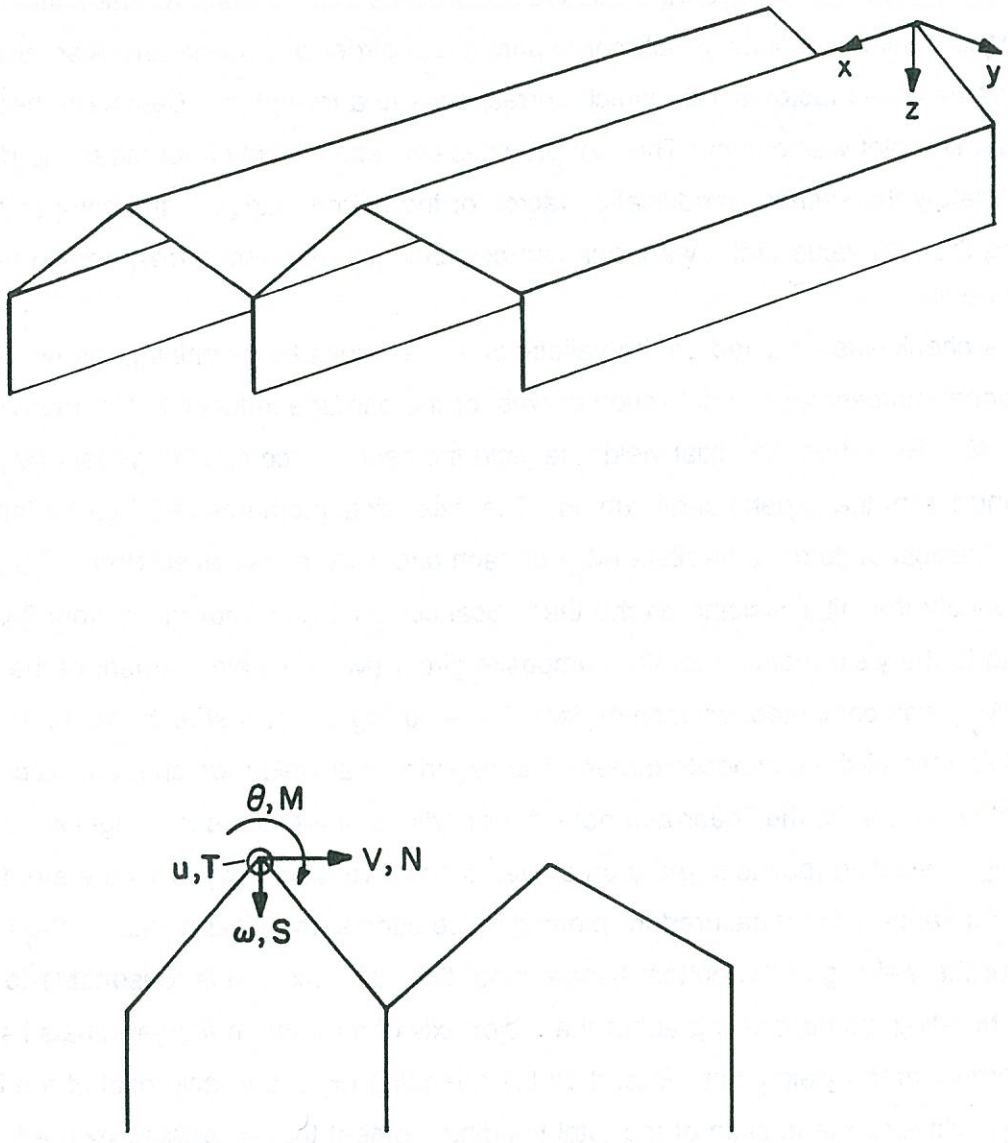

Figure 72. Multiple folded plate structure showing the nodal element displacements and forces.

locations along the span (intermediate diaphragms). Numerous contributions (Avent and Rountree; Chu and Pinjarkar, 1966; Dean and Omid'Varan, 1969; Defries-Skene and Scordelis, 1964; Goldberg and Leve, 1957) to the analysis of folded plate structures are present in the literature. The various analytical procedures available for design computations are broadly based on three different approaches. The earliest of these theories, called the 'ordinary theory', offered an approximate analysis which assumed that the applied loads are transmitted by transverse bending actions to the longitudinal joints, and further by membrane action to the supports. The bending action, also referred to as the slab action, is defined by the behavior of transverse one-way slab strips spanning between the longitudinal joints. The membrane action is modeled using the elementary beam theory applied to the individual plate elements. A subsequent theory which obviates this kind of approximation was termed as the 'elasticity theory'. In this theory, the slab or the flexural stresses are determined by means of classical thin plate theory applied to the plate elements supported along all the four edges, while the membrane actions are defined by the use of plane stress elasticity theory. The most recent approach is the finite element method. Although a powerful and versatile tool of analysis, the finite element technique rarely yields exact results. The accuracy of the computed results depends largely on the modeling of the problem. The modeling, which includes the selection of the discrete element as well as the extent of discretization, is a subjective procedure depending on the specific problem in hand. To achieve a good degree of accuracy, a large number of simultaneous equations need to be solved which requires extensive computer memory. Moreover the analysis does not provide a closed form solution and thus restricts the analytical study of the effect of changing various parameters.

A direct stiffness method based on the elasticity theory was developed by De-Fries Skene and Scordelis (1964) for the analysis of folded plate structures. The method was later extended to the analysis of multiple folded plate structures (Chu and Pinjarkar, 1966). As the name suggests, the method involves a matrix analysis of multiple folded plates using the stiffness approach. The basic assumptions used in the development of the method were:

(1) Each plate is rectangular in shape and uniform in thickness.

(2) The ends of the plates are framed into diaphragms which are infinitely stiff parallel to their own plane but perfectly flexible in the normal direction.

(3) The structure is perfectly elastic.

(4) The intersecting plates are rigidly joined along the fold lines and the angles between the connected plates do not change under the loading.

The development of the method and the underlying theory is described in the original documentation (Defries-Skene and Scordelis, 1964), and will not be included here for the sake of brevity. Only the outline of the method is presented herein.

The method models the folded plate structure as a system of finite number of discrete elements joined together at a finite number of nodal points. In this case, the elements are the individual plate panels while the nodal points are the longitudinal joints or the fold lines. Each nodal point or joint has four degrees of freedom which are:

(1) A displacement u in the longitudinal direction along the joint. The corresponding force, a shear force, is represented as T.

(2) A displacement v in the transverse plane in the horizontal direction. The corresponding force is called N.

(3) A displacement v in the transverse plane in the vertical direction. The corresponding force is referred to as S.

(4) A rotation θ in the transverse plane in the clockwise direction. The related moment is called M.

The positive directions of the nodal degrees of freedom are expressed in Figure 72b with reference to a global coordinate system. The nodal points or the fold lines are subjected to known or unknown forces, as well as known or unknown displacements, each of which corresponds to these degrees of freedom. Accordingly, each element is subjected to four element displacements u, v, w, θ and the related forces T, N, M and S (in the correct order) at each edge. The positive directions of the element displacements and forces are defined with respect to a local or element coordinate system (Figure 73b). The displacements u and v describe the membrane action of the plate element, whereas w and θ represent the flexural or slab displacements. Since the plate has two edges, each connected to a joint, the plate element has eight degrees of freedom. The longitudinal distributions of these displacements and forces are treated by resolving them into harmonic components of the Fourier Series. The necessary equations relating the eight force quantities to the eight displacement quantities for a plate panel are available in the literature mentioned earlier, and are summarized herein.

Membrane Force-Deformation Relationships. An infinitesimal plate element and a typical plate panel subjected to membrane edge forces is shown in Figure 73. The boundary force-deformation relationships for the membrane action were derived by means of plane stress elasticity equations. The resulting equations are given as follows for the i_{th} harmonic and the sign convention shown in Figure 73b.

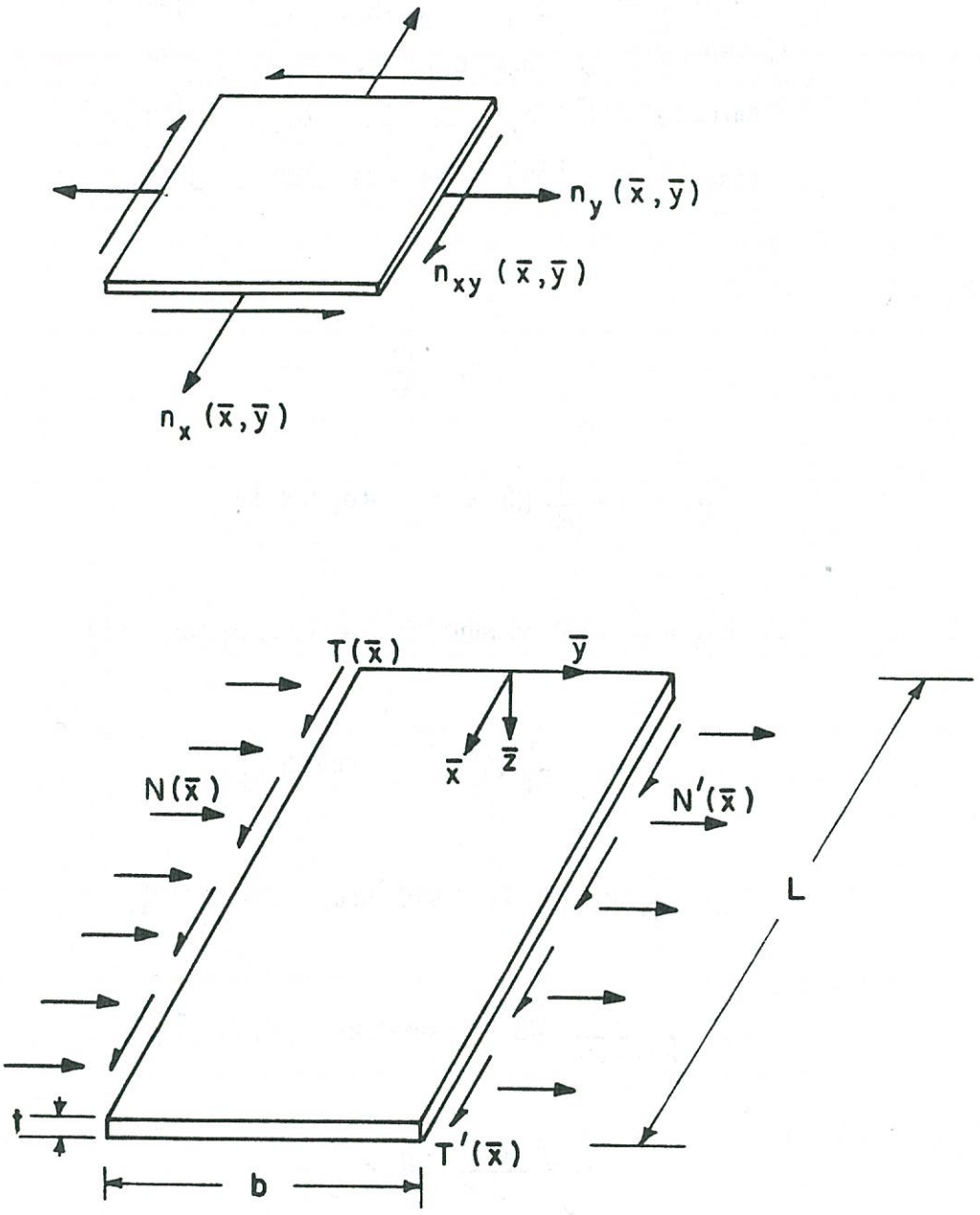

Figure 73. Membrane edge forces on the plate in local coordinate system.

$$\begin{Bmatrix} N_i \sin(\alpha_i \bar{x}) \\ T_i \cos(\alpha_i \bar{x}) \\ N_i' \sin(\alpha_i \bar{x}) \\ T_i' \cos(\alpha_i \bar{x}) \end{Bmatrix} = \frac{K}{b} \begin{pmatrix} b_{11} & -b_{12} & -b_{13} & b_{14} \\ -b_{12} & b_{22} & -b_{14} & -b_{24} \\ -b_{13} & -b_{14} & b_{11} & b_{12} \\ b_{14} & -b_{24} & b_{12} & b_{22} \end{pmatrix} \begin{Bmatrix} V_i \sin(\alpha_i \bar{x}) \\ U_i \cos(\alpha_i \bar{x}) \\ V_i' \sin(\alpha_i \bar{x}) \\ U_i' \cos(\alpha_i \bar{x}) \end{Bmatrix}$$

where,

$$\alpha_i = \frac{i\pi}{b}$$

$$b_{11}, b_{22} = \frac{1}{H_i} [(3-\nu) \sinh 4\beta_i \pm 4(1+\nu) \beta_i]$$

$$b_{13}, b_{24} = \frac{1}{H_i} [2(3-\nu) \sinh 2\beta_i + 4(1+\nu) \beta_i \cosh 2\beta_i]$$

$$b_{14} = \frac{1}{H_i} [4(1+\nu) \beta_i \sinh 2\beta_i]$$

$$b_{12} = \frac{1}{H_i} [(3-\nu)(1-\nu) \sinh^2 2\beta_i - 4(1-\nu)^2 \beta_i^2]$$

$$H_i = \frac{1}{2(1-\nu)\beta_i} [(3-\nu)^2 \sinh^2 2\beta_i - 4(1+\nu)^2 \beta_i^2]$$

$$K = \frac{Et}{1-\nu^2} \; ; \; \beta_i = \frac{a}{2} \alpha_i$$

in which E = modulus of elasticity of the material and, ν = Poisson's ratio.

Flexural Force-Deformation Relationships. The flexural boundary forces on a plate element and panel is shown in Figure 72. The force-deformation relationships for the slab action were determined by applying classical thin plate theory to the individual plate elements supported on all the four edges. The equations for the i_{th} harmonic component and the sign convention shown in Figure 72b are expressed as:

where,

$$\begin{Bmatrix} M_i \\ S_i \\ M_i' \\ T_i' \end{Bmatrix} \sin(\alpha_i \bar{x}) = \frac{D}{b^2} \begin{bmatrix} bd_{11} & d_{12} & bd_{13} & -d_{14} \\ d_{12} & \frac{4\beta_i^2 d_{22}}{b} & d_{14} & \frac{-4\beta_i^2 d_{24}}{b} \\ bd_{13} & d_{14} & bd_{11} & -d_{12} \\ -d_{14} & \frac{-4\beta_i^2 d_{24}}{b} & -d_{12} & \frac{4\beta_i^2 d_{22}}{b} \end{bmatrix} \begin{Bmatrix} \theta_i \\ w_i \\ \theta_i' \\ w_i' \end{Bmatrix} \sin(\alpha_i \bar{x})$$

$$d_{11}, d_{22} = \frac{2\beta_i(\sinh 4\beta_i + 4\beta_i)}{J_i}$$

$$d_{24}, d_{13} = \frac{4\beta_i(2\beta_i \cosh 2\beta_i \pm \sinh 2\beta_i)}{J_i}$$

$$d_{12} = \frac{4\beta_i^2[4(1-\nu)\,\beta_i^2 + (1+\nu)\sinh^2 2\beta_i]}{J_i}$$

$$d_{14} = \frac{16\beta_i^3 \sinh 3\beta_i}{J_i}$$

$$J_i = \sinh^2 2\beta_i - 4\beta_i^2$$

$$D = \frac{Et^3}{12(1-\nu)^2}$$

The applied loads and displacements on the joints are also resolved into Fourier Series components to account for their longitudinal distribution. Equilibrium equations in terms of force-deformation relationships are written for each joint maintaining the compatibility conditions of the structure. A single harmonic component of forces and displacements is considered at one time. The set of simultaneous algebraic equations for the given harmonic is solved to obtain the unknown joint displacements. The joint displacements are transformed

to local coordinates to provide the plate end deformations, which further yield the plate end forces for various plate elements. Only the amplitudes or the characteristic values of the component harmonic function are used in the preceding matrix operations. This makes it possible to treat the fold line as a nodal point and operate with a single value, instead of a function. The results are also in terms of characteristic values and need to be multiplied with the harmonic function to obtain the longitudinal distribution. These steps are repeated for each harmonic. The analysis is conducted for a number of harmonic components. Theoretically, a number of harmonics are needed to represent each loading. However, in practice the higher order terms have a negligible effect and may be neglected. The final result is obtained by superposition of results for different harmonics.

Folded Plate Analysis. The direct stiffness method for analysis of folded plate structures is computationally efficient and straightforward. It involves finite degrees of freedom as the structure need not be discretized along the length. The algebraic matrix operations required are, therefore, relatively fewer and repetitive which makes the method ideal for programming with a micro-computer. The stiffness matrix formed is a band matrix which is not only well-conditioned for inversion, but also economical for storage purposes. Keeping in mind the need for an accurate, simple and efficient procedure of exact analysis, this method was employed for analyzing the response of the composite girder to external restraining forces. A computer program was written for carrying out the analysis. Only the geometry and the material properties of the structure along with the magnitude and location of the applied joint loads need to be input. The format of input is illustrated by a sample set of input data in Appendix I. All the necessary matrix formations and operations are performed internally in the program. A concise flow chart of the program is presented in Appendix H. The output of the program provides the plate boundary forces for the membrane (N and T) and flexural actions (M and S) at each edge. The longitudinal direct stresses at the joints are also computed using the following plane elasticity relation:

$$\sigma_x = E \frac{\delta u}{\delta x} + \nu \frac{P}{t} \tag{33}$$

where u = longitudinal displacement, E = modulus of elasticity, t = thickness of the plate, ν = Poisson's ratio, or neglecting ν,

$$\sigma_x = E \frac{\delta u}{\delta x} \tag{34}$$

The program also computes the moment distribution factor ξ and stiffness modification factor γ for the given section. The value of the stiffness modification factor was calculated for the composite sections considering the transverse in-plane deflections at the midspan of the bottom flange for a static load acting in the same direction.

The W24x76 an W10x39 composite girders were analyzed using the developed program. The analysis was conducted for a midspan transverse load P of 10 kips on one edge of the bottom flange acting parallel to the flange. The resulting plate end forces at the midspan of the girders are tabulated in Appendix J. Figure 74 illustrates the cross-sectional geometry and boundary conditions, element and nodal identification, and the loading used to model the W24x76 and W10x39 girders. As shown in the figure, all the degrees of freedom at the upper edge of the web (plate element 1) were assumed to be restrained in the analysis. The midspan bending moment M_f in the bottom flange (acting about the major axis) was evaluated from the distribution of longitudinal direct stress σ_x. The variation of the longitudinal stress was assumed to be linear between the nodal joints. For instance, considering the element and nodal identification shown in Figure 74, the cross-sectional moment in the bottom flange may be expressed in terms of the longitudinal direct stresses at joints 3 and 4 :

$$M_f = \frac{1}{12} (\sigma_{x4} - \sigma_{x3}) f_f^2 t_f \qquad (35)$$

where the subscripts 3 and 4 stand for the joint #s 3 and 4 and, b_f = flange width and t_f = flange thickness. Thus, M_f represents the restraining moment in the bottom flange plate. The total external restraining moment applied to the bottom flange of the composite girder at midspan was computed as:

$$M_{comp} = \frac{PL}{4} \qquad (36)$$

Thus, for the W10x39 composite girder, the restraining moment M_f in the flange plate was computed as:

$$M_f = 84.54^{k''}$$

and the total external restraining moment is given as:

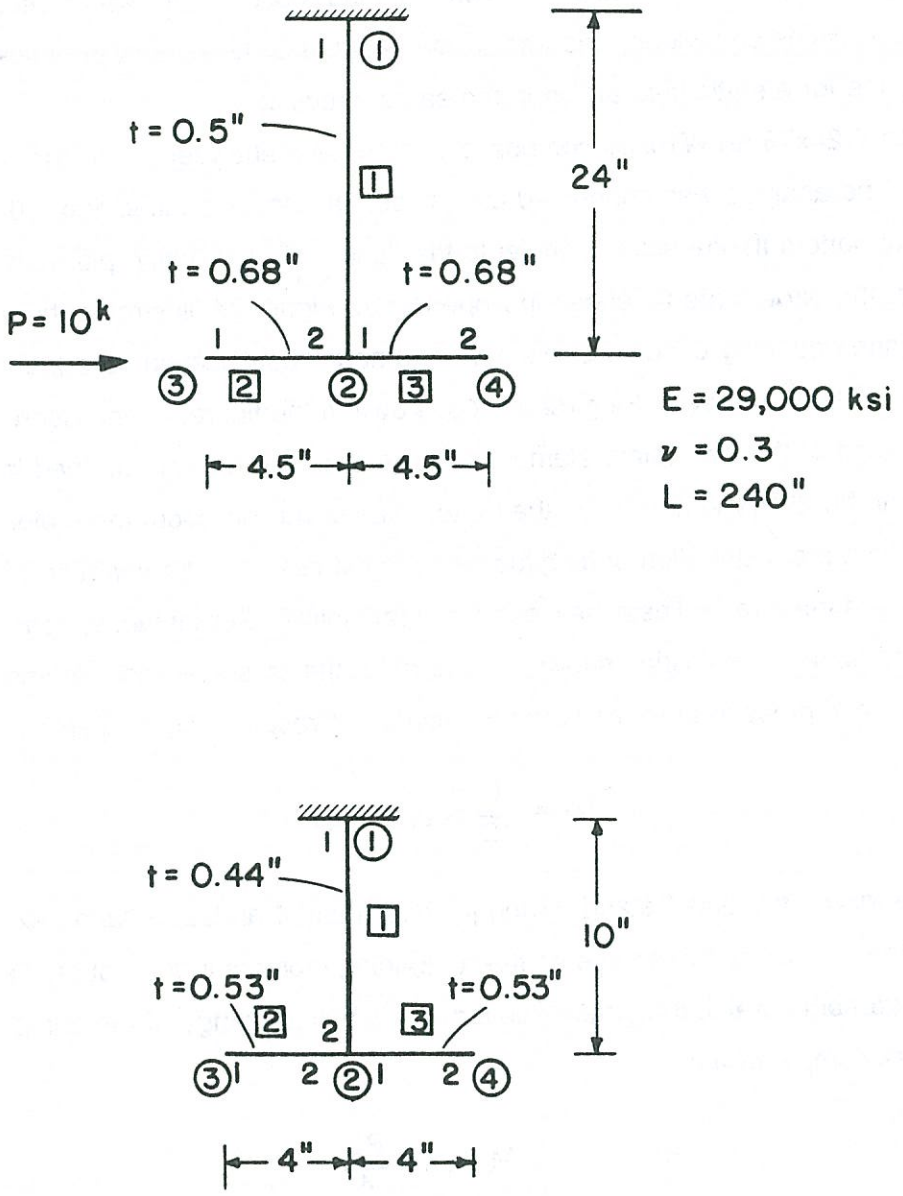

Figure 74. Input information for the W10x39 and W24x76 composite girders.

$$M_{comp} = 600.00^{k''}$$

which provides the moment distribution factor as:

$$\xi = \frac{M_f}{M_{comp}} = 0.147$$

Similarly for the W24x76 composite girder:

$$M_f = 200.16^{k''}$$

$$M_{comp} = 600.00^{k''}$$

which gives the moment distribution factor as:

$$\xi = 0.33$$

The values of the Moment Distribution Factors for the composite girders obtained from the foregoing exact analysis are very much comparable to those estimated from the approximate analysis. The concurrence of the results from the two independent analyses not only verifies the approximate approach but also provides a check for the validity of the computer program developed. It is immediately evident from the computed results in Appendix J that the bottom flange behaves primarily as a membrane under the influence of the external jacking forces. On the other hand, the response of the web is primarily flexural. It may be noted that the basic assumptions of the approximate analysis are consistent with this behavior.

An approximate as well as a more rigorous folded plate analysis has been used herein for evaluating the distribution of external restraining forces in composite girders. The moment distribution factors determined for the tested girders, using the two methods, are presented below:

Composite Girder Test Specimen	Moment Distribution Factor (ξ)		
	Approximate	Folded Plate Analysis	Experimental
W10x39	0.253	0.147	0.183
W24x76	0.335	0.330	0.427

The simplifying assumptions used in the development of the approximate method result in values in the range of 20-30% of the experimental. The experimental values are based on two data points only. A more comprehensive experimental study is required to provide enough test data to establish definitive values. However, this limited data provides a measure of validity to the analytical procedures. Comparison of the values provided by the two approaches indicates that the simplified approach estimates the moment distribution factors for the tested girders to a reasonable degree of accuracy. For the sake of simplicity, an approximate interpolation criteria was used for estimating the stiffness modification factor of a generalized composite girder. On the other hand, the exact method is based on a more rigorous engineering analysis and is thus expected to produced more accurate results. Based on the stiffness approach. It takes into account all the degrees of freedom in the folded plate to provide a closed-form solution. The longitudinal variation of deformations and forces is also calculated by resolving the loads into Fourier series components, analyzing the response for each component and superimposing them. Convergence to the exact results can be obtained by considering a sufficient number of harmonics. In view of the foregoing observations, it is recommended that the direct stiffness method be used for evaluating the moment distribution factors for composite girders. However, when such an exact method is not available, the approximate method may be relied upon to provide reasonable results for practical applications.

Modeling of Simple Span Composite Girders

The present analytical treatment attempts to model the heat-straightening response of a composite girder by reducing the problem to that of a simply supported vee heated plate element dimensionally identical to the bottom flange of the composite girder. The theoretical modeling developed in this section pertains to composite girders which are repaired using the standard heat pattern consisting of a vee heat on the bottom flange in conjunction with a line heat on the web (applied to their plastically deformed regions).

The external constraint (load ratio) on the analogous plate element is assumed to be equal to the effective load ratio parameter for the composite girder. The experimental variation of the average plastic rotations with the effective load ratio was plotted (Figure 75) for the W10x39 and W24x76 composite girders. Only the heating cycles which included the line heat on the web have been considered. The effective load ratio was computed by multiplying the applied load ratio with the moment distribution factor ξ for the composite girder. The values of ξ that were obtained for the composite girders from the exact analysis were used.

The theoretical relationship between the load ratio M/Mp and average plastic rotations for plate elements, as predicted by Equation 4b for a vee angle of 30 degree and heating temperature of 1200°F, was also plotted in Figure 75 and compared with the experimental plots for the composite girders. It is evident from definition that the applied or apparent load ratio (M/M_p) on an isolated plate element equals the effective load ratio, since the entire applied moment is resisted by the plate itself. In other words, the moment distribution factor for a plate element, theoretically, equals unity.

From the analytical expression for plates (Eq 4b), it can be seen that the quantity in the square parenthesis sums the effect of the constraining forces on the plastic rotations. The factor 3.4 M/Mp accounts for the effect of the external restraining forces. The slope of the theoretical plot is governed by this factor. It can be seen from Figure 75, the lower slopes (excluding the effect of hot mechanical straightening) of the experimental plots show an excellent agreement with that of the theoretical plot. Thus, it may be concluded that the effect of the external constraint on the analogous plate element is modeled perfectly by considering the effective load ratio. However, it is also apparent from Figure 75 that for a zero load ratio (no jacking forces), the plastic rotations measured in case of the deep composite girder (W24x76) are substantially larger than the shallow girder (W10x39). In fact, the average plastic rotation for shallow girder is even less than that for a plate element (as predicted by the plate formula). It is self-explanatory that in the absence of the external jacking forces, the heat-straightening response of a structural steel element is governed only by the internal constraint in the member. Since the intercepts of the plots on the x-axis (Figure 75) equal the average plastic rotations corresponding to zero load ratio, they reflect the internal constraining effect in the composite girders. The discrepancy observed on comparing the x intercepts of the plots makes it evident that the internal constraint on the vee action in the bottom flange of the tested composite girders varies from that in a plate element by different amounts. The

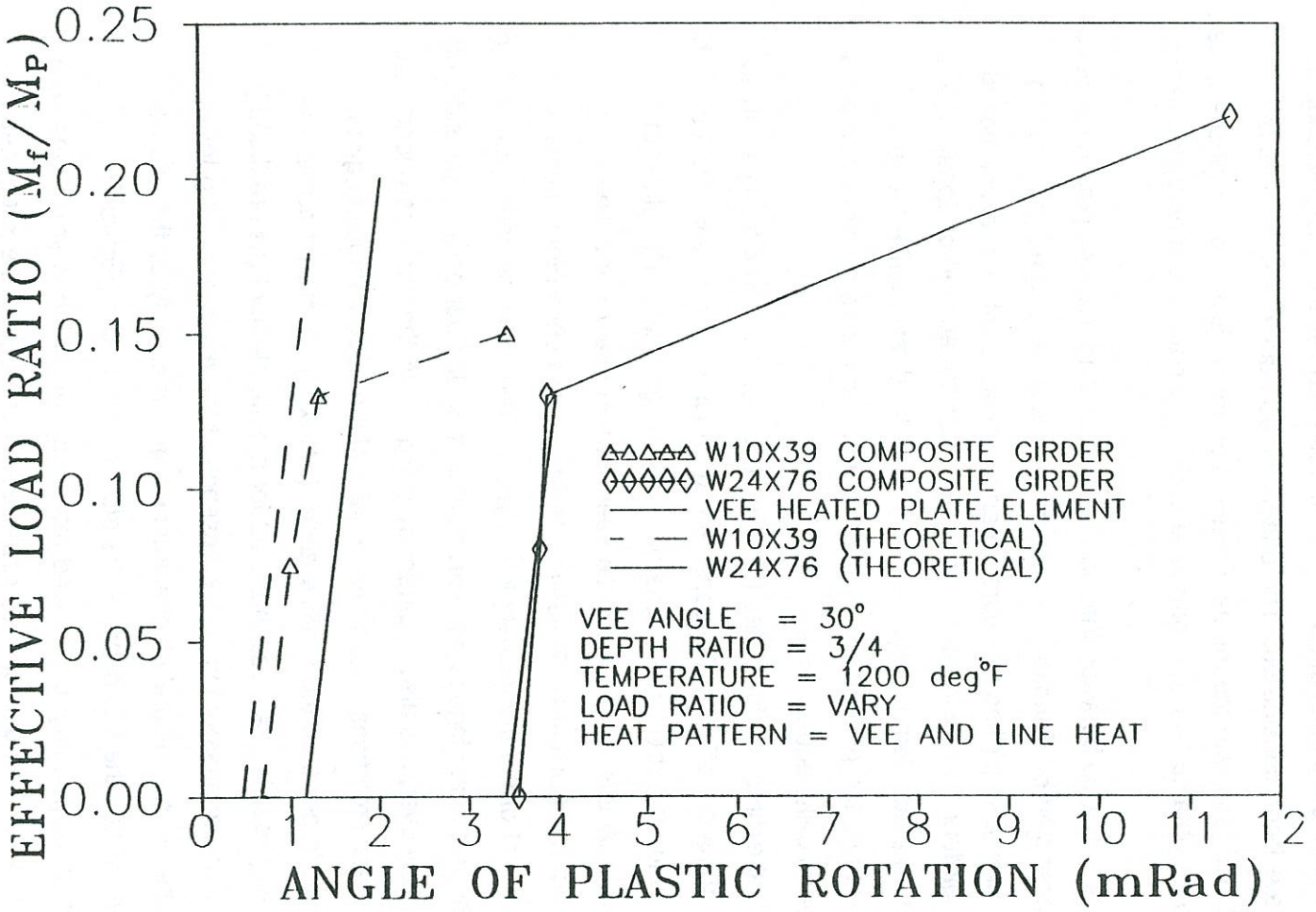

Figure 75. Effective load ratio vs. angle of plastic rotation for tested specimens based on the assumption of a linear moment distribution factor.

intercepts represent the plastic rotations for zero load ratio and thus reflect the internal constraining effect in the plates.

The effect of the internal constraint in the composite girder was modeled by making the following additional assumptions:

(1) The internal constraint in the bottom flange of a composite girder varies linearly with depth to thickness ratio (d/t) of the web.

(2) The internal constraint in a composite girder with a d/t ratio of 37, equals that in an isolated vee heated plate element.

Based on these assumptions, a simple formula was derived for evaluating the plastic rotations in the bottom flange of a composite girder:

$$\phi_{comp} = F_t(T)\, F_l'(M)\, \varepsilon_p(T) \sin \frac{\theta}{3} \qquad (37)$$

where ϕ_{comp} = Plastic rotation in the bottom flange of the composite girder, and d/t_w = depth to thickness ratio of the web in the modified load ratio function, F'_l

$$F_l' = 0.9 + 0.1 \left(\frac{d}{t_w} - 37\right) + 3.4 \frac{M_f}{M_p}$$

For the standard heating temperature of 1200°F, Equation 37 reduces to:

$$\phi_{comp} = 0.00792 \left[0.9 + 0.1 \left(\frac{d}{t} - 37\right) + 3.4 \left(\frac{M_f}{M_p}\right)\right] \sin \frac{\theta}{3}$$

The theoretical variation of the average plastic rotations with the effective load ratio predicted by the preceding formula for the W10x39 and W24x76 composite girders was superimposed on the experimental plots in Figure 75. It is clear that, excluding the data points corresponding to 102% load ratio in case of W10x39 composite girder and 65% load ratio in case of W24x76 composite girder, the analytical formula fits the available experimental data very well. Marked deviations are noted at these points and are attributed to the phenomenon of 'Hot Mechanical Straightening' discussed earlier.

Analytical Treatment of Hot Mechanical Straightening

The available research evidence on the temperature characteristics of steel indicate that the application of a line heat on the web reduces the yield stress of the material along the line by 50%. Accordingly, the yield moment of the web in bending about the minor axis also

decreases in the same proportion along the line heat. Qualitatively speaking, for a certain magnitude of the jacking force, the bending moment in the web about its minor axis along the line heat equals the reduced yield moment. At this jacking force the web begins to yield in minor axis bending at the location of the line heat. For a midspan jacking load on the bottom flange, the yielding commences at the mid-length. As a result, an elasto-plastic hinge is formed in the web at its mid-length. Further increase in load ratio causes an elongation of this yield zone (elasto-plastic hinge). Progressive yielding of the web may result in the formation of a perfect plastic hinge along the line heat, which initiates at the midspan and spreads towards the ends. Yielding of the web along the line heat is accompanied with a redistribution of moments/forces in the folded plate girder. After the onset of yielding in the web, the moment resisted by the bottom flange (M_f) increases non-linearly with the applied jacking forces. Consequently, the plastic rotations obtained in the bottom flange upon performing the vee heat also increase nonlinearly with the applied (apparent) load ratio. The application of a vee heat reduces the yield stress of the bottom flange by half at the location of the vee. If the increased moment in the bottom flange (due to the yielding of the web) exceeds its reduced yield moment, then the bottom flange will also experience yielding under the applied load ratio. The heat-straightening response of the composite girder will exhibit a greater nonlinear increment with the applied jacking force. Eventually, a plastic hinge will be formed in the bottom flange and a failure mechanism will be obtained.

This nonlinear behavior was encountered while studying the W10x39 and W24x76 composite girders and is reflected by the plots of the load ratio vs average plastic rotation for the tested girders. The phenomenon was termed as Hot Mechanical Straightening and was observed at different load ratios in the two girders. From the plots (Figure 67), it may be assessed that the non-linearity in the shallow girder began at some load ratio between 91% and 102%. On the other hand, the deep girder exhibited the phenomenon at an apparent load ratio between 39% and 65%. The analytical treatment developed earlier does not take into account this non-linear behavior, as it is based on the elastic response of the composite girder (linear portion of the moment m versus deflection δ curves). The implication here is that the yielding of the web about the line heat under high load ratios causes a larger share of the applied moment to be distributed to the bottom flange than predicted by the elastic analysis. The deviation observed in the experimental variation (from the theoretical predicted relationship) of the plastic rotations with the effective load ratio for the tested girders at data points corresponding to hot-mechanical straightening verifies the foregoing hypothesis (Figure 75). From Figure 75, it is evident that the plastic rotations displayed by the composite

girders at load ratios in the non-linear range (102% for the W10x39 girder and 65% for the W24x76 girder) are much higher than predicted by the developed analytical model. This implies that the moment distributed to the bottom flange at these load ratios is much greater than calculated by the elastic analysis. In other words, the moment distribution factors are substantially under-estimated by the elastic analysis at the data points in the non-linear range. The effective load ratios at these points need to be revised. Strictly speaking, the developed analytical formulation fails to model the redistribution of moments due to non-linear behavior and thus cannot accurately calculate the moment distribution factors once the initial yield begins in a part of the girder. However, an approximate evaluation of the moment distribution factors was made by modifying the structural model used in the folded plate analysis to simulate the presence of the elasto-plastic hinge. The effect of the yielding in the web was modeled by releasing the rotational restraint at the location of the line heat and applying a restraining moment equal to one-third the initial yield moment of the web in minor axis bending. The folded plate model used for the analysis of the composite girder, with non-linear flexural deformations in the web, is illustrated in Figure 76. Since the line heat is always performed on the yield line, which typically occurs a small distance below the top flange, the portion of the web above the line was assumed to be rigid. The web was assumed to be connected to a hinged support with a partial rotational restraint along the heated line. The moment distribution factors for the data points in the non-linear range were thus computed as 0.33 and 0.59 for the W10x39 and W24x76 composite girders respectively. The experimental variation was re-plotted (Figure 77) by revising moment distribution factors in the range of non-linear behavior. There is a small deviation in the upper portion of the re-plotted curve for the W10x39 composite girder, indicating that hot mechanical straightening may have been initiated in the bottom flange plate, but only slightly. On the other hand, there is a much larger deviation for the case of W24x76 composite girder indicating that hot mechanical straightening plays a significant role at higher load ratios.

As mentioned earlier, the elastic folded plate analysis cannot rigorously model the non-linear behavior of composite girders at high load ratios. However, the critical load ratio which initiates the non-linear phenomenon (that characterizes hot mechanical straightening), can be accurately predicted using the developed analytical approach. The folded plate stiffness method may be used to calculate the stresses in various parts of the girder under a variable load ratio P. The bending moments in the web about the minor axis along the line heat can be compared with the plastic moment capacity of the section at increased temperatures.

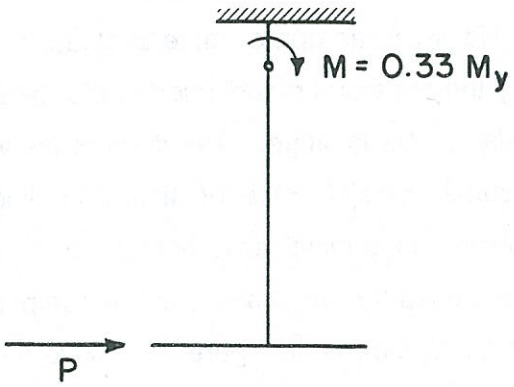

Figure 76. Model for the folded plate analysis of the composite girder with yielding in the web along the line heat.

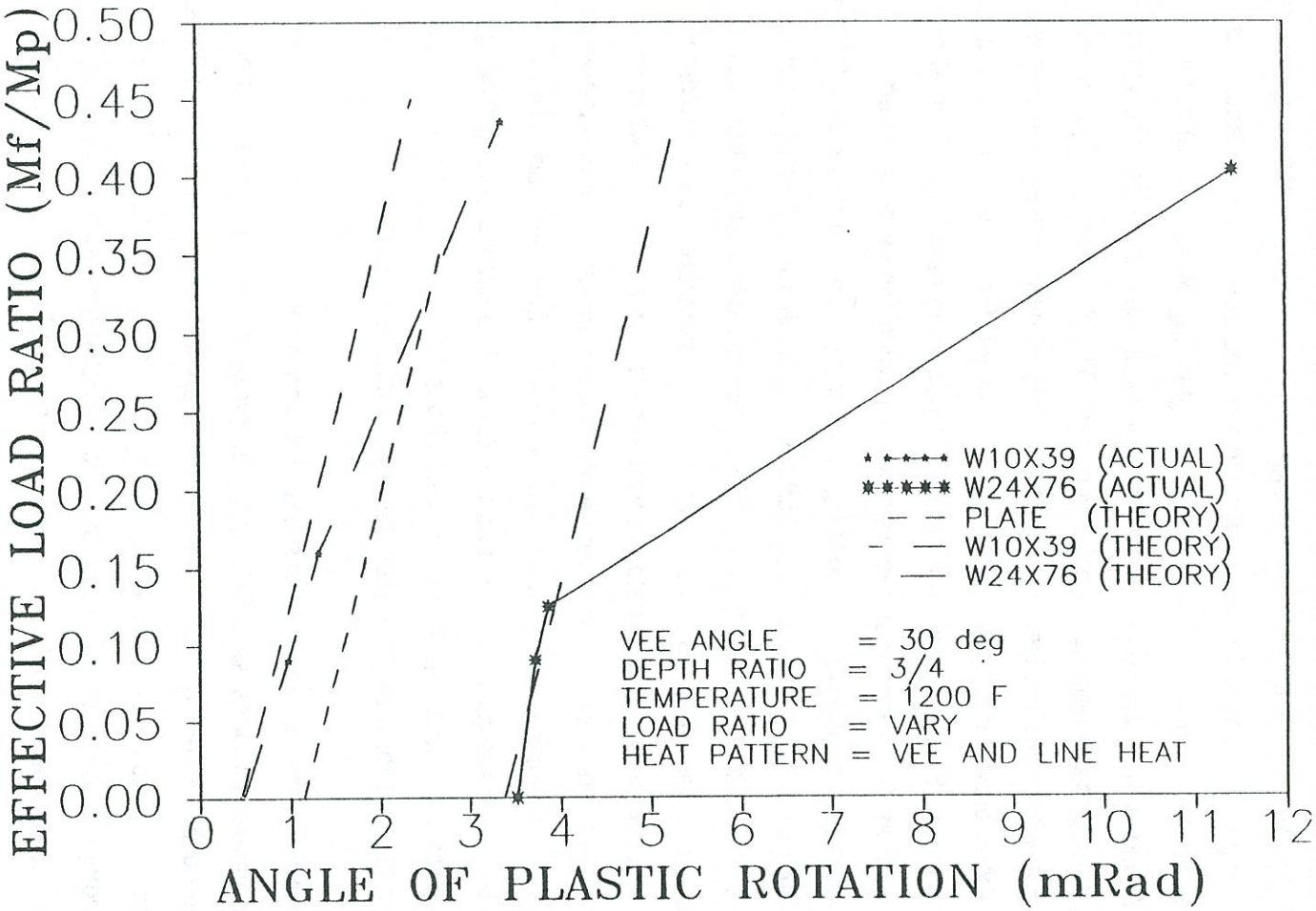

Figure 77. Effective load ratios vs. angle of plastic rotations for revised load ratios in the nonlinear range.

Similar comparisons can be made for bending moments in the bottom flange about the major axis at the location of the vee heat. Hot mechanical straightening may be anticipated to occur if the applied bending moments exceed 50% of the plastic moment capacity in any of the heated sections. The critical apparent load ratios which would initiate non-linear response in the W10x39 and W24x76 composite girders were calculated as 88% and 61% respectively. In both cases the yielding was predicted to commence in the web at midspan. Hence, the initial non-linearity can be attributed to the hot mechanical straightening of the web about the line heat. The points A and B in Figure 67 represent the apparent load ratios beyond which Hot Mechanical Straightening may theoretically be anticipated. The theoretical value for the shallow girder is somewhat conservative considering the experimental results. However, the criteria explained above provides a good estimate of the jacking forces, which may trigger Hot Mechanical Straightening. Since the phenomenon is suspected to cause detrimental effects on the material properties, it is recommended that higher jacking forces be avoided.

For heat-straightening repair of composite girders, it is recommended that a folded plate analysis be used to determine the critical load ratio at which initial yielding occurs during heating. This value should be the maximum apparent load ratio used during the heat-straightening repair. In cases where this type of analysis is unavailable, an approximate limiting value can be estimated from the data presented here. Since the W10x39 and W24x76 composite girders represent a wide range of section geometries, a conservative value can be chosen from the two cases. It is recommended that the effective load ratio in the heat-straightening of composite girders be limited to 12.5%. The corresponding limiting apparent load ratio would be obtained for the specific girder by dividing this value by the moment distribution factor ξ for that girder developed in analytical equations.

Analysis of Composite Girders with Intermediate Diaphragms

The indeterminate response associated with the presence of intermediate lateral bracings in the composite girders was modeled using the analogy of a continuous stiffened beam. The stiffness approach was employed because of its inherent amenability to computer programming. A computer program was developed for the stiffness analysis of three-dimensional framed structures with rigidly connected linear members. The computer-aided analysis was performed for an analogous continuous beam of length equal to that of the composite girder. The continuous beam was considered to be supported at the location of the diaphragms in the composite girder. The stiffness of the beam was taken equal to the effective stiffness of the bottom flange. The effective stiffness of the bottom flange was

evaluated using the stiffness modification factor obtained from Figure 71. The analogy between the bottom flange and a beam is justified on the basis of the assumptions listed. This approach can be applied to the Crowley Bridge case.

The apparent load ratio (M/M_p) on the heat-straightened composite girder at the Crowley Bridge was calculated in the field considering the damaged unbraced span as simply supported at bracings. Strictly speaking, however, the girder is continuous over the bracings and hence, the applied moments are distributed to the other spans (Figure 69). The apparent load ratio on the girder was actually less than 25%. The value of the bending moment at the location of the vee was reevaluated by performing the stiffness analysis of the analogous continuous beam (Figure 69) under the applied jacking force. The value of the apparent load ratio was theoretically revised to 14.3%. The revised value of the apparent load ratio was subsequently multiplied by moment distribution factor ξ for W33x241 composite girder (from Exact analysis) to obtain the effective load ratio in the bottom flange. The angle of plastic rotation for a single vee heat was calculated by substituting the value of the effective load ratio and other involved parameters into Equation 37.

The residual moment in the damaged composite girder on the Crowley Bridge, at the end of the first heating cycle, was evaluated using the approach just described. The plastic rotation produced by the vee heat was taken as the applied loading on the continuous beam. The fixed end actions were calculated assuming an initial deformation in the beam, in the form of an imposed angle at the location of the vee heat. For an imposed angle ϕ at a distance, a, from the support in an unbraced span of length, l, (Figure 76), the fixed end actions are given as:

$$M_A = \frac{2EI\phi}{L^2}(2L-3a) \tag{38a}$$

$$M_B = \frac{2EI\phi}{L^2}(L-3a) \tag{38b}$$

$$R_A = -R_B = \frac{6EI\phi}{L^2}(L-2a) \tag{38c}$$

The angle ϕ was taken equal to the angle of plastic rotation calculated previously. The distance a was given by the distance of the vee heat application from the diaphragm corresponding to support A. The output of the program provided the resultant span end forces and displacements for each span in the analogous beam. From the span end forces, the moment

and the rotation at the center of damage was calculated using elementary structural mechanics. The moment represented the residual moment, while the rotation provided the net plastic rotation caused by a single vee heat at the center of damage. It was found that the residual moment, caused by the first heating cycle, exerted a counter-active load ratio of 18%. Superimposing this with the applied load ratio, it was calculated that the net positive load ratio in the bottom flange during the second heating cycle was only 7%. Further straightening of the bottom flange enlarged the residual moments to a magnitude that overpowered the applied load ratio and suppressed the plastic rotations in the following heating cycles. In the case of the Crowley Bridge, this condition was attained at the end of the fifth heating cycle.

Non-composite Girders

A number of older highway bridges in Louisiana and elsewhere in the United States display non-composite construction. In non-composite bridge construction, the deck slab is attached to the primary supporting girder only at the ends . As a consequence, when such girders are struck by over-height vehicles, the resulting damage pattern can be quite different from that observed in the case of composite girders. A special feature of this study was the repair of a full scale non-composite bridge girder using the method of heat straightening. No reference was found in the literature regarding the study of heat straightening as applied to non-composite bridge girders.

This study involved the repair of a 20 foot long W 24x76 girder, which was damaged three times using a statically applied load to the bottom flange and straightened each time using heat-straightening. In the process, a proposed methodology for the repair of such damage was identified and a complete set of data for repair using a load ratio of 0.25 was obtained. A total of 56 heating cycles were performed.

Experimental Procedure

The member tested was a 20 foot long, A-36 steel W 24x76 girder. The top flange of the girder was connected as a non-composite member to a concrete slab (weighing 600 lb/linear foot) by means of two bolts, one foot away from each end. The girder was connected to the supporting frame by bolts with long slotted holes at one end in order to eliminate any external indeterminacy. The girder was simply supported with diaphragms placed only at the ends .

The damage was induced by statically loading the bottom flange at mid-length with a hydraulic jack to distort the member plastically about the minor axis. Displacements were

measured at nineteen locations along the length for the first two repairs while seventeen locations were used for the final damage. Fifteen measurements were taken along the cross-section at each location as shown in Figure 78. Measurements were taken to the nearest 1/100 of an inch using a U-shaped reference frame mounted on rails.

Throughout the study, the vee heat patterns used were 0.75 depth, 30 degree vees on the bottom flange and 0.5 depth, 45 degree vee heats on the top flange. Heating temperatures were maintained close to 1200°F and regulated using contact pyrometers and temperature crayons. Single orifice oxy-acetylene torches were used for heating. Due to the presence of the slab, the top flange was heated on its lower surface. The bottom flange was also heated on its lower surface. Both top and bottom flanges were heated at the same cross-section along the length during any given cycle.

Primary parameters affecting heat-straightening i.e. vee angle, heating temperature and vee to plate depth ratio, have been studied in the laboratory and reported in the literature. As reported earlier in this report, the behavior of heat straightened, full scale composite girders have also been evaluated. The damage pattern for non-composite girders proved to be quite different from anything observed earlier. The primary objective in the study of non-composite girders was to determine an appropriate method for repairing the damage by testing various heating patterns and evaluating their effect on the straightening process. The external forces applied were passive, self-releasing jacking forces. The observations and results of the three damage and repair sequences performed are reported.

Case SB-8: Initial Damage and Repair of W 24x76 Girder. The initially straight non-composite beam was statically loaded to produce a lateral plastic deformation of 3.9 in. at mid-length of the bottom flange. The top flange deflected by 1 inch. A total load of 40,100 lb was required.

The damaged shape was checked for yield zones using the best third-degree polynomial curve fit through the measured points and by differentiating the polynomial equation to obtain the curvatures along the length. These values were compared to the limiting values of radius of curvature for yield prescribed by Shanafelt and Horn (1984) to determine the extent of yield zones in each flange. This method worked well in the case of the flanges but was too sensitive to be applied to the web. Also, no distinct yield line could be visually identified in the web. The top flange was deformed along the cross-section. Figure 78 shows the extent of the yield zones in the flanges. A series of heating cycles, using different load ratios and vee heats on the top and bottom flanges, were performed.

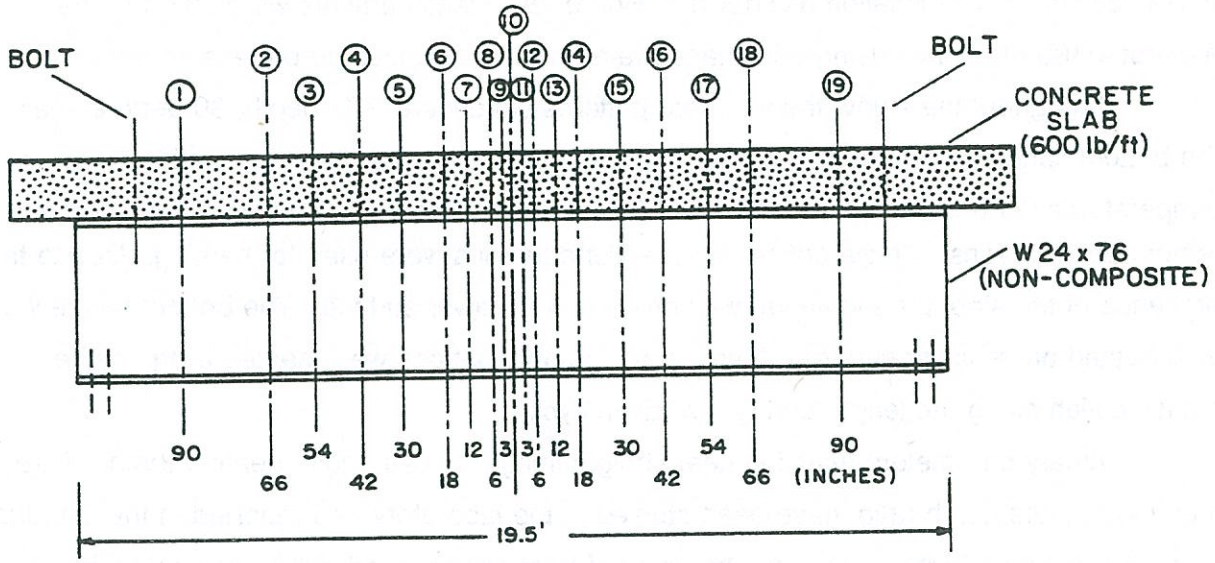

ELEVATION

YIELD ZONES

PT ⑥ TO ⑭ ON BOTTOM FLANGE
PT ⑧ TO ⑫ ON TOP FLANGE
YIELD LINE AT 2½" BELOW FILLET OF TOP FLANGE

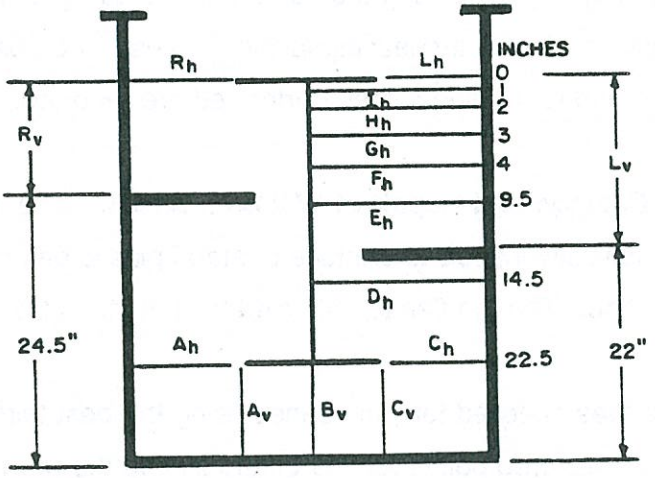

CROSS-SECTIONAL MEASUREMENTS

Figure 78. Experimental set-up for non-composite girder.

The first heating sequence consisted of ten heats at a zero load ratio. The second sequence consisted of 3 cycles at a 0.25 load ratio. Horizontal jacking forces were applied to both flanges. It was determined that the bottom flange was over-heated during some of these cycles. The results of these as well as later cycles are shown in Table 58. A third sequence of ten cycles with a load ratio of 0.25 was followed by a fourth sequence of nine heats with a load ratio of 0.50. The horizontal movement of the bottom and top flange for each cycle are shown in Figures 79a and 79b. The top flange plots appear irregular towards the mid-length due to limitations in measurement, caused by the lateral crimping in the top flange. However the general pattern of movements can be clearly identified.

While the movements of the bottom flange were larger than usual in sequences 1 and 2, unusual behavior was observed at the top flange. During sequence 1, the bottom flange had significant positive plastic rotations but the top flange had consistent negative rotations, as shown in Figure 80c. During sequence 2, the top flange had only one small negative rotation as shown in Figure 80d. However, in sequence 3, the top flange had three large negative rotations which reduced the average rotation significantly as shown in Figure 80e. Clearly, a strong negative force was acting on the top flange and was of a magnitude to overcome a positive jacking force load ratio of 0.50. The force causing the negative rotations probably results from residual stresses caused during damage and friction between the top flange and concrete. Also, the slope of the top flange in the cross section increased with each cycle as shown in Figures 80c, 80d, and 80e. At the end of sequence 3, the bottom flange had straightened and achieved a mid-length translation of 3.6 in. The top flange had translated only 0.57 in. and also displayed a larger slope in cross-section than initially. On plotting the cross-section, a yield zone could clearly be observed, extending between 1.5 to 3.5 inches below the top flange and extending to about 6 feet on either side of the center of damage along the web.

The stages of movement during the SB-8 sequence are shown in Figure 80. In essence, the bottom flange straightened, while the top flange remained damaged. As a result, the web yield line formed as shown in Figure 80e.

It was decided to redamage the beam and to perform a series of tests with line heats and a vertical jacking force on the top flange as shown in Figure 80f.

Case SB-9: Second Re-damage and Repair of W 24x76. The girder was redamaged in a fashion similar to the first case. The bottom flange was plastically deformed by 3.77 in. at midlength while the top flange exhibited a sympathetic horizontal movement of

Table 58. Summary of Experimental Results for Girder SB-8.

Heating Sequence (1)	Heating Cycle (2)	Top & Bottom Vee Heat Location (Pt. #) (3)	Line Heat Location (Pt. #) (4)	Load Ratio (M/M_p) (5)	Plastic Rotation for Bottom vee (mRad) (6)	Plastic Rotation for Top Vee (mRad) (7)
1^1	1	11	--	0.0	9.2309	3.8330
	2	12	--	0.0	-1.6635	-5.0827
	3	8	--	0.0	4.5769	-3.9992
	4	10	--	0.0	0.7489	-0.0834
	5	8	--	0.0	5.9903	1.4997
	6	12	--	0.0	3.2455	-2.4995
	7	12	--	0.0	6.6585	3.5832
	8	10	--	0.0	0.0024	-7.9153
	9	12	--	0.0	3.5794	-2.4992
	10	10	--	0.0	4.5794	0.5001
				Average	3.6944	-1.2663
2^1	1	10	--	0.19	5.0794	4.9150
	2	12	--	0.19	5.2466	2.9990
	3	13	--	0.19	6.1636	3.5826
3	1	13	--	0.19	4.9998	0.9999
	2	13	--	0.19	3.9151	1.9164
	3	13	--	0.19	0.9997	2.0831
	4	8	--	0.19	2.7492	1.6665
	5	9	--	0.19	1.4996	0.0003
	6	8	--	0.19	0.9998	1.5833
	7	8	--	0.19	0.7498	-0.250
	8	9	--	0.19	0.3332	0.5000
	9	8	--	0.19	1.6666	1.4999
	10	8	--	0.19	-0.4165	0.58333
				Average	1.2996	1.0582

Heating Sequence	Heating Cycle	Top & Bottom Vee Heat Location (Pt. #)	Line Heat Location (Pt. #)	Load Ratio (M/M_p)	Plastic Rotation for Bottom vee (mRad)	Plastic Rotation for Top Vee (mRad)
(1)	(2)	(3)	(4)	(5)	(6)	(7)
4	1	9	--	0.39	4.1659	2.7499
	2	8	--	0.39	0.6665	-3.332
	3	9	--	0.39	4.4995	4.3332
	4	8	--	0.39	1.2499	-1.5833
	5	8	--	0.39	4.2497	3.4166
	6	9	--	0.39	2.5832	0.6667
	7	8	--	0.39	-0.6667	0.9166
	8	10	--	0.39	2.21499	0.2500
	9	9	--	0.39	0.5000	-0.7500
				Average	2.1665	0.7407

[1]Bottom flange was overheated in cycles 1-13 in sequences 1 and 2.

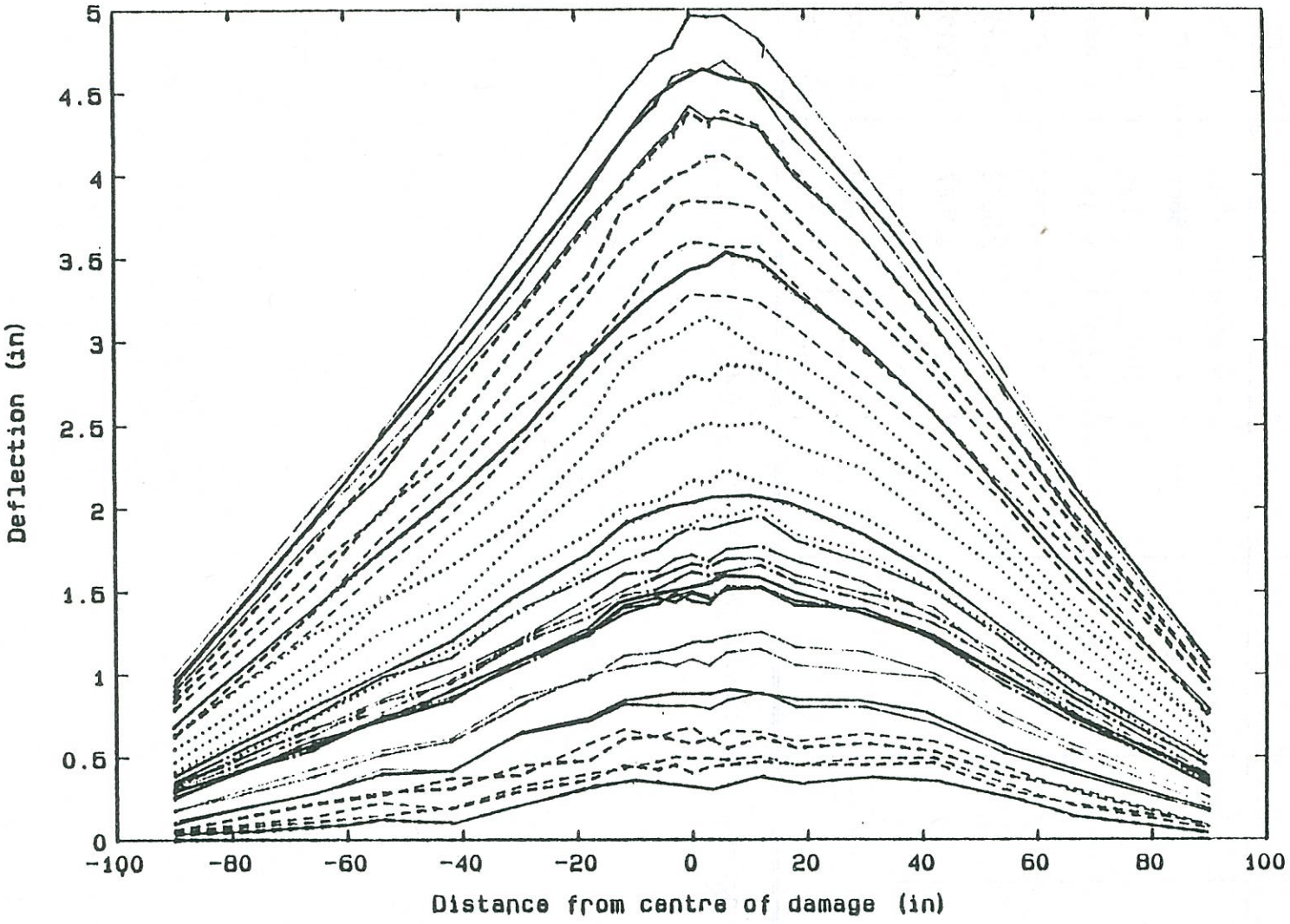

Figure 79a. Deformations of bottom flange of girder SB-8 for 32 heating cycles.

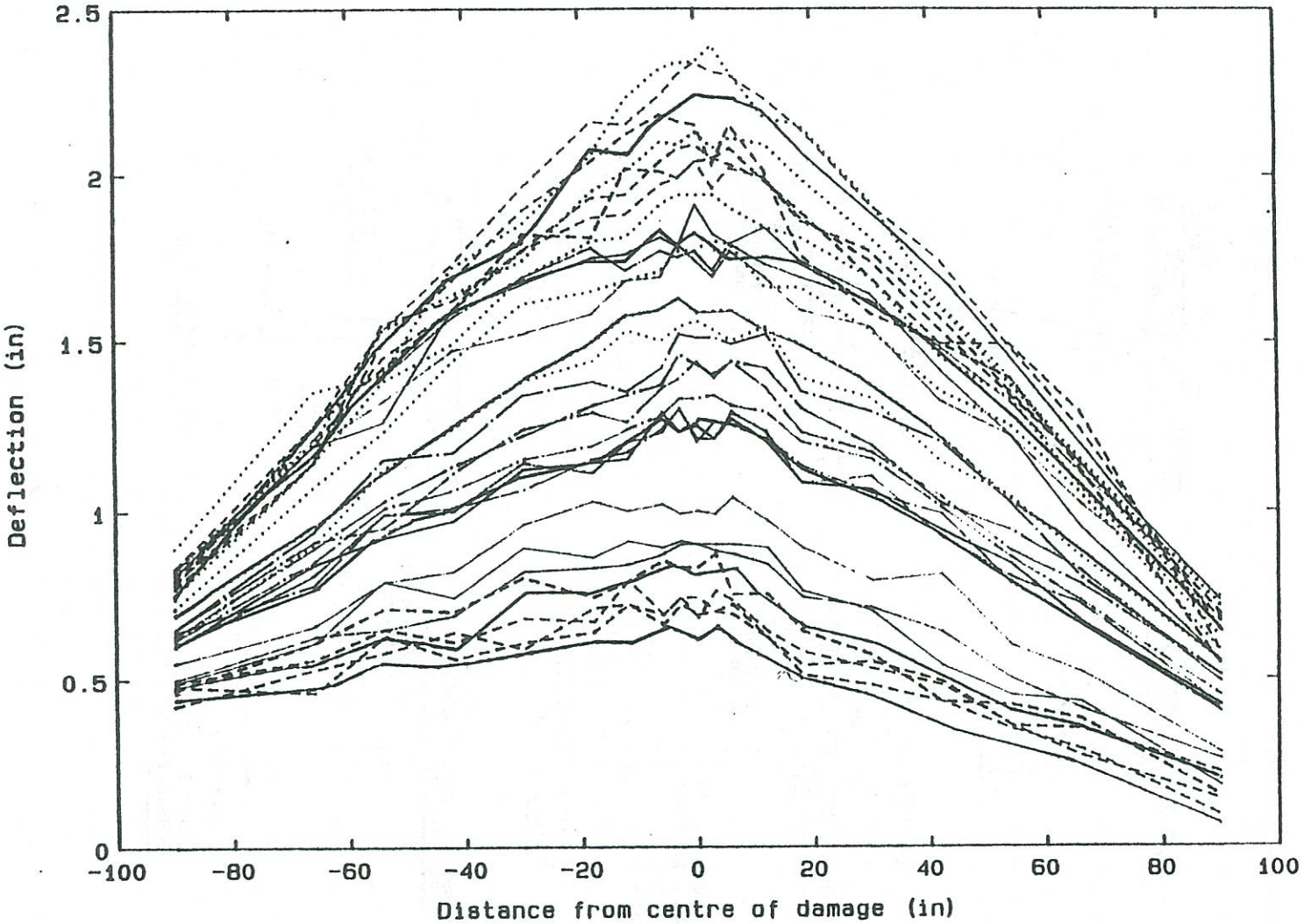

Figure 79b. Deformations of top flange of girder SB-8 for 32 heating cycles.

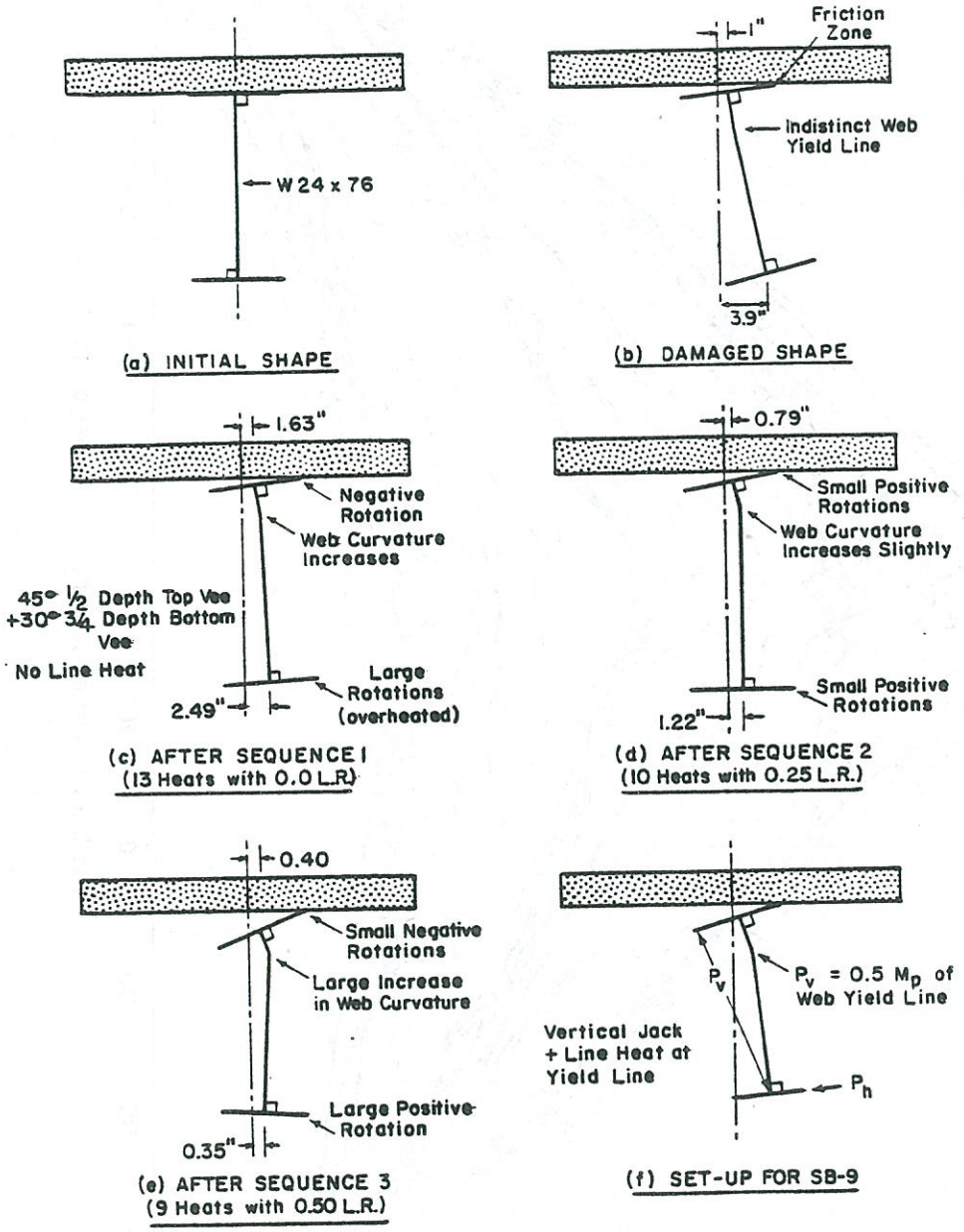

Figure 80. Sequential of SB-8 during various heating sequences.

1.16 in. and a vertical downward deflection of 1.175 inches. A series of nineteen heats were performed using a zero load ratio and varying the heating sequences as indicated in Table 59. Figures 81a and 81b demonstrate the movements of girder SB-9. A vertical jacking force was applied on the top flange at the midlength as shown in Figure 80f. The line heat was placed over a 12 ft length, 6 ft to either side of the center of damage along the web yield line.

The vee heat locations on the flanges were varied. One or both flanges were heated, strip heats and line heats were applied. The combination that worked the best was to heat the bottom flange first and then the web line. The top flange was not heated in this case but still showed positive movement. Strip heats were not effective in improving the heat-straightening response.

Case SB-10: Third Damage and Repair of W 24x76. Based on the tests on SB-9, it was decided to re-damage the beam and to carry out the straightening process using the following methodology:

(1) Place a horizontal jack on the bottom flange and a vertical jack as shown in Figure 80f;

(2) Vee heat the bottom flange;

(3) Line heat the web yield line;

(4) Repeat this methodology until the slopes of both flanges are identical.

This process is referred to as Phase I. The beam behaves similarly to a composite beam. The significant aspect of this phase is the use of the vertical jacking force, whose horizontal component must be balanced by a horizontal jacking force. The magnitude of the vertical jacking force was based on a 0.5 web load ratio, which causes 0.5 times the plastic moment capacity of a 12 ft line along the web. It is advisable not to heat the top flange until the web yield line vanishes.

Once the web yield line vanishes, Phase 2 is initiated. A horizontal load is applied to both flanges and vee heats are performed on top and bottom flanges. A line heat is carried out along the web.

The beam was redamaged for the second time to cause a bottom flange deflection of 4.61 in. The top flange sympathetically deflected by 2.15 in. and displayed a vertical downward deflection of 1.62 in. in the cross-section, relative to the ends, at the center of damage.

The Phase I heating pattern was applied using 10 heating cycles with: a 0.25 effective horizontal load ratio; a line heat 11 ft long, 2.5 in. below the top flange; a web load ratio of 0.5; and a 30 degree, 3/4 depth bottom flange vee. By the end of Phase I, the slopes of both

Table 59. Summary of Experimental Results for Girder SB-9.

Heating Sequence	Heating Cycle	Top & Bottom Vee Heat Location (Pt. #)	Line Heat Location (Pt. #)	Load Ratio (M/M_p)	Plastic Rotation for Bottom vee (mRad)	Plastic Rotation for Top Vee (mRad)
(1)	(2)	(3)	(4)	(5)	(6)	(7)
5[1]	1	--	3-17	0.0	-3.5770	-1.3331
	2	--	2-18	0.0	-5.3225	-4.4158
	3	--	2-18	0.0	1.8294	5.6656
				Average		
6[2]	1	10	2-16	0.0	1.7467	-7.1655
	2	7	2-18	0.0	2.7444	3.8326
	3	9	2-18	0.0	-1.9960	-4.0825
	4	8	2-18	0.0	2.5784	-0.8332
	5	10	2-18	0.0	-0.4993	-0.7497
	6	8	2-18	0.0	-0.9979	-0.0832
	7	10	2-18	0.0	3.7430	0.4165
				Average	1.0456	-0.3749
7[3]	1	8	2-18	0.0	-0.4159	1.9162
	2	10	2-18	0.0	-1.8299	-0.5832
	3	8	2-18	0.0	0.5822	-0.7499
	4	10	2-18	0.0	4.3257	4.9990
				Average	0.6655	1.3955
8[4]	1	7	2-18	0.0	1.3311	-1.7496
9[5]	1	12	--	0.0	0.6657	0.7498
10[6]	1	8	--	0.0	1.6640	1.4164
	2	10	--	0.0	0.7489	-3.7492
	3	8	--	0.0	0.0985	0.6664
				Average	0.6379	-0.5555

[1]Vertical jacking + line, no vee heats
[2]Top and bottom vees + vertical jacking + line
[3]Only bottom vee + vertical jacking + line
[4]Top + bottom vee + line
[5]Top + bottom vee only
[6]Top + bottom vee + rectangular strip heat

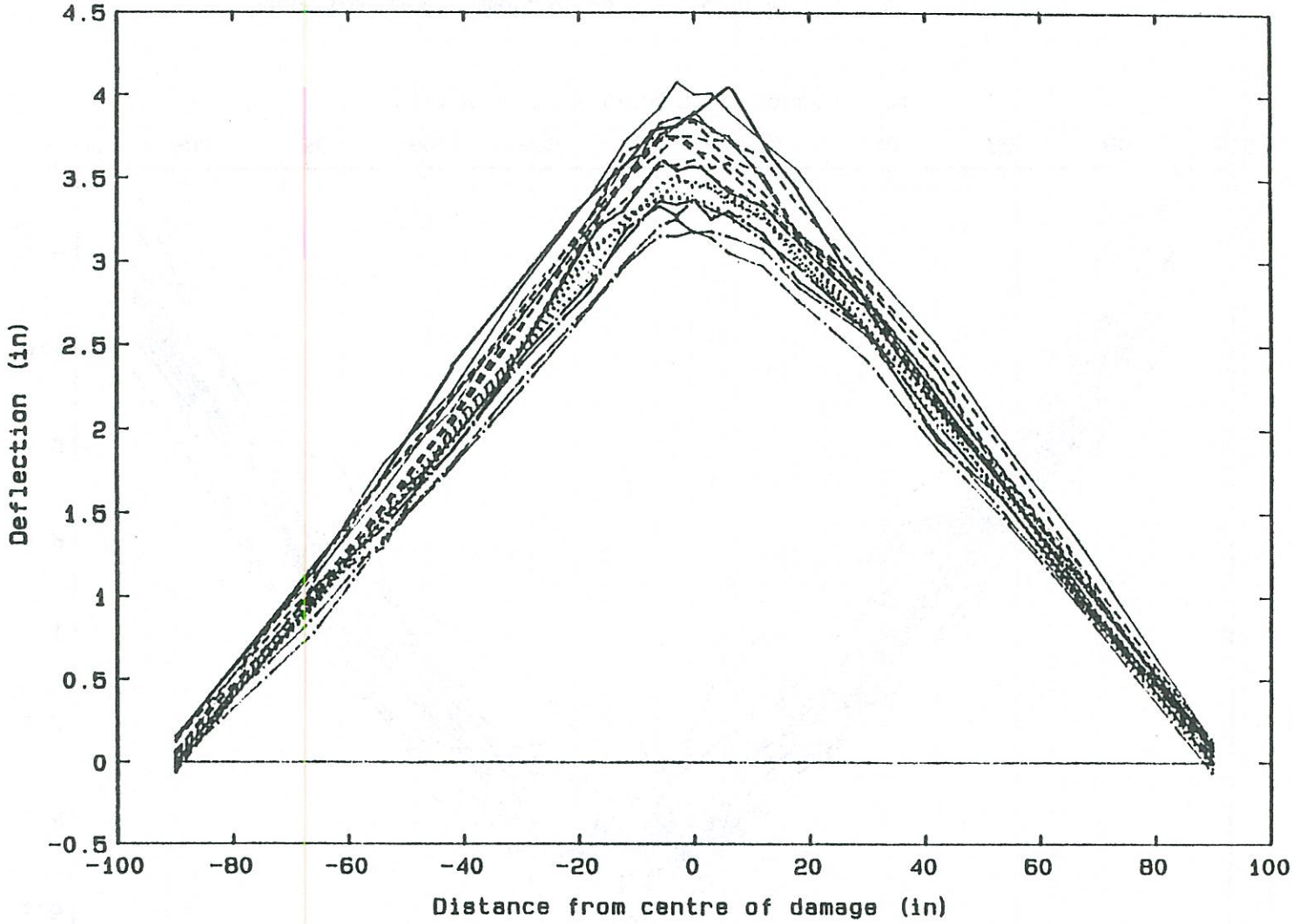

Figure 81a. Deformations of bottom flange of girder SB-9 for 19 heating cycles.

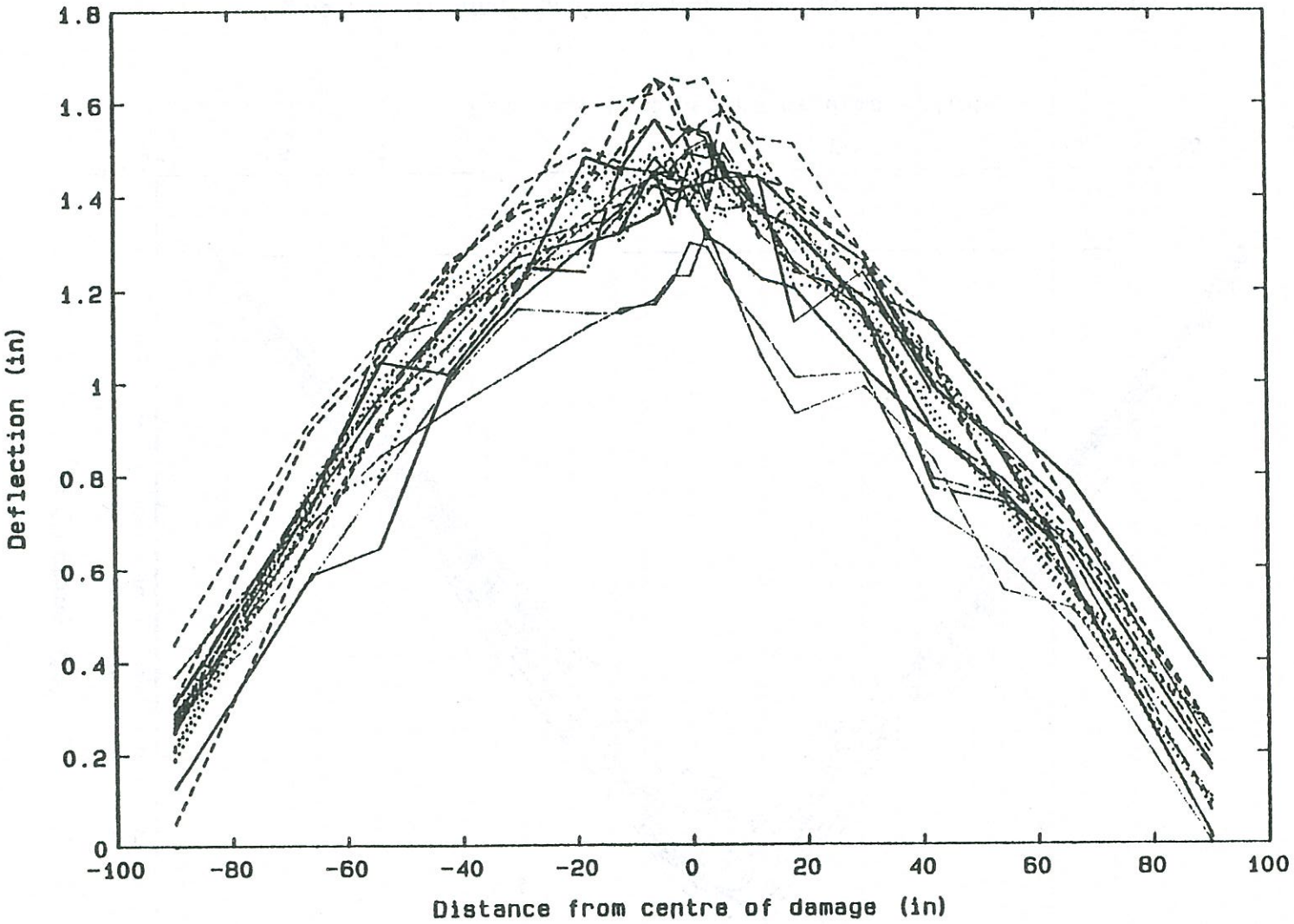

Figure 81b. Deformations of top flange of girder SB-9 for 19 heating cycles.

flanges in the cross-section were equal and the yield line along the web had vanished. The average plastic rotation of the bottom flange was 1.7800 mRad while the top flange showed an average plastic rotation of 0.7600 mRad. Negative movements occurred in four heating cycles. The randomly occurring negative rotation was consistently observed during the tests. However, the average plastic rotations were positive and the heat straightening process was effective.

Eight heating cycles were performed in Phase II to complete the repair. Vee heats and horizontal jacking forces were applied to both the flanges. A 0.25 load ratio was applied to each flange. After 8 cycles, the average plastic rotation for the bottom flange was 0.67 mRad while that for the top flange was 0.64 mRad. Both flanges straightened at a similar rate. Overall, the bottom flange translated 1.94 in. in 18 heats while the top flange translated by 0.77 in. The heat-straightening response is tabulated in Table 60. The horizontal movement of the flanges can be seen in Figure 83a and 83b. The rotation of the top flange about the yield line is shown in Figure 84. Thus, the two phase methodology was effective for straightening non-composite girders.

Recommended Methodology for Non-Composite Girder Repair

Additional testing is required before a methodology can be finalized. Based on the above experiments, a two-phase repair methodology for non-composite girder repair should be investigated further. The methodology is shown in Figure 82.

Phase I: After applying a horizontal jacking force to the bottom flange and a vertical jacking force between the flanges, perform a vee heat to the bottom flange and a line heat along the web yield line. Continue this phase until the cross-sectional slopes of the top and bottom flange are the same at the center of damage.

Phase II: First apply both a horizontal jacking force to both flanges and a vertical jacking force between the top and bottom flanges. Perform vee heats on both flanges and continue to heat the web yield line until the beam straightens.

At any stage during phase II, if the cross-sectional slope of the bottom flange exceeds that of the top flange, phase I should be reapplied until the slopes become identical.

Table 60. Summary of Experimental Results for Girder SB-10.

Heating Sequence	Heating Cycle	Top & Bottom Vee Heat Location (Pt. #)	Line Heat Location (Pt. #)	Load Ratio (M/M_p)	Plastic Rotation for Bottom vee (mRad)	Plastic Rotation for Top Vee (mRad)
(1)	(2)	(3)	(4)	(5)	(6)	(7)
	1	10	2-18	0.19	4.3883	1.3904
	2	9	2-18	0.19	1.2642	2.2330
	3	10	2-18	0.19	1.8601	-0.6781
	4	8	2-18	0.19	2.0684	1.8166
	5	9	2-18	0.19	2.9502	6.2590
11[1]	6	10	2-18	0.19	0.8042	-4.6362
	7	8	2-18	0.19	6.4580	-0.1404
	8	9	2-18	0.19	-4.6559	-0.7024
	9	8	2-18	0.19	1.5939	1.7100
	10	10	2-18	0.19	1.0997	0.0242
				Average	1.7831	0.7557
	1	8	4-16	0.19	3.6626	-1.4145
	2	11	4-16	0.19	-4.4474	1.0561
	3	8	4-16	0.19	3.8462	4.4278
	4	9	4-16	0.19	-4.5685	-5.7960
12[2]	5	10	4-16	0.19	3.8758	1.8505
	6	8	4-16	0.19	-0.8576	1.4291
	7	9	4-16	0.19	1.0852	0.8333
	8	8	4-16	0.19	2.7567	2.4417
				Average	0.6692	0.6038

[1]Bottom vee + line + vertical jacking + horizontal load on bottom flange
[2]Top + bottom vee + horizontal load on both flanges

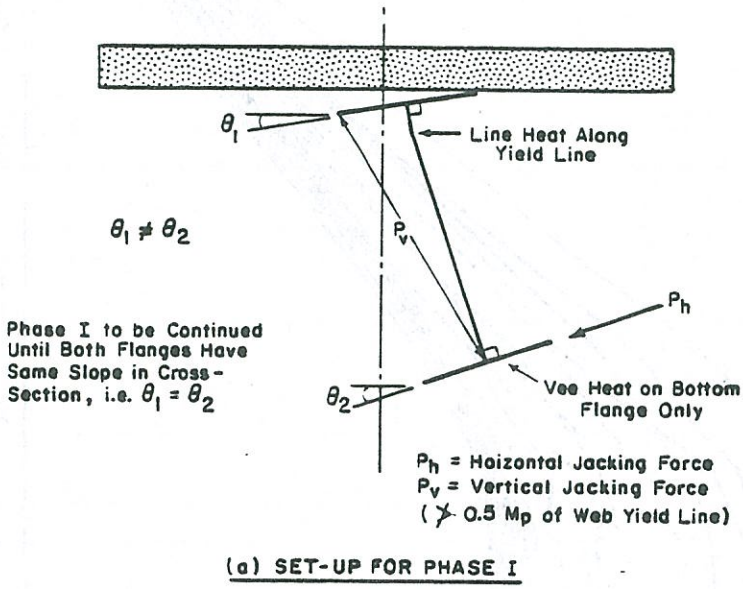

(a) SET-UP FOR PHASE I

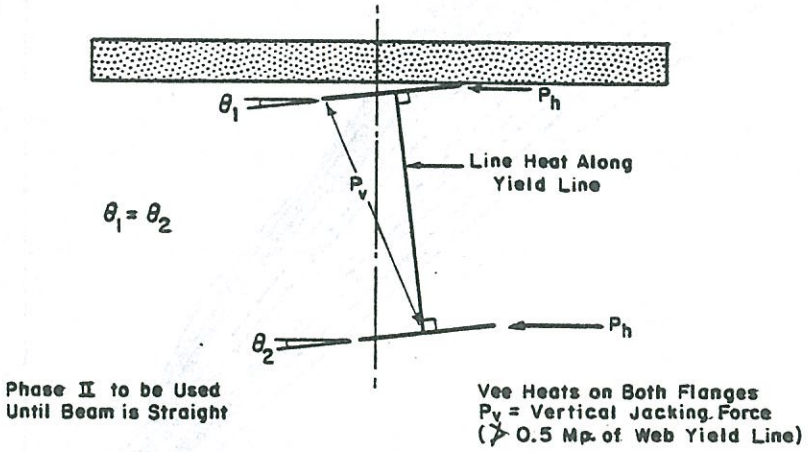

(b) SET-UP FOR PHASE II

Figure 82. Methodology for non-composite girder repair.

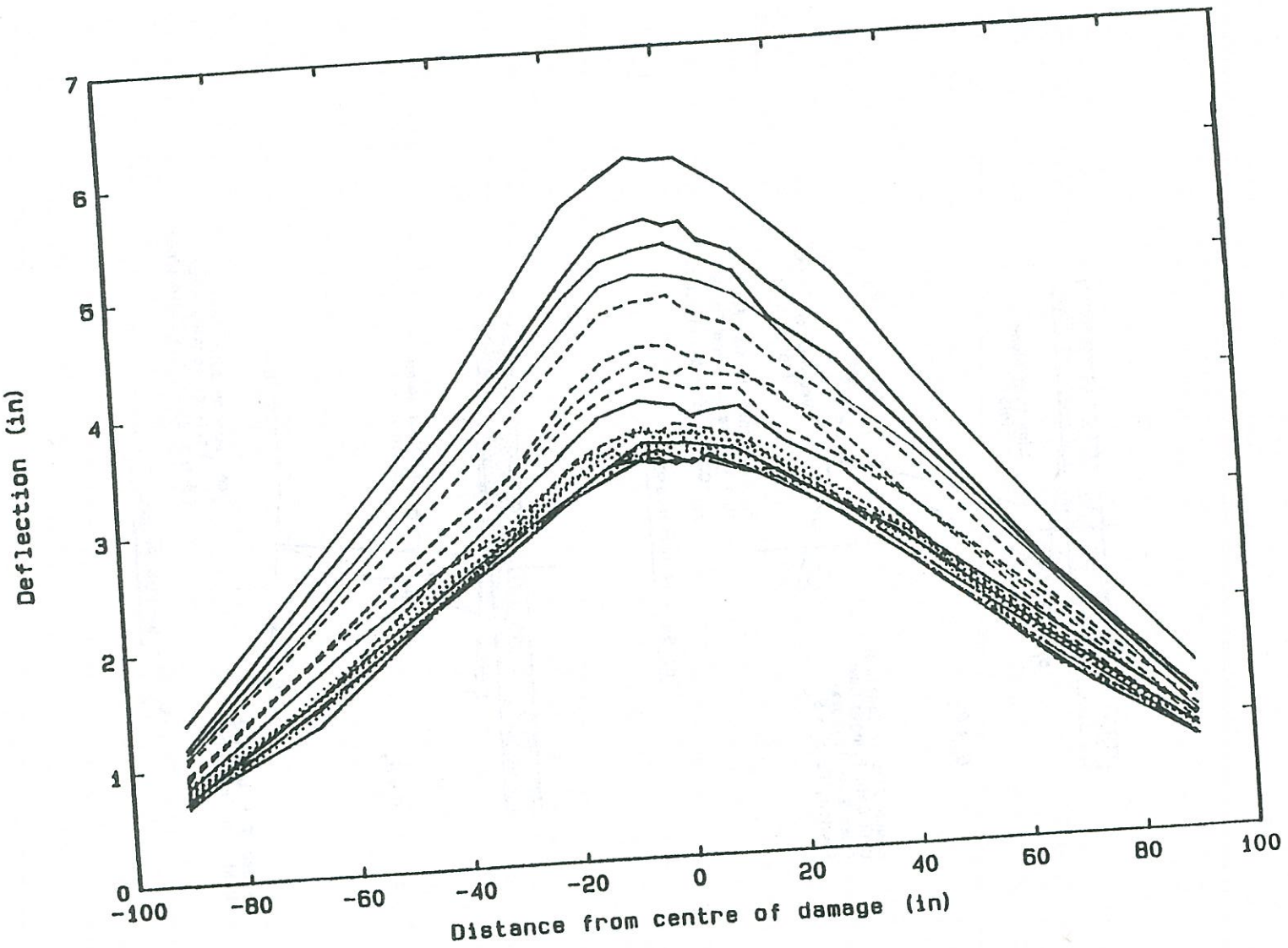

Figure 83a. Deformations of bottom flange of girder SB-10 for 18 heating cycles.

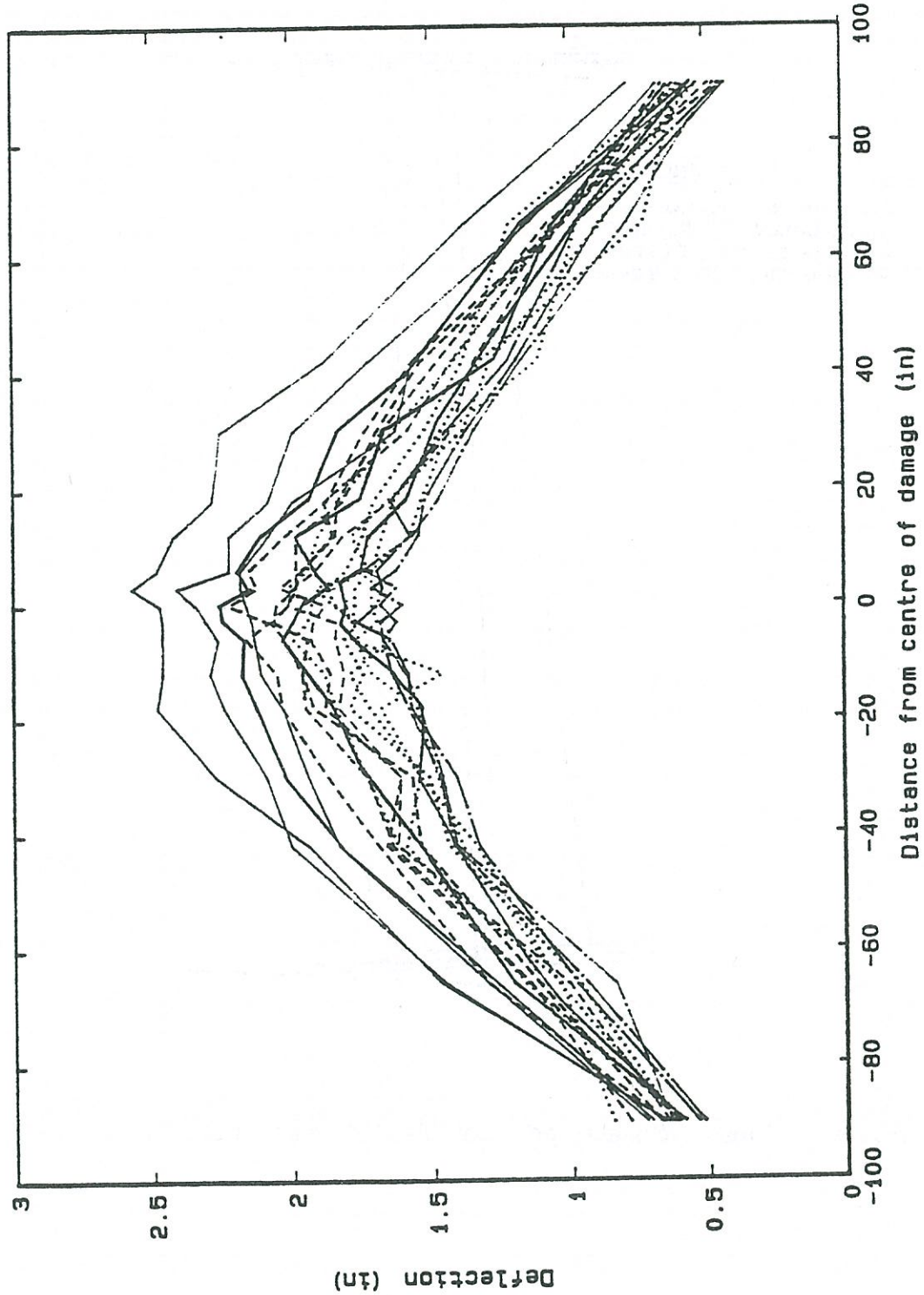

Figure 83b. Deformations of top flange of girder SB-10 for 18 heating cycles.

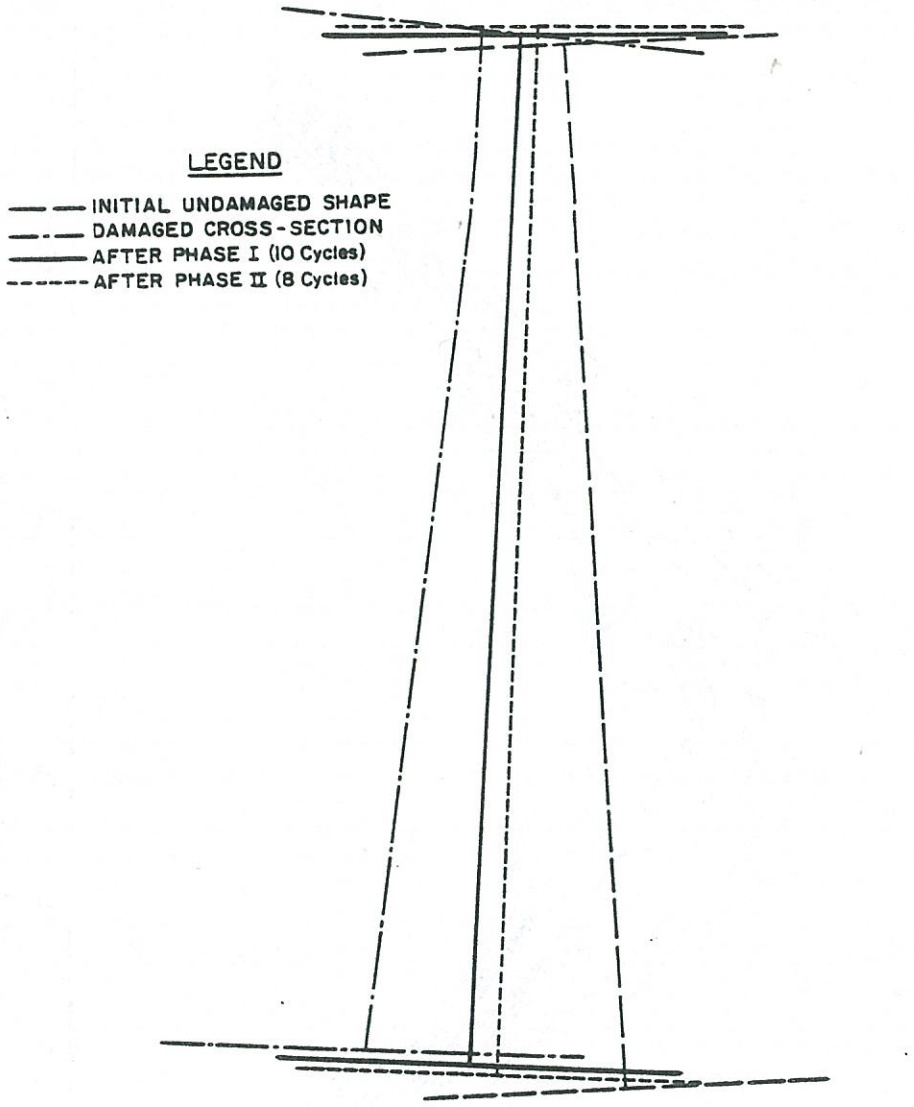

Figure 84. Cross sectonal response of SB-10 at center of damage.

Analysis of Results

A graphical presentation of the plastic rotation data for the above tests is given in Figure 85 and 86. During the tests, the jacking force required to apply the load ratios was calculated using an assumed yield stress of 36 ksi. However, a tensile test on a sample from the unheated region of the girder indicated that the actual yield stress of the steel was 46.5 ksi. Thus, the effective applied load ratios were 0.19 and 0.39, respectively, rather than the originally assumed values of values of 0.25 and 0.50. These actual values have been used for the analysis.

In Figure 85, lines 1 and 2 show the plastic rotations predicted by the plate formula for 30 degree and 45 degree vee heats. Line 3 shows the bottom flange test values for sequences 2 and 3. Line 4 shows the top flange values for sequences 2 and 3 using all 10 cycles in sequence 3. Line 5 shows the same values ignoring the negative rotations. A comparison of lines 4 and 5 indicates the substantial nature of these negative values and their retarding effect on the top flange rotations. The average bottom flange plastic rotations for SB-10 during Phases I and II are shown in Figure 86. The theoretical plastic rotations from the Category W wide flange equation (Eq. 15) and the plastic rotations for the composite W24x76 evaluated earlier on in this study are also shown. When the results for the non-composite case are compared to the results obtained for composite beams at the 0.25 load ratio, the plastic rotations are much lower for the non-composite girder. The rotations in the composite case can be interpolated in Figure 67 as 3.8 mRad as compared to 1.78 mRad for the Phase I heats wherein both sequences use a bottom vee and web line heat but the latter sequence also uses vertical jacking forces. The plastic rotations for Phase II are similarly much lower than those theoretically predicted by Eq. 15 for Category W shapes.

An important aspect that appears in all the tests performed on the non-composite beams is the retarding effect of the slab on the top flange movements. In Figure 85, the plots of Load ratio v/s Plastic rotation show that although a 45 degree vee was used, the top flange shows lower rotation than the bottom flange which had a 30 degree vee.

It can be observed from the tests that the top and bottom flanges move at similar rates for Phase II. However the top flange is required to move through a smaller deflection than the bottom flange in order to straighten the beam. The top flange would regain its original configuration before the bottom flange. In this case the process was stopped prior to completely straightening the girder. However, once the top flange is straight, only the bottom flange should be heated.

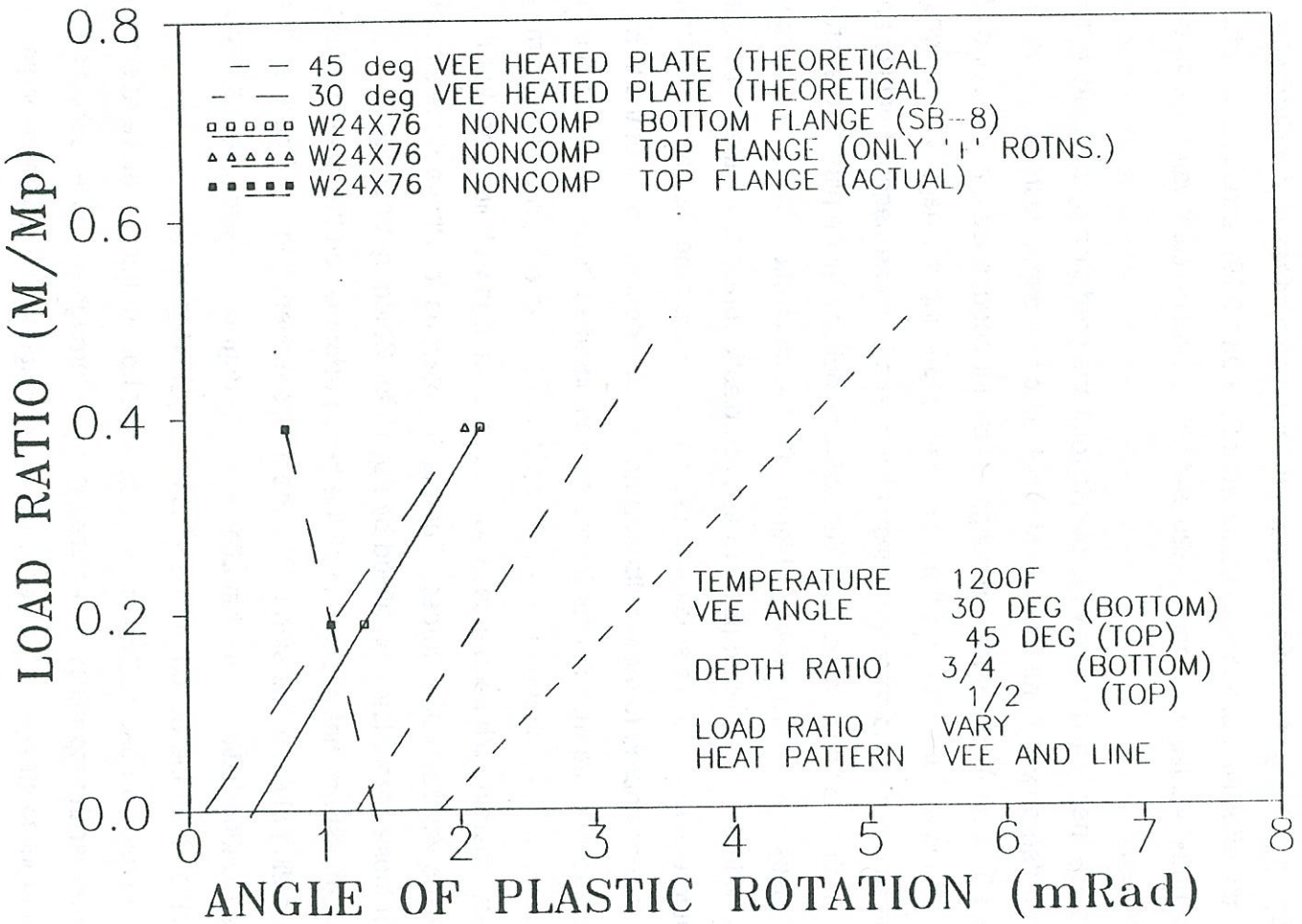

Figure 85. Plot of plastic rotation vs. load ratio for SB-8.

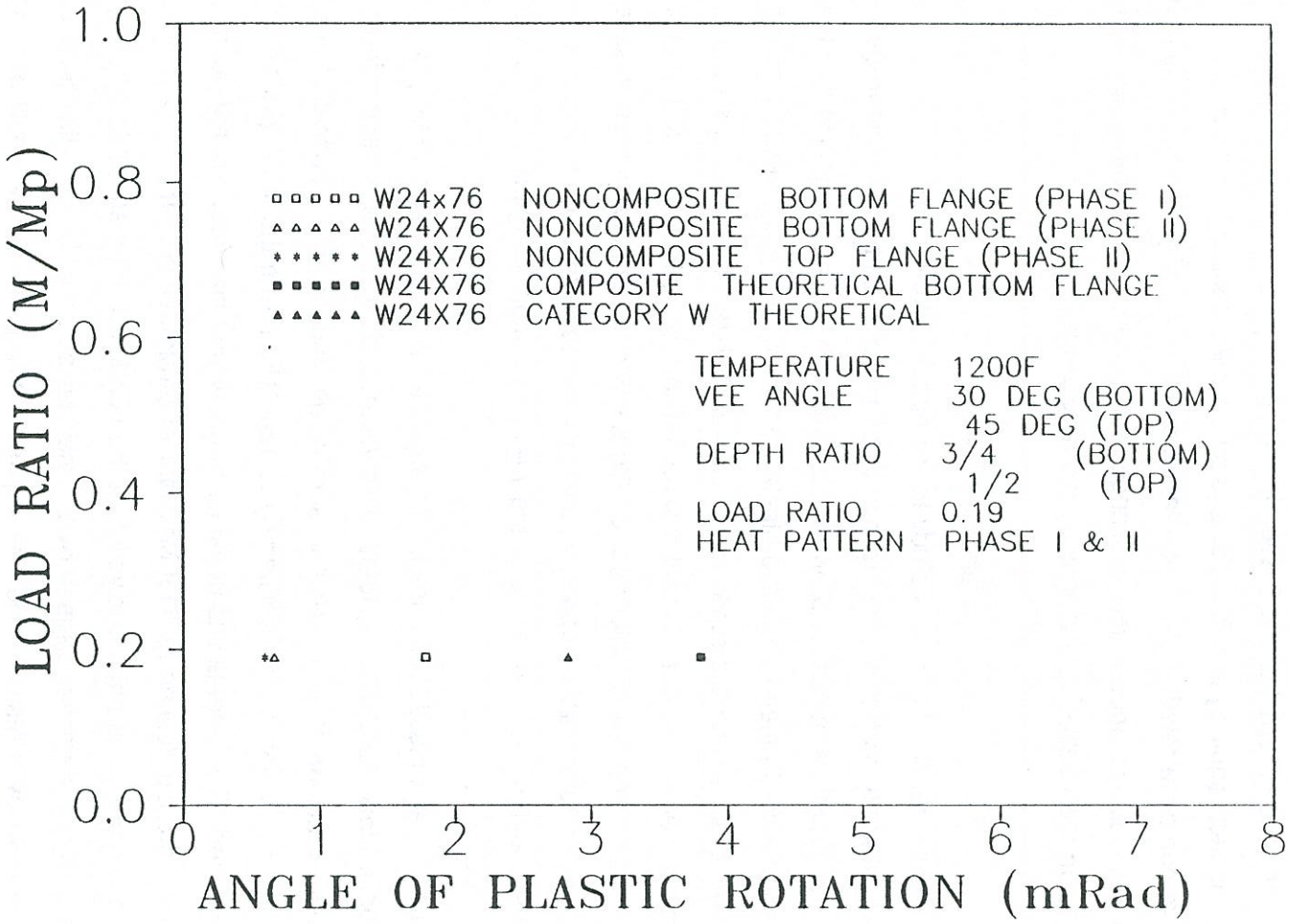

Figure 86. Plot of plastic rotation vs. load ratio for SB-10.

The only consistent data available for predicting this movement has been obtained in the 18 cycles performed on SB 10. Further tests using load ratios of 0.0 and 0.50 and the prescribed methodology are required in order to reliably quantify the behavior. An analytical formula to predict the plastic rotations could then be developed and used to predict the number of heats required to repair a given level of damage.

The other aspect requiring additional analysis is to determine the number of heats required to ensure complete rotation of the top flange about the web yield line. This number would depend on the relative slope of the top flange in the cross-section with respect to the bottom flange and on the vertical web yield line load ratio used.

Conclusions

The conclusions reached from this study for composite girders are:

(1) A past study on the heat-straightening behavior of composite bridge girders established that a vee heat on the bottom flange in conjunction with a line heat on the web (in their respective plastic curvature regions) constitute an effective heating pattern for the repair of composite girders. The present study verified this fact and offered additional research evidence to indicate that the inclusion of a half-depth rectangular heat on the web does not influence the plastic rotations appreciably. However, they do tend to reduce the buckling of the web due to differential shortening of the web and bottom flange at the location of the vee.

(2) The average plastic rotations in a composite girder increase linearly with the applied load ratio (jacking force). However, a deviation is observed from the linear relationship at a certain load ratio, beyond which dramatically large plastic rotations (higher than predicted by extrapolation from the linear pattern) are obtained. The anomalous behavior at excessive load ratios is attributed to the phenomenon defined as 'Hot Mechanical Straightening'. It was concluded from the elastic folded plate analysis that the non-linear heat-straightening response of tested girders was caused by the yielding of the web about its minor axis at relatively low stresses under the applied jacking forces as a result of elevated temperatures associated with the line heat. The critical load ratio which initiates the non-linear response (that characterizes hot mechanical straightening) depends on the geometry of the composite girder. A criteria has been developed using the folded plate analysis for predicting this critical load ratio for

a generalized composite girder. The critical load ratio in this case was found to be higher for the shallow girder.

(3) The redundant interactions at the web-flange interface of the composite girder stiffens the response of the bottom flange to the external jacking forces. The stiffening effect of the web depends on the girder geometry and diminishes with the depth to thickness ratio of the web. A stiffness modification factor was estimated for the bottom flange in the W10x39 as well as W24x76 composite girders. A design chart (Figure 71) is provided to obtain the stiffness modification factor for a generalized composite girder.

(4) Because of the indeterminate web-flange interaction, the bending moments produced by the external restraining forces are distributed among both the bottom flange and web. Only that fraction of the applied bending moment which is distributed to the bottom flange is effective in providing external restraint to the vee. In case of significant web effects, the definition of the load ratio used previously is deceptive as it does not reflect the external constraint in the bottom flange. The external constraint in the bottom flange is more rationally represented by the 'effective load ratio' parameter computed as the ratio of fractional bending moment distributed to the bottom flange to its plastic moment capacity at the location of the vee heat. An approximate analysis was developed to estimate the moment distributed to the bottom flange in a generalized W shaped composite girder. The results of the approximate analysis were verified by conducting an exact elastic analysis. The exact analysis uses a matrix stiffness approach based on folded plate theory. The effective load ratio, defined earlier, may be computed using either approach.

(5) The redundant forces at the web-flange interface impose a negative internal constraint on the vee action in the bottom flange and inhibits the heat-straightening response (plastic rotations) of the bottom flange in a composite girder. The impedance to the straightening effect is more pronounced for shallow beams. As established in the past research, the presence of the yield line in the web tends to magnify these counter-productive redundant forces. A line heat on the web along with the vee heat in the bottom flange is quite effective in mitigating these negative constraining forces.

(6) A simple formula was derived for computing the plastic rotations in a simple span composite girder.

(7) The plastic rotation at the location of the vee heat in a heat-straightened continuous span composite girder (with intermediate lateral bracings) produces indeterminate forces/moments at the braced sections. These redundant forces provide a negative internal constraint to the vee in the form of a residual moment at that location. The progressive movement of the bottom flange due to heat-straightening results in an accumulation of the residual moment which may become large enough to overpower the positive effect of the applied load ratio and deter further plastic rotations. These moments need to be evaluated and balanced by increasing the applied jacking forces at the end of each heating cycle. A simplistic analytical approach was presented to approximate the magnitude of the residual moment at the end of each heating cycle. The residual moment in the bottom flange of a composite girder may be assessed by analyzing the indeterminate forces/moments in an analogous continuous beam with an initial deformation in the form of an imposed bend at the location of the vee heat. The stiffness of the analogous beam is given by the effective stiffness of the bottom flange.

(8) A conclusive recommendation on the repair of non-composite girders cannot yet be made. Additional testing and evaluation is required to finalize a procedure. However, a proposed methodology for future study is proposed.

Chapter 5

HEAT STRAIGHTENING OF DAMAGED BRIDGE TRUSS MEMBERS SUBJECTED TO AXIAL COMPRESSION

Introduction

An important aspect to be addressed in the study of the heat straightening response of damaged bridge structural components is the effect of axial compression on the repair process. Truss members damaged by over-height vehicles typically include lateral wind bracing elements which may carry a substantial axial load. Other truss members in bridges are also susceptible to damage due to impact of passing vehicles.

The factors evaluated in this phase of the study were the effects of the P-Delta moments on the repair process and the effect of load ratio on the magnitude of the plastic rotations.

A study of the response of two A-36 steel girders was conducted. An HP 12x53 was tested for minor axis damage (Category W) and a W 10x39 was tested for major axis damage (Category S). During the repair, both beams were subjected to axial compression of 0.35 times the AISC allowable axial load. A total of 70 heating cycles were performed. Load ratios of 0.0, 0.25 and 0.50 were used in each case. A zero load ratio sequence with an axial load of 0.175 times the allowable axial load was also conducted in the case of the Category W damage.

Experimental Procedure

The girders were tested in the HEAT facility. The specimens used were 20 foot long, A-36 steel girders. Girders SB-11, SB-12, SB-13 and SB-14 were damaged about the minor axis while girders SB-15, SB-16 and SB-17 were damaged about the major axis.The damage was induced symmetrically about the center of damage using statically loaded hydraulic jacks. The girders were simply supported and diaphragms were placed only at the ends. No axial loads were applied during the damage process. The axial force was applied by means of the assembly shown in Figure 87a and 87b. Lateral jacking forces were applied by means of hydraulic jacks. Measurements were taken to the nearest 1/100 in by means of a scale at 19 locations along the length with 10 points per cross-section. The heating was carried out using single orifice oxyacetylene torches. The patterns used were 3/4 depth 45 degree vees and a strip heat on the web (for Category W only). The outside surface of the bottom flange and the

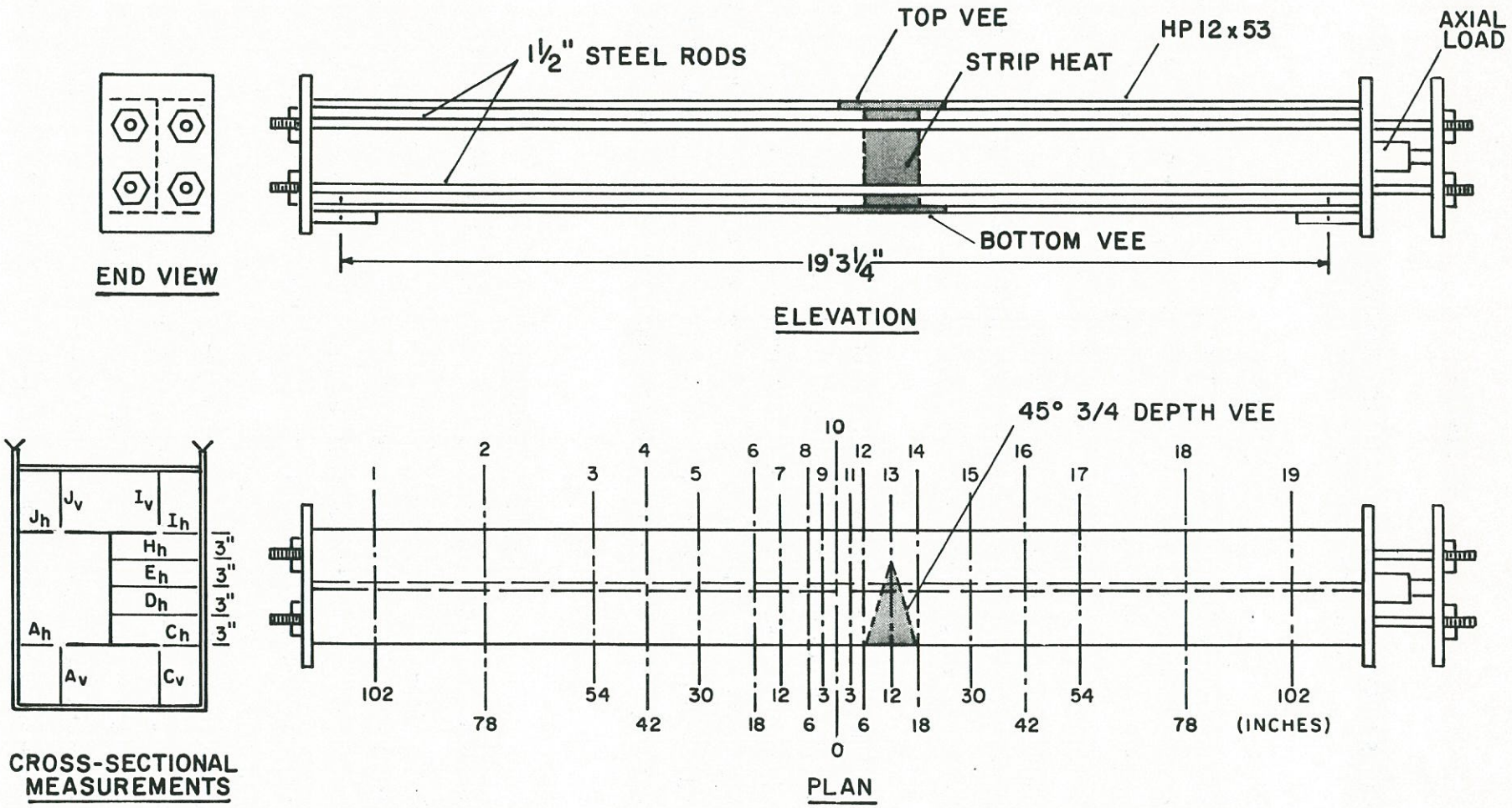

Figure 87a. Experimental set-up for Category W compression members.

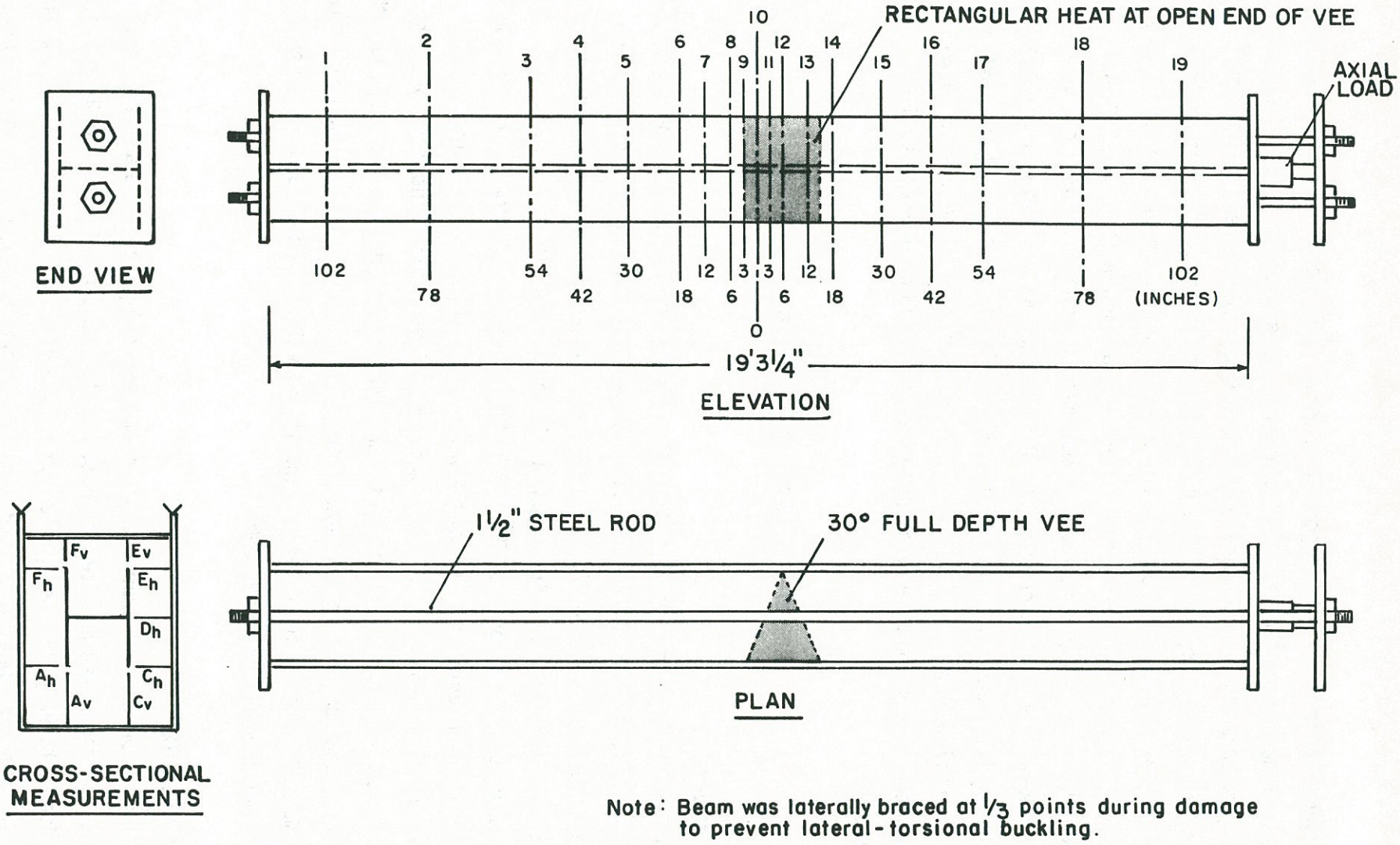

Figure 87b. Experimental set-up for Category S compression members.

top flange were heated in case of Category W as shown in Figure 87a. The web and the outer surface of the flange, at the open end of the vee, were heated in case of Category S as shown in Figure 87b. The vee heat used on the web was a 30 degree full depth vee.

With the axial load applied, a moment in the member is created due to the P-delta effect. This moment tends to impede the heat straightening process as it acts to magnify the damage. The approach used here was to cancel out this moment with the application of the lateral jacking force. After each cycle, the moment resulting from the axial force acting through the new midpoint deflection was computed. The jacking force was adjusted to include the specified load ratio plus a moment to cancel out the P-delta moment at the center of damage. The load ratio for these tests is defined as the ratio of the moment at the center of damage due to the jacking force divided by the plastic moment of the cross-section about the axis of damage.

Description of Test Results

Category W: SB-11

The HP 12x53 girder, which was tested for the category W case, was damaged and repaired three times using load ratios of 0.50, 0.25 and zero. The three sequences are represented as SB-11, SB-12 and SB-13 respectively. A load of 21 kips was required to induce a deflection of 3.36 in. on the initially straight beam. Ten heating cycles were performed using a load ratio of 0.50. The loads during damage and repair were applied on both the flanges symmetrically. Both flanges were vee heated simultaneously using two torches. A strip heat on the web was then carried out. The plastic rotations are given in Table 61. An average plastic rotation of 5.16 mRad was achieved over the ten cycles in the top flange while the bottom flange showed an average plastic rotation of 5.9140 mRad. The beam translated 3.41 in. during the ten cycles. The movements of the beam over these ten cycles are shown in Figure 88a and 88b.

Category W: SB-12

The same beam was redamaged using a load of 21 kips to induce a deflection of 3.66 in. Ten heating cycles were performed using a load ratio of 0.25. An identical method was used for the heating. An average plastic rotation of 3.7910 mRad was achieved over the ten cycles in the top flange while the bottom flange compared similarly with an average plastic rotation of 3.9090 mRad. The beam translated by 2.15 in. during the ten cycles. The

Table 61. Summary of Experimental Results for Category W Compression Members SB-11 through SB-14.

Heating Sequence	Heating Cycle	Vee Heat Location	Load Ratio (M/M_p)	Top Flange Plastic Rotation (millirad)	Bottom Flange Plastic Rotation (millirad)
(1)	(2)	(3)	(4)	(5)	(6)
	1	10	0.42	13.2547	8.7179
	2	12	0.42	5.4923	8.1797
	3	10	0.42	8.4864	4.8165
	4	12	0.42	5.3247	6.2913
	5	8	0.42	4.3683	4.0071
SB-11[1]	6	12	0.42	4.6950	5.3586
	7	10	0.42	4.0534	2.2629
	8	8	0.42	2.0714	0.5733
	9	12	0.42	3.2653	12.9488
	10	10	0.42	0.5967	5.9791
			Average	5.1608	5.9135
	1	10	0.21	9.4827	7.7712
	2	12	0.21	2.4859	-9.2918
	3	12	0.21	4.4216	16.7501
	4	10	0.21	3.3983	0.2364
	5	12	0.21	7.9809	4.3655
SB-12[1]	6	8	0.21	-1.6673	4.0847
	7	12	0.21	3.905	1.7441
	8	13	0.21	0.9460	2.0939
	9	10	0.21	3.6806	4.9742
	10	8	0.21	3.2758	6.3705
			Average	3.7910	3.9099
	1	10	0.0	5.6589	1.0120
SB-13[1]	2	12	0.0	0.9119	1.2036
	3	8	0.0	1.9011	1.8783

Heating Sequence	Heating Cycle	Vee Heat Location	Load Ratio (M/M_p)	Top Flange Plastic Rotation (millirad)	Bottom Flange Plastic Rotation (millirad)
(1)	(2)	(3)	(4)	(5)	(6)
SB-13[1] (cont.)	4	10	0.0	2.5771	1.1814
	5	12	0.0	1.2717	1.3725
	6	10	0.0	0.6976	-0.1576
	7	14	0.0	2.3405	1.2941
	8	12	0.0	0.1575	2.1265
	9	10	0.0	1.0917	-0.8999
	10	12	0.0	2.6563	1.2713
			Average	1.9264	1.0283
SB-14[2]	1	12	0.0	-0.4278	0.0111
	2	10	0.0	3.5683	0.3374
	3	10	0.0	-2.8144	0.5964
	4	10	0.0	0.8554	0.5852
	5	8	0.0	1.9022	1.3278
	6	10	0.0	0.1012	0.3826
	7	12	0.0	0.1575	0.1574
	8	10	0.0	-0.9789	-0.9223
	9	13	0.0	1.7781	2.6892
	10	10	0.0	2.5438	1.0351
			Average	0.6685	0.6200

[1]An axial load of 0.35 times the allowable axial load (based on AISC specifications) was maintained during straightening

[2]An axial load of 0.175 times the allowable axial load (based on AISC specifications) was maintained during straightening

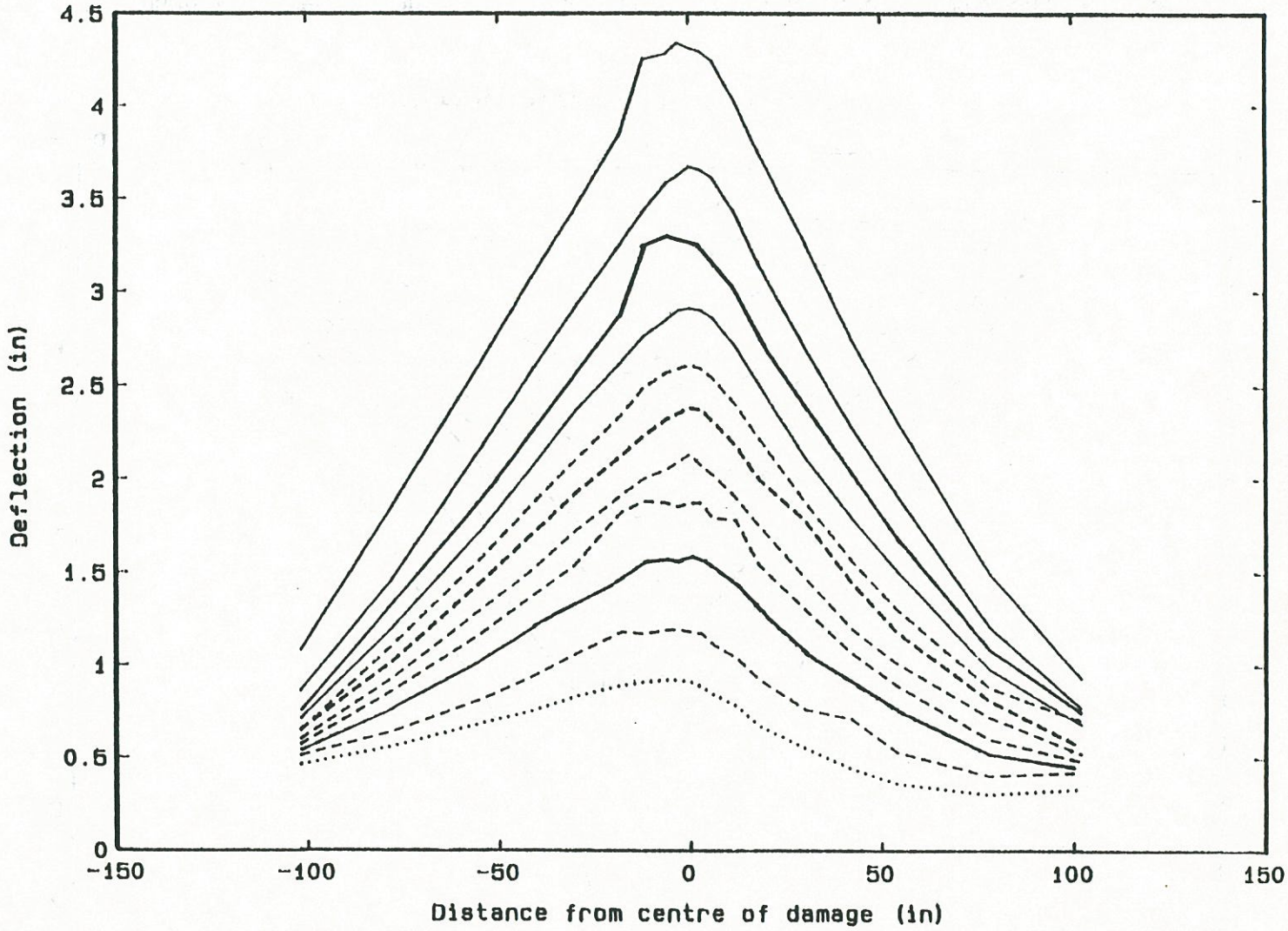

Figure 88a. Deformations of bottom flange over 10 heating cycles for compression member SB-11.

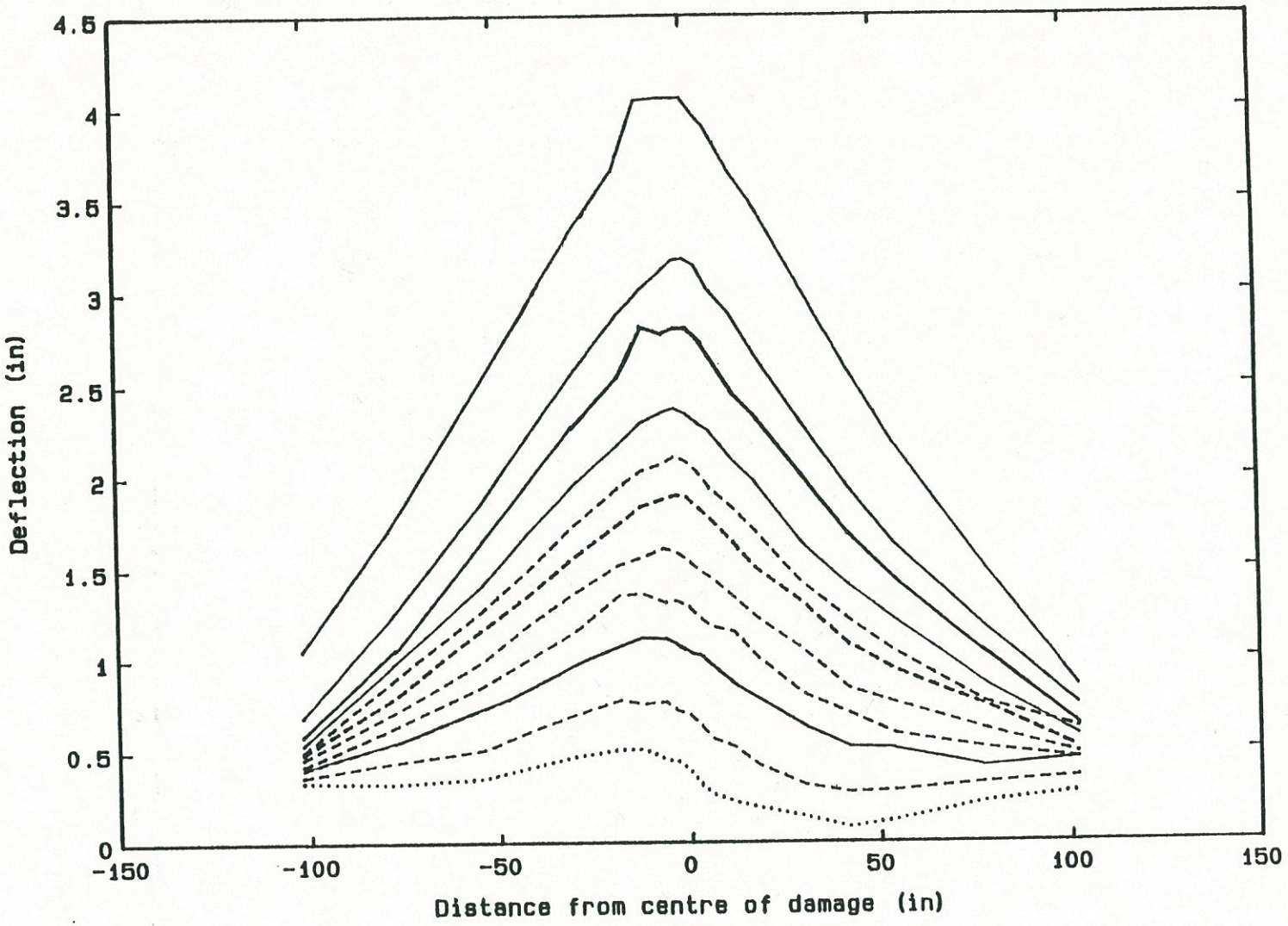

Figure 88b. Deformations of top flange over 10 heating cycles for compression member SB-11.

movements of the beam over these ten cycles are shown in Figure 89a and 89b and the plastic rotations are shown in Table 61.

Category W: SB-13

The same beam was redamaged using a damage load of 21 kips to induce a deflection of 3.25 in. Ten heating cycles were performed using a load ratio of zero. A lateral jacking force was applied only to balance the P-delta effect. An average plastic rotation of 1.9270 mRad was achieved over the ten cycles in the top flange while the bottom flange showed an average plastic rotation of 1.0280 mRad. The beam translated 0.86 in. during the ten cycles. The movements of the beam over the ten heating cycles are shown in Figure 90a and 90b and the plastic rotations are shown in Table 61.

Category W: SB-14

The applied axial load was then reduced to 0.175 times the allowable axial load and a further series of ten cycles using a zero load ratio were performed. An average plastic rotation of 0.6690 mRad was achieved over the ten cycles in the top flange while the bottom flange showed an average plastic rotation of 0.6200 mRad. The beam translated 0.37 in. during the ten cycles. The movements of the beam over these twenty heating cycles are shown in Figure 91a and 91b and the plastic rotations are tabulated in Table 61.

Category S: SB-15

The W10x39 girder, which was damaged about the strong axis, was damaged and repaired three times using load ratios of 0.00, 0.25 and 0.50. In order to prevent lateral torsional buckling of the beam during damage, the beam was laterally braced at the third points. There was a tendency for lateral torsional buckling due to the large load required to induce major axis damage on a full-scale girder. The bracings were removed during the repair sequence in order to prevent any influence on the plastic rotations. The three sequences are represented as SB-15, SB-16 and SB-17 respectively. A load of 28.98 kips was required to induce a deflection of 1.70 in. on the initially straight beam. Thirteen heating cycles were performed using a load ratio of zero. The vee heats were changed from 45 degree to 30 degree vees after the third cycle in order to minimize local distortion and maintained at 30 degrees for the rest of the Category S cycles. The loads during damage and repair were applied directly to the web. First, the web was vee heated. Then a strip heat, on the flange at the open end of the vee, was carried out. The strip heat progressed from the top

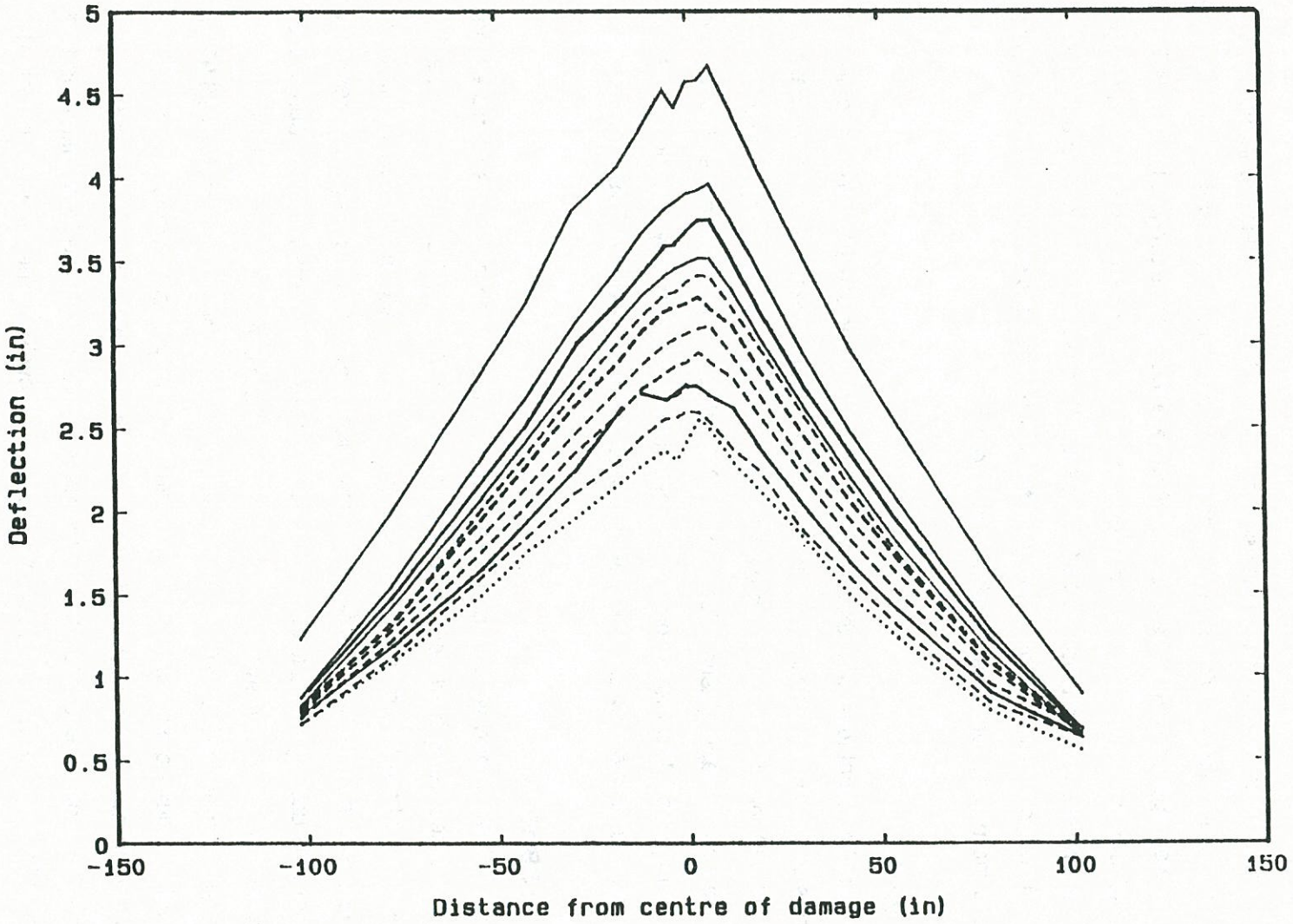

Figure 89a. Deformations of bottom flange over 10 heating cycles for compression member SB-12.

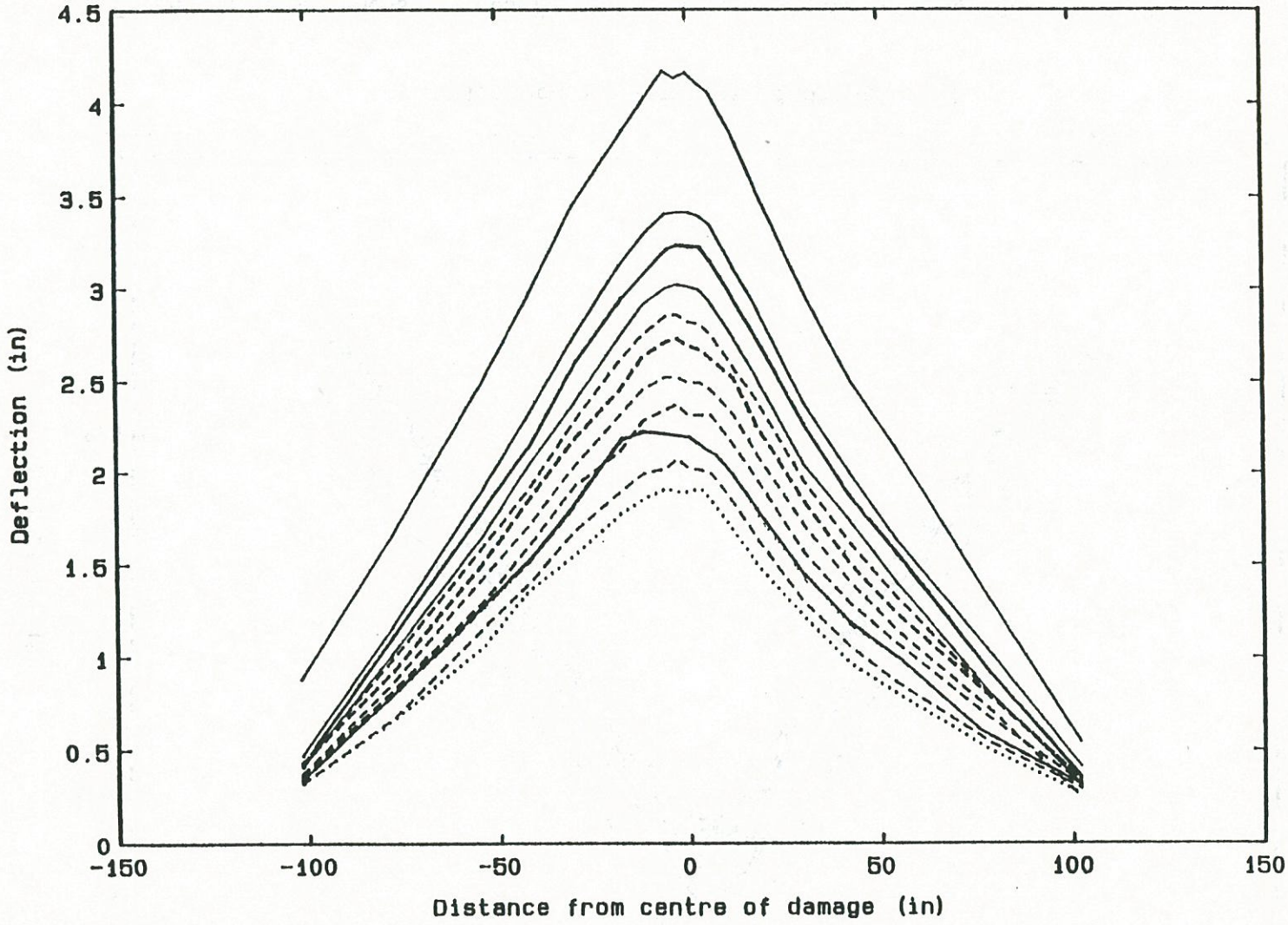

Figure 89b. Deformations of top flange over 10 heating cycles for compression member SB-12.

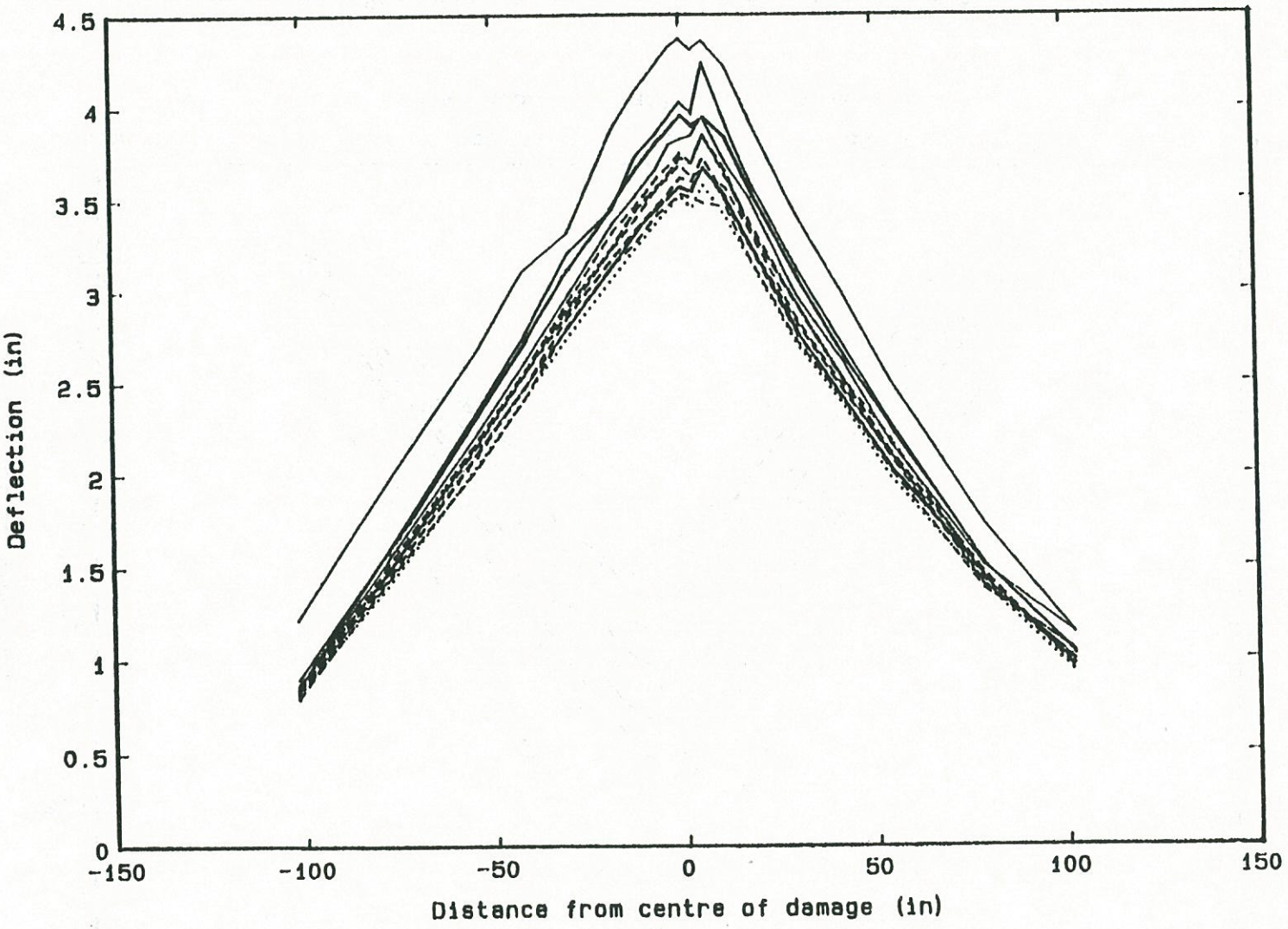

Figure 90a. Deformations of bottom flange over 10 heating cycles for compression member SB-13.

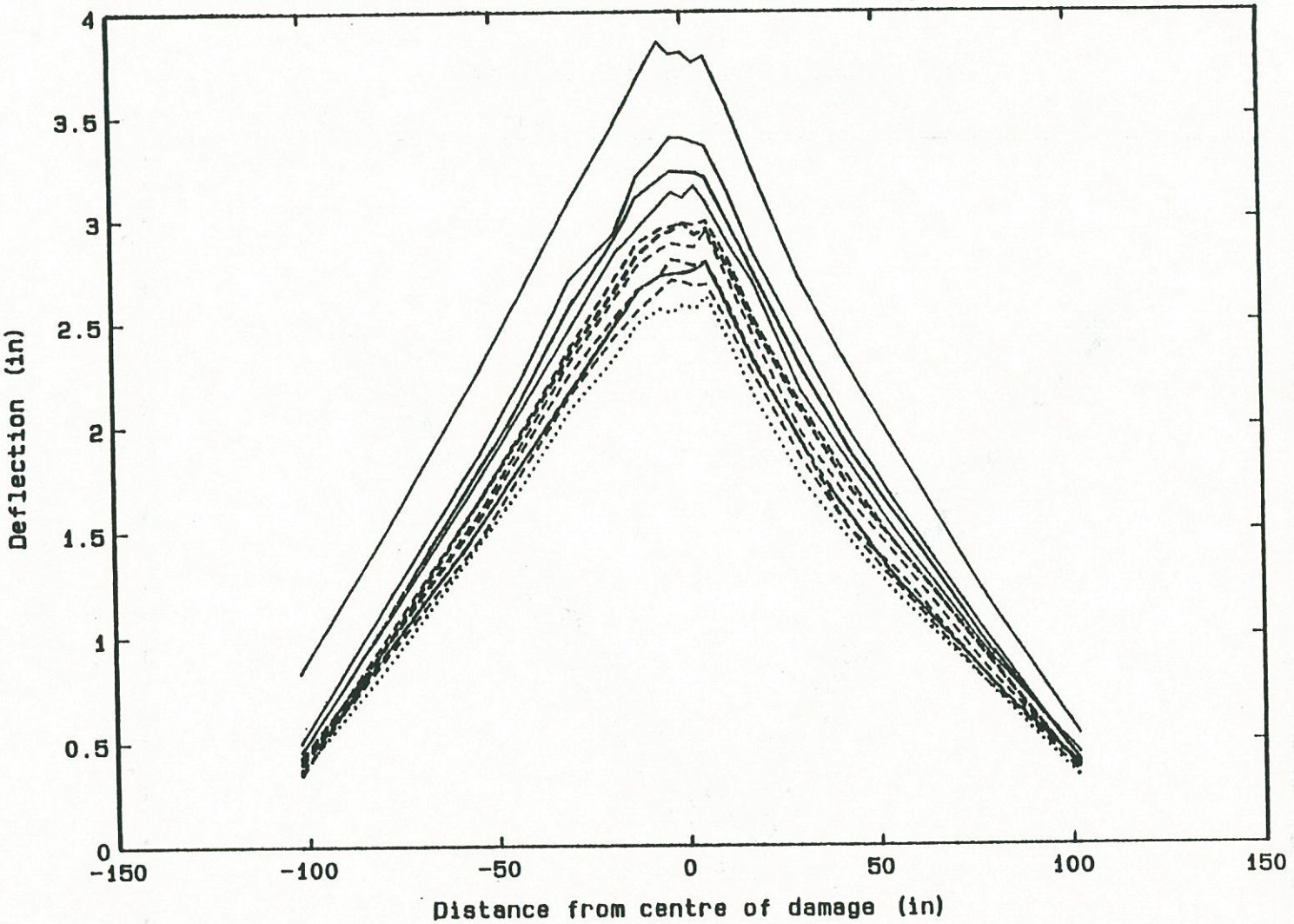

Figure 90b. Deformations of top flange over 10 heating cycles for compression member SB-13.

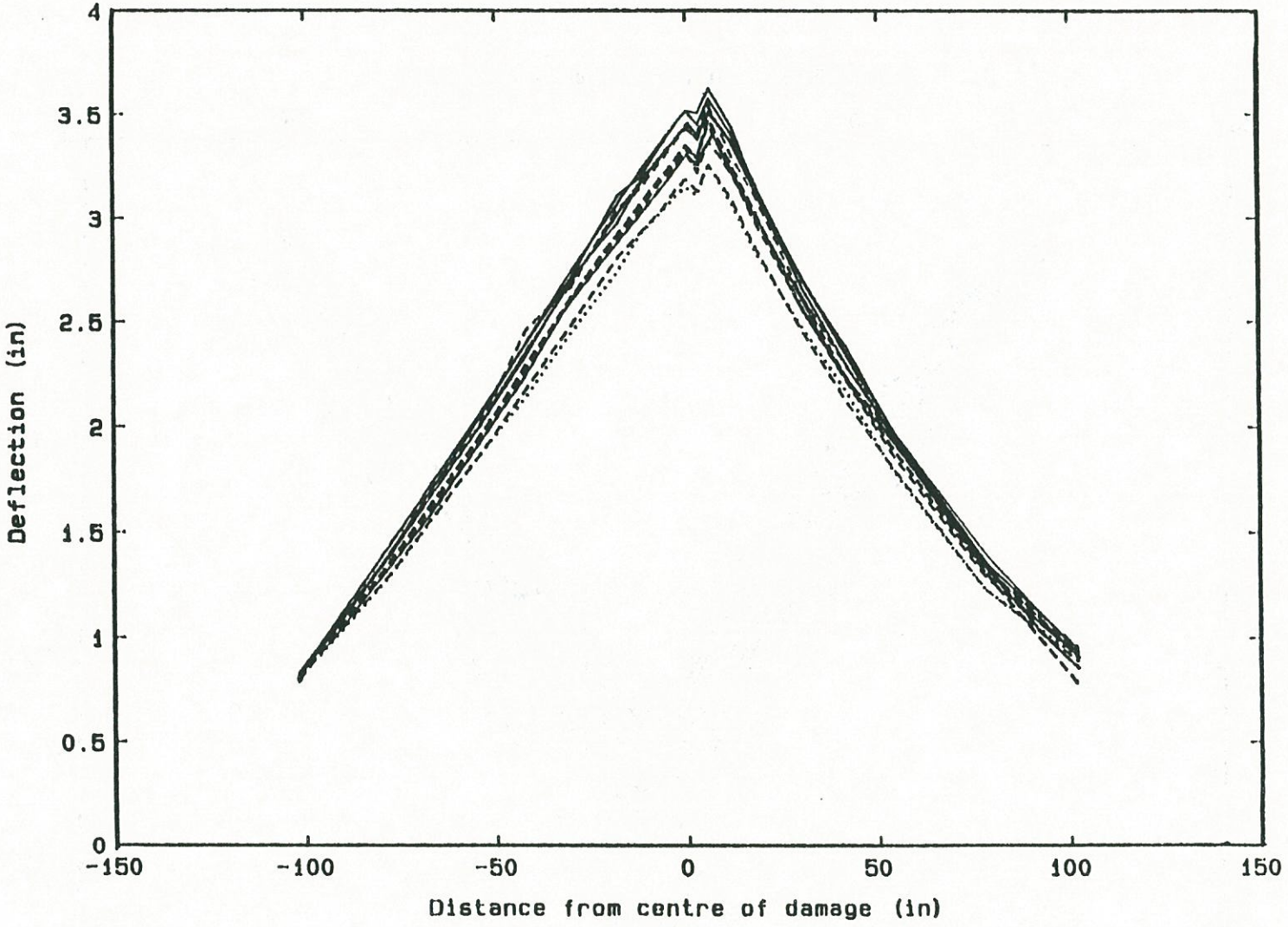

Figure 91a. Deformations of bottom flange over 10 heating cycles for compression member SB-14.

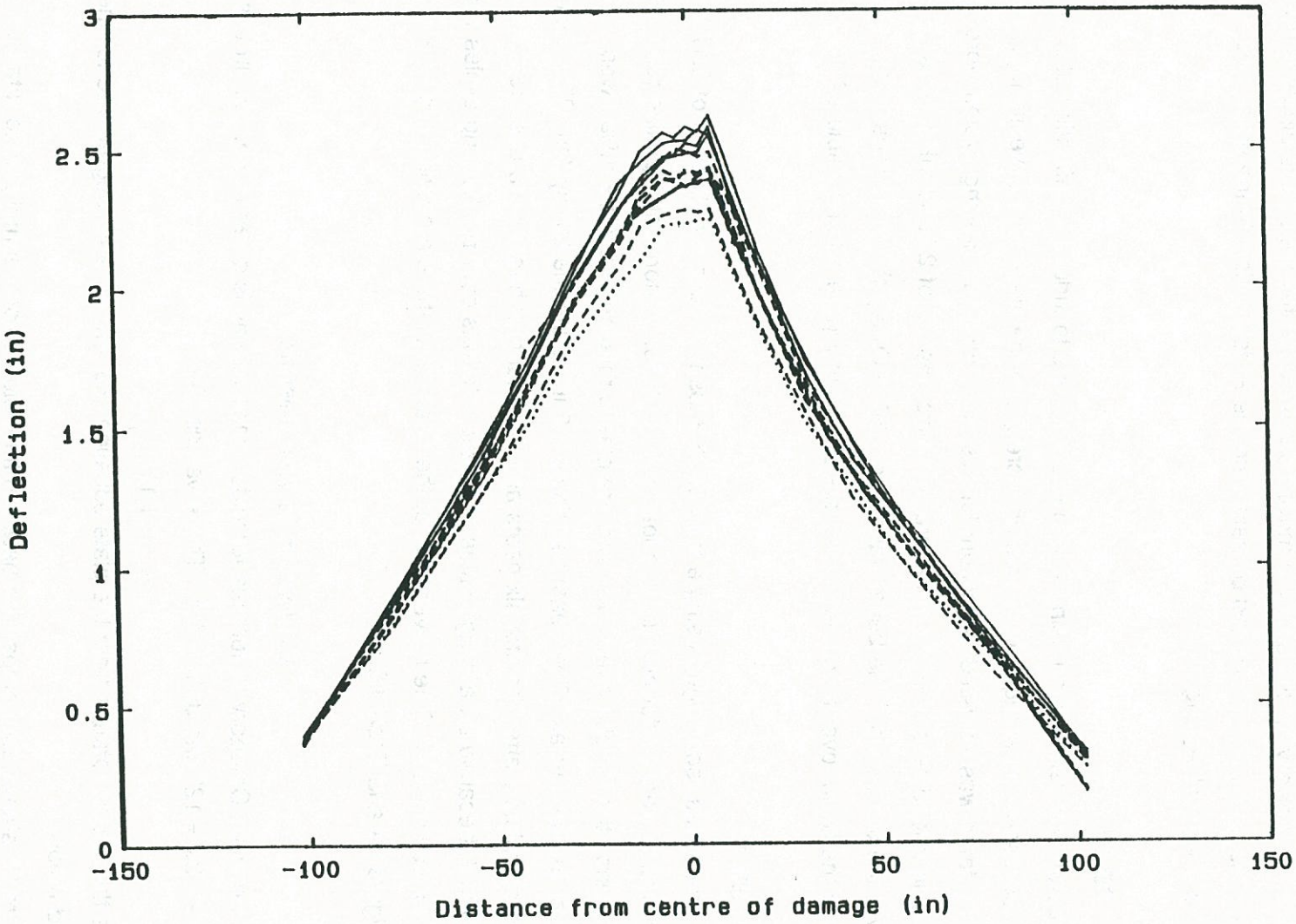

Figure 91b. Deformations of top flange over 10 heating cycles for compression member SB-14.

to the bottom of the flange. An average plastic rotation of 1.1370 mRad was achieved over the ten cycles. The beam translated 0.99 in. during the thirteen cycles.

The movements of the beam over the ten cycles are shown in Figure 92 and in Table 62. There was a tendency for the beam to move downwards in the weak axis direction during the heating cycles. This was prevented by balancing the P-delta effect in the weak axis direction using a vertical jacking force.

Category S: SB-16

The beam was redamaged using a load of 28.98 kips to induce a deflection of 2.34 in. After every successive redamage, there was an increase in the weak axis deflection. The vertical jacking force was adjusted to account for this behavior. Ten heating cycles were performed using a load ratio of 0.25. An average plastic rotation of 2.8268 mRad was achieved over the ten cycles. The beam translated 1.60 in during the ten cycles. The movements of the beam over these ten cycles are shown in Figure 93 and Table 62.

Category S: SB-17

The beam was redamaged using a load of 26.8 lbs to induce a deflection of 2.17 in. Ten heating cycles were performed using a load ratio of 0.50. A horizontal jacking force was applied to balance the P-delta effect. An average plastic rotation of 5.7753 mRad was observed over the ten cycles. The beam translated 3.2 in during the ten cycles. The beam straightened completely after the first six heats and the final four heats were used to over-straighten it, because an average value of plastic rotations over ten heating cycles was being used for comparison. The movements of the beam over the ten heating cycles are shown in Figure 94 and Table 62.

Evaluation of Test Results

The previous Category W formula for wide flange beams is given in Eq. 15. In this case, w = 12", bs = 12" and ds/w = 0.5. These values give,

$$\phi_w = 1.125\ \phi_p$$

where ϕ_p is the plastic rotation from the plate equation (Eq. 4b) for a 45 degree vee for the applied load ratios.

Figure 95 shows the comparison between the actual experimental plastic rotations and those obtained from Eq. 15. Mean values of the actual rotations of the top and bottom flange have been used. The yield strength of the steel was initially assumed to be 36 ksi. The

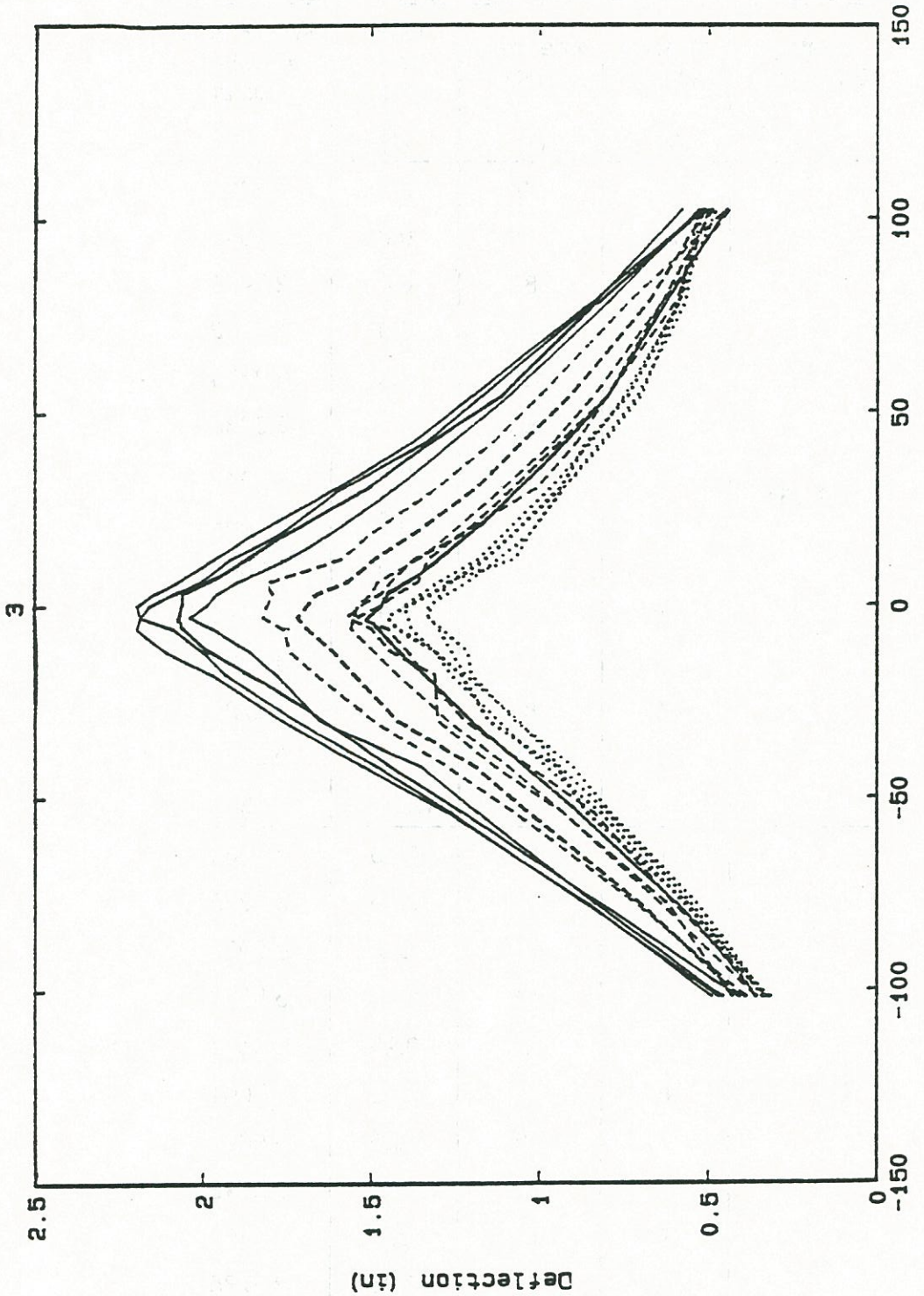

Figure 92. Deformations of web over 13 heating cycles for compression member SB-15.

Table 62. Summary of Experimental Results for Category S Compression Members SB-15 through SB-17.

Heating Sequence (1)	Heating Cycle (2)	Vee Heat Location (3)	Load Ratio (M/M_p) (4)	Web Plastic Rotation (millirad) (5)
SB-15[2]	1[1]	10	0.0	1.8012
	2[1]	12	0.0	0.9344
	3[1]	8	0.0	2.7471
	4	10	0.0	1.3512
	5	12	0.0	2.8584
	6	8	0.0	2.3982
	7	10	0.0	1.339
	8	10	0.0	0.0004
	9	7	0.0	-0.6643
	10	12	0.0	2.7024
	11	10	0.0	0.7432
	12	8	0.0	1.2723
	13	10	0.0	-0.5291
			Average	1.1372
SB-16[2]	1	10	0.25	3.6465
	2	12	0.25	2.7352
	3	8	0.0	0.6076
	4	10	0.25	5.8200
	5	12	0.25	3.3437
	6	8	0.25	1.7001
	7	10	0.25	3.6028
	8	8	0.25	2.2743
	9	12	0.0	1.9592
	10	10	0.25	2.5785
			Average	2.8268

Heating Sequence (1)	Heating Cycle (2)	Vee Heat Location (3)	Load Ratio (M/M_p) (4)	Web Plastic Rotation (millirad) (5)
SB-17[2]	1	10	0.50	11.3706
	2	8	0.50	3.7532
	3	12	0.50	3.2316
	4	10	0.50	6.8912
	5	8	0.50	5.0900
	6	10	0.50	5.3603
	7	8	0.50	3.5022
	8	10	0.50	3.6824
	9	8	0.50	4.2791
	10	10	0.50	8.5916
			Average	5.7753

[1]Indicates 45° heat
[2]An axial load of 0.35 times the allowable axial load (based on AISC specifications) was maintained during heat straightening

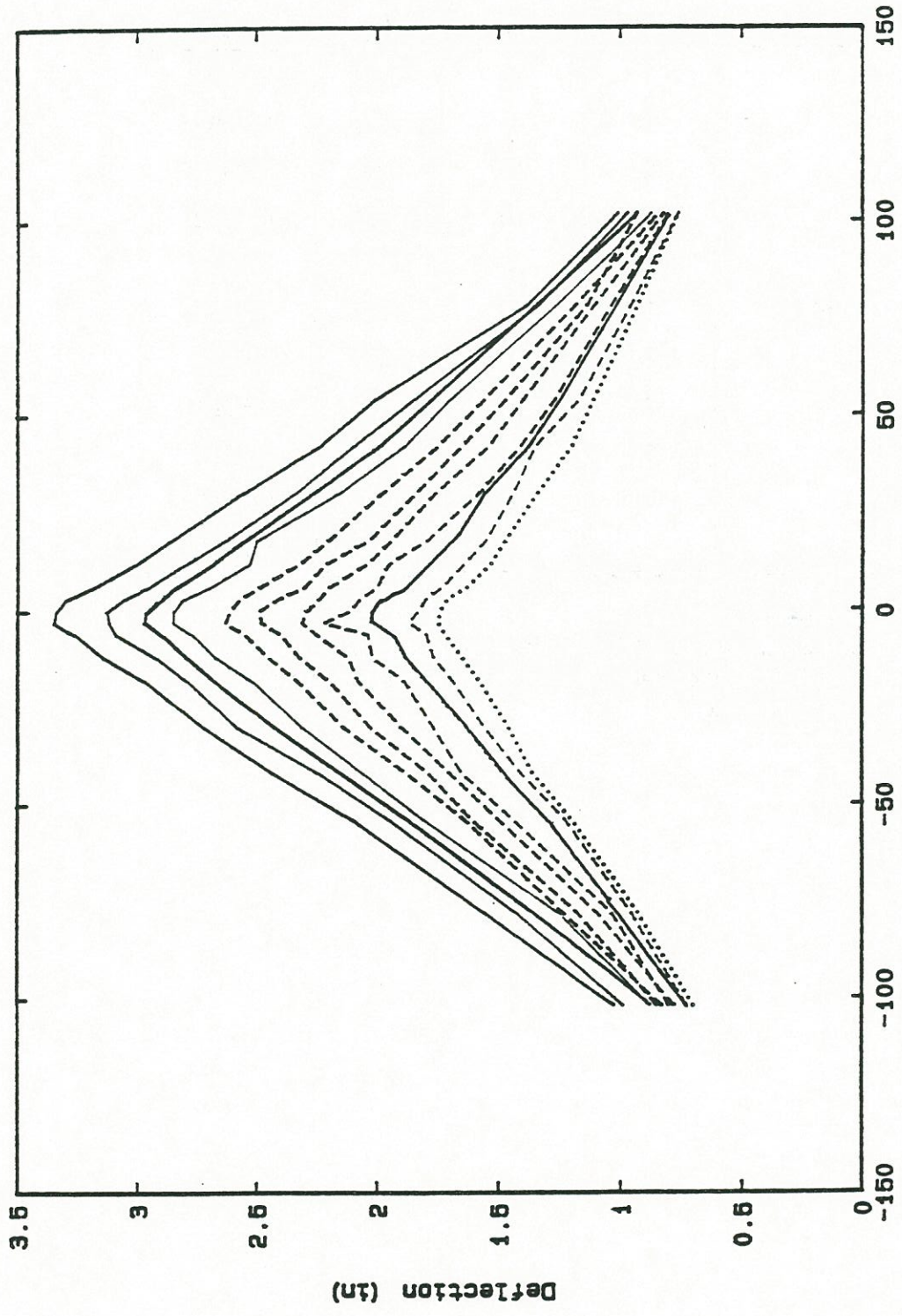

Figure 93. Deformations of web over 10 heating cycles for compression member SB-16.

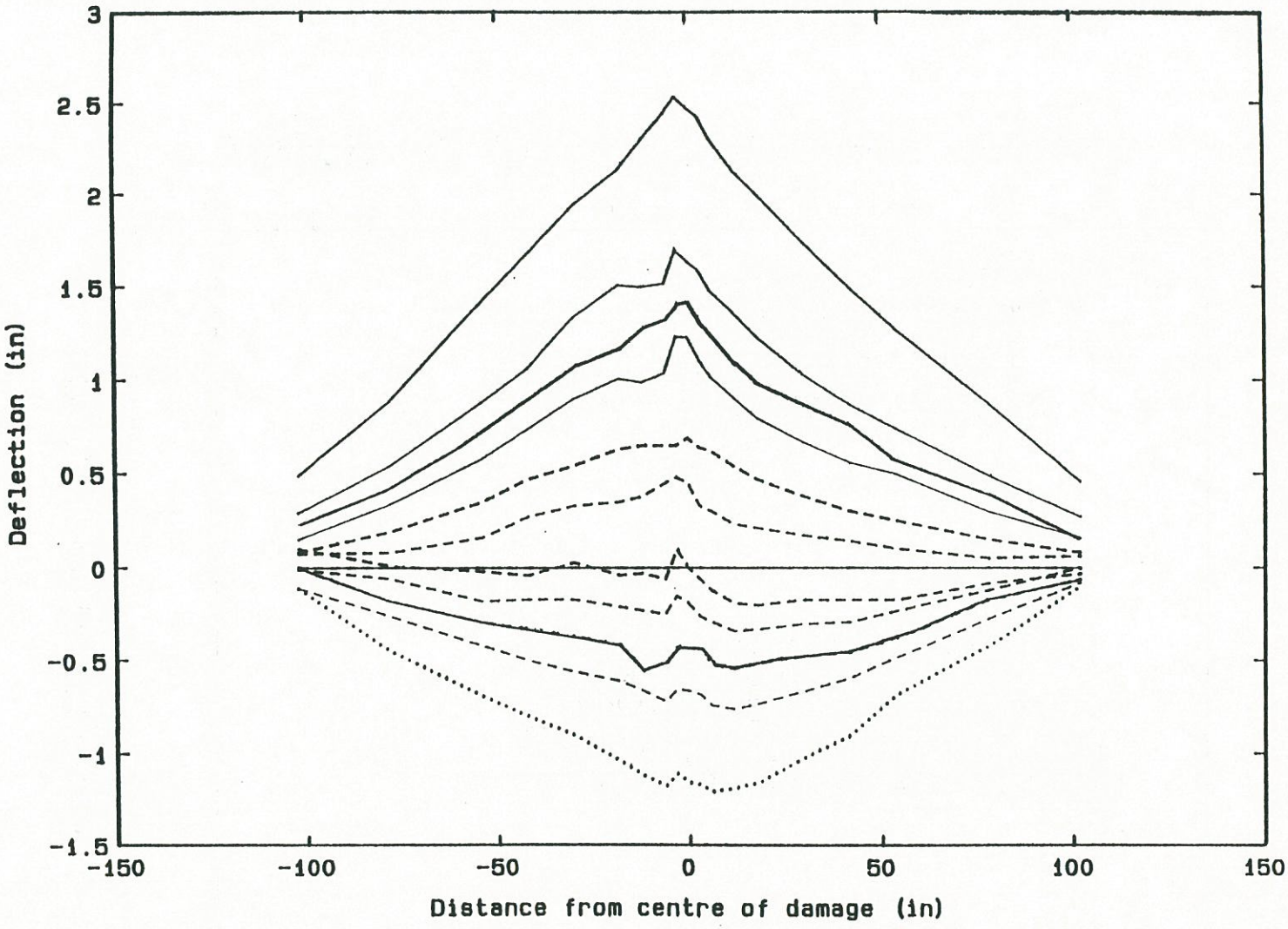

Figure 94. Deformations of web over 10 heating cycles for compression member SB-17.

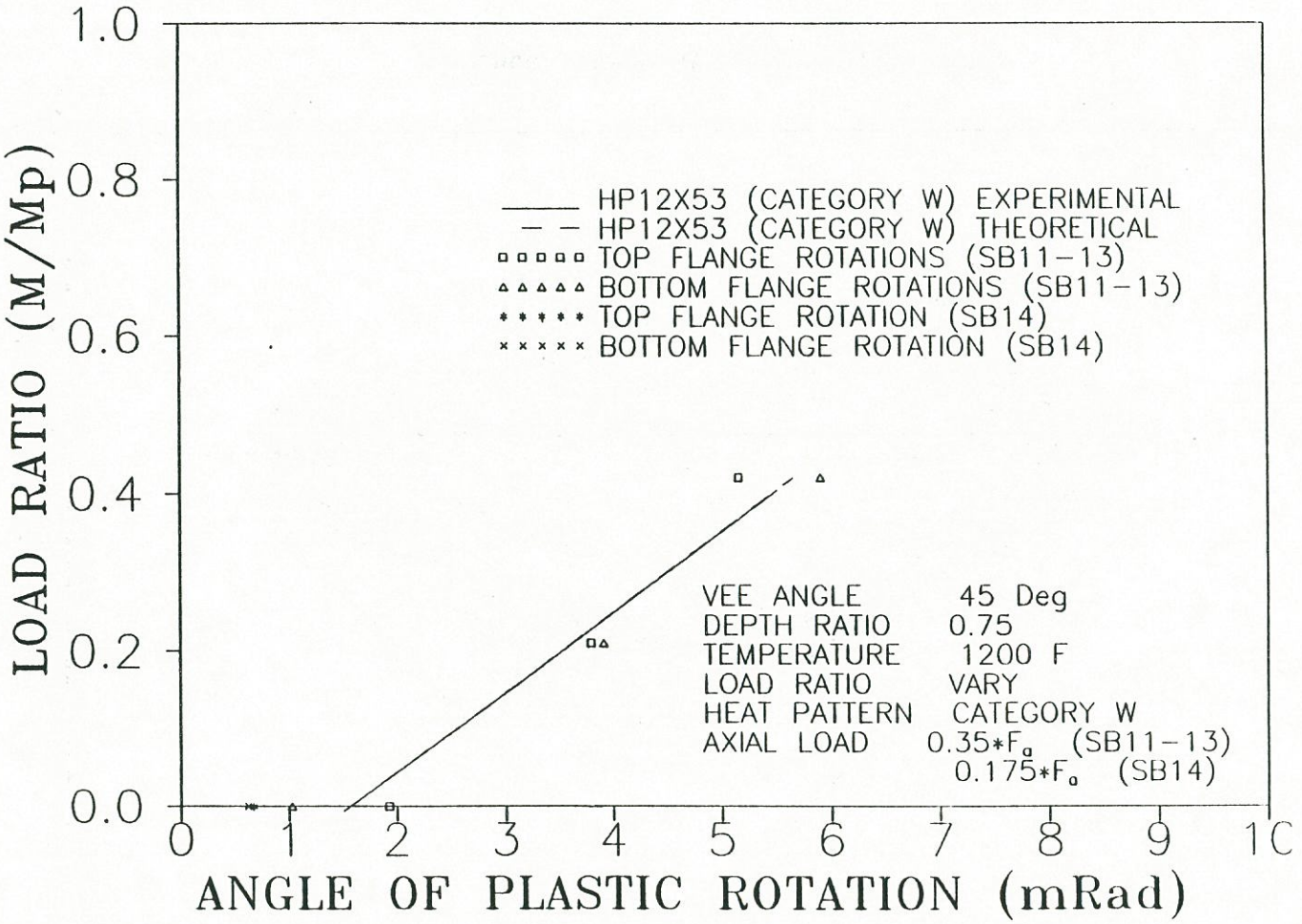

Figure 95. Plot of load ratio vs. plastic rotation for Category W compression members.

results of the tensile tests on an unheated specimen from the beam revealed that the actual yield stress was 42.5 ksi. The effective applied load ratios were determined to be 0.21 and 0.42, instead of 0.25 and 0.50 as initially assumed. In Figure 95, the experimental and the theoretical values are not consistent with each other. The axial force seems to retard plastic rotations at low load ratios and accelerate them at higher load ratios. This behavior is explained by considering that for low constraining forces the entire cross section is in compression. The compression forces at the apex region of the vee will tend to result in shortening of that region as compared to cases where that region is in tension. This behavior will result in smaller plastic rotations. Once the constraining forces are large enough to cancel out these compression forces at the apex region of the vee, the plastic rotations are larger and, in fact, accelerate movement because the axial force is uniformly distributed over the open end of the vee creating a larger net compression force that an equivalent bending stress. To compensate for this effect, it is assumed that the axial load effect is linear. The mathematical formula has the form

$$\phi_{ax} = \phi''_w \tag{39a}$$

where ϕ''_w is the wide flange beam equation for weak axis damage

$$\phi''_w = F_t(T)\, F''_l(M)\, \varepsilon_p(T)\, [1 + \frac{1}{4}\, \frac{d_s b_s}{w^2}]\, \sin\, \frac{\theta}{3} \tag{39b}$$

with the modified load ratio function defined as

$$F''_l(M) = 0.9\, (1 - \frac{k}{2}\, \frac{f_a}{F_a}) + 3.4\, \frac{M}{M_p}\, (1 + \frac{k}{2}\, \frac{f_a}{F_a}) \tag{39c}$$

and k = 1.40. The moment, M, includes the P-delta effect and the constraint effect.

The plastic rotations for the ten heating cycles with an axial load equal to 0.175 times the allowable axial load are low and do not agree with the theory or with other experimental results. However, during this sequence, the heats were being performed on a beam which was nearly straight as can be observed in Figure 91a and 91b. As a result, the jacking force required to balance the P-delta moments was small. The pressure gauge used for measuring the applied jacking force was not sensitive enough to accurately measure this small applied force. Thus, the P-delta effect probably had a negative influence on the plastic rotations.

The previous Category S formula for wide flange beams is given by Eq. 18. In our case, w = 10", bs = 8" and ds/w = 1. These values give,

$$\phi_s = 1.4\ \phi_p$$

where ϕ_p is the plastic rotation from the plate equation (Eq. 4b) for a 30 degree vee for the applied load ratios.

Figure 96 shows the comparison between the actual experimental plastic rotations of the web and those obtained from Robinson's formula. Here the actual yield stress for the unheated specimen was 37.5 ksi which is close to the assumed value of 36 ksi. The values of the actual tensile strengths of all field tested girders are given in Table 63. The experimental and theoretical values differ in a manner similar to the weak axis case. Again, assuming the axial effect is linear, the equation for predicting plastic rotations is

$$\phi_{as} = \phi''_s \tag{40}$$

where ϕ''_s is defined by

$$\phi''_s = F_t(T)\ F''_l(M)\ \varepsilon_p(T)\ [1 + \frac{1}{2}\ \frac{d_s b_s}{w^2}]\ \sin\ \frac{\theta}{3}$$

and the modified load ratio function is

$$F''_l(M) = 0.9\ (1 - k\ \frac{f_a}{F_a}) + 3.4\ \frac{M}{M_p}\ (1 + k\ \frac{f_a}{F_a})$$

and k = 1.4.

Conclusions

A study of the heat straightening response of bridge girders subjected to axial compression has been carried out. Seventy heating cycles were performed. Beams subjected to both major and minor axis damage were evaluated. Three different load ratios were used in each case. The previously presented methodologies for Category S and Category W heats were followed. A complete set of plastic rotations for each case was obtained. The axial load applied was equal to 0.35 times the AISC allowable value. The results of the test were compared to the theoretical formulae for wide flange beams. The basic conclusions from this study are

(1) The methodologies developed in the laboratory for the Category S and Category W heats can be successfully applied to full-scale girders.

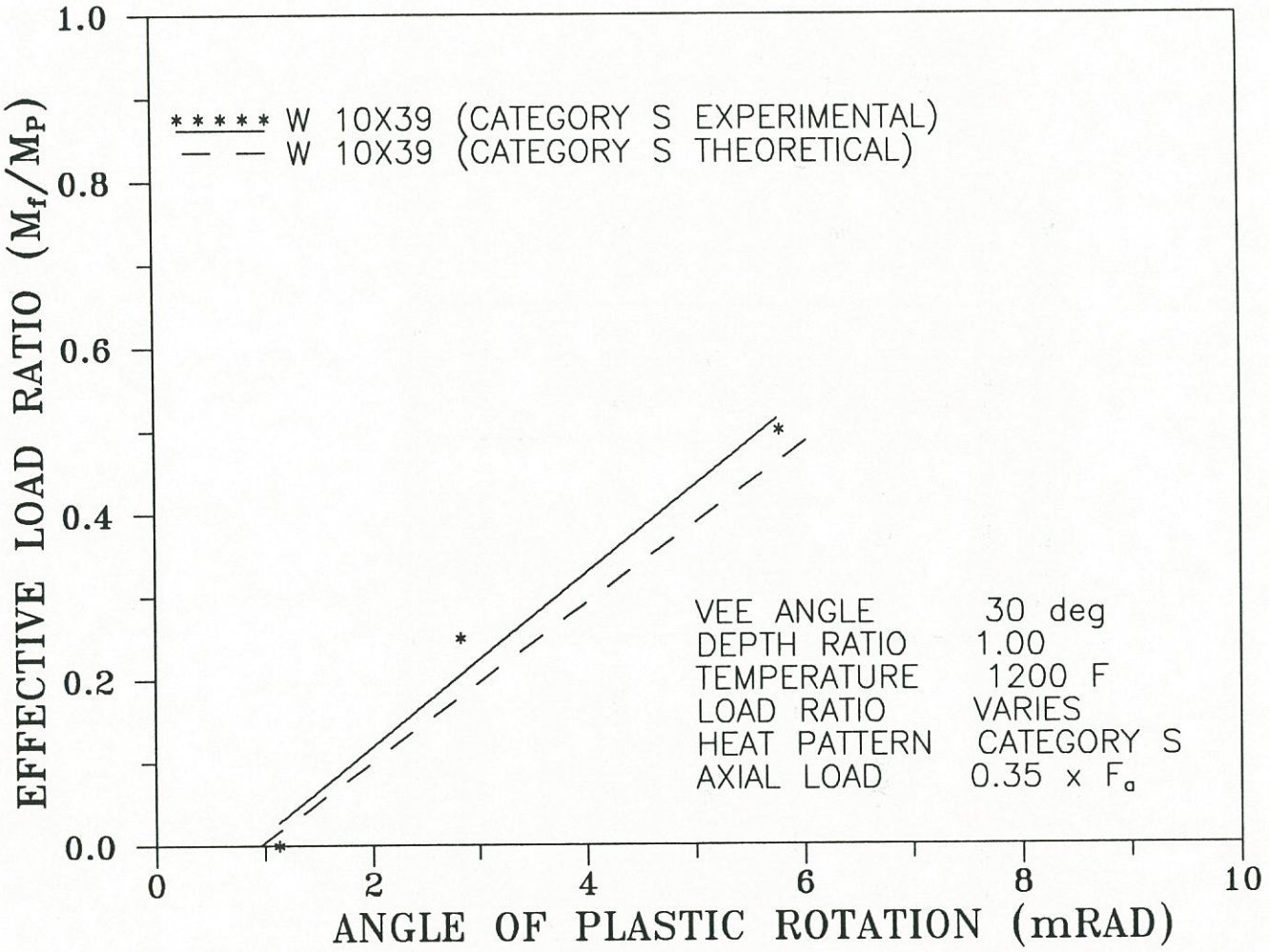

Figure 96. Plot of load ratio vs. plastic rotation for Category S compression members.

Table 63. Tensile test results for field-tested A-36 steel girders.

Beam Type	Designation	Tensile Strength (ksiP	Yield Strength (ksi)	Percent Elongation (2" gauge length)
W10x39 (Composite)	SB1, SB2	63.45	39.50	44.20
W24x76 (Composite)	SB3 ~ SB6	69.06	46.60	40.60
W24x76 (Composite)	SB7	71.15	41.27	41.40
W24x76 (Noncomposite)	SB8 ~ SB10	69.99	46.50	40.60
WP12x53 (Axial Category W)	SB11 ~ SB14	71.84	42.78	35.90
W10x39 (Axial Category S)	SB15 ~ SB17	61.63	37.28	40.60

(2) The Category W formula for beams without axial loads must be modified for Category W beams subjected to axial compression and the P-delta moments superimposed the jacking force moments.

(3) The Category S formula for beams without axial loads fits a similar pattern for Category S beams subjected to axial compression.

(4) The jacking forces used should include as a minimum a component producing a moment at the damaged section equal and opposite to the moment produced by the axial force acting through the deflection at the damaged section. In considering limitations on the jacking forces, this component should be omitted.

(5) Axial forces in conjunction with small or negligible lateral constraining forces tend to retard moment when compared to an equivalent beam with no axial load. However, for axial loads combined with large lateral constraining forces, the movements are magnified.

Chapter 6

COMPUTER ANALYSIS FOR DESIGNING REPAIRS

A computer program was written to aid in the damage assessment and design of heat-straightening repair. The listing of the programs and sample inputs and outputs are included in Appendix K. The users manual for the program is given in this chapter.

An Introduction to the 'HEAT' Program

The 'HEAT' program is an interactive software system which computerizes the design of the heat-straightening repair process for global effects of damage. This program can handle twelve different commonly-observed damage types for the damaged girder. The 'HEAT' software can be used by the repair technician to determine the following repair parameters:

(1) the degree of damage

(2) the heating patterns and repair methodology to be used

(3) the number of heats required to straighten the member

(4) the magnitude of the external jacking force to be applied during repair.

The software can be used in the IBM PC environment. The software is fully interactive and the input is minimal. Results appear interactively on screen. Detailed results with an input echo appear in a file 'heat.r' while a brief summary of results can be found in file 'heat.s'.

An additional program 'INDET' is also included. This program is designed to determine:

(1) the plastic rotations for a heating cycle

(2) the residual moments caused by heat-straightening in girders with diaphragms

Results appear interactively on screen and in file 'indet.r'.

A glossary of heat-straightening terms is given, followed by a step-by-step explanation of how to use the program. Sample Inputs and Outputs and the program listings for both programs are given in the appendix. It should be noted that this program is based on experimental and analytical heat-straightening research conducted at LSU until December 1992. The program is mostly based on research presented in this report. The details of heat-straightening research can be found in the references listed at the end of this manual. However, it must be noted that while most parameters affecting the heat-straightening process

are now well-defined, some important aspects of heat-straightening are still under scientific study.

A Glossary of Heat-Straightening Terms

The list given below contains a glossary of the heat-straightening terminology used in the program. Each term is clearly defined in the context of the 'HEAT' and 'INDET' programs.

'HEAT' - An interactive program for Heat-straightening repair design.

'INDET' - An interactive program to determine plastic rotations and residual moments in girders with intermediate diaphragms.

Heat-Straightening - An in-situ repair technique for structural steel repair wherein damage is repaired by heating all yield zones, in predetermined heating patterns, to no more than 1200 deg F, with the application of passive external jacking forces, such that the load ratio does not exceed 0.33. The steel must be convection-cooled.

Axial Load Ratio - The ratio of the axial load acting on the undamaged member to the allowable AISC axial load for the undamaged member.

Damage type - A condition which indicates the type of member to be repaired.

Category S damage - A category of global damage in which the damaged member deforms about its major (or strong) axis (Figure 2b).

Category W damage - A type of global damage in which the damaged member deforms about its minor (or weak) axis (Figure 2a).

Center of damage - The point of maximum damage, usually the point of impact.

Composite girder - A deck-girder system in which the deck slab is attached compositely to the girder along its length (Figure 57).

Damaged Element - The damaged element is the plate element in the damaged member which has undergone major axis damage.

Damaged Member - The plate, angle, channel or W shape which has undergone plastic deformations during damage.

Degree of Damage - The angle through which the damaged element must move during the heat-straightening process in order to re-attain its undamaged configuration.

- The yield strain for the undamaged steel. The damage strains must not exceed 100 times the yield strain if heat-straightening is to be used for the repair.

External Jacking Force - A passive, self-releasing external force used to expediate the heat-straightening process by preventing reverse movements in the initial stages of the heating cycle.

Global Damage - The component of damage associated with bending or twisting of a member. The other component is local damage which is associated with localized deformations in the form of bulges or crimps.

Heating Cycle - A single unit of the heat-straightening process. It consists of heating time and cooling time.

Heating Pattern - The patterns in which heat is applied to the yield zones to cause straightening. Most commonly used patterns are vees, lines and strips

Heating Sequence - A group of heating cycles used during heat-straightening.

Heating Temperature - The temperature to which the steel is heated during repair. The heating temperature must not exceed 1200 deg F for carbon steel

Line Heat - A heating pattern used to repair minor axis bends in plate elements. It consists of a single, continuous pass of a torch along a yield line.

Load Ratio - A dimensionless parameter to express the magnitude of the external jacking force to be applied. The load ratio is defined as the ratio of the applied moment in the heated zone due to the jacking force to the plastic moment capacity of the reference shape.

Non-Composite girder - A deck-girder system in which the deck is not attached compositely to the girder along its length, and is attached only at the supports (Figure 78).

P-delta Effect - The additional moment caused by the axial load in an axially loaded girder due to the damage displacement at the center of damage. The P-delta moments retard the heat straightening process and must be compensated by an additional applied external jacking force.

Plastic Rotation - Plastic rotation is a dimensionless parameter used to quantify the heat-straightening response of a member. It is the relative change in the degree of damage during a single heating cycle. It can be calculated based on an analytical formula (1) (Figure 1).

Recommended Methodology - A step-by-step procedure detailing the heat-straightening procedure for a given damage type.

Reference Stations - Four locations, two on each side of the zone of damage, located away from the yield zones, where the ordinates are measured off a datum line parallel to the undamaged span of the girder, to obtain the damage ordinates (Figure 97).

Residual Moment - The moments caused in indeterminate girders due to damage inducement. Residual moments may retard the heat-straightening process and must be compensated for by the external jacking force (Figure 100).

Stiffening leg - A plate element which stiffens the major damaged element in a rolled shape, e.g., the web of a Category W damaged wide flange (Figure 26).

Stiffness Modification Factor - A factor used to determine the fraction of the applied external force applied at the bottom flane which is carried by the bottom flange of a composite girder (Figure 71).

Strip Heats - A rectangular heating pattern used to heat yield zones on the stiffening element in damaged rolled shapes (Figure 2a).

Unsupported span - The span between two diaphragms, one on each side of the center of damage in an indeterminate member. It is the simply supported span in a determinate member (Figure 100).

Vee Angle - The angle of the apex of a vee heat (Figure 1).

Vee Depth - The perpendicular distance from vee apex to vee base (Figure 1).

Vee Heat - A triangular heating pattern used to repair major axis bends. The apex of the vee points in the direction of desired girder movement (Figure 1).

Vee Width - The width of the base of the vee heat (Figure 1).

Yield Zones - Zones on the damaged member which have undergone plastic deformations during the damage.

Using the 'HEAT' Program

General Input Procedure

The 'HEAT' program is an on-screen interactive program. The program will demand input values and decision codes from the user at different stages in its operation. Integer and real values can be input for numerical data. The on-screen input query specifies the units of

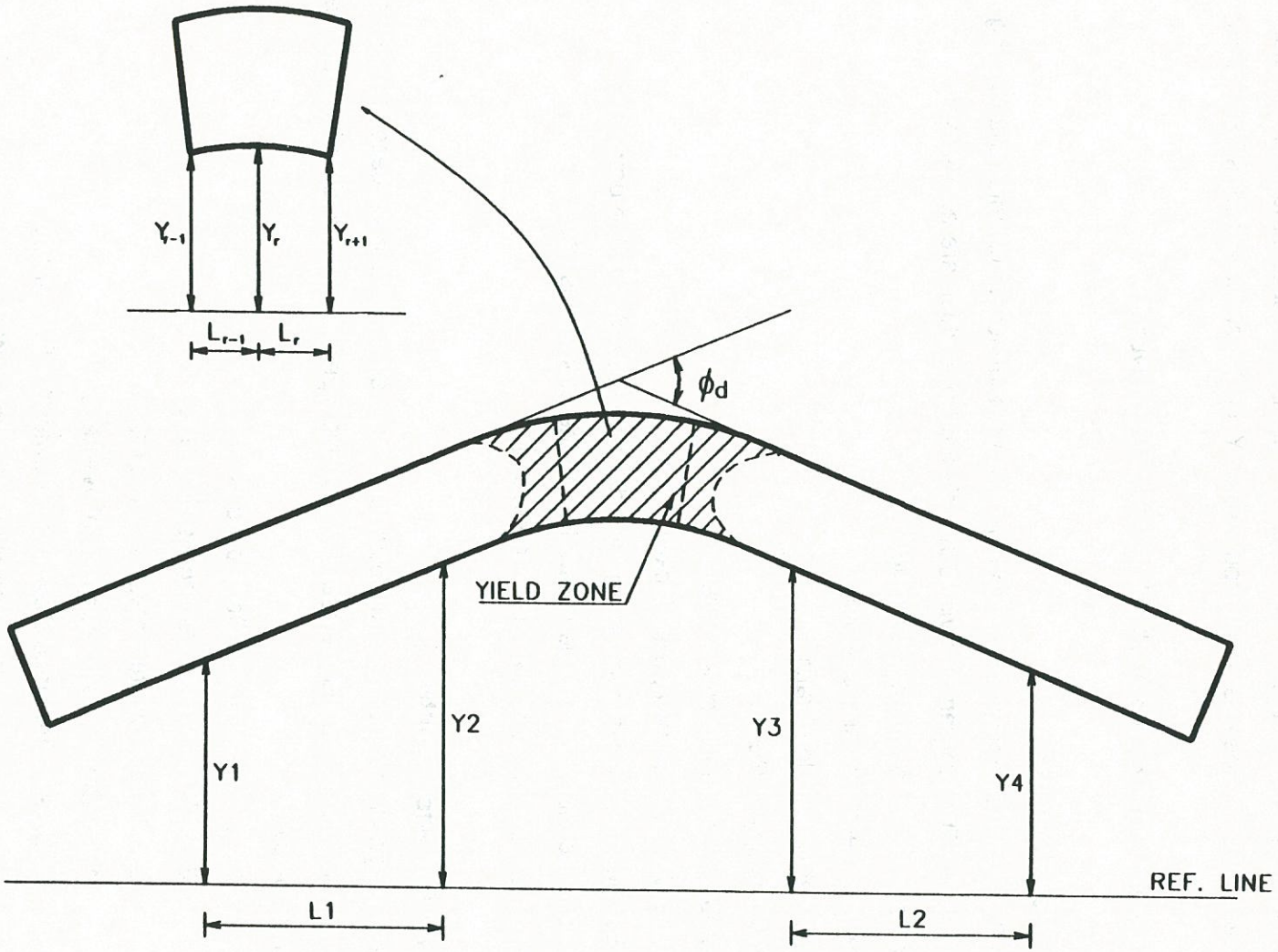

Figure 97. Offset measurements to calculate degree of damage.

the desired input. The decision codes are 'Y' & 'N'. Apostrophes are required before and after the decision character for the decision codes.

The command 'heat' initiate the program. The program will first ask the user: "Would you like to continue? (Y/N):". The user must input either 'Y' or 'N' for the answers 'yes' or 'no' respectively.

If the answer is 'Y', the program will ask for the damage type.

Structure of the 'HEAT' Program

The 'HEAT' program has been designed in a modular manner to minimize the running time and the input time. The program is divided into six modules which are as follows:

(1) Damage types for damaged member

(2) Member geometry and properties

(3) External applied load ratio

(4) Methodology of Repair

(5) Number of heating cycles for repair

(6) Magnitude of external applied jacking force

The member geometry & yield stress and the damage ordinates of the damaged member at four reference stations must be known before the program is used.

The modules are explained in the following sections.

Damage Types for Damaged Member

The 'HEAT' program can be used to design the heat straightening process for twelve different damage types of the damaged member. The twelve types are identified for input by the number codes given below.

1 ... Indeterminate Composite W shape

2 ... Determinate Composite W-shape

3 ... Determinate Category S W-shape

4 ... Determinate Category W W-shape

5 ... Axially-loaded Determinate Category S W-shape

6 ... Axially-loaded Determinate Category W W-shape

7 ... Determinate Category S Channel

8 ... Determinate Category W Channel

9 ... Determinate Category S Angle

10 ... Determinate Category W Angle

11 ... Determinate Category S Plate

12 ... Determinate Non-composite W-shape

The user must input the number code for the damage type in question.

Member Geometry and Properties

The member geometry and properties and geometry of the section are to be entered next. For rolled shapes, the input must include flange width, flange thickness, web depth, web thickness and yield stress of the steel, respectively. For angles, either leg can be considered as the flange depending on the damage type selected. For plates, only the plate width, plate thickness and the yield stress are to be input. All units are required to be in inches and kips.

External Applied Load Ratio

The value of the applied external load ratio is the next input. The value of the load ratio for repair must not exceed a value of 0.33, for any damaged member. In the case of composite girders, the load ratio must not exceed a value of 0.125. These limits are imposed to prevent hot mechanical straightening during repair.

Any desired value from zero to the above limits can be specified. The maximum values will give the fastest results and are hence the best choices. If the jacking arrangement dictates otherwise, a lower value can be used.

At this stage, the program asks if the user wishes to determine the number of heats required to heat-straighten the beam. If the user enters 'N', the program moves directly to the final module (VI), where the external jacking forces are calculated. This step eliminates the need for the intermediate steps if the methodology and number of heats have already been determined. These values normally need to found only once before the repair commences. The jacking force, however, may change during the repair because of P-delta moments and residual indeterminate moments for axially-loaded and composite beams respectively, and may need to be evaluated at regular intervals during the repair process.

If the user enters 'Y', the methodology of repair is determined next.

Methodology of Repair

The program provides the user with the degree of damage and the geometry of the vee heats to be used in the repair. Important repair parameters are also input in this module. The program does not give the step-by-step repair procedure but this procedure can be found in a

following section, along with illustrations, for the various damage types. The recommended methodologies must be followed for efficient repair.

(i) The program first determines the Degree of damage for the damaged member.

The program asks the user to enter four values for the undamaged distances of the four reference stations from the left end of the unsupported span (in feet) and the unsupported span (in feet). Two reference stations must be located on either side of the center of damage, at a safe distance away from the yield zones.

Next, the program asks the user for the damage ordinates of the damaged element from the four reference stations (in inches).

Based on these values, the program outputs the degree of damage of the damaged member in radians and in degrees. If this value exceeds 12 deg, the damage strains must be less than 100 times ε_y if heat straightening repair is to be used.

(ii) The program then calculates the vee geometry.

The user is first asked for the heating temperature (in deg F). This value must not exceed 1200 deg F. A lower value will give slower results and the value of 1200 deg F is recommended for repair. Lower temperatures may be used if necessary. The user is then asked for the depth of vee desired (in inches). The recommended value is the full width of the damaged element. However, if absolutely necessary a lower value of vee depth can be entered for practical purposes.

The program then outputs the values of vee width (in) and vee angle (deg). It also asks the user to refer to this manual for the step-by-step repair procedure.

Number of Heats Required for Repair

The number of heats required for repair are calculated based on analytical models developed during the research (1). It is important to know this value in advance to estimate the time and resources required for a repair project. Depending on the damage type selected, some values may have to be input at this stage.

If the damage type is 5 or 6, i.e., if the girder is axially loaded, the program will ask the user for the axial load ratio. The applied axial load acting on the undamaged member can be determined from structural analysis. The allowable axial load on the undamaged member can be determined from Tables 3.36-3.50 in the AISC LRFD Steel Designer's manual. The ratio of applied axial load to allowable axial load is the axial load ratio. This ratio must be entered by the user.

If the damage type is 7,8,9 or 10 i.e. channels and angles, the program will ask the user for the distance from the apex of the vee to the stiffening element. This value must be entered by the user in inches.

The program then outputs the number of heating cycles needed for repair.

In case of non-composite girders, no method exists for determining the number of heats for repair. In this case, the program outputs the number of heats required to straighten the damaged bottom flange, considering it as an unrestrained plate element. This method gives the minimum number of heats required and only a rough estimate can be made by the user of the total number of heats required.

Magnitude of External Applied Jacking Force

The program asks if the user wishes to determine the magnitude of the external jacking force. If the user inputs 'N', the program is terminated. If the user inputs 'Y', the program calculates the magnitude of the external applied load based on certain values which must be input.

The program asks if there is any strong axis damage in the web. The user must input either 'Y' or 'N' depending on the case.

The program asks for the shorter distance of the vee-heat from the supports (in feet). The user must input the desired value. It is a good practice to place the jack at least one foot away from the vee heated area. The program asks for the distance of the jack (in feet) from the other end of the span. The program then asks for the distance between the supports of the heated span (in feet).

Depending on the damage type, the program may request further information. If the selected damage type is 5 or 6, i.e. axially loaded girder, the program will ask for the axial load (in kips) and the current deflection at the center of damage (in). If the selected damage type is 1, i.e. indeterminate composite girder, the program will ask for the value of the residual moment, which must be determined from the 'INDET' program discussed later in this chapter. The user must input this value. In the case of composite girders, the program uses a stiffness modification factor in the calculation of the jacking load. The jacking load will be conservative because the program calculates the force considering the damaged unsupported span as a simple span.

The program then outputs the magnitude of the jacking force required to create the desired load ratio.

The program is then terminated. The following chapter discusses the step-by-step recommended methodologies for girder repair.

Recommended Methodologies for Repair

There are certain guidelines which must be followed in the heat-straightening repair of members irrespective of the damage types. These guidelines are presented below.

General Guidelines for Heat-Straightening Repair

(1) Damaged members must not be repaired more than twice by heat-straightening

(2) Damage strain must not exceed 100 times the yield strain.

(3) The yield zones must be visually identified.

(4) Yield zones must be checked for hairline fractures.

(5) All yield zones must be heated but elastic zones must not be heated.

(6) Jacking forces must be passive, calibrated and carefully monitored during repair.

(7) Jacking forces must be directed to produce moments tending to reduce damage curvature.

(8) Jacking forces must be adjusted periodically to account for residual moments and P-delta effects.

(9) Heating temperature must be monitored during repair.

(10) Vee heat locations must be varied within the yield zone by at least one vee width after every heat

(11) Two or more vees may be heated simultaneously in the yield zone.

(12) Vee width must not exceed six inches.

(13) Heating temperatures must not exceed 1200 deg F for carbon steel and 1000 deg F for constructional alloy steel.

(14) The steel must be allowed to air cool.

(15) Vee heats must be used to repair major axis bends, line heats to repair minor axis bends and strip heats to heat minor axis bends in the stiffening element.

Repair Methodologies

The basic practice followed for different damage types is the same.

(1) The reference stations are marked and the initial measurements are taken.

(2) The 'HEAT" program is used to determine the degree of damage, vee geometry, number of heats and jacking force.

(3) The external jacking force is applied using calibrated gages.

(4) The recommended heating patterns given in the following sections, are applied to the yield zones.

(5) The member is allowed to air-cool.

(6) Measurements are taken after the beam has cooled to the ambient temperature.

Recommended Heating Patterns

The heating patterns for the various types of members are given below. All figures are given at the end of the chapter for easy reference.

(1) Plates with strong axis bends:

Use vee heats as shown in Figure 1.

(2) Category W Angles and Channels:

Use vee heats with strip heats as shown in Figures 98 and 100.

(3) Category S Angles and Channels:

Use vee heats with strip heats as shown in Figures 98 and 100.

(4) Category S wide flange beams (with or without axial load):

Use vee heats with strip heats as shown in Figure 99.

(5) Category W wide flange beams (with or without axial load):

Use vee heats with strip heats as shown in Figure 99.

(6) Composite deck-girder systems:

Use heating pattern shown in Figure 101.

(7) Non-Composite deck-girder systems:

Use heating pattern shown in Figure 82.

The above guidelines, methodologies and heating patterns can be used appropriately to conduct the heat-straightening repair of a damaged steel member.

The following section gives the details of the 'INDET' program.

Using the 'INDET' Program

General Information on Input Procedures

The 'INDET' program is identical in terms of the general input procedures to the 'HEAT' program. The only change is that the output is stored in file 'indet.r' in this case. The command 'indet' will initiate the program.

This program is used to determine the plastic rotation obtained in a heating cycle and to determine the residual moment caused in a composite girder by these movements. The girder is considered to be continuous over the diaphragms. The residual moments hinder the heat-straightening process and must be compensated for by the external jacking force. These

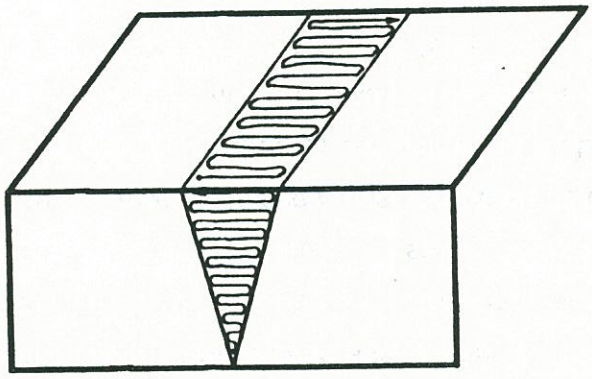

(a) Stiffening element at open end of vee
(Heat vee first and then rectangle)

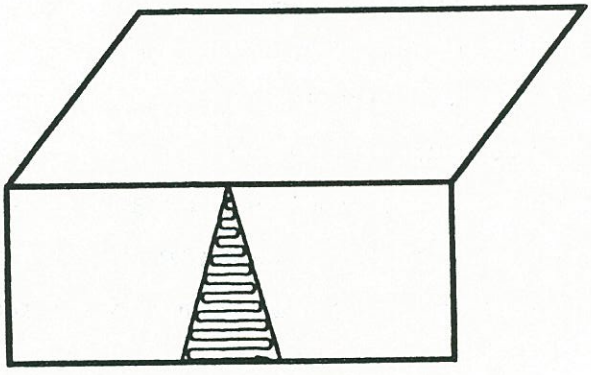

(b) Stiffening element at apex of vee
(Vee heat only)

Figure 98. Heating patterns for category S or W angles.

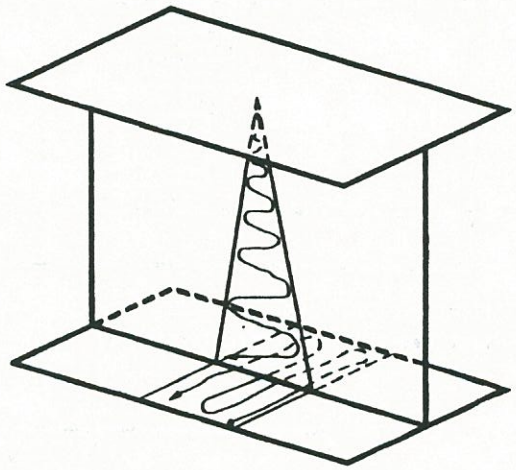

(a) Heating configuration for category S wide flange
(Heat vee first and then rectangle)

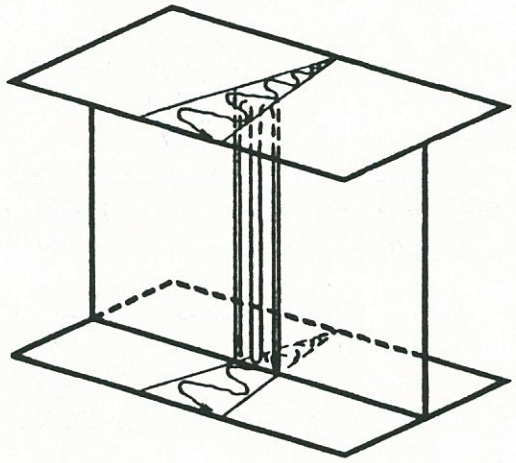

(b) Heating configuration for category W wide flange
(Heat vees simultaneously and then rectangle)

Figure 99. Heating patterns for category S or W wide flange beams (with or without axial load).

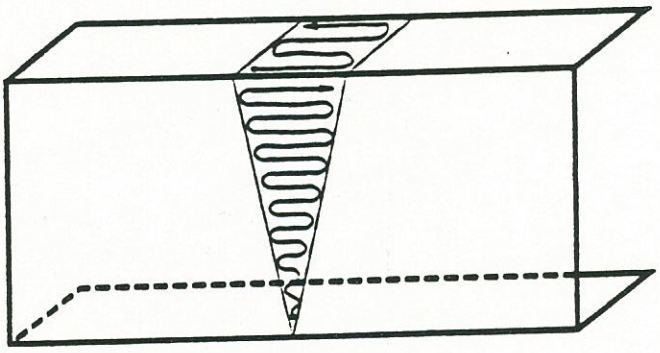

(a) Category S damage
(Heat vee first and then rectangle)

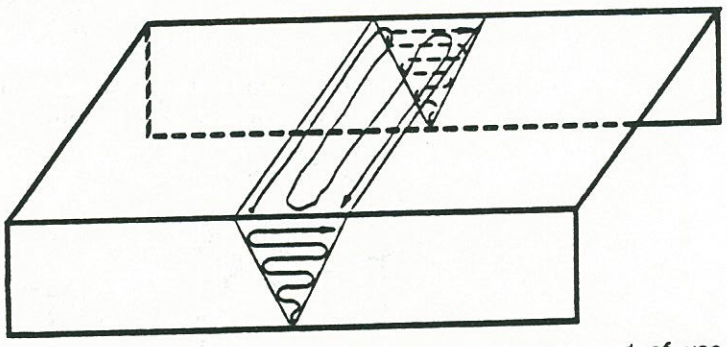

(b) Category W damage with stiffening element at open end of vee
(Heat both vees simultaneously and then rectangle)

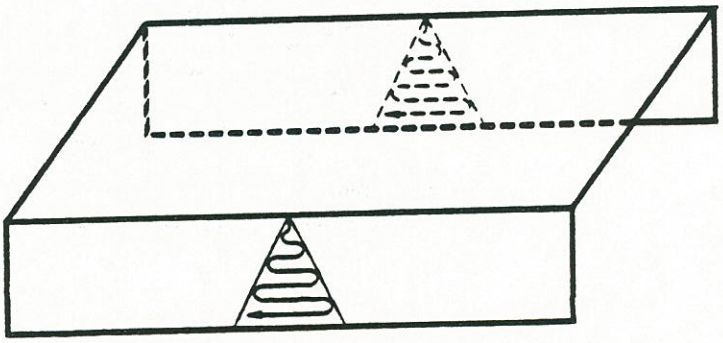

(c) Category W damage with stiffening element at apex of vee
(Heat vees simultaneously)

Figure 100. Heating patterns for category W or W channels.

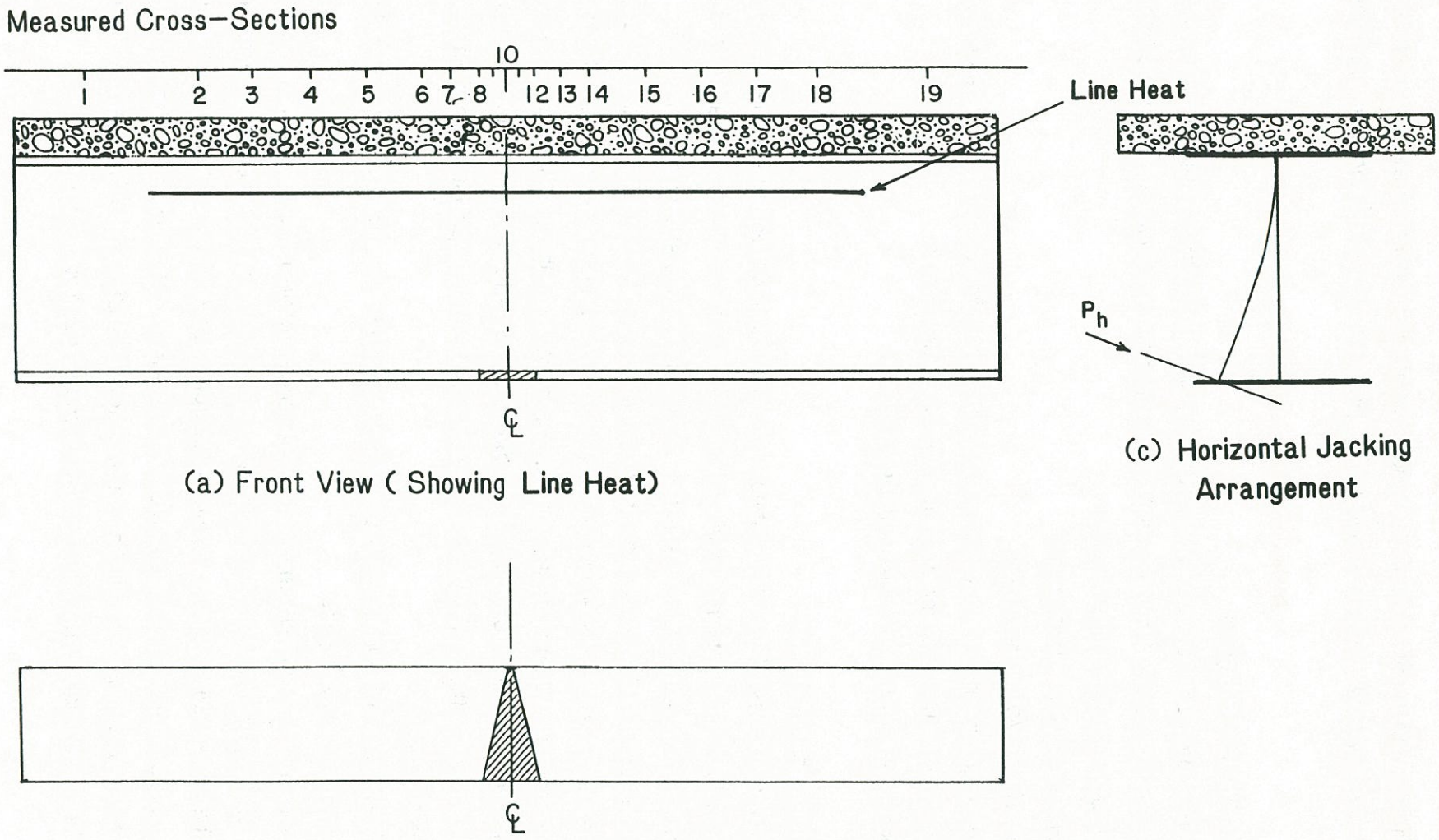

Figure 101. Heating patterns for composite deck-girder systems.

moments will change with every heating cycle and must be evaluated after every four cycles to be input in the 'Jacking force' module of the 'HEAT' program for the indeterminate composite girder case.

Structure of the 'INDET' Program

The 'INDET' program has also been designed in a modular manner to minimize the running time and the input time. The program is divided into three modules which are as follows:

(1) Structural parameters for girder.

(2) Heat-straightening response

(3) Residual Moments caused.

The member geometry & yield stress and the damage ordinates of the damaged member at four reference stations must be known before the program is used.

The modules are explained in the following sections.

Structural Parameters for Girder

The program first asks if the user wishes to find the residual moments. If the input is 'N', it enters the module II for Heat-straightening response. If the input is 'Y', it asks for input regarding the structural parameters of the girder. A sample input is shown in Figure 102.

(1) The user is asked for the number of spans, number of joints, number of support restraints and number of diaphragms in the indeterminate girder. The spans referred to are the unsupported spans in between the diaphragms. The joints include the end supports and the diaphragm locations. The number of support restraints is the total number of restraints at the joints against X and Y translation and Z rotation.

(2) The next set of inputs are the joint index number, X-coordinate and Y-coordinate (in feet) for each joint.

(3) The next set of inputs are the member index number, Jth joint number, Kth joint number, width of the bottom flange and the thickness of the bottom flange (in).

(4) The next set of inputs is the restrained joint number, followed by the X, Y translational and Z rotational restraint at the joint. "1" signifies a restrained degree of freedom while "0" signifies an unrestrained DOF, e.g., a fixed joint is "1 1 1". The diaphragm joints are considered as roller supports hence "0 1 0".

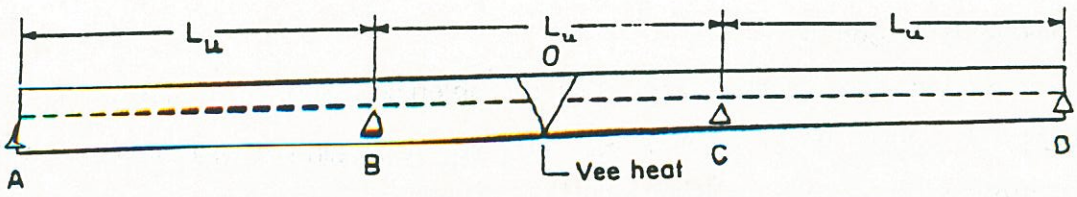

(a) . Bottom Flange of the Composite Girder with the Diaphragm Locations

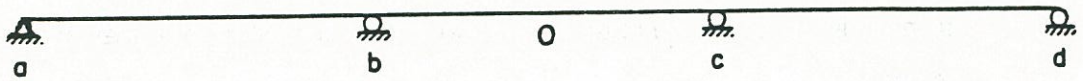

(b) . Idealized Beam

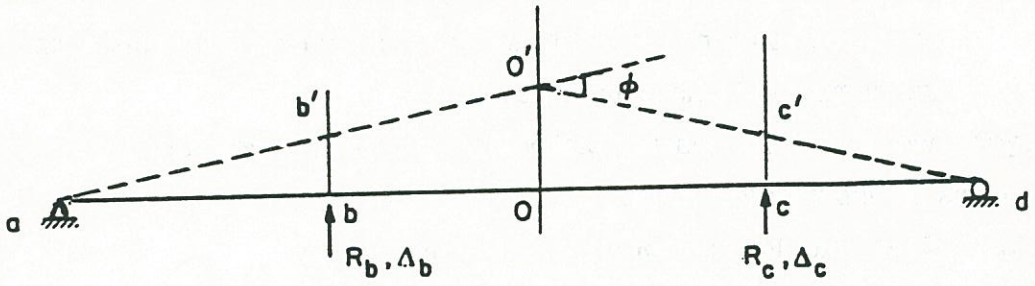

c) Released structure for idealised beam showing redundant forces.

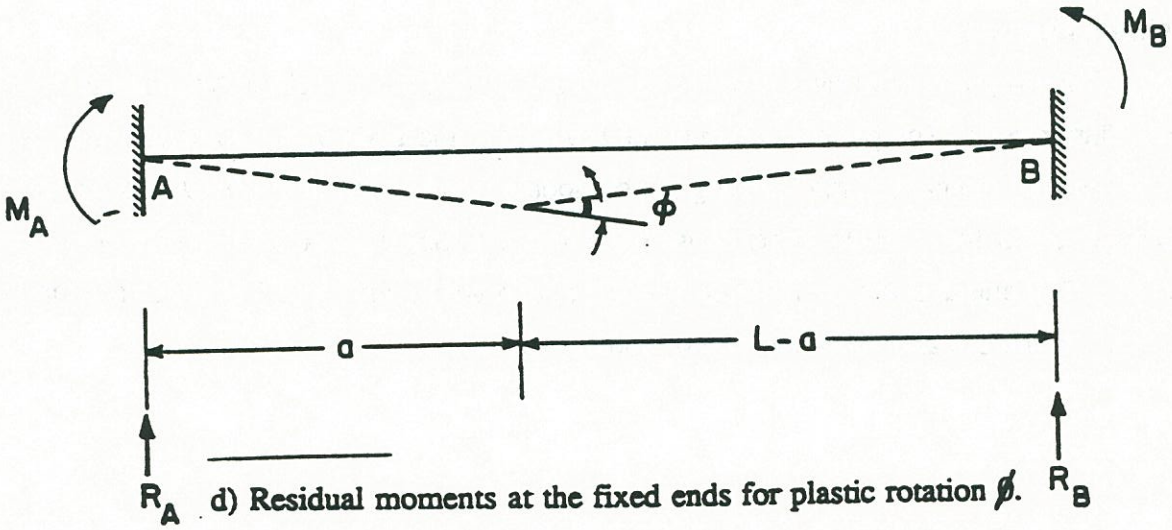

d) Residual moments at the fixed ends for plastic rotation ϕ.

Figure 102. Sample structure parameters and residual moments for 'INDET' program.

Heat-Straightening Response

The second module calculates the heat straightening response of the member for a heating cycle. The plastic rotation is then input as a load to obtain the residual moments.

The program first asks if the user wishes to calculate the plastic rotations. If not the user can directly input a previously calculated value. If the user inputs 'N', the program asks for the plastic rotation directly. If the user inputs 'Y', the program asks for the following input.

(1) The program asks for the locations of the four reference stations from the Jth end of the damaged span (in feet).

(2) The next input is the number of heating cycles for which the plastic rotation is desired.

(3) The next set of input is the four damage measurements after the cycle, previous to the ones for which the plastic rotation is to be calculated.

(4) The next set of input is the four damage measurements after every cycle for which the plastic rotation is to be calculated. The nunmber of inputs must be equal to the number of heats input in step (2).

The program will output the plastic rotation (rad) for each cycle after the damage measurements are input for that cycle.

(5) Then enter the number of heated members.

(6) Input the member index number of each heated member.

(7) Enter the plastic rotation (rad), either directly or from step (4), over a cycle or a set of cycles, and input the location of the vee heat (ft), from the Jth node of the span.

Residual Moments

The program performs a stiffness analysis to output the values of the residual moments at the diaphragms. The positive value of the moment at the ends of the damaged span is input as the residual moment in the 'Jacking force' module (module VI) of the 'HEAT' program. The jacking force is then recalculated considering the increasing value of the retarding residual moment. The output gives the residual moment at end action number 3 & 6, which are the Z-axis moments at the Jth and Kth node of the member respectively.

Chapter 7

SUMMARY, CONCLUSIONS AND RECOMMENDATIONS

Summary

Reported here are the results of over four years of research on heat-straightening of damaged steel. The study began with an exhaustive investigation of simple plate elements in the laboratory to establish the important parameters associated with the method. Not only were the various factors affecting heat-straightening quantified, but a rational formula was derived to predict the amount of straightening which would occur after a single vee heat as a function of these parameters. The key parameters were found to be heating temperature, vee angle, and constraining force. The formula developed is suitable for hand computations and design office use.

The next step was to extend the study to rolled shapes. Angles, channels and wide flange beams were damaged and heat straightened under controlled laboratory conditions to determine the factors affecting behavior. While the factors affecting plates were found to be equally important for rolled shapes, two other variables were determined to influence rolled shape behavior. Rolled shapes can be viewed as consisting of two types of cross section plate elements: primary and stiffening. The primary elements consist of plate elements bent about their local major axis when damaged. Vee heats are applied to these elements during repair. Stiffening plate elements are perpendicular to primary elements and are typically either bent about their minor axis or experience tension or compression when damaged. Strip heats are applied to these elements during repair. The sections may or may not be symmetrical. The cross section geometry introduces two effects. One is identified as the geometric effect and relates to the location of the stiffening elements at either the top, center, or bottom of the primary element. The other is the principle axis effect which relates to whether the primary elements coincide with the principle axis or not. Both factors have been quantified through extensive laboratory testing. In addition, an analytical investigation led to the conclusion that degree of straightening could be predicted by formulas using the plate equation as their basis. In essence, multiplication factors reflecting both the geometric and principle axis effects were introduced into the plate equation. The results were simple formulas to predict heat-straightening movements in angles, channels or wide flange beams about either their major or minor axis. Again, the formulas developed are suitable for hand computation and design office use.

The next phase of the research moved to large scale experimentation in which full-size steel bridge components were investigated. The focal point has been deck-girder systems in which the steel girder is compositely connected to the deck. However, noncomposite girders were also studied. The bottom flange of such structures is frequently damaged by over-height vehicles traveling the underpass. Tests were conducted in an outdoor facility in which 20 ft. long girders, ranging in depth from 10 to 24 inches, were damaged and repaired. All tests were conducted with a deck loading in place. Analytical studies were also conducted which have resulted in simple formulas for predicting behavior during heat-straightening. An additional factor influencing behavior was the role of the constraining force in indeterminate structures. When a lateral constraining force is applied to the bottom flange, a portion of the force is transferred through the web to the top flange and deck. Thus, the apparent moment induced in the bottom flange (based on assuming the entire force is carried by the bottom flange) is considerably higher than the actual moment. Since the actual flange moment is the governing factor related to constraining force, this behavior must be accounted for in developing analytical models. In addition, the diaphragms typically found in this type of structure result in an indeterminate beam over rigid supports for lateral loads applied to the bottom flange. Even adjusting for the web effect, an indeterminate analysis is often required when diaphragms are present. Procedures were developed to: (1) determine the effective stiffness of the bottom flange; (2) compute the residual moments caused as a result of the damage; (3) compute the effective bottom flange moment due to a specified applied constraining force; and (4) predict the rate of restoration per heat cycle. This phase of the study led to the refinement of heating patterns to be used for both composite and noncomposite girders. However, an analytical treatment of noncomposite girders was not developed because the experimental data base was too small for an adequate comparison. As a capstone to this phase of the project, a damaged girder in an actual bridge was repaired. Measurements were taken to verify the results determined analytically.

Finally, full scale wide flange rolled shapes were tested and evaluated in axial compression to simulate truss members. The experimental results for both major and minor axis damage differed from that of wide flange sections without axial loads. For small or negligible lateral constraining forces, the rate of straightening was less. The implication being that axial forces hinder straightening movements without significant applied constraining forces. However, for large lateral constraining forces, the straightening movements were larger than an equivalent member without axial loads implying that the axial forces magnify movements under these conditions. An analytical model was developed which incorporates the axial load effect. Again,

the basic plate equation forms the basis for this formula with multiplication factors employed to compensate for the axial loads.

As the research progressed from simple plate elements in the laboratory to full scale field tests, a continually decreasing number of experiments were conducted. A part of the reason was that as certain factors were identified and evaluated, it was not necessary to re-evaluate at the next stage. Additionally, as the specimens became larger and the structural configuration more complex, only a limited number of tests could be conducted within the scope of the project. However, some aspects require additional testing for a complete assessment of the behavior. To put the scope of the entire testing program in perspective, the following summary is presented.

Type of Element	Number of Specimens	Number of Heats
Undamaged elements		
Small plates	94	383
Small angles	6	18
Small Channels	12	36
Small wide flanges	29	164
Sub-Total	141	601
Damaged elements		
Small plates	10	336
Small angles	5	29
Small channels	1	14
Small wide flanges	5	297
Sub-Total	21	676
Damaged structural systems		
Large composite girders	3	137
Large noncomposite girders	1	69
Large axially loaded girders	2	73
Field repair of actual bridge	1	10
Sub-Total	7	289
Total	169	1566

Conclusions

As a result of using this experimental data to verify analytical formulations, some reliable formulas for predicting behavior have been developed. The most highly reliable is the basic plate equation for plastic rotations which forms the basis for all the analytical work. The research here differs from past work in that the emphasis has been placed on straightening damaged members in which a large number of heating cycles are employed. Previous research has been almost exclusively limited to heating initially straight members for only a few cycles. As a result of this emphasis, reliable data has been obtained for angles, channels and wide flange beams as well as composite girders and axially loaded wide flange members. This data has been used to verify the analytical modeling. The primary limitation on the modeling for rolled shapes is that a full range of different size sections have not been tested. More testing of damaged rolled shapes and noncomposite girders is needed to fine-tune and complete the analytical study.

From an engineering perspective, the most significant result of this research are the analytical procedures developed.. These results will enable engineers to assess damage, analyze the required parameter variations, design the heat-straightening repair, and compute the type and number of heating cycles to complete the repair. In most cases, the design formulations are suitable for hand computations and either field or design office use. While it was originally envisioned that a computer program would be required to facilitate the design of heat-straightening repairs, the simplicity of the formulas means that hand computations are feasible. The only required use of a computer analysis is for the treatment of indeterminate systems to determine constraining force effects. For most cases, any standard frame analysis package will be satisfactory. The only possible exception is for composite girders with intermediate diaphragms. However, most standard programs can handle this aspect also with the coefficients provided in this report. A computer program has been developed for the analysis of all basic cases and is given in an appendix.

An important issue that has limited the use of heat-straightening is the concern about material property changes. Most previous research has evaluated material properties after the application of only a small number of heats and usually on undamaged members. The investigation was also conducted on members that had been damaged and repaired. It can be concluded that yield stress and tensile stress increase slightly after repair, although higher values were typically located near the apex of the vee. The modulus of elasticity showed a decrease at the open end and varied at other locations. There were no indications that the material property changes should limit the use of heat straightening.

Residual stress distributions were measured for angle, channel and wide flange sections. The peak values were typically in the 20 ksi range which is similar to those found in welded built-up sections. This level of residual stress should not be detrimental.

The results of this research have shown that heat-straightening repair is a valid procedure for repairing structural steel. It has been found that the degree of damage can best be defined as the angle of rotation between non-yielded portions on both sides of a plastic hinge yield zone. The length of the yield zone is a relatively unimportant consideration. More important is the type of damage. A classification system has been developed to more clearly define damage in three categories: S for major axis bending, W for minor axis bending, and T for torsional damage. Methodologies for heat straightening each type have been defined.

However, there are limiting situations in applying heat-straightening repair. One consideration is the occurrence of sudden cracking during repairs. While reported occasionally in field applications, no explanations have been advanced. The cracking phenomena has been reproduced in an experimental environment while repairing a composite girder. An unusually high jacking force was being used when the crack occurred. The failure is attributed to this excessive force. Since jacking forces are rarely measured in field repairs, it is not surprising that cracking sometimes occurs. It is recommended that jacking forces be limited to that which produces a moment in the heated zone not to exceed one-third of the plastic moment capacity. It is also recommended that jacking forces not be allowed unless the jacks are gauged to control the applied force and a structural analysis is performed to determine what the limiting force should be.

A second limiting factor may be the degree of damage. This study is the first to explore this facet. Specimens were damaged so that the extreme fiber strain equalled 100 times the yield strain. These members were successfully repaired indicating that limiting strains are at least that high.

A third limiting factor is repetitive damage and successive heat-straightening repair. In one test, a fatigue type crack appeared during the fourth damage/repair cycle. In a second test series, plates were damage and repaired up to eight different times. Material properties varied little after two cycles but began to change significantly after the fourth cycle. In particular, yield stresses increased dramatically, while tensile stress did not change. As a result, the material takes on the stress-strain characteristics of a brittle material. Based on these considerations, it is recommended that damaged steel members not be repaired more than twice by heat straightening.

Recommendations

One area which has not been addressed is the heat-straightening repair of localized damage such as bulges and crimps. These localized damage zones can be quite severe. Current field practice is to use hot mechanical straightening to correct this type of damage. It is believed that effective patterns and methodology can be developed so that this type of damage can be engineered in a manner similar to that presented here for overall member damage.

A second area of need is to apply the research of this project to actual repair situations. A selected number of bridges with the various categories of damage should be field repaired with careful instrumentation and monitoring of the results. This data will allow for the fine-tuning of both the analysis and methodology of heat-straightening.

A third need is to investigate the fatigue characteristics of heat-straightened members. At present, no guidance exists as to possible limitations. As a result, some authors recommend that fracture critical members not be heat straightened. It is the opinion of the writers that this is too severe of a limitation. However, research is needed to verify this concept.

A fourth need is to develop procedures for assessing the degree of damage in terms of the reduced capacity of the structure. Factors to be evaluated include the effects of unsymmetrical damaged cross-sections, lateral and torsional buckling strength reductions due to distortion, and strength losses due to localized bulges and buckles. Such analysis would enable the engineer to base the decision to repair on a quantitative analysis.

A final need is to conduct additional laboratory experiments on rolled shapes and built-up members typically used in bridge design. A greater variety in member sizes would provide further verification of the analytical models. Built-up member tests have not been conducted and may require special considerations.

REFERENCES

American Institute of Steel Construction (1986), Manual of Steel Construction, Load Resistance Factor Design, 1st edition.

American Railway Engineering Association (1946), Shortening Eyebars to Equalize the Stress," Bulletin No. 460.

Avent, R. R. (1987), "Use of Heat-Straightening Techniques for Repair of Damaged Steel Structural Elements in Bridges," Phase 1: Interim Report, Louisiana Transportation Research Center, Louisiana State University, Baton Rouge.

Avent, R. R. and Boudreaux, R. J. (1987), "Heat-Straightening Effects on the Behavior of Plates and Rolled Shapes," Second Interim Report of Phase 1, Louisiana Transportation Research Center, Louisiana State University, Baton Rouge.

Avent, R. R. and Fadous, G. M. (1987), "Heat-Straightening Effects on the Behavior of Full-Scale Simulated Bridge Girders," First Interim Report of Phase 2, Louisiana Transportation Research Center, Louisiana State University, Baton Rouge.

Avent, R. R., (1989), "Heat-Straightening of Steel: Fact and Fable," Journal of Structural Engineering, ASCE, Vol. 115, No. 11, November.

Avent, R. R. and Fadous, G. M. (1989a), "Heat-Straightening Prototype Damaged Bridge Girders," Journal of Structural Engineering, ASCE, Vol. 115, No. 7, July.

Avent, R. R. and Fadous, G. M. (1989b), "Heat-Straightening Techniques for Repair of Damaged Steel in Bridges," Final Report, Louisiana Transportation Research Center, Louisiana State University, Baton Rouge.

Avent, R. R. and Rountree, E. G. (1974), "field Analysis of Saw-tooth Folded Plates,"

Avent, R. R., and Wells, S. (1979), "Factors Affecting the Strength of Thin-Wall Welded Columns," Engineering and Industrial Research Station Report No. MSSU-EIRS-CE-79-7, Mississippi State University, Mississippi State, MS, May.

Avent, R. R., and Wells, S. (1982), "Experimental Study of Thin-Web Welded H Columns," Journal of the Structural Division, ASCE, Vol. 108, No. ST7, July.

Barsom, J. M. and Rolfe, S. T. (1987), Fracture & Fatigue Control in Structures - Applications of Fracture Mechanics, 2nd Edition, Prentice-Hall, Englewood Cliffs, New Jersey.

Benjamin, J. R. and Cornell, C. A. (1970), Probability, Statistics, and Decision for Civil Engineers, McGraw-Hill, New York.

Bernard, P. and Schulze, K. (1966), "Flame Straightening in Ship-building," Mittelunge der BEFA (Beratungsstelle fur Autogen Technik), Vol. 17, No. 11, pp. 206 (German).

Blodget, O. W. (1972), "Distortion . . . How Metal Properties Affect It," Welding Engineer, February, pp. 40-46.

Boudreaux, R. J. (1987), "Heat Straightening of Steel: Identifying the Important Parameters and Predicting Member Response," MS Thesis, Louisiana State University, Baton Rouge.

Brockenbrough, R. L.(1970), "Theoretical Stresses and Strains from Heat Curving," Journal of the Structural Division, ASCE, Vol. 96, No. ST7, Proc. Paper 7410, July, pp. 1421-1444.

Brockenbrough, R. L. and Johnston, B. G. (1970), "Criteria for Heat Curving Steel Beams and Girders," Journal of the Structural Division, ASCE, Vol. 96, No. ST10, October, pp. 2209-2226.

Brockenbrough, R. L. and Ives, K. D. (1970), "Experimental Stresses and Strains from Heat Curving," Journal of the Structural Division, ASCE, Vol. 96, No. ST7, Proc. Paper 7400, July, pp. 1305-1331.

Brockenbrough, R. L. and Johnston, B. G. (1968), USS Steel Design Manual, U.S. Steel Corporation, Pittsburgh, PA.

Burbank, B. B. (1968), "Straightening Distorted Weldments," Report to the Ship Structure Committee, Report No. SR-185, July.

Ciesicki, H. and Butler, S. (1958), "Flame Camber Your Own Beams," Industry and Welding, April.

Cku, K. and Pinjarakar, S. G. (1966), "Multiple Folded Plate Structures," Journal of the Structural Division, ASCE, Vol. 92, No. ST2, Proc. Paper 4791.

Crooker, T. W. and Harrison, H. L. (1965), "The Effects of Flame Cambering on the Bending Strengths of I-Beams," Welding Journal, Vol. 44, No. 12, December, Research Supplement, pp. 545s-548s.

deBejar, L. A., Robinson, P. F. and Avent, R. R., "Risk Consistent Estimate of Heat-Straightening Applications. I: Plates," Journal of Structural Engineering, ASCE, (submitted for review).

deBejar, L. A., Robinson, P. F. and Avent, R. R., "Risk Consistent Estimate of Heat-Straightening Applications. II: Beams," Journal of Structural Engineering, ASCE, (submitted for review).

Dean, D. L. and Omid'Varan, C. (1969), "Analysis of Ribbed Plates," Journal of the Structural Division, ASCE, Vol. 95, No. ST3, Proc. Paper 6474, pp. 411-440.

De-Fries-Skene, A. and Scordelis, A. C. (1964), "Direct Stiffness Solution for Folded Plates," Journal of the Structural Division, ASCE, Vol. 90, No. ST4, pp. 15-47.

Ditman, O. (1961), "Determination of Thermal Shrinkage in Structural Steel," MS Thesis, University of Washington.

Engineering-News Record (1959), "How Fire Destroyed and Fire Repaired Air Force Hangers," June 18, pp. 50-53.

Fadous, G. M. (1987), "Heat-Straightening Effects on the Behavior of a Full-Scale Simulated Bridge Girder," MS Thesis, Louisiana State University, Baton Rouge.

"Flame Buckled This Steel . . . And Flame Straightened It," (1959), Part 1, Welding Engineer, February, pp. 43.

For Chin, W. (1962), "Linear Shrinkage of Steel," MS Thesis, University of Washington.

Gipson, G. S. and Ortiz, J. C. (1986), "Toward an Analytical Description of the Heat-Straightening Phenomenon - The Thermal Problem," SECTAM XIII Proceedings.

Goldberg, J. E. and Leve, H. L. (1957), "Theory of Prismatic Folded Plate Structures," International Associates of Bridge and Structural Engineering, Memoirs, Vol. 17, pp. 59-86.

Graham, R. (1975), "Investigation of Flame Straightening Methods for Steel Structures," Boeing Co. Manufacturing Development Report, MDR 2-32075, October 30.

Harrison, H. L. (1952), "Straightening Structural Members in Place," Welding Journal, Vol. 31, No. 5, May Research Supplement, pp. 257s-262s.

Harrison, H. L. and Mills, B. D., Jr. (1951), "Effects of Light Peening on the Yielding of Steel," Welding Journal, Vol. 30, No. 5, May Research Supplement, pp. 251s-253s.

Harrison, H. L. (1950), "A Study of the Holt Method of Heat (Contraction) Straightening," MS Thesis, University of Washington.

Hicks, C. R. (1982), Fundamental Concepts in the Design of Experiments, Third Edition, Holt, Rhinehart and Winston, New York.

Higgins, T. R. (1966), "Discussion on the Effects of Flame Cambering on the Bending Strength of I-Beams," Welding Journal, Vol. 45, No. 6, June Research Supplement, pp. 284s-288s.

Holt, J. E. (1955), "Flame Straightening: A Friend in Need," Welding Engineer, Vol. 40, No. 10, October, pp. 44-46, No. 12, December, pp. 30-31.

Holt, J. E. (1938), Contraction as a Friend in Need, Typed and Copyrighted.

Holt, R. E. (1971), "Primary Concepts in Flame Bending," Welding Engineer, Vol. 56, No. 6, June, pp. 416-424.

Holt, R. E. (1965), "Flame Straightening Basics," Welding Engineer, Vol. 50, No. 9, September, pp. 49-53.

Holt, R. E. (1977), "How to Control and Correct Warping," Welding Design and Fabrication, June, pp. 98-102.

Horton, D. L. (1973), "Heat Curved Mild Steel Wide Flange Sections: An Experimental and Theoretical Analysis," MS Thesis, University of Washington.

Issa, R. R. (1978), "An Experimental Study of Various Factors Affecting the Bond Strength of Epoxy Repaired Timber Structures," MS Thesis, Mississippi State University.

Kihara, H., Hisida, M. and Fujita, Y. (1961), "On the Residual Stresses Due to Spot Heating," Document No. X-267-61, International Institute of Welding, Commission X.

"Kinks Go Up in Flames," (1981), Engineering News Record, April 9, p. 17.

Maeda, T. and Yada, T. (1963), "Fundamental Nature of Shrinkage Distortion Due to Spot Heating on a Rectangular Plate," Document No. X-327-63, International Institute of Welding, Commission X.

Maeda, T. and Yada, T. (1961), "Investigation of Shrinkage Due to Multiple Spot Heating," Document No. X-268-61, International Institute of Welding, Commission X.

Masubuchi, K. (1960), "Calculation and Measurement of Residual Stresses Due to Spot Heating," Document No. X-259-60, International Institute of Welding, Commission X.

Moberg, K. L. (1979), "Damage Assessment and Contraction Straightening of Steel Structures," MS Thesis, University of Washington.

Morris, J. J. (1949), "Controlled Distortion - An Aid to Metal Working," Welding Journal, Vol. 28, No. 11, November, pp. 1080-1082.

Meyers, P. S. (1976), "Fundamentals of Heat Flow in Welding," Welding Research Council Bulletin, No. 123, July.

Newman, E. M. (1959), "Repair of Fire Damaged Structural Steel," Military Engineer, No. 344, November-December, pp. 448-450.

Nicholls, J. I. and Weerth, D. E. (1972), "Investigation of Triangular Heats Applied to Mild Steel Plates," Engineering Journal, AISC, October, pp. 137-141.

"Oxyacetylene Torches Straighten Fire-Warped Steel," (1959), Welding Engineer, March, pp. 31-34.

Pattee, H. E., Evans, R. M. and Monroe, R. E. (1970), "Effect of Flame and Mechanical Straightening on Material Properties of Weldments," Summary Report on Ship Structure Committee on Project SR-185, Straightening Distorted Weldments.

Pattee, H. E., Evans, R. M. and Monroe, R. E. (1969), "Flame Straightening and Its Effect on Base Metal Properties," Summary Report to Ship Structure Committee concerning the first phase of Project SR-185, Straightening Distorted Weldments, Battelle Memorial Institute, Columbus, Ohio, August.

Pfeiffer, R. (1963), "The Flame Straightening of Sheeting and Sheet Metal Structures," Mitteilungen der BEFA, Vol. 14, No. 9, pp. 1-7 (German).

"Phase I Report on Folded Plate Construction" (1963), Task Committee on Folded Plate Construction, Journal of Structural Division, ASCE, Vol. 89, No. ST6, Proc. Paper 3741, pp. 365-406.

Roeder, C. W. (1986), "Experimental Study of Heat Induced Deformation," Journal of Structural Engineering, ASCE, Vol. 112, No. 10, October, pp. 2247-2262.

Roeder, C. W. (1987), "Predictions of Deformations Due to Heat Curving," Bridges and Transmission Line Structures, ASCE, New York, pp. 101-110.

Roeder, C. W. (1985), "Use of Thermal Stress for Seismic Damage Repair," Final Report on NSF Grant CEE-82-05260, University of Washington, Seattle, October.

Rothman, R. L. (1973), "Flame Straightening Quenched and Tempered Steels in Ship Construction," Ship Structures Committee, Report No. 247.

Rothman, R. L. and Monroe, R. E. (1973), "Effect of Temperature and Strain Upon Ship Steels," Ship Structures Committee, Report No. 235.

Shanafelt, G. O. and Horn, W. G. (1984), "Guidelines for Evaluation and Repair of Damaged Steel Bridge Members," NCHRP Report No. 271, Transportation Research Board, National Research Council, Washington, DC, June.

Structural Stability Research Council (SSRC) (1976), Guide to Stability Design Criteria for Metal Structures, Third Edition, John Wiley & Sons, New York.

Thatcher, W. M. (1967), "Horizontally Curved Steel Girders - Fabrication and Design Considerations," Engineering Journal, AISC, July.

Tsalman, L. B. (1959), "Straightening Welded Structures by Heating with an Oxy-Acetylene Flame," Welding Production, 5, pp. 29-31 (Russian).

U.S. Steel Corporation (1966), "Steels for Elevated Temperature Service," ADUSS 43-1089.

Wanatabe, M. and Satoh, K. (1951), "On the Correction of Distortion in Welded Thin Plate Structures," Journal of the Japan Welding Society, Vol. 20, pp. 194-202 (Japanese).

Weerth, D. E. (1971), "Theoretical and Experimental Analysis of Heat Curved Mild Steel," MS Thesis, University of Washington.

Yoch, A. E. (1957), "Flame Cambering of Beams for Bridges," Welding Engineer, Vol. 42, No. 2.

APPENDIX A

RESIDUAL STRESSES (UNDAMAGED PLATES)

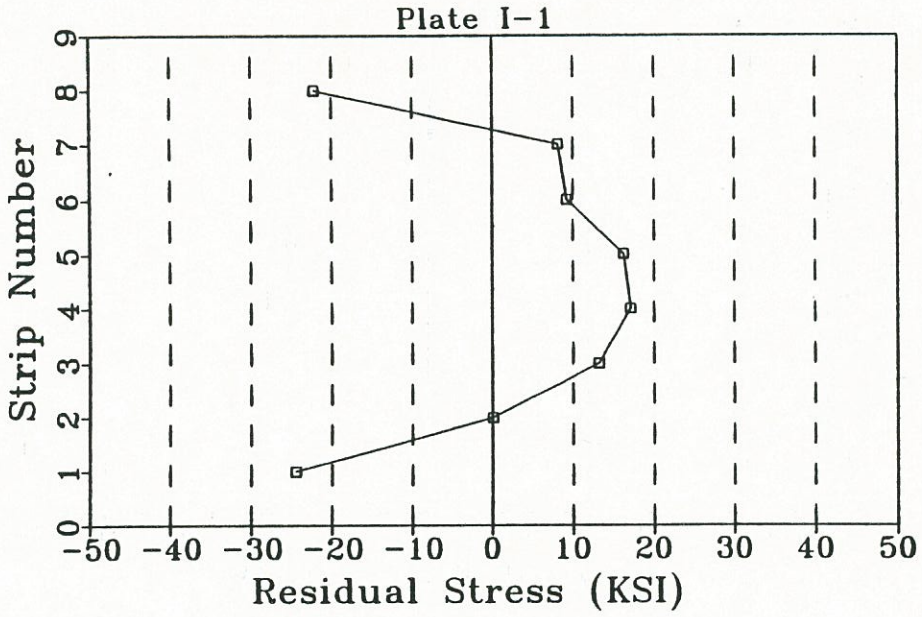

Figure A1. Stresses in plate I-1 (20° vee, M/M_p = 0.00, depth ratio = 1.00).

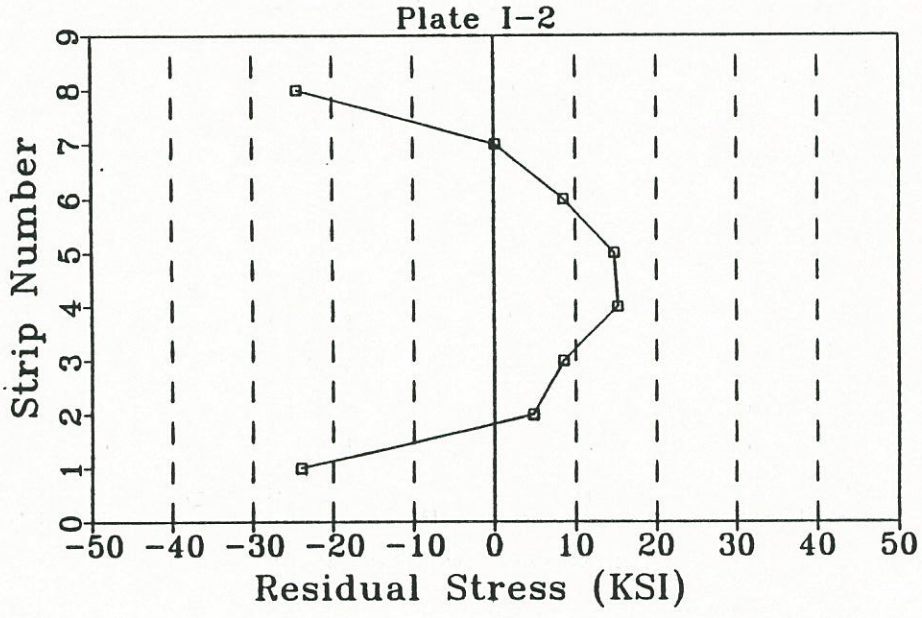

Figure A2. Stresses in plate I-2 (45° vee, M/M_p = 0.00, depth ratio = 1.00).

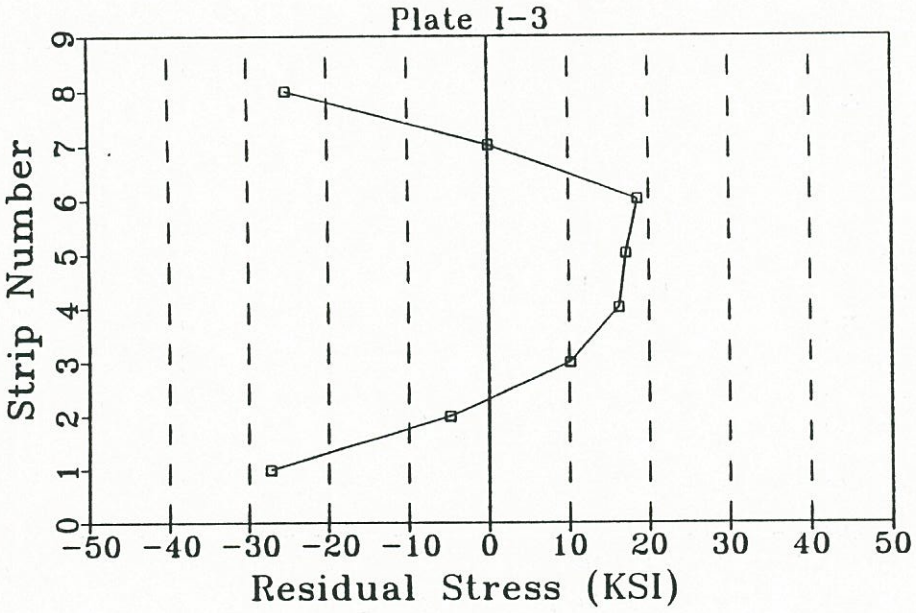

Figure A3. Stresses in plate I-3 (60° vee, M/M_p = 0.00, depth ratio = 1.00).

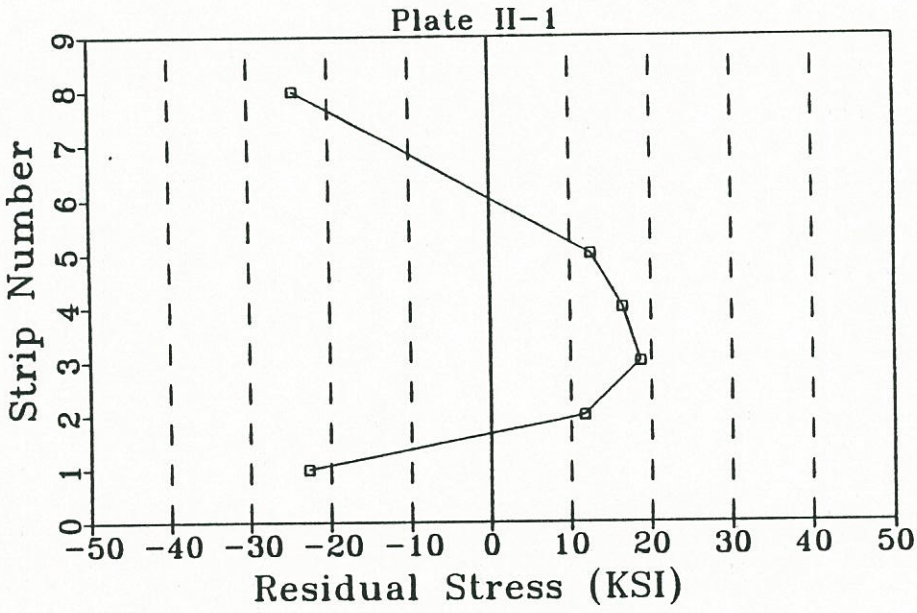

Figure A4. Stresses in plate II-1 (20° vee, M/M_p = 0.00, depth ratio = 1.00).

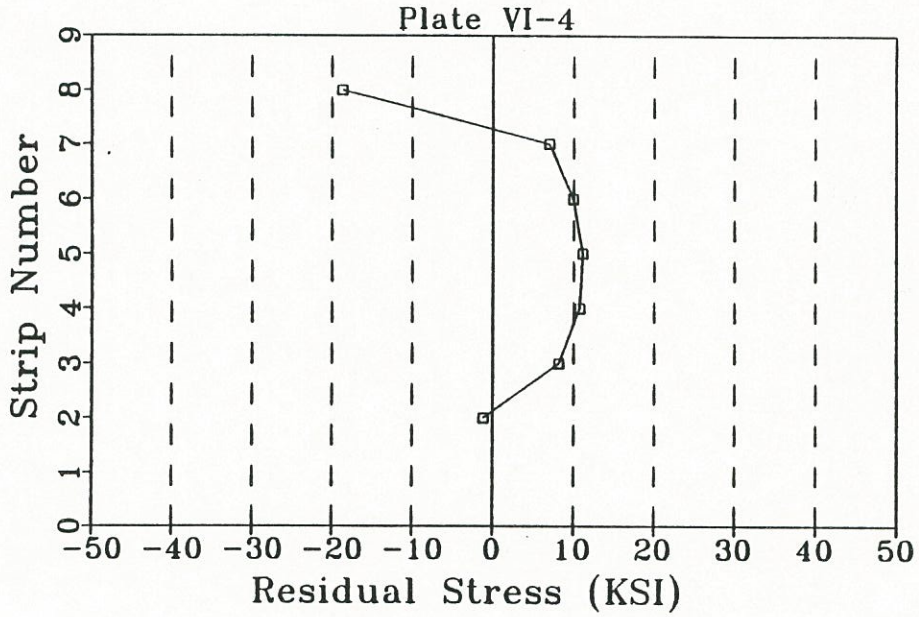

Figure A5. Stresses in plate VI-4 (45° vee, M/M_p = 0.50, depth ratio = 0.75).

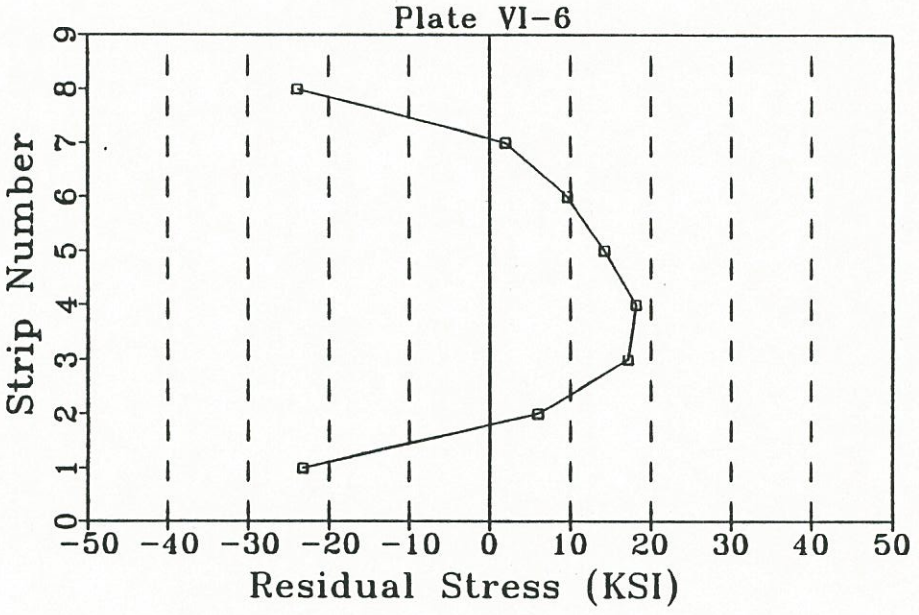

Figure A6. Stresses in plate VI-6 (45° vee, M/M_p = 0.00, depth ratio = 0.75).

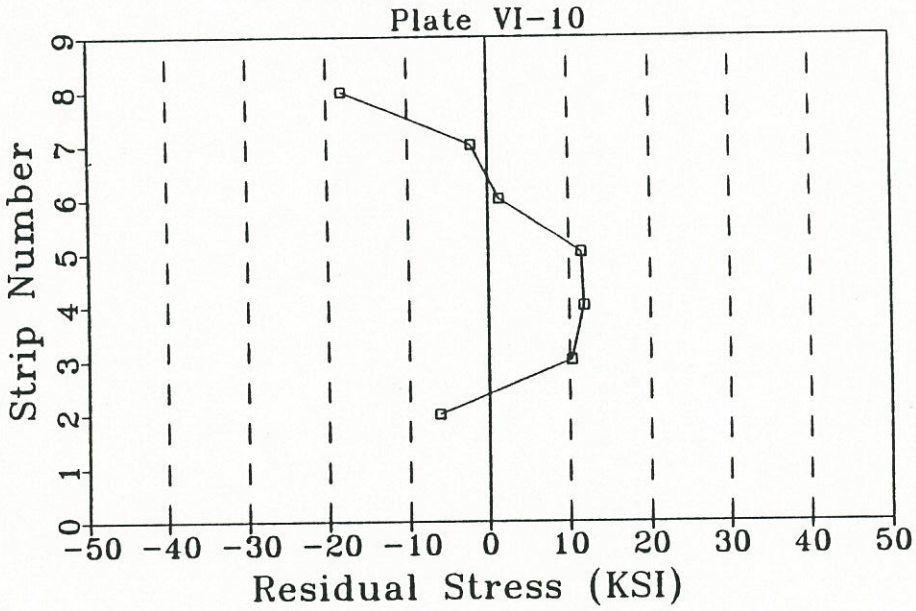

Figure A7. Stresses in plate VI-10 (82° vee, M/M_p = 0.50, depth ratio = 0.75).

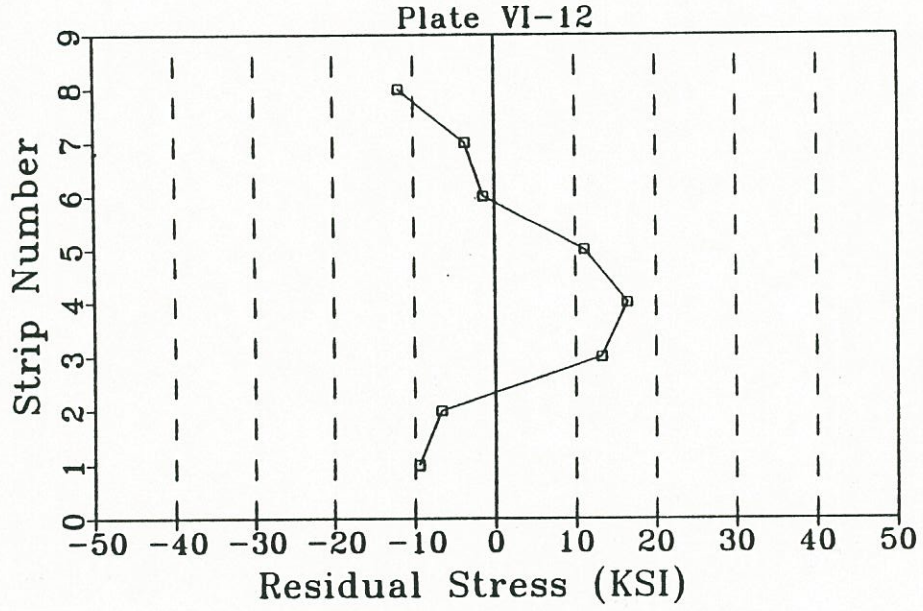

Figure A8. Stresses in plate VI-12 (82° vee, M/M_p = 0.00, depth ratio = 0.75).

APPENDIX B

PLASTIC ROTATIONS (DAMAGED PLATES)

Plastic Rotations in Milliradians

Plate XXV-3

1	6.381	2	4.717	3	-0.224	4	4.015
5	4.205	6	6.143	7	1.417	8	3.434
9	4.283	10	7.790	11	5.619	12	5.000
13	10.497	14	4.183	15	4.353	16	5.408
17	3.594	18	4.364	19	2.485	20	3.615
21	7.289	22	3.465	23	4.460		

Plate XXV-5

1	7.049	2	7.072	3	8.532	4	3.945
5	8.351	6	6.934	7	5.731	8	6.951
9	6.243	10	6.273	11	7.254	12	7.794
13	8.100						

Plate XXV-6

1	15.977	2	16.687	3	5.350	4	8.627
5	7.882	6	7.071	7	3.348	8	5.349
9	6.322	10	6.479	11	6.467	12	4.591
13	4.671	14	9.984	15	3.996	16	6.108
17	5.840	18	5.781	19	5.113	20	3.686
21	2.253	22	2.023	23	4.276	24	4.242
25	5.791	26	5.282	27	6.003	28	1.684
29	4.494	30	2.384	31	5.914	32	0.785
33	3.400	34	2.955	35	5.185		

Plastic Rotations in Milliradians

Plate XXV-7

1	6.632	2	8.064	3	8.255	4	8.127
5	2.574	6	2.935	7	5.900	8	8.000
9	6.644	10	6.228	11	2.870	12	3.225
13	7.940	14	5.368	15	3.950	16	7.479
17	2.910	18	11.558	19	12.121	20	7.181
21	3.926	22	2.001	23	4.266	24	4.327
25	5.226	26	4.931	27	1.980	28	4.725
29	3.302	30	3.859	31	4.412	32	3.762
33	5.937	34	4.372	35	1.911	36	5.289
37	4.759	38	5.472	39	10.323	40	8.300
41	3.366	42	5.850	43	10.552	44	4.477
45	4.607	46	2.876	47	5.608	48	10.254
49	6.330	50	6.231	51	2.524	52	5.923
53	9.332	54	4.379	55	2.545	56	3.240
57	4.560	58	8.455				

Plate XXV-8

1	7.795	2	4.465	3	4.451	4	4.317
5	8.042	6	5.528	7	4.140	8	5.580
9	5.700	10	5.611	11	6.457	12	2.624
13	4.528	14	5.359	15	4.579	16	3.920
17	6.170	18	-0.820	19	4.485	20	2.895
21	2.625						

Plastic Rotations in Milliradians

Plate XXV-4

Ht #	P.R.	Ht #	P.R.	Ht #	P.R.
1	2.506	36	6.036	71	7.490
2	9.638	37	3.003	72	4.359
3	-3.984	38	4.250	73	3.682
4	10.555	39	2.330	74	3.982
5	5.475	40	5.980	75	1.441
6	-3.768	41	0.241	76	1.924
7	2.839	42	5.465	77	4.173
8	3.582	43	1.544	78	2.453
9	4.101	44	3.875	79	2.329
10	7.883	45	0.350	80	4.120
11	3.604	46	8.535	81	3.817
12	3.516	47	7.337	82	3.418
13	4.204	48	5.046	83	3.628
14	6.636	49	4.024	84	1.048
15	4.578	50	1.812	85	2.915
16	2.498	51	1.675	86	1.428
17	5.109	52	2.489	87	9.952
18	2.330	53	3.156	88	7.757
19	2.436	54	3.350	89	-0.180
20	4.782	55	2.434	90	4.741
21	7.160	56	3.079	91	2.613
22	1.046	57	3.025	92	0.839
23	2.556	58	2.907	93	6.156
24	5.015	59	1.147	94	3.803
25	-0.233	60	4.342	95	3.508
26	3.695	61	3.803	96	5.638
27	9.314	62	6.164	97	1.165
28	14.585	63	1.878	98	2.699
29	5.270	64	4.542	99	0.895
30	6.704	65	4.057	100	1.505
31	3.811	66	5.167	101	0.735
32	4.972	67	3.622	102	1.695
33	3.692	68	3.981	103	1.830
34	3.277	69	2.314	104	2.070
35	5.112	70	3.679	105	4.620
--	-----	--	-----	106	9.675

Plastic Rotations in Milliradians

Plates:	XXV-9	XXV-10	XXV-11	XXV-12
Ht #	P.R.	P.R.	P.R.	P.R.
1	4.137	2.286	5.404	5.808
2	4.239	3.527	18.663*	5.074
3	3.538	2.508	-8.177*	4.799
4	1.492	2.749	4.585	2.530
5	2.044	1.993	2.928	5.414
6	4.630	2.795	4.228	6.595
7	-0.073	3.813	6.870	2.279
8	3.396	1.672	2.351	5.195
9	1.641	1.815	4.418	3.440
10	2.072	2.324	2.996	3.891
11	3.595	1.420	5.294	4.925
12	2.167	0.763	3.434	0.793
13	1.993	3.060	2.335	2.092
14	2.480	1.734	1.822	4.728
15	1.499	0.602	7.941	4.853
16	2.842	2.676	3.546	6.636
17	0.531	2.868	1.707	4.380
18	4.071	1.653	5.426	4.766
19	0.375	0.279	2.971	-1.825
20	2.592	3.449	4.286	8.325

*Error in measurement between these two heats.

Note: The heating temperature for plates XXV-9 through XXV-12 was 1100°F.

APPENDIX C

RESIDUAL STRESSES (DAMAGED PLATES)

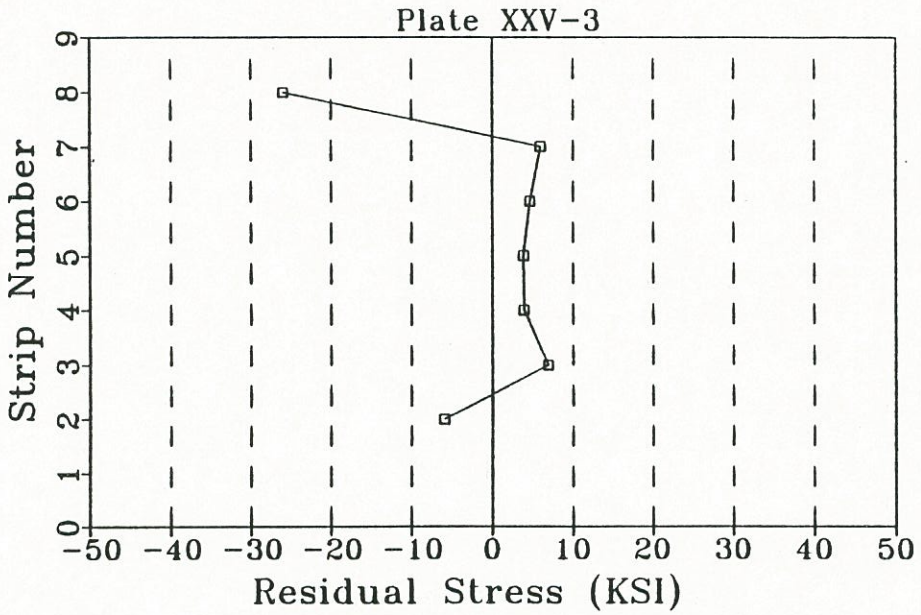

Figure C1. Stresses in plate XXV-3 (45° vee, M/M_p = 0.25, depth ratio = 1.00, angle of damage = 6.40°, assumed E = 29,000 ksi).

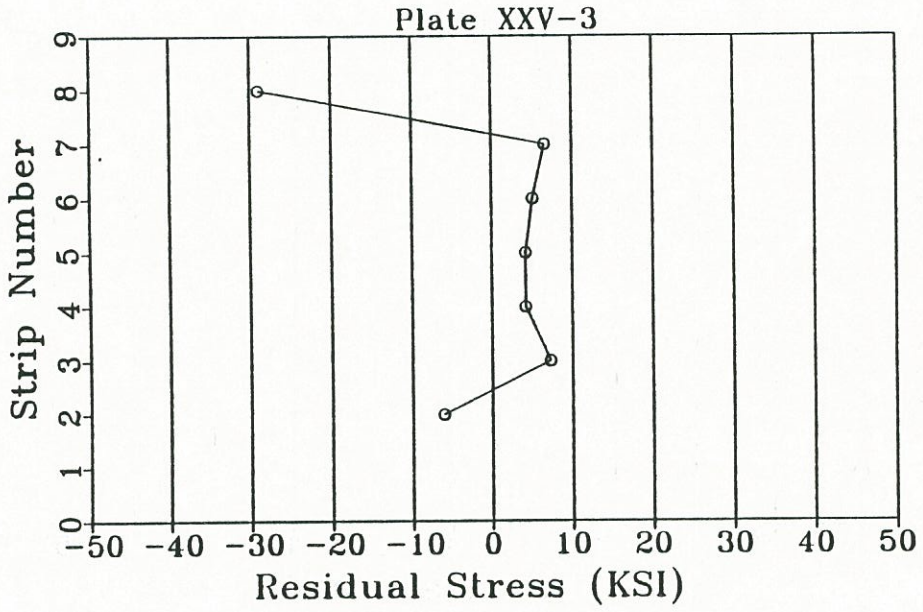

Figure C2. Stresses in plate XXV-3 (45° vee, M/M_p = 0.25, depth ratio = 1.00, angle of damage = 6.40°, assumed E from tensile test results).

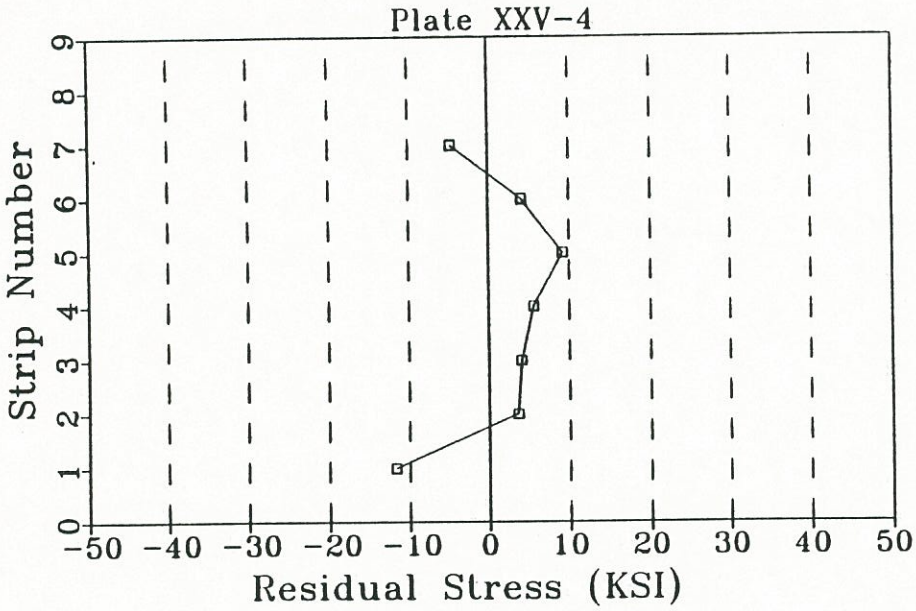

Figure C3. Stresses in plate XXV-4 (45° vee, M/M_p = 0.25, depth ratio = 1.00, angle of damage = 6.40°, assumed E = 29,000 ksi).

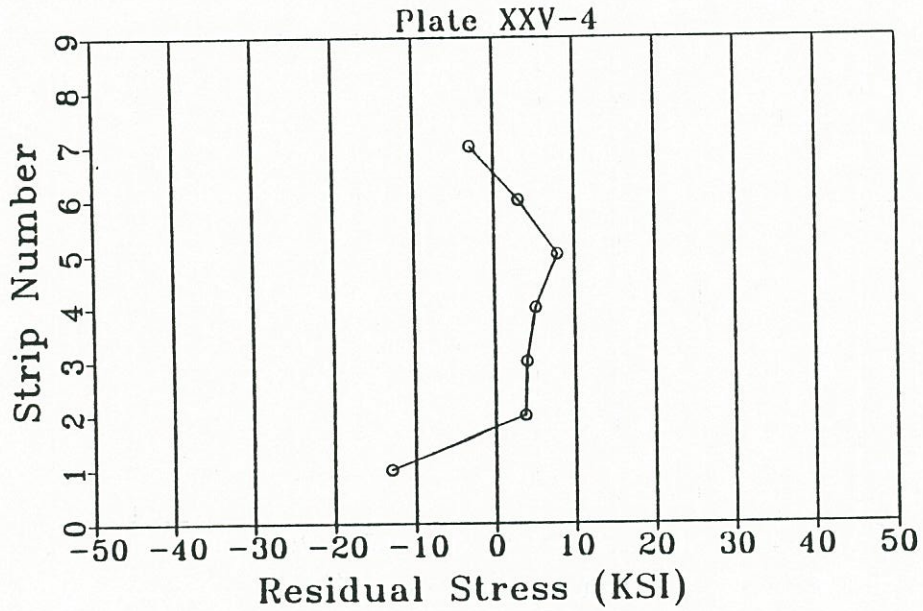

Figure C4. Stresses in plate XXV-4 (45° vee, M/M_p = 0.25, depth ratio = 1.00, angle of damage = 23.62°, using E from tensile test results).

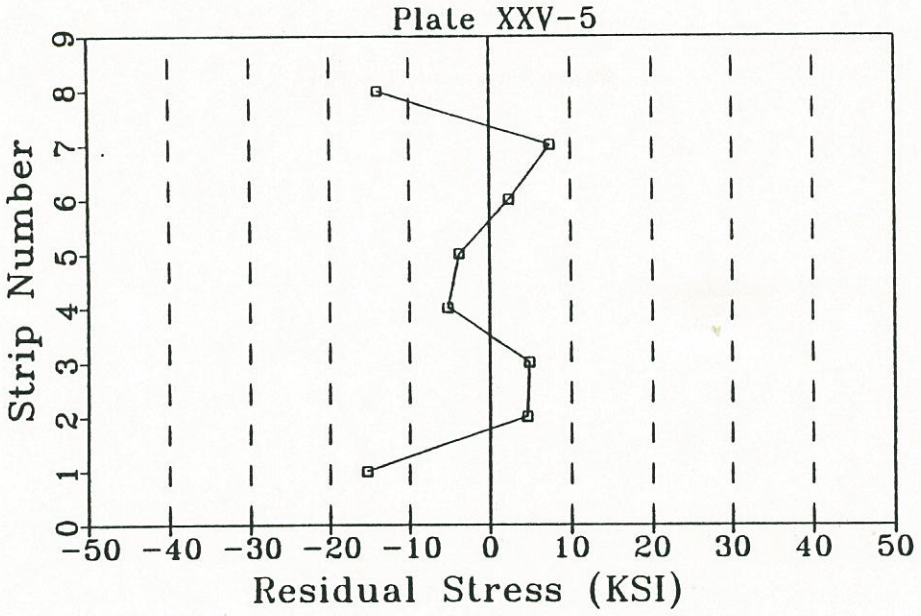

Figure C5. Stresses in plate XXV-5 (45° vee, M/M_p = 0.50, depth ratio = 1.00, angle of damage = 5.58°, assumed E = 29,000 ksi).

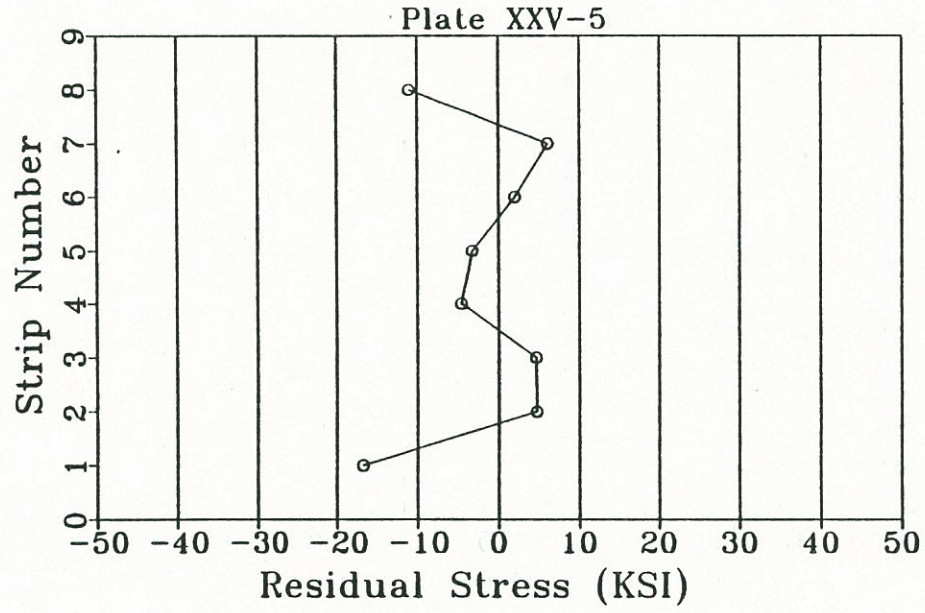

Figure C6. Stresses in plate XXV-5 (45° vee, M/M_p = 0.50, depth ratio = 1.00, angle of damage = 5.58°, using E from tensile test results).

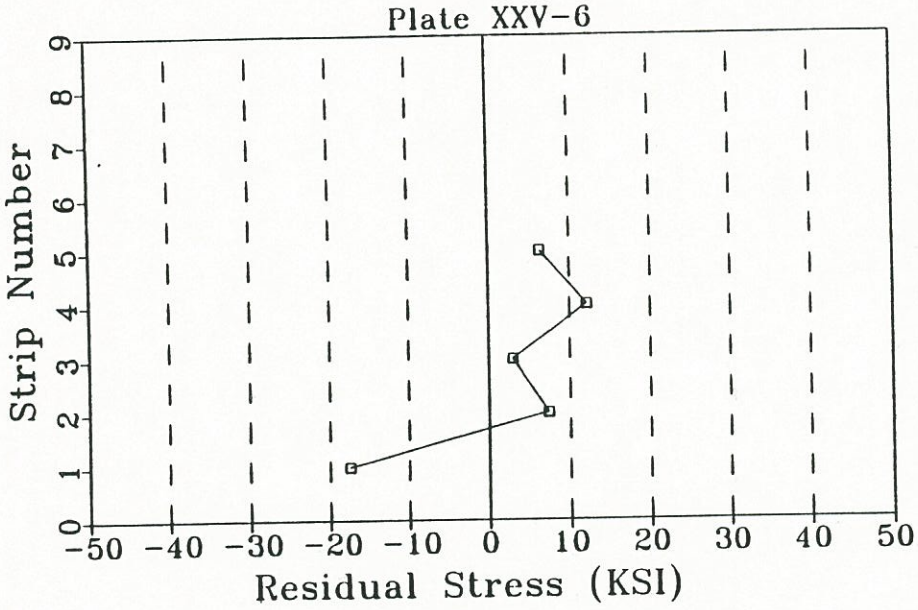

Figure C7. Stresses in plate XXV-6 (45° vee, M/M_p = 0.50, depth ratio = 1.00, angle of damage = 11.80°, assumed E = 29,000 ksi).

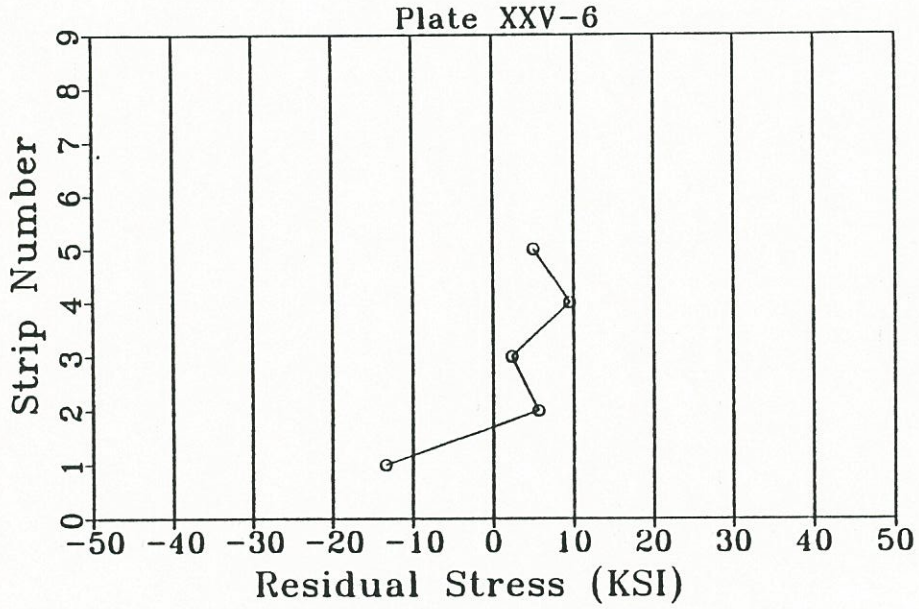

Figure C8. Stresses in plate XXV-6 (45° vee, M/M_p = 0.50, depth ratio = 1.00, angle of damage = 11.80°, using E from tensile test results).

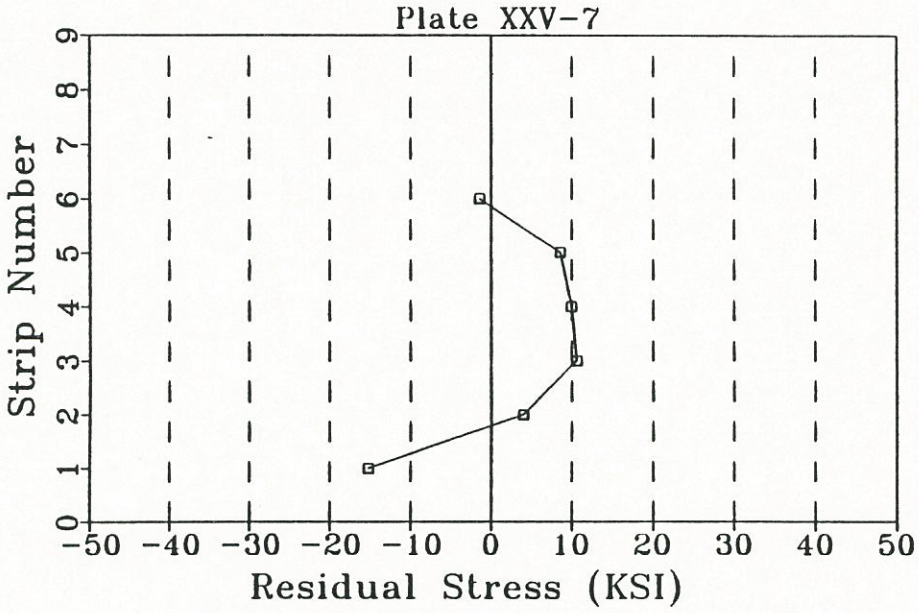

Figure C9. Stresses in plate XXV-7 (45° vee, M/M_p = 0.33, depth ratio = 1.00, angle of damage = 18.77°, assumed E = 29,000 ksi).

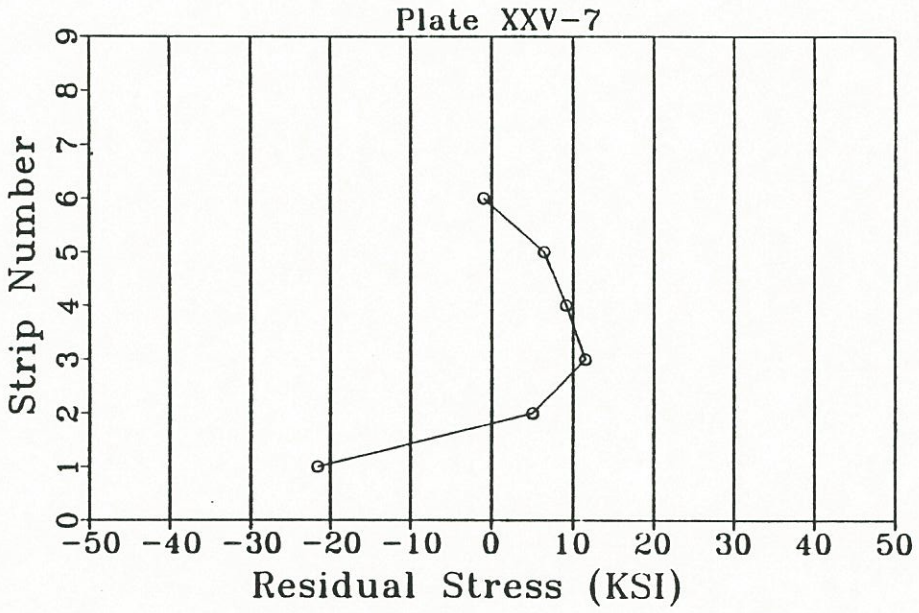

Figure C10. Stresses in plate XXV-67 (45° vee, M/M_p = 0.33, depth ratio = 1.00, angle of damage = 18.77°, using E from tensile test results).

APPENDIX D

PLATE THICKNESSES* (AFTER REPAIR)

*Refer to Figure 24 in text for points of measurement.

Plate XXV-3

Strip	Thickness (inches) at Location: aa	a	b	c	d	e	ee
1	0.495	0.504	0.513	0.520	0.513	0.506	0.495
2	0.495	0.502	0.505	0.523	0.503	0.500	0.495
3	0.495	0.501	0.506	0.532	0.503	0.505	0.495
4	0.495	0.507	0.518	0.543	0.507	0.502	0.495
5	0.495	0.507	0.524	0.538	0.512	0.500	0.495
6	0.495	0.503	0.523	0.532	0.516	0.498	0.495
7	0.495	0.503	0.519	0.535	0.510	0.498	0.495
8	0.495	0.503	0.517	0.538	0.510	0.500	0.495

Plate XXV-4

Strip	Thickness (inches) at Location: aa	a	b	c	d	e	ee
1	0.495	0.516	0.536	0.630	0.538	0.517	0.495
2	0.495	0.525	0.542	0.679	0.532	0.520	0.495
3	0.495	0.525	0.539	0.692	0.524	0.525	0.495
4	0.495	0.526	0.590	0.690	0.560	0.538	0.495
5	0.495	0.519	0.599	0.677	0.557	0.521	0.495
6	0.495	0.507	0.588	0.654	0.576	0.515	0.495
7	0.495	0.501	0.563	0.621	0.554	0.502	0.495
8	0.495	0.499	0.551	0.602	0.532	0.497	0.495

Plate XXV-5

Strip	Thickness (inches) at Location: aa	a	b	c	d	e	ee
1	0.495	0.510	0.514	0.490	0.512	0.505	0.495
2	0.495	0.504	0.510	0.498	0.509	0.503	0.495
3	0.495	0.502	0.505	0.513	0.504	0.500	0.495
4	0.495	0.500	0.506	0.517	0.503	0.499	0.495
5	0.495	0.499	0.514	0.514	0.505	0.495	0.495
6	0.495	0.496	0.511	0.516	0.505	0.495	0.495
7	0.495	0.494	0.508	0.522	0.504	0.501	0.495
8	0.495	0.500	0.509	0.522	0.509	0.499	0.495

Plate XXV-6

Strip	Thickness (inches) at Location: aa	a	b	c	d	e	ee
1	0.495	0.511	0.521	0.481	0.522	0.506	0.495
2	0.495	0.516	0.522	0.521	0.523	0.515	0.495
3	0.495	0.518	0.520	0.545	0.521	0.517	0.495
4	0.495	0.522	0.530	0.561	0.533	0.522	0.495
5	0.495	0.516	0.534	0.556	0.527	0.520	0.495
6	0.495	0.510	0.545	0.530	0.528	0.511	0.495
7	0.495	0.506	0.549	0.556	0.534	0.510	0.495
8	0.495	0.497	0.537	0.533	0.535	0.498	0.495

Plate XXV-7

Strip	Thickness (inches) at Location: aa	a	b	c	d	e	ee
1	0.495	0.513	0.528	0.515	0.534	0.492	0.495
2	0.495	0.513	0.519	0.573	0.519	0.505	0.495
3	0.495	0.512	0.524	0.599	0.515	0.511	0.495
4	0.495	0.518	0.557	0.603	0.521	0.520	0.495
5	0.495	0.512	0.568	0.588	0.517	0.516	0.495
6	0.495	0.503	0.563	0.582	0.521	0.512	0.495
7	0.495	0.499	0.542	0.581	0.519	0.509	0.495
8	0.495	0.487	0.523	0.548	0.505	0.496	0.495

Plate XXV-8

Strip	Thickness (inches) at Location: aa	a	b	c	d	e	ee
1	0.495	0.501	0.506	0.507	0.505	0.500	0.495
2	0.495	0.499	0.502	0.502	0.497	0.495	0.495
3	0.495	0.495	0.493	0.521	0.491	0.502	0.495
4	0.495	0.496	0.491	0.524	0.488	0.496	0.495
5	0.495	0.490	0.489	0.521	0.485	0.492	0.495
6	0.495	0.489	0.488	0.518	0.484	0.492	0.495
7	0.495	0.495	0.503	0.524	0.502	0.497	0.495
8	0.495	0.499	0.501	0.522	0.502	0.498	0.495

APPENDIX E

RESIDUAL STRESSES (UNDAMAGED WIDE FLANGES)

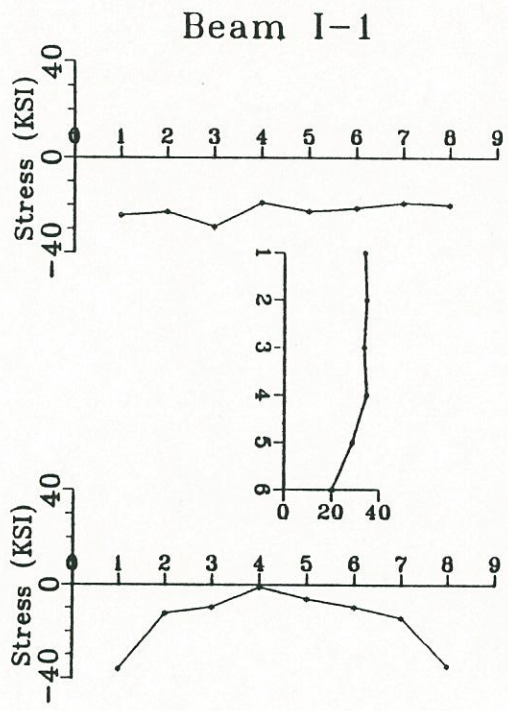

Figure E1. Stresses in Beam I-1 (20° vee, M/M_p = 0.00, depth ratio = 1.00).

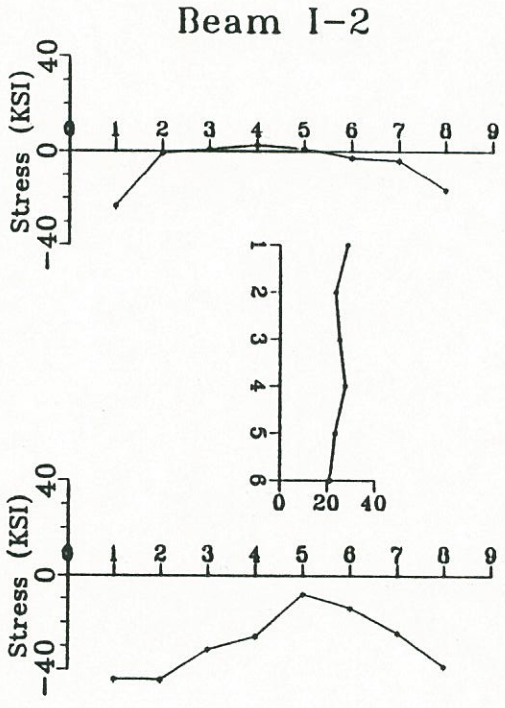

Figure E2. Stresses in Beam I-2 (45° vee, M/M_p = 0.00, depth ratio = 1.00).

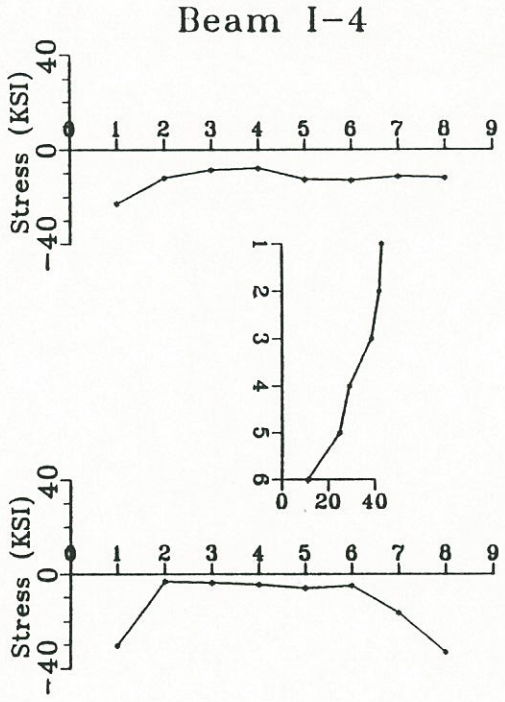

Figure E3. Stresses in Beam I-4 (30° vee, M/M_p = 0.00, depth ratio = 1.00).

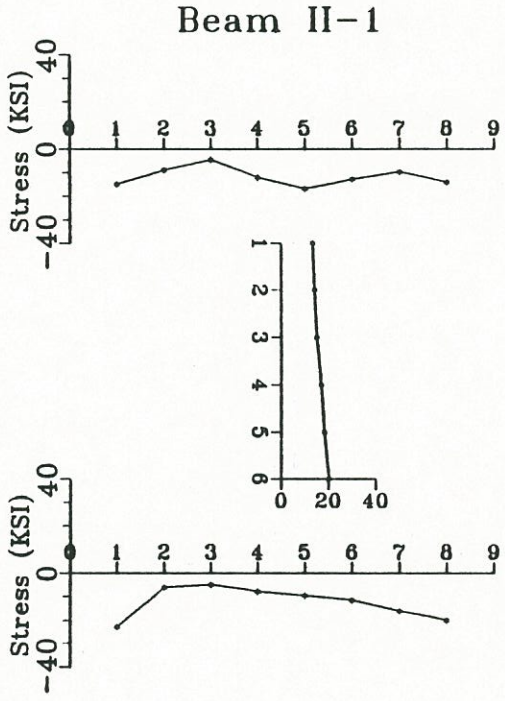

Figure E4. Stresses in Beam II-1 (20° vee, M/M_p = 0.00, depth ratio = 1.00).

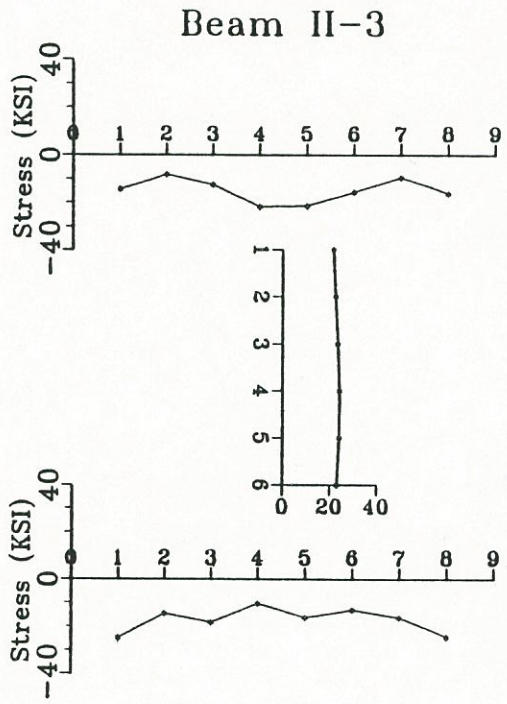

Figure E5. Stresses in Beam II-3 (45° vee, M/M_p = 0.00, depth ratio = 1.00).

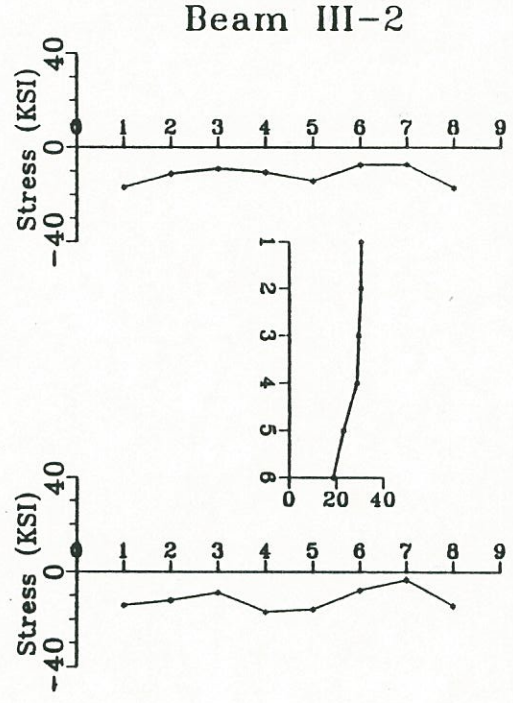

Figure E6. Stresses in Beam III-2 (20° vee, M/M_p = 0.50, depth ratio = 1.00).

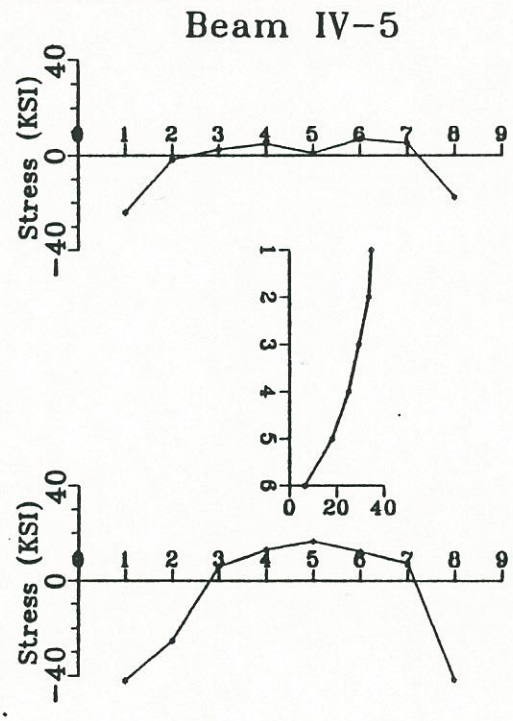

Figure E7. Stresses in Beam IV-5 (45° vee, M/M_p = 0.25, depth ratio = 1.00).

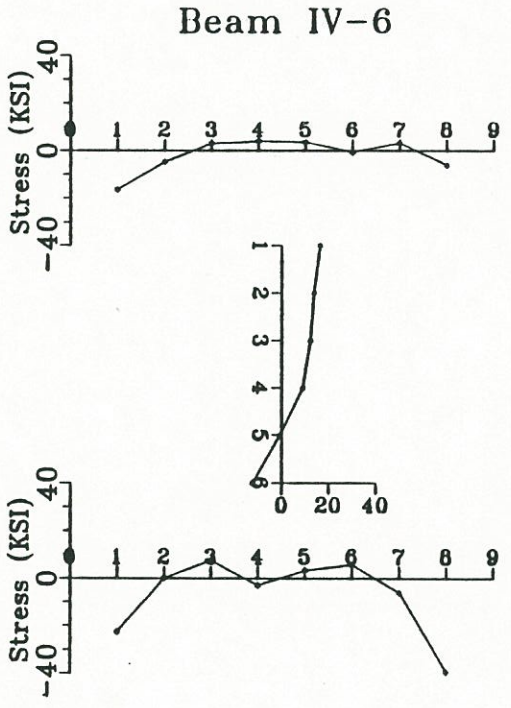

Figure E8. Stresses in Beam IV-6 (45° vee, M/M_p = 0.50, depth ratio = 1.00).

APPENDIX F

PLASTIC ROTATIONS (DAMAGED WIDE FLANGES)

Plastic Rotations in Milliradians

	First Repair Cycle				Second Repair Cycle		
Beam:	XXI-1	XXI-2	XXI-3	XXI-4	XXI-2	XXI-3	XXI-4
Ht 1	10.97	12.16	6.15	10.39	11.93	10.23	9.84
2	4.93	5.52	7.61	10.06	6.12	5.30	5.68
3	5.27	5.88	5.70	8.00	5.16	4.92	6.43
4	5.18	5.70	6.85	6.38	6.64	5.98	7.80
5	7.54	4.16	6.85	7.15	8.69	8.29	6.18
6	7.53	6.45	7.64	6.45	4.94	5.4	1.21*
7	8.36	8.54	5.01	4.77	0.74	4.72	6.39
8	8.12	5.82	7.40	6.84	6.52	5.76	7.60
9	10.66	8.01	8.77	6.89	4.77	2.88	7.00
10	7.04	7.85	7.34	6.41	5.73	5.92	5.65
11	5.52	6.35	7.00	7.18	7.76	7.16	6.64
12	7.05	7.59	7.83	5.90	7.11	5.76	5.47
13	6.35	7.97	6.35	4.46	7.09	6.15	6.94
14	5.22	7.16	6.46	4.98	7.34	5.47	5.72
15	3.38	6.17	5.00	5.00	6.35	5.20	5.18
16	6.15	4.03	5.50	4.82	6.44	5.70	6.01
17	7.12	3.74	5.45	3.49	4.64	4.28	5.70
18	2.75	4.19	5.52	5.25	4.82	4.30	----
19	0.43	4.53	----	----	5.90	2.41	----
20	6.67	3.81	----	----	6.37	6.69	----
21	----	----	----	----	7.39	4.30	----
22	----	----	----	----	5.20	4.75	----
23	----	----	----	----	8.34	----	----

*Load applied after heat.

Plastic Rotations in Milliradians

	3rd Repair Cycle		4th Repair Cycle		5th R.C.
Beam:	XXI-3	XXI-4	XXI-3	XXI-4	XXI-4
Ht 1	11.199	11.598	7.158	9.941	10.214
2	4.693	6.420	9.744	7.611	4.986
3	7.794	7.343	7.120	10.086	7.121
4	7.348	2.898	2.292	6.022	5.056
5	8.654	5.729	8.652	9.082	9.217
6	7.847	7.618	8.812	8.298	6.948
7	4.948	4.473	5.420	2.609	3.126
8	5.691	6.386	6.928	8.054	8.301
9	5.580	6.252	7.357	8.078	5.895
10	4.478	4.949	4.703	5.176	2.408
11	6.437	7.380	4.321	3.872	5.199
12	5.875	5.468	4.276	4.772	8.351
13	3.602	3.083	4.750	3.174	6.416
14	5.966	6.910	5.471	4.480	6.485
15	4.773	6.934	7.475	4.729	5.697
16	5.449	3.783	7.769	3.310	3.761
17	5.270	4.503	1.013*	2.162	5.743
18	6.621	5.990	7.342	7.634	4.775
19	5.450	4.481	5.000	6.374	1.194
20	-----	2.973	5.248	6.914	3.311
21	-----	7.725	6.071	-----	5.000

*Load applied after heat.

Plastic Rotations in Milliradians

		Beam XXI-4		
		6th Repair	7th Repair	8th Repair
Ht #	1	14.892	11.378	14.183
	2	11.687	8.488	11.970
	3	10.209	6.986	11.393
	4	8.863	8.000	10.679
	5	8.753	9.757	9.019
	6	8.372	6.432	7.604
	7	9.545	10.911	8.349
	8	8.533	4.050	11.435
	9	4.729*	5.761	8.285
	10	6.013	6.865	9.300
	11	5.382*	7.429*	7.409
	12	7.905	8.533	4.054*
	13	4.527*	6.440*	19.457
	14	-----	6.193	-----
	15	-----	8.085	-----
	16	-----	14.975	-----

* These heats consisted of 1 vee only (All other heats on this page consisted of two vees). Two vees were used during the final three repairs of beam XXI-4 due to time constraints.

APPENDIX G

RESIDUAL STRESSES (DAMAGED WIDE FLANGES)

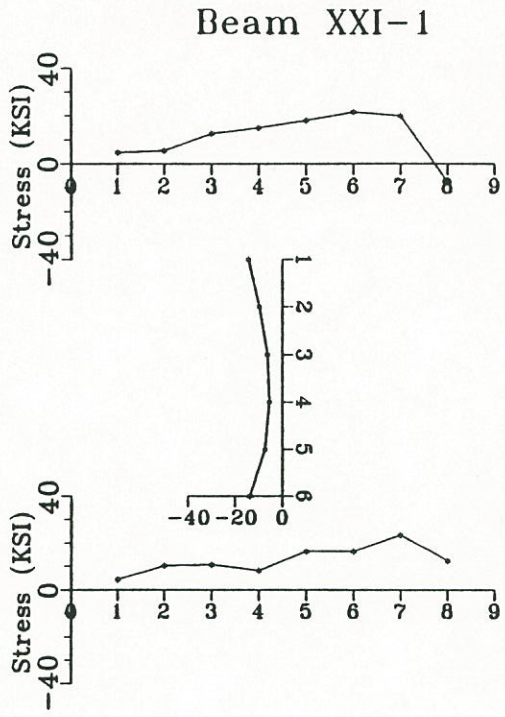

Figure G1. Stresses in beam XXI-1, region B (1 damage/repair cycle, assumed value of E = 29,000 ksi).

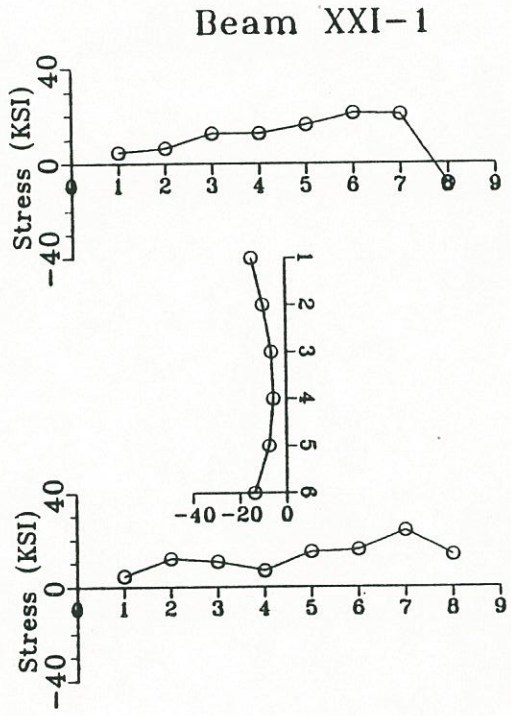

Figure G2. Stresses in beam XXI-1, region B (1 damage/repair cycle, using E from tensile test results).

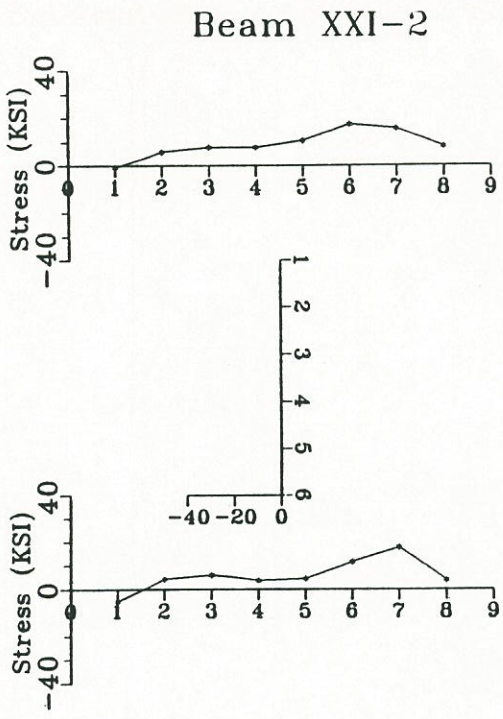

Figure G3. Stresses in beam XXI-2, region B (2 damage/repair cycle, assumed value of E = 29,000 ksi).

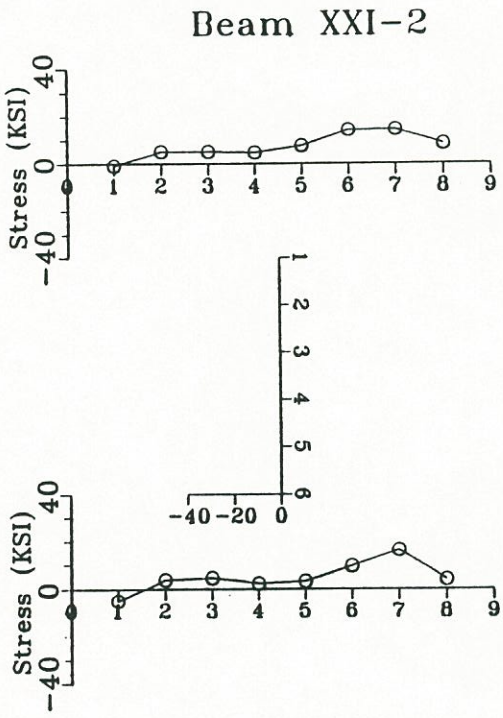

Figure G4. Stresses in beam XXI-2, region B (2 damage/repair cycle, using E from tensile test results).

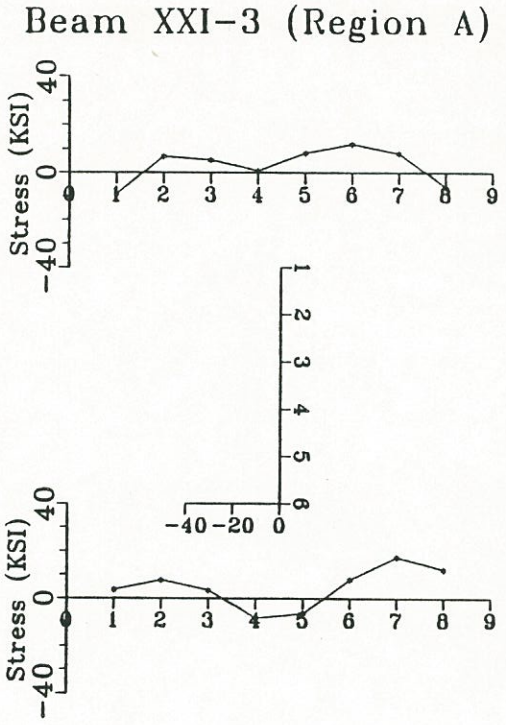

Figure G5. Stresses in beam XXI-3, region A (4 damage/repair cycle, assumed value of E = 29,000 ksi).

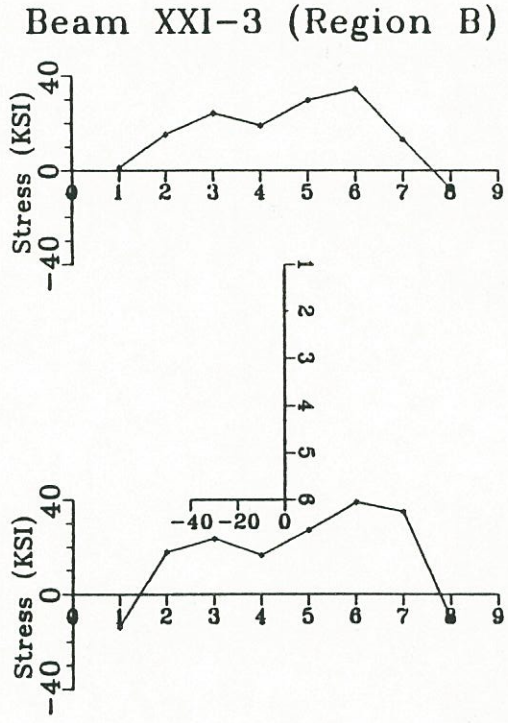

Figure G6. Stresses in beam XXI-3, region B (4 damage/repair cycle, assumed value of E = 29,000 ksi).

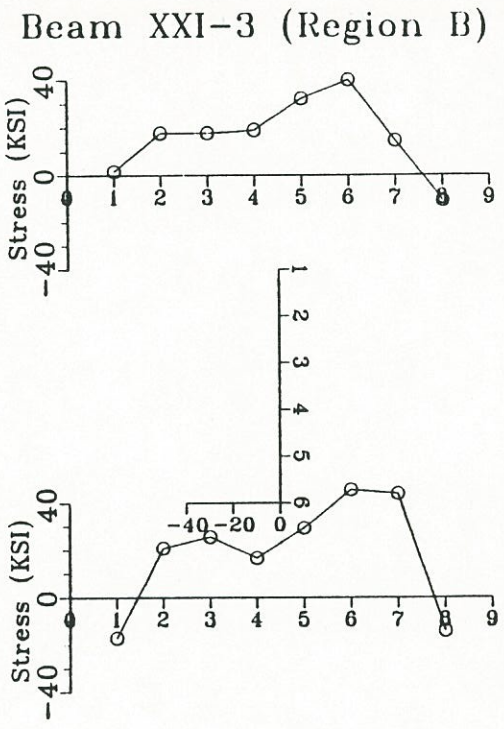

Figure G7. Stresses in beam XXI-3, region B (4 damage/repair cycle, using E from tensile test results).

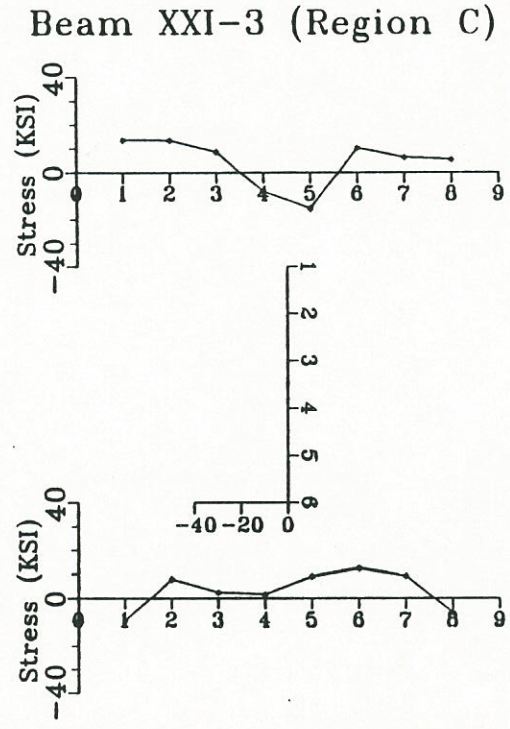

Figure G8. Stresses in beam XXI-3, region C (4 damage/repair cycle, assumed value of E = 29,000 ksi).

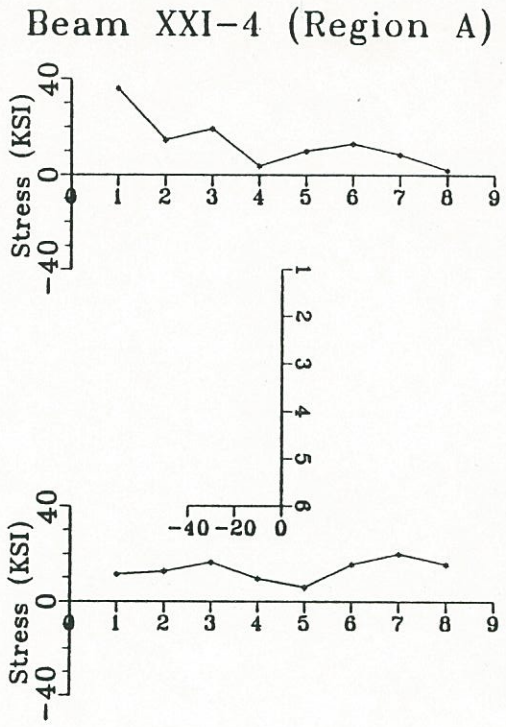

Figure G9. Stresses in beam XXI-4, region A (8 damage/repair cycle, assumed value of E = 29,000 ksi).

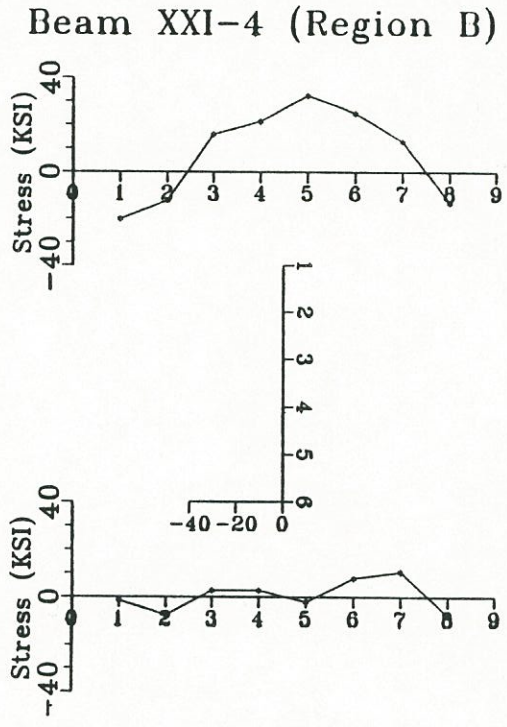

Figure G10. Stresses in beam XXI-4, region B (8 damage/repair cycle, assumed value of E = 29,000 ksi).

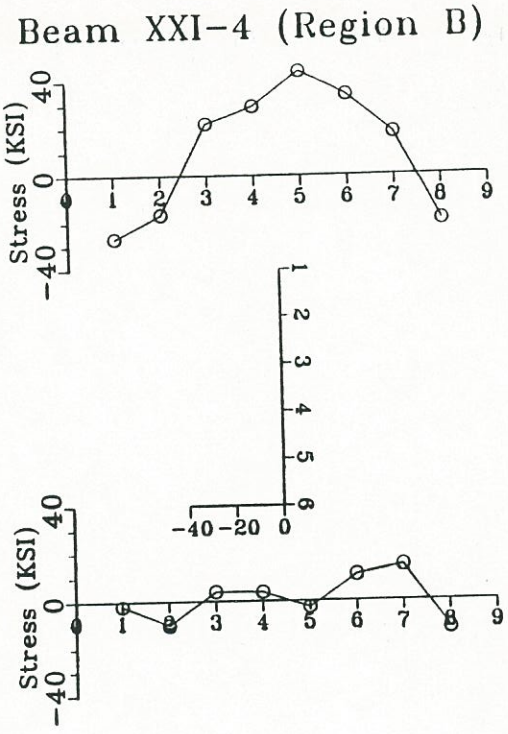

Figure G11. Stresses in beam XXI-4, region B (8 damage/repair cycle, using E from tensile test results).

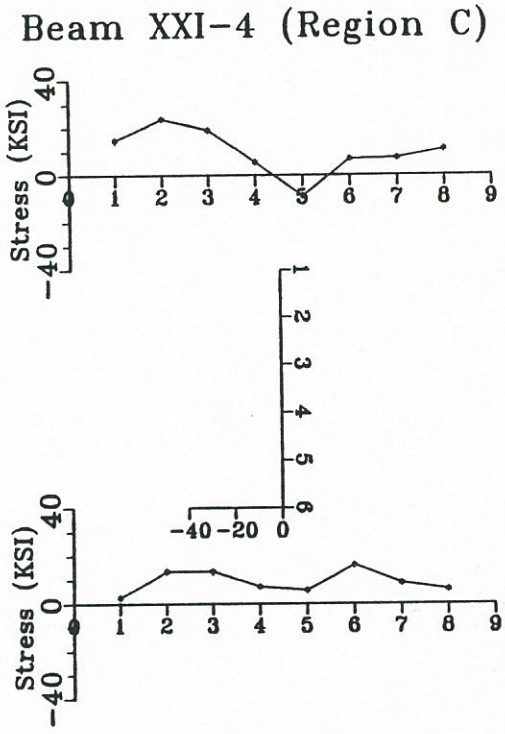

Figure G12. Stresses in beam XXI-4, region C (8 damage/repair cycle, assumed value of E = 29,000 ksi).

APPENDIX H

FLOWCHART OF COMPUTER PROGRAM FOR FOLDED PLATE ANALYSIS

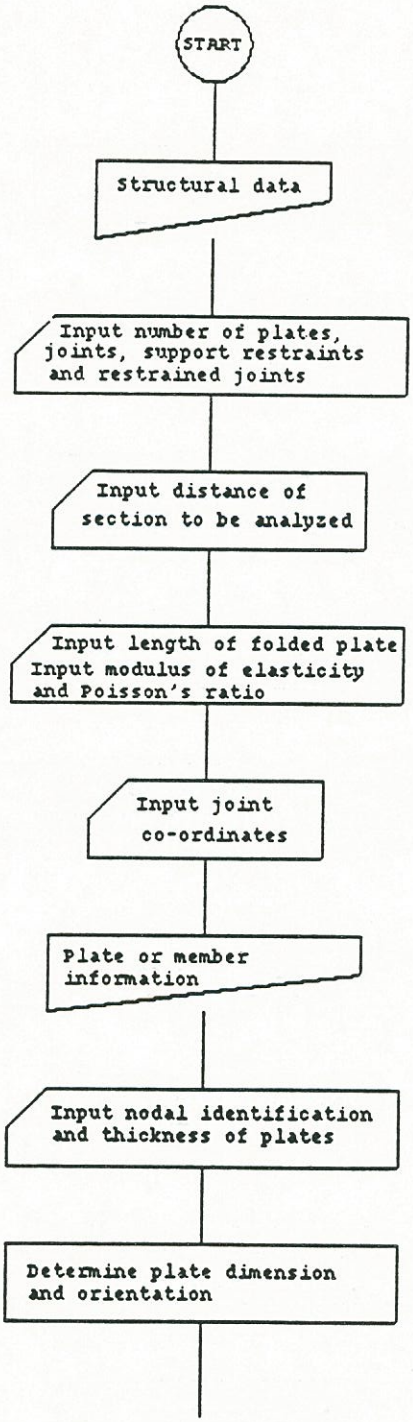
START
Structural data
Input number of plates, joints, support restraints and restrained joints
Input distance of section to be analyzed
Input length of folded plate
Input modulus of elasticity and Poisson's ratio
Input joint co-ordinates
Plate or member information
Input nodal identification and thickness of plates
Determine plate dimension and orientation

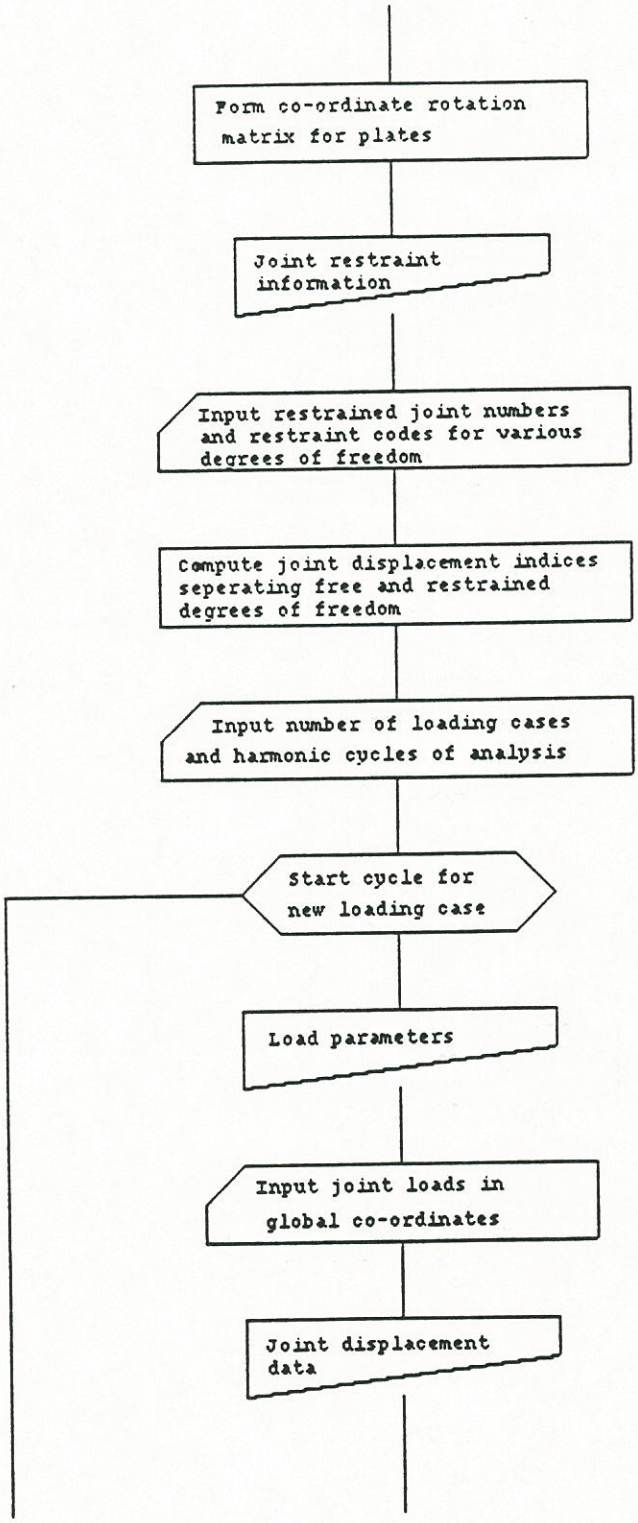
Form co-ordinate rotation matrix for plates
Joint restraint information
Input restrained joint numbers and restraint codes for various degrees of freedom
Compute joint displacement indices seperating free and restrained degrees of freedom
Input number of loading cases and harmonic cycles of analysis
Start cycle for new loading case
Load parameters
Input joint loads in global co-ordinates
Joint displacement data

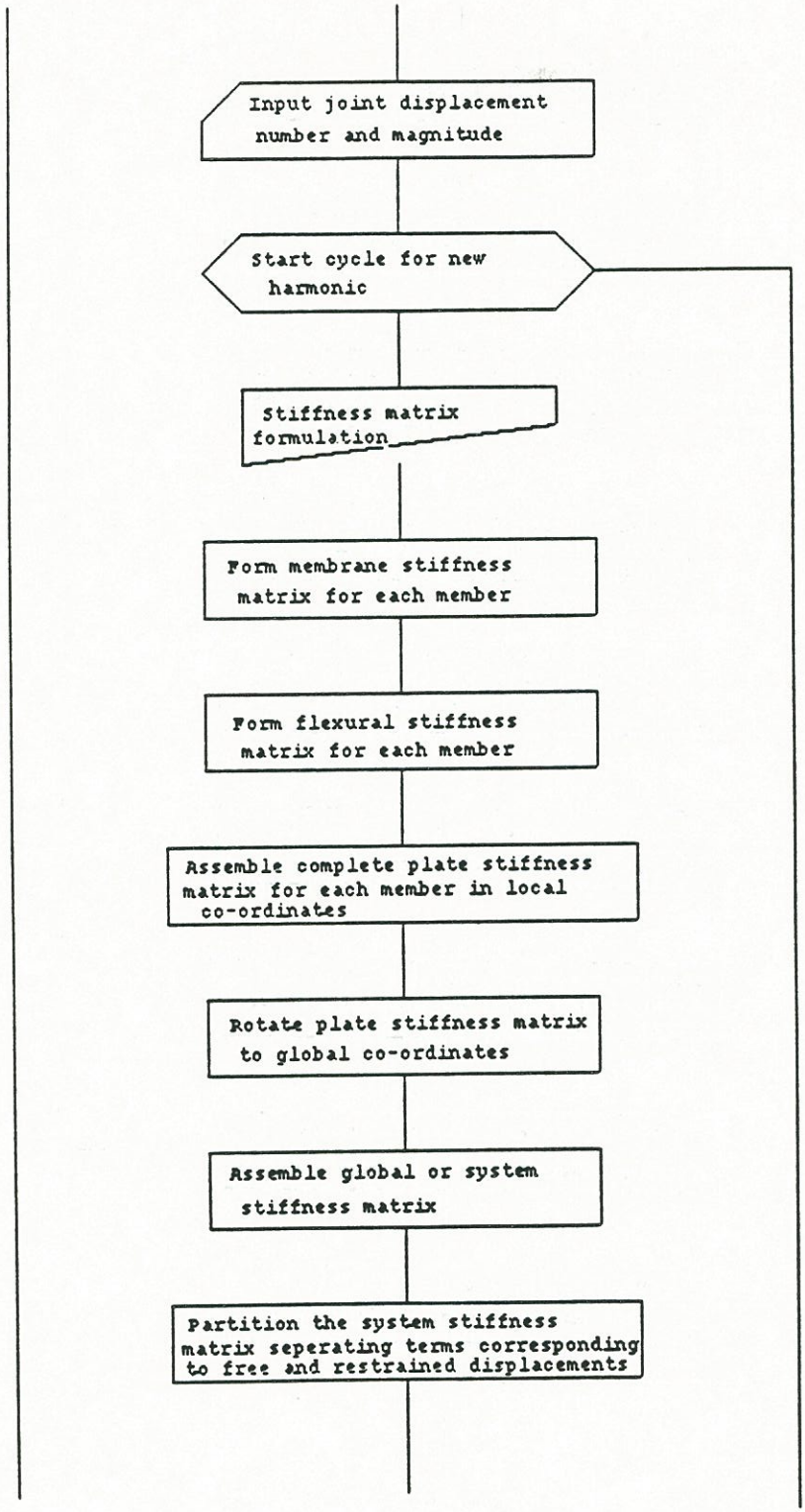
Input joint displacement number and magnitude
Start cycle for new harmonic
Stiffness matrix formulation
Form membrane stiffness matrix for each member
Form flexural stiffness matrix for each member
Assemble complete plate stiffness matrix for each member in local co-ordinates
Rotate plate stiffness matrix to global co-ordinates
Assemble global or system stiffness matrix
Partition the system stiffness matrix seperating terms corresponding to free and restrained displacements

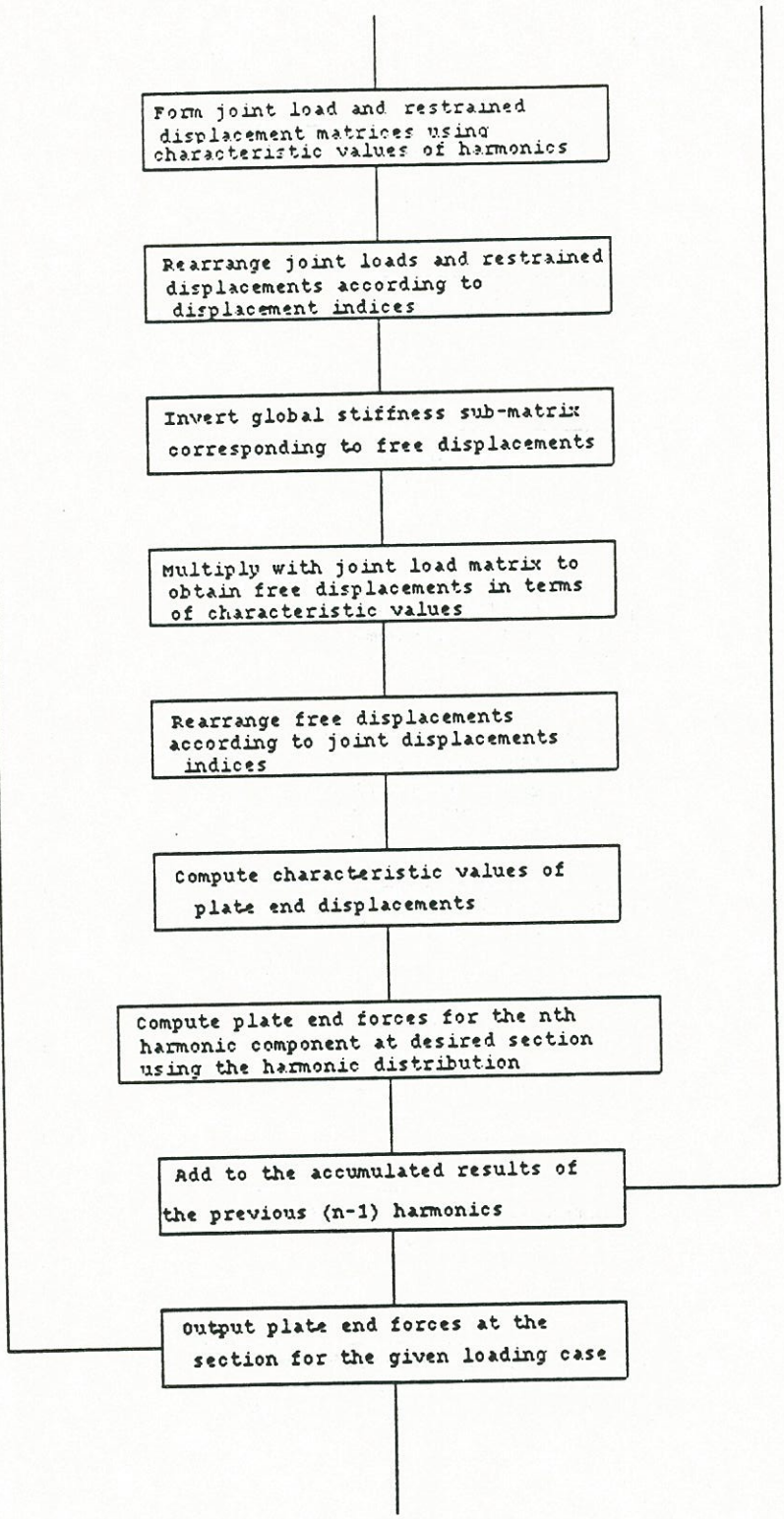
Form joint load and restrained displacement matrices using characteristic values of harmonics
Rearrange joint loads and restrained displacements according to displacement indices
Invert global stiffness sub-matrix corresponding to free displacements
Multiply with joint load matrix to obtain free displacements in terms of characteristic values
Rearrange free displacements according to joint displacements indices
Compute characteristic values of plate end displacements
Compute plate end forces for the nth harmonic component at desired section using the harmonic distribution
Add to the accumulated results of the previous (n-1) harmonics
Output plate end forces at the section for the given loading case

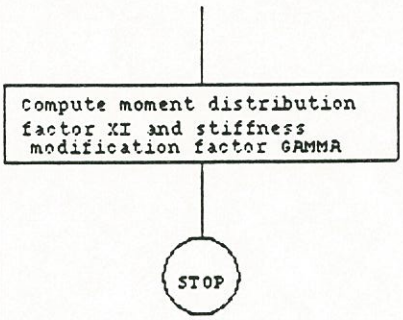
Compute moment distribution factor XI and stiffness modification factor GAMMA
STOP

APPENDIX I

SAMPLE INPUT DATA FOR THE COMPUTER SOFTWARE DEVELOPED FOR EXACT ANALYSIS OF FOLDED PLATE STRUCTURE

STRUCTURAL DATA

NP	NJ	NR	NRJ
3	4	4	1

STRUCTURAL PARAMETERS

LEN	E	U
240	29000	0.3

JOINT COORDINATES

JOINT #	Y	Z
1	0	0
2	0	24
3	-4.5	24
4	4.5	24

PLATE IDENTIFICATION

PLATE #	JTH NODE	KTH NODE	THICKNESS
1	1	2	0.44
2	3	2	0.687
3	2	4	0.687

JOINT RESTRAINT CODES

JOINT #	JR1	JR2	JR3	JR4
1	1	1	1	1

LOAD PARAMETERS

NLC	NHC	NLJ
1	9	1

ACTIONS AT JOINTS

JOINT #	AJ1	AJ2	AJ3	AJ4
3	10.000	0	0	0

XJ1	XJ2	XJ3	XJ4
120.00	0	0	0

QJ1	QJ2	QJ3	QJ4
0	0	0	0

X11	X12	X13	X14
0	0	0	0

X21	X22	X23	X24
0	0	0	0

SUPPORT DISPLACEMENTS

NSD	DSJ
0	0

APPENDIX J

SUMMARY OF RESULTS FROM THE COMPUTER AIDED FOLDED PLATE ANALYSIS OF THE TESTED GIRDERS FOR A JACKING LOAD OF 10 KIPS ON THE BOTTOM FLANGE AT MIDSPAN

RESULTS FOR W 10 X 39 GIRDER

SECTION AT 0.5 SPAN

PLATE END ACTIONS

PLATE#	EDGE#	N	T	M	S	SIGMA
1	1	-0.01	0.0	1.02	0.12	0.0
	2	0.0	0.0	0.13	-0.12	0.05
2	1	0.42	0.0	0.0	0.0	-
14.91						
	2	-0.26	0.0	-0.06	0.0	0.05
3	1	0.15	0.0	-0.06	0.0	0.05
	2	0.0	0.0	0.0	0.0	14.99

XI = 0.14
GAMMA = 31.20

RESULTS FOR W 24 X 76 GIRDER

SECTION AT 0.5 SPAN

PLATE END ACTIONS

PLATE#	EDGE#	N	T	M	S	SIGMA
1	1	-0.01	0.0	1.44	0.07	0.0
	2	0.0	0.0	0.17	-0.07	0.05
2	1	0.43	0.0	0.0	0.0	-
21.77						
	2	-0.25	0.0	-0.08	0.0	0.05
3	1	0.17	0.0	-0.08	0.0	0.05
	2	0.0	0.0	0.0	0.0	21.84

XI = 0.33
GAMMA = 4.31

APPENDIX K

COMPUTER PROGRAM LISTINGS AND SAMPLE INPUTS/OUTPUTS

```
C     PROGRAM FOR DETERMINING NUMBER OF HEATS REQUIRED TO C
HEAT-STRAIGHTEN A DAMAGED BRIDGE GIRDER
C                          .... lOUISIANA ST. U., 1992

      INTEGER BC,HT,VAD
      REAL LR,LU,LLV,LJ,NHR,MP,MF,MA,MR
      CHARACTER ANS,ANS1,ANS2,ANS3,ANS4,ANS5
C     OPEN (5,FILE='HEAT.D')
      OPEN(8,FILE='HEAT.R')
      OPEN(7,FILE='HEAT.S')
      WRITE (8,*)
      WRITE (*,*)
      WRITE (7,*)
      WRITE (7,*)
      WRITE (8,*)
      WRITE (*,*)
      WRITE (8,*) '           #####  H. E. A. T.  #####'
      WRITE (8,*) '         ==============================='
      WRITE (8,*)
      WRITE (8,*)'A State-of-Art Software for Heat Straightening Repair'
      WRITE (8,*)
      WRITE (8,*)'Dept. of Civil Engineering, Louisiana St. Univ., 1992'
      WRITE (8,*)
      WRITE (8,*)
      WRITE (8,*) 'This program generates:'
      WRITE (8,*) '1. The degree of damage of the damaged girder.'
      WRITE (8,*) '2. The number of heating cycles required for repair.'
      WRITE (8,*) '3. The repair methodology and heat pattern details.'
      WRITE (8,*) '4. The magnitude of the external jacking forces.'
      WRITE (8,*)
      WRITE (8,*)
      WRITE (7,*) '           #####  H. E. A. T.  #####'
      WRITE (7,*) '         ==============================='
      WRITE (7,*)
      WRITE (7,*)'A State-of-Art Software for Heat Straightening Repair'
      WRITE (7,*)'Dept. of Civil Engineering, Louisiana St. Univ., 1992'
      WRITE (7,*)
      WRITE (7,*) 'This file contains the summary of the results for'
      WRITE (7,*) 'the HEAT program : '
      WRITE (*,*)
      WRITE (*,*)'           #####  H. E. A. T.   #####  '
      WRITE (*,*)'         ==============================='
      WRITE (*,*)
      WRITE (*,*)'A State-of-Art Software for Heat Straightening Repair'
      WRITE (*,*)
      WRITE (*,*)'Dept. of Civil Engineering, Louisiana St. Univ., 1992'
      WRITE (*,*)
      WRITE (*,*)
      WRITE (*,*)'This program generates:'
      WRITE (*,*)'1. The degree of damage of the damaged girder.'
      WRITE (*,*)'2. The number of heating cycles required for repair.'
      WRITE (*,*)'3. The repair methodology and heat pattern details.'
      WRITE (*,*)'4. The magnitude of the external jacking forces.'
      WRITE (*,*)
      WRITE (*,*)
      WRITE (*,*)'Would you like to continue? (Y/N)'
      READ (*,*) ANS
      IF(ANS.NE.'Y') GOTO 9999
      WRITE (8,*)
      WRITE (*,*)
```

```
      WRITE (8,*)
      WRITE (*,*)
      WRITE (7,*)
      WRITE (7,*)
C     BOUNDARY CONDITIONS OF MEMBER
C     Input the number code for Damage type. The codes are
C     Indeterminate Composite W-shape                    .. 1
C     Determinate Composite W-shape                      .. 2
C     Determinate Category 'S' W-shape                   .. 3
C     Determinate Category 'W' W-shape                   .. 4
C     Axially-loaded Determinate Category 'S' W-shape    .. 5
C     Axially-loaded Determinate Category 'W' W-shape    .. 6
C     Determinate Category 'S' Channel                   .. 7
C     Determinate Category 'W' Channel                   .. 8
C     Determinate Category 'S' Angle                     .. 10
C     Determinate Category 'W' Angle                     .. 11
C     Determinate Category 'S' Plate                     .. 12
C     Determinate Non-composite W-shape                  .. 12
      WRITE(*,*)'I.]  DAMAGE TYPE FOR THE DAMAGED MEMBER'
      WRITE(8,*)'I.]  DAMAGE TYPE FOR THE DAMAGED MEMBER'
      WRITE(*,*)'Available number codes for damage type are:'
      WRITE(*,*)'Indeterminate Composite W-shape                    .. 1'
      WRITE(*,*)'Determinate Composite W-shape                      .. 2'
      WRITE(*,*)'Determinate Category S W-shape                     .. 3'
      WRITE(*,*)'Determinate Category W W-shape                     .. 4'
      WRITE(*,*)'Axially-loaded Determinate Category S W-shape      .. 5'
      WRITE(*,*)'Axially-loaded Determinate Category W W-shape      .. 6'
      WRITE(*,*)'Determinate Category S Channel                     .. 7'
      WRITE(*,*)'Determinate Category W Channel                     .. 8'
      WRITE(*,*)'Determinate Category S Angle                       .. 9'
      WRITE(*,*)'Determinate Category W Angle                       .. 10'
      WRITE(*,*)'Determinate Category S Plate                       .. 11'
      WRITE(*,*)'Determinate Non-composite W-shape                   .. 12'

      WRITE(*,*)
      WRITE(8,*)'Available number codes for damage type are:'
      WRITE(8,*)'Indeterminate Composite W-shape                    .. 1'
      WRITE(8,*)'Determinate Composite W-shape                      .. 2'
      WRITE(8,*)'Determinate Category S W-shape                     .. 3'
      WRITE(8,*)'Determinate Category W W-shape                     .. 4'
      WRITE(8,*)'Axially-loaded Determinate Category S W-shape      .. 5'
      WRITE(8,*)'Axially-loaded Determinate Category W W-shape      .. 6'
      WRITE(8,*)'Determinate Category S Channel                     .. 7'
      WRITE(8,*)'Determinate Category W Channel                     .. 8'
      WRITE(8,*)'Determinate Category S Angle                       .. 9'
      WRITE(8,*)'Determinate Category W Angle                       .. 10'
      WRITE(8,*)'Determinate Category S Plate                       .. 11'
      WRITE(8,*)'Determinate Non-composite W-shape                   .. 12'

      WRITE(8,*)
      WRITE(*,*)'Enter number code for damaged member type:'
      READ(*,*) BC
      WRITE(8,*)'The number code entered for member type is :',BC
      WRITE(8,*)
      WRITE(*,*)
      WRITE(8,*)
      WRITE(*,*)
C     MEMBER DATA
C     Input the Geometry and yield stress of the heated section:
C     Enter the flange width, flange thickness, web depth, web thickness
```

```
C     for W-shapes, channels and angles and value of yield stress
C     Enter plate width & thickness for plates and value of yield stress

      WRITE(*,*)'II.]  MEMBER GEOMETRY AND PROPERTIES:'
      WRITE(8,*)'II.]  MEMBER GEOMETRY AND PROPERTIES:'
      IF(BC.EQ.11) GOTO 91
      WRITE(*,*)'Enter values for Flange width, Flange thickness, Web'
      WRITE(*,*)'depth, Web thickness (in) and Yield Stress (ksi)'
      WRITE(8,*)'Values entered for Flange width, Flange thickness, Web'
      WRITE(8,*)'depth, Web thickness (in) and Yield Stress (ksi) are'
      READ(*,*) BF,TF,DW,TW,FY
      WRITE(8,12) BF,TF,DW,TW,FY
12    FORMAT (F7.3,5X,F7.3,5X,F6.3,5X,F6.3)
      GOTO 92
91    WRITE(*,*)'Enter Plate width, thickness(in) & Yield Stress(ksi):,'
      WRITE(8,*)'Plate width, thickness(in) and Yield Stress(ksi) are:'
      READ(*,*) BF,TF,FY
      WRITE(8,13) BF,TF,FY
13    FORMAT (F7.3,5X,F7.3,5X,F6.2)
92    WRITE(*,*)
      WRITE(8,*)
      WRITE(*,*)
      WRITE(8,*)
C     LOAD RATIO
      WRITE(*,*)'III.]  EXTERNAL LOAD RATIO'
      WRITE(8,*)'III.]  EXTERNAL LOAD RATIO'
      IF(BC.NE.1) GOTO 121
      WRITE(*,*)'The maximum allowable Load Ratio for repair is 0.125'

      WRITE(*,*)'Enter value of the desired Load Ratio for repair:'
      GOTO 93
121   WRITE(*,*)'The maximum allowable Load Ratio for repair is 0.33'
      WRITE(*,*)'Enter value of the desired Load Ratio for repair:'
93    READ(*,*) LR
      WRITE(8,*)'The Load Ratio selected for repair is :'
      WRITE (8,803) LR
803   FORMAT (2X,F5.3)
      WRITE(8,*)
      WRITE(*,*)
      WRITE(8,*)
      WRITE(*,*)
C     MODULE FOR CALCULATING METHODOLOGY
      WRITE(*,*)'Do you wish to calculate the number of heats required'
      WRITE(*,*)'to heat-straighten the damaged girder? (Y/N):'
      READ (*,*) ANS1
      IF(ANS1.NE.'Y') GOTO 240
      WRITE(8,*)'Do you wish to calculate the Number of Heats required'
      WRITE(8,*)'to heat-straighten the damaged girder? (Y/N):   ',ANS1
      WRITE(*,*)
      WRITE(8,*)
      WRITE(*,*)'IV.]  METHODOLOGY OF REPAIR'
      WRITE(8,*)'IV.]  METHODOLOGY OF REPAIR'
C     MODULE FOR DEGREE OF DAMAGE
      WRITE(*,*)'i] Degree of damage of member:'
      WRITE(8,*)'i) Degree of Damage of member:'
      WRITE(7,*)'I] DEGREE OF DAMAGE OF MEMBER'
C     Input values of locations of four reference stations from left end
C      of the unsupported damaged span (ft), unsupported span (ft)
      WRITE (*,*)'Enter the distance of four Reference Stations from'
      WRITE (*,*)'left end of unsupported span:'
```

```
      READ(*,*) RS1,RS2,RS3,RS4
      WRITE (8,*)'The distance of four Reference Stations from the'
      WRITE (8,*)'left end of unsupported span:'
      WRITE (8,10) RS1,RS2,RS3,RS4
10    FORMAT (F6.2,5X,F6.2,5X,F6.2,5X,F6.2)
      WRITE (*,*)
      WRITE (8,*)
C     Input values of ordinates of damaged beam at the four reference
C      stations
      S1=RS1*12.
      S2=RS2*12.
      S3=RS3*12.
      S4=RS4*12.
      WRITE (*,*) 'Enter values for the Damage Measurements of the'
      WRITE (*,*) 'bottom flange at the four reference stations (in):'
      READ(*,*) O1,O2,O3,O4
      WRITE (8,*) 'Values input for the Damage Measurements along the'
      WRITE (8,*) 'bottom flange at the four reference stations (in):'
      WRITE (8,11) O1,O2,O3,O4
11    FORMAT (F8.3,5X,F8.3,5X,F8.3,5X,F8.3)
      WRITE (8,*)
      WRITE (*,*)
C     Degree of damage calculations
      TH1=ABS(ATAN((O2-O1)/(S2-S1)))
      TH2=ABS(ATAN((O3-O4)/(S4-S3)))
      PHID=TH1+TH2
      DEGD= PHID*180./3.142
      WRITE(8,*) '## OUTPUT:  Degree of damage (rad) is :'
      WRITE(8,804) PHID
      WRITE(8,*) '## OUPUT:   Degree of damage (deg) is : '
      WRITE (8,805) DEGD
      WRITE(7,*) 'degree of damage (rad) is :'
      WRITE(7,804) PHID
      WRITE(7,*) 'degree of damage (deg) is : '
      WRITE (7,805) DEGD
      WRITE(*,*) 'OUTPUT:  Degree of damage (rad) is :'
      WRITE(*,804) PHID
      WRITE(*,*) 'OUTPUT:  Degree of damage (deg) is : '
      WRITE (*,805) DEGD
804   FORMAT (2X,F6.4)
805   FORMAT (2X,F6.2)
      IF(DEGD.GT.12.) GOTO 120
      GOTO 125
C     If the degree of damage > 12 degrees, the damage strains
C     need to be checked
120   WRITE(8,*) '## NOTE : As Degree of damage > 12 degrees:'
      WRITE(8,*) '      Check for epsY is required i.e. eps < 100*epsY'
      WRITE(*,*) 'NOTE :As Degree of damage > 12 degrees:'
      WRITE(*,*) '    Check for epsY is required i.e. eps < 100*epsY.'
      WRITE(7,*) 'NOTE :As Degree of damage > 12 degrees:'
      WRITE(7,*) '    Check for epsY is required i.e. eps < 100*epsY.'
125   WRITE(8,*)
      WRITE(*,*)
      WRITE(8,*)
      WRITE(7,*)
C     MODULE FOR HEATING PATTERNS AND AVG. PLASTIC ROTATION
C     BASED ON BOUNDARY CONDITIONS
C     Deciding the heating pattern i.e heating temp.,epsP, F(T)
      WRITE(8,*) 'ii)  Heating Pattern Details:'
      WRITE(7,*) 'II] HEATING PATTERN DETAILS'
```

```
      WRITE(*,*) 'ii)  Heating Pattern Details:'
      WRITE(*,*) 'Maximum Heating Temperature is 1200 deg F'
      WRITE(*,*)'Enter the desired Heating Temperature in deg F:'
      READ(*,*) HT
      WRITE(8,*)'The Heating Temperature selected is (deg F):'
      WRITE(8,*) HT
808   FORMAT (2X, F7.2)
      IF (HT.EQ.1200) GOTO 126
      FT = 0.5 + 0.00125*(HT-750.)
      EP1= (.001*HT**2. + 6.1*HT - 415.) / 10.**6.
      EP2=  -720000. + 4200.*HT- 2.75*HT**2.
      EP3= 806. * (500000. + 1333.*HT- 1.111*HT**2.)
      EP= EP1-(EP2/EP3)
      FTEP= FT*EP
      GOTO 127
126   FTEP=0.00792
C     Deciding the Vee angle
127   WRITE(*,*) 'Full-Depth Vees are highly recommended.'
      WRITE(*,*)'Enter the desired Depth of Vee (in):'
      READ(*,*) VD
      WRITE(8,*) 'Vee Depth selected is (in):'
      WRITE (8,907) VD
907   FORMAT(2X,F5.2)
      WRITE(7,*) 'Vee Depth selected is (in):'
      WRITE (7,807) VD
807   FORMAT(2X,F5.2)
      VB=2*VD*TAN(0.3927)
      VA=0.7854
      VAD=45
      IF (VB.LE.6.) GOTO 128
      VB=2*VD*TAN(0.2618)
      VA=0.5236
      VAD=30
      IF (VB.LE.6.) GOTO 128
      VB=2*VD*TAN(0.1745)
      VA=0.3490
      VAD=20
      IF (VB.LE.6.) GOTO 128
      VB=2*VD*TAN(0.0873)
      VA= 0.1746
      VAD=10
128   WRITE(*,*) 'OUTPUT :   Vee Angle (deg) is:'
      WRITE(*,810) VAD
810   FORMAT (2X,I2)
      WRITE(*,*) 'OUTPUT:   Vee Width (in) is:'
      WRITE(*,911) VB
911   FORMAT (2X,F6.2)
      WRITE(8,*) '## OUTPUT:   Vee Angle (deg) is:'
      WRITE(8,912) VAD
912   FORMAT (2X,I2)
      WRITE(8,*) '## OUTPUT:    Vee Width (in) is:'
      WRITE(8,913) VB
913   FORMAT (2X,F6.2)
      WRITE(7,*) 'Vee Angle (deg) is:'
      WRITE(7,914) VAD
914   FORMAT (2X,I2)
      WRITE(7,*) 'Vee Width (in) is:'
      WRITE(7,915) VB
915   FORMAT (2X,F6.2)
      WRITE(*,*)
```

```
      WRITE(8,*)
      WRITE(7,*)
      WRITE(*,*)'NOTE: The Users manual illustrates the recommended'
      WRITE(*,*)'repair methodology for the damage type selected.'
      WRITE(8,*)'NOTE: The Users manual illustrates the recommended'
      WRITE(8,*)'repair methodology for the damage type selected.'
      WRITE(*,*)
      WRITE(8,*)
      WRITE(*,*)
      WRITE(8,*)
C      Average plastic rotation per cycle & No. of heats required for
repair
      WRITE(*,*)'V.]  NUMBER OF HEATING CYCLES REQUIRED FOR REPAIR'
      WRITE(8,*)'V.]  NUMBER OF HEATING CYCLES REQUIRED FOR REPAIR'
      WRITE(7,*)'III]  NUMBER OF HEATING CYCLES REQUIRED FOR REPAIR'
      TES=FTEP*SIN(VA/3.)
      PHIPL=TES*(.9+3.4*LR)
      IF(BC.NE.1) GOTO 130
      PHIAV=TES*(0.9+0.1*(DW/TW-37.)+3.4*LR)
      GOTO 228
130   IF(BC.NE.2) GOTO 140
      PHIAV=TES*(0.9+0.1*(DW/TW-37.)+3.4*LR)
      GOTO 228
140   IF(BC.NE.3) GOTO 150
      PHIAV=PHIPL*(1.+0.5*BF/DW)
      GOTO 228
150   IF(BC.NE.4) GOTO 160
      PHIAV=PHIPL*(1.+0.125*DW/BF)
      GOTO 228
160   IF(BC.NE.5) GOTO 170
      WRITE(*,*)'Enter value of Axial Load Ratio for undamaged member'
      WRITE(*,*)'i.e. Applied Axial Load/ Allowable Axial Load:'
      READ(*,*) AX
      WRITE(8,*)'Value of Axial Load ratio entered is: '
      WRITE (8,815) AX
815   FORMAT (2X, F7.3)
      WRITE(*,*)'Enter distance from Apex of vee to Stiffening leg (in)'
      READ(*,*) DS
      WRITE(8,*)'Distance from Apex of vee to Stiffening leg (in) is :'
      WRITE(8,816) DS
816   FORMAT(2X, F6.2)
      PHIAV=TES*(1.+.5*DS*BF/DW**2.)*(.9*(1.-1.4*AX)+3.4*LR*(1.+1.4*AX))
      GOTO 228
170   IF(BC.NE.6) GOTO 180
      WRITE(*,*)'Enter value of Axial Load Ratio for undamaged member'
      WRITE(*,*)'i.e. Applied Axial Load/ Allowable Axial Load'
      READ(*,*) AX
      WRITE(8,*)'Value of Axial Load ratio entered is: '
      WRITE (8,818) AX
818   FORMAT (2X, F7.3)
      WRITE(*,*)'Enter distance from Apex of vee to Stiffening leg (in)'
      READ(*,*) DS
      WRITE(8,*)'Distance from Apex of vee to Stiffening leg (in) is :'
      WRITE(8,817) DS
817   FORMAT(2X, F6.2)
      PHIAV=TES*(1.+.25*DS*BF/DW**2.)*(.9*(1.-.7*AX)+3.4*LR*(1.+.7*AX))
      GOTO 228
180   IF(BC.NE.7) GOTO 190
      WRITE(*,*)'Enter distance from Apex of vee to Stiffening leg (in)'
      READ(*,*) DS
```

```
      WRITE(8,*)'Distance from Apex of vee to Stiffening leg (in) is :'
      WRITE(8,819) DS
819   FORMAT(2X, F6.2)
      PHIAV=PHIPL*(1.+0.5*BF*DS/DW**2.)
      GOTO 228
190   IF(BC.NE.8) GOTO 200
      WRITE(*,*)'Enter distance from Apex of vee to Stiffening leg (in)'
      READ(*,*) DS
      WRITE(8,*)'Distance from Apex of vee to Stiffening leg (in) is :'
      WRITE(8,821) DS
821   FORMAT(2X, F6.2)
      PHIAV=PHIPL*(1.+0.25*DW*DS/BF**2.)
      GOTO 228
200   IF(BC.NE.9) GOTO 210
      WRITE(*,*)'Enter distance from Apex of vee to Stiffening leg (in)'
      READ(*,*) DS
      WRITE(8,*)'Distance from Apex of vee to Stiffening leg (in) is :'
      WRITE(8,822) DS
822   FORMAT(2X, F6.2)
      PHIAV=PHIPL*(1.+0.5*BF*DS/DW**2.)*(1.+2.*LR)
      GOTO 228
210   IF(BC.NE.10) GOTO 220
      WRITE(*,*)'Enter distance from Apex of vee to Stiffening leg (in)'
      READ(*,*) DS
      WRITE(8,*)'Distance from Apex of vee to Stiffening leg (in) is :'
      WRITE(8,823) DS
823   FORMAT(2X, F6.2)
      PHIAV=PHIPL*(1.+0.5*DW*DS/BF**2.)*(1.+2.*LR)
      GOTO 228
220   IF(BC.NE.11) GOTO 230
      PHIAV=PHIPL
228   NHR= PHID/PHIAV
      INHR= NHR+1.
      WRITE(*,*) 'OUTPUT: The Number of Heating Cycles required for'
      WRITE(*,*) '        repair is:',INHR
      WRITE(8,*) '## OUTPUT: The No. of Heating Cycles required for'
      WRITE(8,*) '           repair is:',INHR
      WRITE(7,*) 'The Number of Heating Cycles for repair is:',INHR
      GOTO 231
230   IF(BC.NE.12) GOTO 231
      PHIAV=PHIPL
      NHR= PHID/PHIAV
      INHR= NHR + 1.
      WRITE(*,*)'NOTE:   The theoretical number of heats for repair is'
      WRITE(*,*)'indeterminable for Non-Composite girders. The minimum'
      WRITE(*,*)'number of heats required for repair of the bottom'
      WRITE(*,*)'flange, considering it as a free plate, is :', INHR
      WRITE(8,*)'NOTE:   The theoretical number of heats for repair is'
      WRITE(8,*)'indeterminable for Non-Composite girders. The minimum'
      WRITE(8,*)'number of heats required for repair of the bottom'
      WRITE(8,*)'flange, considering it as a free plate, is :',INHR
      WRITE(7,*)'NOTE:   The theoretical number of heats for repair is'
      WRITE(7,*)'indeterminable for Non-Composite girders. The minimum'
      WRITE(7,*)'number of heats required for repair of the bottom'
      WRITE(7,*)'flange, considering it as a free plate, is :',INHR
C826   FORMAT (2X,I4)
231   WRITE(*,*)
      WRITE(8,*)
      WRITE(*,*)
      WRITE(8,*)
```

```
      WRITE(7,*)
      WRITE(7,*)
C     PROGRAM FOR DETERMINING APPLIED EXTERNAL JACKING FORCE
240   WRITE(*,*)'Do you wish to find the External Jacking Force (Y/N)?'
      READ(*,*) ANS2
      WRITE(8,*)'Do you wish to find the Jacking Force (Y/N)?:   ',ANS2
      IF(ANS2.NE.'Y') GOTO 9999
      WRITE(*,*)
      WRITE(8,*)
      WRITE(*,*)'VI.]  MAGNITUDE OF EXTERNAL APPLIED JACKING FORCE'
      WRITE(8,*)'VI.]  MAGNITUDE OF EXTERNAL APPLIED JACKING FORCE'
      WRITE(7,*)'IV]  MAGNITUDE OF EXTERNAL APPLIED JACKING FORCE'
      WRITE(*,*)
      WRITE(8,*)
      WRITE(*,*)'Is there Strong Axis Damage in the Web?(Y/N):'
      READ(*,*) ANS3
      WRITE(8,*)'Is there Strong Axis Damage in the Web? (Y/N):   ',ANS3
      WRITE(*,*)
      WRITE(8,*)
      WRITE(*,*)'Enter shorter distance of vee from support (ft)'
      READ(*,*) LLV
      WRITE(8,*)'Shorter distance of vee from support (ft):'
      WRITE(8,830) LLV
830   FORMAT (2X,F6.2)
      WRITE(*,*)
      WRITE(8,*)
      WRITE(*,*)'Enter distance of jack from other support (ft)'
      READ(*,*) LJ
      WRITE(8,*)'Distance of jack from from other support is (ft):'
      WRITE(8,829) LJ
829   FORMAT (2X,F6.2)
      WRITE(*,*)
      WRITE(8,*)
      WRITE(*,*)'Enter distance between supports of heated span (ft)'
      READ(*,*) LU
      WRITE(8,*)'Distance between supports for vee-heated span is (ft):'
      WRITE(8,831) LU
831   FORMAT (2X,F6.2)
      WRITE(*,*)
      WRITE(8,*)
      IF (BC.EQ.11) GOTO 241
      IF(ANS3.NE.'Y') GOTO 241
      MP=FY*TW*DW**2./4.
      GOTO 242
241   MP=FY*TF*BF**2./4.
242   MA=MP*LR
      MR=0.0
C     WRITE(*,*) 'MP,FY,BF,TF,LR,MA',MP,FY,BF,TF,LR,MA
C      WRITE(8,*) 'MP,FY,BF,TF,LR,MA',MP,FY,BF,TF,LR,MA
      IF(BC.EQ.1) GOTO 250
      IF(BC.EQ.2) GOTO 300
      IF(BC.EQ.5 .OR. BC.EQ.6 ) GOTO 350
      IF(BC.EQ.12) GOTO 450
      IF(BC.EQ.4 .OR. BC.EQ.8) GOTO 545
      GOTO 540
C     composite indeterminate(1)
250   UI=DW/TW
      IF(UI.LT.64.) GOTO 251
      GM=1.
      GOTO 252
```

```
251   GM=0.1344*(64.-DW/TW)+1.
252   WRITE(*,*)'NOTE :   Stiffness Modification Factor is :'
      WRITE(*,938) GM
938   FORMAT(2X, F8.2)
      WRITE(8,*)'NOTE :   Stiffness Modification Factor is :'
      WRITE(8,832) GM
832   FORMAT (2X,F6.3)
      WRITE(*,*)
      WRITE(8,*)
      WRITE(7,*)
      WRITE(*,*)'NOTE: Use INDET program to determine Residual Moments'
      WRITE(*,*) 'Enter a positive value of Residual Moment (k-ft):'
      WRITE(*,*)
      READ (*,*) MR
      WRITE(8,*) 'Value of Residual Moment input is (k-ft):'
      WRITE(8,836) MR
      WRITE(*,*)
      WRITE(8,*)
836   FORMAT (2X, F8.2)
      MA=MA*GM+(MR/12.)*GM
      PJ= LU* MA/(LLV*LJ*12.)
      GOTO 550
C     composite determinate(2)
300   UI=DW/TW
      IF(UI.LT.64.) GOTO 301
      GM=1.
      GOTO 302
301   GM=0.1344*(64.-DW/TW)+1.
302   WRITE(*,*)'NOTE :   Stiffness Modification Factor is :'
      WRITE(*,837) GM
837   FORMAT(2X, F8.2)
      WRITE(8,*)'NOTE :   Stiffness Modification Factor is :'
      WRITE(8,937) GM
937   FORMAT(2X, F8.2)
      WRITE(*,*)
      WRITE(8,*)
      MA=MA*GM
      PJ= LU* MA/(LLV*LJ*12.)
      GOTO 550
C     Axially loaded (5,6)
350   WRITE(*,*)'Enter the Axial Load (kips) and the current Deflection'
      WRITE(*,*)'at the center of damage(in):'
      READ(*,*)PAX,DELX
      WRITE(8,*)'Axial Load (kips) and Current Deflection at the'
      WRITE(8,*)'center of damage (in) are:'
      WRITE (8,841) PAX,DELX
841   FORMAT (2X,F6.2,10X,F5.2)
      WRITE(*,*)
      WRITE(8,*)
      MR=PAX*DELX
      IF(ANS3.EQ.'Y') GOTO 351
      MA=2.*MA+MR
      GOTO 550
351   MA=MA+MR
      PJ= LU* MA/(LLV*LJ*12.)
      GOTO 550
C     Non composite case
450   PJ= LU* MA/(LLV*LJ*12.)
      WRITE(*,*)'OUTPUT: For Non-composite case,'
      WRITE(*,*)'The required external Jacking Force (kips) for the'
```

```
      WRITE(*,*)'bottom flange, considering it as a free plate, is:'
      WRITE(*,87) PJ
      WRITE(8,*)'## OUTPUT: For Non-composite case,'
      WRITE(8,*)'The required external Jacking Force (kips) for the'
      WRITE(8,*)'bottom flange, considering it as a free plate, is:'
      WRITE(8,87) PJ
      WRITE(7,*)'iv) For Non-Composite case, Jacking Force (kips) for'
      WRITE(7,*)'the bottom flange, considering it as a free plate:'
      WRITE(7,87) PJ
87    FORMAT (2X,F5.2)
      GOTO 560
C     All other determinate cases (3,4,7-11)
540   PJ= LU* MA/(LLV*LJ*12.)
      GOTO 550
545   MA=2.*MA+MR
      PJ= LU* MA/(LLV*LJ*12.)
550   WRITE(*,*)
      WRITE(8,*)
      WRITE(*,*)'OUTPUT: Required external jacking Force is (kips):'
      WRITE(*,958)PJ
958   FORMAT (2X, F5.2)
      WRITE(7,*)'Required external jacking Force is (kips):'
      WRITE(7,957)PJ
957   FORMAT (2X, F5.2)
      WRITE(8,*)'## OUTPUT: Required external Jacking Force is (kips):'
      WRITE(8,853)PJ
853   FORMAT (2X, F5.2)
560   WRITE(8,*)
      WRITE(*,*)
      WRITE(8,*)
      WRITE(*,*)
      WRITE(8,*)
      WRITE(7,*)
      WRITE(7,*)
      WRITE(*,*)
      WRITE(8,*)'                [ End of file: heat.r ]'
      WRITE(7,*)'                [ End of file: heat.s ]'
      WRITE(*,*)'  [ Detailed results of program are in file: heat.r ]'
      WRITE(*,*)'    [ A summary of the results is in file: heat.s ]'
      WRITE(8,*)
      WRITE(7,*)
      WRITE(8,*)'##########################################################'
      WRITE(*,*)'###############   End of Program   ###################'
      WRITE(7,*)'##########################################################'
9999  CLOSE (5)
      CLOSE (8)
      CLOSE (7)
      STOP
      END
```

```
C  PROGRAM FOR ANALYSIS OF A INDETERMINATE SPACE FRAME
C  WITH HEAT-STRAIGHTENED MEMBERS FOR CALCULATING RESIDUAL  C   FORCES
C                                    Louisiana St. U., 1992
       REAL LEN,MIY,MIZ,LENGTH
       REAL X(15),Y(15),Z(15),XF(15),YF(15),ZF(15)
       DIMENSION JJ(15),KK(15)
       REAL AX(15),XI(15),YI(15),ZI(15)
C       REAL ALPHA(15)
       DIMENSION JRL(30),IA(15),ID(30),IM(12),BF(15),TF(15)
       CHARACTER ANS,ANS2,ANS3,ANS4, ANS5,ANS6
       REAL R(3,3,15),RT(12,12,15),RTT(12,12,15)
       REAL XP(15),YP(15),ZP(15),EL(15),FEA(12)
       REAL S(30,30),SM(12,12),SMRT(12,12,15),SMS(12,12)
       REAL SFF(30,30),SFFI(30,30),SFS(30,30),SSF(30,30),SSS(30,30)
       REAL AJ(30),AMLA(12,15),AML(12,15),AMS(12,15),AE(30),AMD(12)
       REAL A(30),AFS(30),AM(12,15),AF(30)
       REAL DJ(30),DS(30),DF(30),FSA(30),ASF(30),ASS(30),AS(30)
C       COMMON/A/PXM,PYM,PZM,DXJ,DYJ,DZJ
C       COMMON/B/UDXM,UDYM,UDZM,TXM,DTJ
       COMMON/C/LEN,FEA
       COMMON/E/SFF
       COMMON/F/SFFI
       COMMON/G/PHIY,DHY,PHIZ,DHZ
       COMMON/H/FEAH(12)
       COMMON/P/LENGTH,E,MIY,MIZ
C      OPEN (5,FILE='INDET.D')
       OPEN(8,FILE='INDET.R', STATUS='NEW')
       WRITE(*,*)
       WRITE(*,*)
       WRITE(*,*)'          #####  I  N  D  E  T   #####'
       WRITE(*,*)'        ==================================='
       WRITE(*,*)'  A Program to calculate Residual Moments caused'
       WRITE(*,*)'       at Diaphragms by Heat Straightening '
       WRITE(*,*)'Dept. of Civil Engineering, Louisiana St. Univ., 1992'

       WRITE(*,*)
       WRITE(*,*)
       WRITE(*,*)'Would you like to find the Residual Moments? (Y/N):'
       READ(*,*) ANS5
       WRITE(*,*)
       WRITE(*,*)
       WRITE(8,*)
       WRITE(8,*)
       WRITE(8,*)'          #####  I  N  D  E  T   #####'
       WRITE(8,*)'        ==================================='
       WRITE(8,*)'A Program to calculate Plastic Rotations and Residual'
       WRITE(8,*)' Moments at diaphragms caused by Heat Straightening'
       WRITE(8,*)'Dept. of Civil Engineering, Louisiana St. Univ., 1992'

       WRITE(8,*)
       WRITE(8,*)
       WRITE(8,*)
       WRITE(8,*)
       WRITE(8,*)'Would you like to find the Residual Moments? (Y/N):'
      1,ANS5
       WRITE(8,*)
       IF(ANS5.EQ.'N') GOTO 9999
       WRITE(8,*)'I]  STRUCTURAL PARAMETERS'
       WRITE(*,*)'I]  STRUCTURAL PARAMETERS'
       WRITE(8,*)
```

```
      WRITE(*,*)
C     STRUCTURAL DATA
      WRITE(*,*)'i)  Enter No. of Spans, No. of Joints, No. of Support'
      WRITE(*,*)'Restraints and No. of Diaphragms in damaged girder:'
      READ(*,*) NM,NJ,NR2,NRJ
      WRITE(8,*)'i)  No. of Spans, No. of Joints, No. of Support'
      WRITE(8,*)'Restraints and No. of Diaphragms for girder are:'
      WRITE(8,*) NM,NJ,NR2,NRJ
C     STRUCTURAL PARAMETERS
C      WRITE(*,*)'MODULUS OF ELASTICITY'
      E = 29000.
      G = 1.
C     JOINT COORDINATES
      WRITE(8,*)
      WRITE(*,*)
      WRITE(*,*)'ii) Enter Joint Index nos, X & Y coordinates (ft):'
      WRITE(8,*)'ii) Joint Index nos, X & Y coordinates (ft) are:'
      DO 100 J=1,NJ
      READ(*,*) J,XF(J),YF(J)
      WRITE(8,61) J,XF(J),YF(J)
61    FORMAT(2X,I3,6X,F7.3,6X,F7.3)
      X(J)=XF(J)*12.
      Y(J)=YF(J)*12.
      Z(J)= 0.
100   CONTINUE
C      MEMBER INFORMATION
      WRITE(8,*)
      WRITE(*,*)
      WRITE(*,*)'iii) Enter Span No., Jth Node, Kth node, width of'
      WRITE(*,*)'bottom flange (in), bottom flange thickness (in):'
      WRITE(8,*)'iii) Span No., Jth Node, Kth node, bottom flange'
      WRITE(8,*)'width (in), bottom flange thickness (in):'
      DO 200 I=1,NM
      READ(*,*) I,JJ(I),KK(I),BF(I),TF(I)
      WRITE(8,62) I,JJ(I),KK(I),BF(I),TF(I)
62    FORMAT (2X,I3,5X,I3,5X,I3,5X,F7.4,5X,F7.4)
      XI(I)=1.
      YI(I)=1.
      ZI(I)= TF(I)*BF(I)**3./12.
      AX(I)= BF(I)*TF(I)
      IA(I)=0
      GOTO 200
C      IF(IA(I).EQ.0) GO TO 200
C      WRITE(*,*)'IS ALPHA,THE ANGLE BETWEEN MEMBER Z AXIS AND '
C      WRITE(*,*)'STRUCTURAL Z AXIS AVAILABLE?'
C      READ(5,*) ANS
C      IF(ANS.NE.'Y') GO TO 210
C      READ(5,*)ALPHA(I)
C      GO TO 200
C      WRITE(*,*)'INPUT X,Y,Z COORDINATES OF POINT P'
C 210  READ(5,*) XP(I),YP(I),ZP(I)
200   CONTINUE
      NDJ=6
      ND=NDJ*NJ
      NR=NR2+3*NJ
      N=ND-NR
      MD=2*NDJ
C     JOINT RESTRAINTS
      WRITE(8,*)
      WRITE(*,*)
```

```
      WRITE(*,*)'iv) Restrainted Joint Data:'
      WRITE(8,*)'iv) Restrainted Joint Data:'
      DO 300 J=1,ND
300   JRL(J)=0
      WRITE(*,*)'    Enter the Restrained Joint Index number first. '
      WRITE(*,*)'Next, enter 3 Restraint Code Nos. for X & Y trans-'
      WRITE(*,*)'alations and Z rotation at the Restrained joint'
      WRITE(*,*)'1= Restrained displacement, 2= Free displacement)'
      WRITE(*,*)'    Enter the above values for all restrained joints'
      WRITE(*,*)'in sequence:'
      WRITE(8,*)'    Restrained Joint Index numbers are given first.'
      WRITE(8,*)'Next, 3 Restraint Code Nos. for X & Y transalations'
      WRITE(8,*)'and Z rotation at the Restrained joint are given.'
      WRITE(8,*)'1= Restrained displacement, 2= Free displacement)'
      WRITE(8,*)'    The above values for all restrained joints are:'

      DO 310 J=1,NRJ
      READ (*,*) K
      K6=6*K
      READ(*,*) JRL(K6-5),JRL(K6-4),JRL(K6)
      WRITE(8,63) K,JRL(K6-5),JRL(K6-4),JRL(K6)
63    FORMAT ( 2X,I3,5X,I3,2X,I3,2X,I3)
      JRL(K6-3)=1
      JRL(K6-2)=1
      JRL(K6-1)=1
310   CONTINUE
C FORMULATION OF ROTATION MATRIX FOR MEMBERS
      DO 400 I=1,NM
      J=JJ(I)
      K=KK(I)
      XCL=X(K)-X(J)
      YCL=Y(K)-Y(J)
      ZCL=Z(K)-Z(J)
      EL(I)=SQRT(XCL*XCL+YCL*YCL+ZCL*ZCL)
      CX=XCL/EL(I)
      CY=YCL/EL(I)
      CZ=ZCL/EL(I)
      CXZ=SQRT(CX*CX+CZ*CZ)
      IF(IA(I).EQ.0) GO TO 410
C PRINCIPAL AXES OF MEMBER INCLINED TO STRUCTURAL AXES
C      IF(ANS.EQ.'Y')GO TO 410
C      XPS=XP(I)-X(J)
C      YPS=YP(I)-Y(J)
C      ZPS=ZP(I)-Z(J)
410   IF(CXZ.GT.0.001) GOTO 420
C VERTICAL MEMBER
      R(1,1,I)=0.0
      R(1,2,I)=CY
      R(1,3,I)=0.0
      R(2,1,I)=-CY
      R(2,2,I)=0.0
      R(2,3,I)=0.0
      R(3,1,I)=0.0
      R(3,2,I)=0.0
      R(3,3,I)=1.0
      IF(IA(I).EQ.0) GOTO 400
C PPAL AXES INCLINED TO STRUCTURAL AXES
C      IF(ANS.EQ.'Y') GOTO 415
C      SQ=SQRT(XPS*XPS+ZPS*ZPS)
C      COSA=-XPS/SQ
```

```
C       SINA=ZPS/SQ
C       GO TO 416
C 415   COSA=COS(ALPHA(I))
C       SINA=SIN(ALPHA(I))
C 416   R(2,1,I)=-CY*COSA
C       R(2,3,I)=SINA
C       R(3,1,I)=CY*SINA
C       R(3,3,I)=COSA
C       GO TO 400
C INCLINED MEMBER
420    R(1,1,I)=CX
       R(1,2,I)=CY
       R(1,3,I)=CZ
       R(2,1,I)=-CX*CY/CXZ
       R(2,2,I)=CXZ
       R(2,3,I)=-CY*CZ/CXZ
       R(3,1,I)=-CZ/CXZ
       R(3,2,I)=0.0
       R(3,3,I)=CX/CXZ
       IF(IA(I).EQ.0)GO TO 400
C INCLINED MEMBERS WITH PPAL AXES INCLINED TO STRUCTURAL AXES
C       IF(ANS.EQ.'Y') GO TO 425
C       YPG=R(2,1,I)*XPS+R(2,2,I)*YPS+R(2,3,I)*ZPS
C       ZPG=R(3,1,I)*XPS+R(3,2,I)*YPS+R(3,3,I)*ZPS
C       SQ=SQRT(YPG*YPG+ZPG*ZPG)
C       COSA=YPG/SQ
C       SINA=ZPG/SQ
C       GO TO 426
C 425   COSA=COS(ALPHA(I))
C       SINA=SIN(ALPHA(I))
C 426   R(2,1,I)=(-CX*CY*COSA-CZ*SINA)/CXZ
C       R(2,2,I)=CXZ*COSA
C       R(2,3,I)=(-CY*CZ*COSA+CX*SINA)/CXZ
C       R(3,1,I)=(CX*CY*SINA-CZ*COSA)/CXZ
C       R(3,2,I)=-CXZ*SINA
C       R(3,3,I)=(CY*CZ*SINA+CX*COSA)/CXZ
400    CONTINUE
C CALCULATION OF COMPLETE ROTATION MATRIX
       DO 500 K=1,NM
       DO 500 I=1,MD
       DO 500 J=1,MD
500    RT(I,J,K)=0.0
       DO 600 K=1,NM
       DO 600 I=1,3
       DO 600 J=1,3
       RT(I,J,K)=R(I,J,K)
       RT(I+3,J+3,K)=R(I,J,K)
       RT(I+6,J+6,K)=R(I,J,K)
600    RT(I+9,J+9,K)=R(I,J,K)
C JOINT DISPLACEMENT INDEXES
       N1=0
       DO 700 J=1,ND
       N1=N1+JRL(J)
       IF(JRL(J).GT.0)GO TO 720
       ID(J)=J-N1
       GO TO 700
720    ID(J)=N+N1
700    CONTINUE
C STIFFNESS MATRIX FORMULATION
       DO 800 J=1,ND
```

```
      DO 800 K=1,ND
800   S(J,K)=0.0
C MEMBER STIFFNESS MATRIX
      DO 900 I=1,NM
      DO 810 J=1,12
      DO 810 K=1,12
810   SM(J,K)=0.0
      SKAX=E*AX(I)/EL(I)
      SKB2Z=4.0*E*ZI(I)/EL(I)
      SKB2Y=4.0*E*YI(I)/EL(I)
      SKTX=G*XI(I)/EL(I)
      SKB3Y=1.5*SKB2Y/EL(I)
      SKB4Y=2.0*SKB3Y/EL(I)
      SKB3Z=1.5*SKB2Z/EL(I)
      SKB4Z=2.0*SKB3Z/EL(I)
      SM(1,1)=SKAX
      SM(2,2)=SKB4Z
      SM(3,3)=SKB4Y
      SM(4,4)=SKTX
      SM(5,5)=SKB2Y
      SM(6,6)=SKB2Z
      SM(7,7)=SKAX
      SM(8,8)=SKB4Z
      SM(9,9)=SKB4Y
      SM(10,10)=SKTX
      SM(11,11)=SKB2Y
      SM(12,12)=SKB2Z
      SM(1,7)=-SKAX
      SM(2,6)=SKB3Z
      SM(2,8)=-SKB4Z
      SM(2,12)=SKB3Z
      SM(3,5)=-SKB3Y
      SM(3,9)=-SKB4Y
      SM(3,11)=-SKB3Y
      SM(4,10)=-SKTX
      SM(5,9)=SKB3Y
      SM(5,11)=SKB2Y/2.0
      SM(6,8)=-SKB3Z
      SM(6,12)=SKB2Z/2.0
      SM(8,12)=-SKB3Z
      SM(9,11)=SKB3Y
C GENERATE TERMS IN LOWER TRIANGULAR HALF OF SM
      DO 910 J=1,11
      DO 910 K=J+1,12
910   SM(K,J)=SM(J,K)
C TRANSPOSE OF RT MATRIX-[RTT]
      DO 920 J=1,12
      DO 920 K=1,12
920   RTT(K,J,I)=RT(J,K,I)
C ROTATION OF MEMBER STIFFNESS MATRIX TO STRUCTURAL AXES
C MULTIPLY [SM] AND [RT]
      DO 930 J=1,MD
      DO 930 K=1,MD
      SMRT(J,K,I)=0.0
      DO 930 L=1,MD
      SMRT(J,K,I)=SMRT(J,K,I)+SM(J,L)*RT(L,K,I)
930   CONTINUE
C MULTIPLY [RTT] AND [SMRT]
      DO 940 J=1,MD
      DO 940 K=1,MD
```

```
      SMS(J,K)=0.0
      DO 940 L=1,MD
940   SMS(J,K)=SMS(J,K)+RTT(J,L,I)*SMRT(L,K,I)
      IM(1)=6*JJ(I)-5
      DO 941 J=2,6
941   IM(J)=IM(J-1)+1
      IM(7)=6*KK(I)-5
      DO 942 J=8,12
942   IM(J)=IM(J-1)+1
C FORMULATION OF GLOBAL STIFFNESS MATRIX
      DO 950 J=1,MD
      I1=IM(J)
      IR=ID(I1)
      DO 950 K=1,MD
      I2=IM(K)
      IC=ID(I2)
      S(IR,IC)=S(IR,IC)+SMS(J,K)
950   CONTINUE
900   CONTINUE
C PARTITIONING THE STIFFNESS MATRIX
      DO 1110 J=1,N
      DO 1110 K=1,N
1110  SFF(J,K)=S(J,K)
      DO 1120 J=1,N
      DO 1120 K=N+1,ND
1120  SFS(J,K-N)=S(J,K)
      DO 1130 J=N+1,ND
      DO 1130 K=1,N
1130  SSF(J-N,K)=S(J,K)
      DO 1140 J=N+1,ND
      DO 1140 K=N+1,ND
1140  SSS(J-N,K-N)=S(J,K)
C LOAD PARAMETERS
C ACTIONS AT JOINTS
      DO 1141 J=1,ND
1141  AJ(J)=0.0
C      WRITE(*,*)'INPUT #OF LOADED JOINTS'
C      READ(5,*)NLJ
       NLJ = 0
      IF(NLJ.EQ.0) GO TO 1299
C      DO 1200 J=1,NLJ
C      WRITE(*,*)'INPUT THE JOINT # AND JOINT LOADS CORRESPONDING TO'
C      WRITE(*,*)'SIX DISPLACEMENT COORDINATES IN GLOBAL SYSTEM'
C      READ(5,*)K,AJ(6*K-5),AJ(6*K-4),AJ(6*K-3),AJ(6*K-2),AJ(6*K-1)
C     *,AJ(6*K)
C 1200 CONTINUE
C MEMBERS LOADS
1299  WRITE(*,*)
      WRITE(*,*)
      WRITE(8,*)
      WRITE(8,*)
      WRITE(*,*)'II] HEAT STRAIGHTENING DATA:'
      WRITE(8,*)'II] HEAT STRAIGHTENING DATA:'
      WRITE(*,*)
      WRITE(8,*)
C     MODULE FOR CALCULATING PLASTIC ROTATIONS
9999  WRITE(*,*)'    Would you like to determine the Plastic Rotations'
      WRITE(*,*)'induced by Heat straightening repair (Y/N):'
      READ(*,*) ANS6
      WRITE(8,*)'    Would you like to determine the Plastic Rotations'
```

```
      WRITE(8,*)'induced by Heat straightening repair (Y/N):     ',ANS6

      WRITE(*,*)
      WRITE(8,*)
      IF(ANS6.NE.'Y') GOTO 893
C     Input values of locations of four reference stations from left end
C      of the unsupported damaged span (ft), unsupported span (ft)
      WRITE (*,*)'i) Enter distance of Four Reference Stations from'
      WRITE (*,*)'left end of unsupported span before heating cycle:'
      READ(*,*) RS1,RS2,RS3,RS4
      WRITE (8,*)'   Distances of the Four Reference Stations from the'
      WRITE (8,*)'left end of unsupported span before heating cycle:'
      WRITE (8,10) RS1,RS2,RS3,RS4
10    FORMAT (F6.2,5X,F6.2,5X,F6.2,5X,F6.2,5X,F6.2)
      WRITE (*,*)
      WRITE (8,*)
C     Input values of ordinates of damaged beam at the four reference
C      stations
      S1=RS1*12.
      S2=RS2*12.
      S3=RS3*12.
      S4=RS4*12.
C      WRITE (*,*)'   Enter the Number of Heating Cycles for which the'
C      WRITE (*,*)'plastic rotation is desired:'
C      READ(*,*) NHTSE
C      WRITE (8,*)'   The Number of Heating Cycles for which the '
C      WRITE (8,*)'plastic rotation is desired is:',NHTSE
C      WRITE(*,*)
C      WRITE(8,*)
      NHTSE=1
      WRITE (*,*)'   Enter values for the Measurements along the bottom'
      WRITE (*,*)'flange at the four stations (in) for initial'
      WRITE (*,*)' damaged configuration and current heating cycle:'
      WRITE (8,*)'   Values input for the Measurements along the bottom'
      WRITE (8,*)'flange at the four stations (in) for initial '
      WRITE (8,*)'configuration and each heating cycle:'
      NHTS=NHTSE+1
      THX=0.
      DO 876, JUJU=1,NHTS
      READ(*,*) O1,O2,O3,O4
      WRITE (8,11) O1,O2,O3,O4
11    FORMAT (F8.3,5X,F8.3,5X,F8.3,5X,F8.3)
C     Angle of damage calculations
      TH1= ATAN((O2-O1)/(S2-S1))
      TH2= ATAN((O3-O4)/(S4-S3))
      TH = TH1+TH2
      IF(JUJU.NE.1) GOTO 877
      THX = TH
      GOTO 876
877   PHI= THX-TH
      IBHIK= JUJU-1
C     WRITE (*,*) 'TH1, TH2, THX, TH', TH1, TH2, THX, TH
      WRITE(8,*) 'Heating Cycle No.      :', IBHIK
      WRITE(8,*) 'Plastic Rotation (rad) :', PHI
      WRITE(*,*) 'Heating Cycle No.      :', IBHIK
      WRITE(*,*) 'Plastic Rotation (rad) :', PHI
      THX = TH
      WRITE(8,*)
876   CONTINUE
893   IF(ANS5.NE.'Y') GOTO 2400
```

```
      WRITE(*,*)
      WRITE(8,*)
      DO 1298 I=1,NM
      DO 1298 J=1,MD
      AMLA(J,I)=0.0
      AML(J,I)=0.0
1298  AMS(J,I)=0.0
      WRITE(*,*)'ii) Enter the Number of Heated Members:'
      READ(*,*) NLM
      WRITE(8,*)'ii) The Number of Heated Members is:',NLM
      IF(NLM.EQ.0) GO TO 1399
      DO 1300 M=1,NLM
      DO 1301 J=1,MD
      FEA(J)=0.0
1301  FEAH(J)=0.0
      WRITE(*,*)
      WRITE(8,*)
      WRITE(*,*)'iii) Enter the Member Index No. of Heated Member:'
      READ(*,*)I
      WRITE(8,*)'iii) The Member Index No. of Heated Member:',I
      LEN=EL(I)
      MIY=YI(I)
      MIZ=ZI(I)
      LENGTH=LEN
C      WRITE(*,*)'WOULD YOU LIKE TO INPUT MEMBER END FORCES DIRECTLY?'
C      READ(5,*)ANS2
C      ANS2 = N
C      IF(ANS2.EQ.'Y')GO TO 1308
C      WRITE(*,*)'ARE THERE ANY MEMBER LOADS?'
C      READ(5,*)ANS3
C       ANS3 = N
C       IF(ANS3.NE.'Y')GO TO 1305
C      WRITE(*,*)'INPUT POINT LOADS IN DIRECTION OF MEMBER AXES'
C      WRITE(*,*)'XM,YM,AND ZM AXES AND DISTANCES FROM JTH NODE'
C      READ(5,*)PXM,PYM,PZM,DXJ,DYJ,DZJ
C      WRITE(*,*)'INPUT DISTRIBUTED LOADS IN XM,YM AND ZM DIRECTIONS'
C      READ(5,*)UDXM,UDYM,UDZM
C      WRITE(*,*)'INPUT TORQUE IN XM DIRECTION,DISTANCE FROM JTH NODE'
C      READ(5,*)TXM,DTJ
C      CALL FEAC
C      WRITE(*,*)'IS THE MEMBER HEATED?'
C1305  READ(5,*)ANS4
 1305  ANS4 = 'Y'
      WRITE(*,*)
      WRITE(8,*)
      WRITE(*,*)'iv)  Enter Plastic Rotation and Vee heat distance from'
      WRITE(*,*)'Jth Node of heated span (ft) for the heating cycle:'
      READ(*,*) PHIZ, DHZF
      WRITE(8,*)'iv)  Plastic Rotation and Vee heat distance from Jth'
      WRITE(8,*)'Node of heated span (ft) for the heating cycle are:'
      WRITE(8,69) PHIZ, DHZF
69    FORMAT(2X,F9.7,5X,F5.2)
      DHZ=DHZF*12.
      PHIY = 0.
      DHY = 0.
      CALL FEAV
      GO TO 1309
C     WRITE(*,*)' INPUT ADDITIONAL MEMBER END ACTIONS FOR 12 MEMBER END'
C 1308 READ(5,*)(AMLA(J,I),J=1,MD)
1309  DO 1310 J=1,MD
```

```
1310  AML(J,I)=FEA(J)+FEAH(J)+AMLA(J,I)
      DO 1321 J=1,MD
      DO 1321 K=1,MD
1321  AMS(J,I)=AMS(J,I)+RTT(J,K,I)*AML(K,I)
1300  CONTINUE
C CALCULATION OF EQUIVALENT JOINT LOAD MATRIX
1399  DO 1398 J=1,ND
1398  AE(J)=0.0
      DO 1400 I=1,NM
      IM(1)=6*JJ(I)-5
      DO 1401 J=2,6
1401  IM(J)=IM(J-1)+1
      IM(7)=6*KK(I)-5
      DO 1402 J=8,12
1402  IM(J)=IM(J-1)+1
      DO 1400 J=1,MD
      I1=IM(J)
      AE(I1)=AE(I1)-AMS(J,I)
1400  CONTINUE
C COMBINED JOINT LOADS
      DO 1420 J=1,N
1420  AF(J)=0.0
      DO 1421 J=1,NR
      FSA(J)=0.0
1421  DS(J)=0.0
      N1=0
      DO 1500 J=1,ND
      JR=ID(J)
      N1=N1+JRL(J)
      IF(JRL(J).GT.0)GO TO 1501
      AF(JR)=AJ(J)+AE(J)
      GO TO 1500
1501  FSA(N1)=-AJ(J)-AE(J)
1500  CONTINUE
      DO 1550 J=1,ND
1550  DJ(J)=0.0
C INPUT SUPPORT DISPLACEMENTS
C      WRITE(*,*)' INPUT # OF SUPPORT DISPLACEMENTS'
C      READ(5,*)NSD
       NSD = 0
       IF(NSD.EQ.0) GO TO 1699
C      DO 1600 I=1,NSD
C      WRITE(*,*)' INPUT SUPPORT DISPLACEMENT COORDINATE'
C      READ(5,*)J
C      WRITE(*,*)'INPUT SUPPORT DISPLACEMENTS'
C1600  READ(5,*)DJ(J)
C FORMING SUPPORT DISPLACEMENT MATRIX
C      N1=0
C      DO 1610 J=1,ND
C      N1=N1+JRL(J)
C      IF(JRL(J).EQ.0) GO TO 1610
C      DS(N1)=DJ(J)
C1610  CONTINUE
C MULTIPLY [SFS] AND [DS]
1699  DO 1700 J=1,N
      AFS(J)=0.0
      DO 1700 K=1,NR
1700  AFS(J)=AFS(J)+SFS(J,K)*DS(K)
C SUBTRACT [AJS]FROM [AF]
      DO 1720 J=1,N
```

```
1720  A(J)=AF(J)-AFS(J)
C INVERT [SFF]
      CALL INVR(N)
C MULTIPLY [SFFI] AND [A]
      DO 1800 J=1,N
      DF(J)=0.0
      DO 1800 K=1,N
1800  DF(J)=DF(J)+SFFI(J,K)*A(K)
C REARRANGING DISPLACEMENTS
      N1=0
      DO 1900 K=1,ND
      N1=N1+JRL(K)
      IF(JRL(K).GT.0) GO TO 1900
      DJ(K)=DF(K-N1)
1900  CONTINUE
      WRITE(*,*)
      WRITE(8,*)
      WRITE(*,*)
      WRITE(8,*)
      WRITE(*,*)'III] RESIDUAL MOMENTS'
      WRITE(8,*)'III] RESIDUAL MOMENTS'
      WRITE(8,*)
      WRITE(*,*)
C      WRITE(*,*)'i)  Displacement Number Code    Displacement (in,rad)'
C      WRITE(8,*)'i)  Displacement Number Code    Displacement (in,rad)'
      DO 1910 J=1,ND
      IF(DJ(J).EQ.0.) GOTO 1910
C       WRITE(8,24)J,DJ(J)
C       WRITE(*,24)J,DJ(J)
C24     FORMAT(13X,I2,18X,F18.6)
1910  CONTINUE
C       WRITE(*,*)
C       WRITE(8,*)
C MEMBER END ACTIONS
C       WRITE(*,*)'i)  Member End Actions:'
C       WRITE(8,*)'i)  Member End Actions:'
C       WRITE(*,*)
C       WRITE(8,*)
      DO 2000 I=1,NM
      IM(1)=6*JJ(I)-5
      IM(7)=6*KK(I)-5
      DO 2001 J=2,6
2001  IM(J)=IM(J-1)+1
      DO 2002 J=8,12
2002  IM(J)=IM(J-1)+1
      DO 2005 J=1,MD
      AMD(J)=0.0
      AM(J,I)=0.0
      DO 2010 K=1,MD
      I1=IM(K)
2010  AMD(J)=AMD(J)+SMRT(J,K,I)*DJ(I1)
2005  AM(J,I)=AML(J,I)+AMD(J)
      WRITE(8,*)'Member End Actions for Span Number:',I
C      WRITE(8,*)'  End Action Number Code     Member End Action (k,in)'

      WRITE(*,*)'Member End Actions for Span Number:',I
C     WRITE(*,*)'  End Action Number Code     Member End Action (k,in)'

      WRITE(8,*)'   End Action no.              Residual moment(k-in)'
```

```
      WRITE(*,*)'   End Action no.              Residual moment(k-in)'

      DO 2000 J=1,MD
C     IF(AM(J,I).EQ.0.) GOTO 2000
      IU = J/6
      HU2= IU*6.
      IF(HU2.NE.J) GOTO 2000
      IHU3= J/2.
      WRITE(*,22) IHU3,AM(J,I)
      WRITE(8,22) IHU3,AM(J,I)
22    FORMAT(13X,I2,18X,F18.3)
2000  CONTINUE
      WRITE(*,*)
      WRITE(8,*)
C CALCULATE SUPPORT ACTIONS
C     [SSF]*[DF]
      DO 2100 J=1,NR
      ASF(J)=0.0
      DO 2100 K=1,N
2100  ASF(J)=ASF(J)+SSF(J,K)*DF(K)
C     [SSS]*[DS]
      DO 2150 J=1,NR
      ASS(J)=0.0
      DO 2150 K=1,NR
2150  ASS(J)=ASS(J)+SSS(J,K)*DS(K)
      DO 2200 J=1,NR
2200  AS(J)=ASF(J)+ASS(J)+FSA(J)
      N1=0
C     WRITE(8,*)'iii) Support Displacement Code   Displacement (in,rad)'
C     WRITE(*,*)'iii) Support Displacement Code   Displacement (in,rad)'
      DO 2300 J=1,ND
      N1=N1+JRL(J)
      IF(AS(N1).EQ.0.) GO TO 2300
C      WRITE(8,22)J,AS(N1)
C      WRITE(*,22)J,AS(N1)
C21    FORMAT(13X,I2,24X,F18.6)
2300  CONTINUE
2400  WRITE(8,*)
      WRITE(8,*)
      WRITE(8,*)'           [ End of File: indet.r ]'
      WRITE(8,*)
      WRITE(8,*)'###############  End of Program  ####################'
      WRITE(*,*)
      WRITE(*,*)
      WRITE(*,*)'     [ Results of program are in file: indet.r ]'
      WRITE(*,*)
      WRITE(*,*)'###############  End of Program  ####################'
      CLOSE (5)
      CLOSE (8)
      STOP
      END

C       SUBROUTINE FEAC
C CALCULATE FIXED END MEMBER ACTIONS
C       REAL L
C       COMMON/A/PXM,PYM,PZM,AX,AY,AZ
C       COMMON/B/UDXM,UDYM,UDZM,TXM,AT
C       COMMON/C/L,FEA(12)
C       BX=L-AX
C       BY=L-AY
```

```
C       BZ=L-AZ
C       BT=L-AT
C       FEA(1)=-PXM*(BX**2.)*(3*AX+BX)/(L**3.)-UDXM*L/2.
C       FEA(7)=-PXM*(AX**2.)*(AX+3*BX)/(L**3.)-UDXM*L/2.
C       FEA(2)=-PYM*(BY**2.)*(3*AY+BY)/(L**3.)-UDYM*L/2.
C       FEA(8)=-PYM*(AY**2.)*(AY+3*BY)/(L**3.)-UDYM*L/2.
C       FEA(3)=-PZM*(BZ**2.)*(3*AZ+BZ)/(L**3.)-UDZM*L/2.
C       FEA(9)=-PZM*(AZ**2.)*(AZ+3*BZ)/(L**3.)-UDZM*L/2.
C       FEA(6)=-PYM*AY*(BY**2.)/(L**2.)-UDYM*(L**2.)/12.
C       FEA(12)=PYM*(AY**2.)*BY/(L**2.)+UDYM*(L**2.)/12.
C       FEA(5)=PZM*AZ*(BZ**2.)/(L**2.)+UDZM*(L**2.)/12.
C       FEA(11)=-PZM*(AZ**2.)*BZ/(L**2.)-UDZM*(L**2.)/12.
C       FEA(4)=-TXM*BT/L
C       FEA(10)=-TXM*AT/L
C       RETURN
C       END

      SUBROUTINE FEAV
C     TO CALCULATE FIXED END ACTIONS DUE TO THE VEE HEATS
      REAL L,KY,KZ,MY,MZ
      COMMON/G/PY,DY,PZ,DZ
      COMMON/H/FEAH(12)
      COMMON/P/L,EM,MY,MZ
      KY=2*EM*MY/(L*L)
      KZ=2*EM*MZ/(L*L)
      FEAH(1)=0.0
      FEAH(7)=0.0
      FEAH(2)=-3*KZ/L*PZ*(L-2*DZ)
      FEAH(8)=-FEAH(2)
      FEAH(3)=-3*KY/L*PY*(L-2*DY)
      FEAH(9)=-FEAH(3)
      FEAH(4)=0.0
      FEAH(10)=0.0
      FEAH(5)=KY*PY*(2*L-3*DY)
      FEAH(11)=KY*PY*(L-3*DY)
      FEAH(6)=-KZ*PZ*(2*L-3*DZ)
      FEAH(12)=-KZ*PZ*(L-3*DZ)
      RETURN
      END

      SUBROUTINE INVR(N)
      REAL MAX
      INTEGER POS
      COMMON/E/A(30,30)
      COMMON/F/B(30,30)
      DO 101 I=1,N
      DO 101 J=1,N
101   B(I,J)=0.0
      DO 100 I=1,N
100   B(I,I)=1.0
      DO 1000 I=1,N
      MAX=ABS(A(I,I))
      POS=I
      DO 200 J=I,N
      IF(ABS(A(J,I)).LE.MAX) GOTO 200
      MAX=ABS(A(J,I))
      POS=J
200   CONTINUE
      MAX=A(POS,I)
      IF(ABS(MAX).LE.1.0E-6)GO TO 2000
```

```
      DO 210 J=1,N
      TEMP=A(I,J)
      A(I,J)=A(POS,J)
      A(POS,J)=TEMP
      TEMP=B(I,J)
      B(I,J)=B(POS,J)
      B(POS,J)=TEMP
210   CONTINUE
      DO 220 J=1,N
      A(I,J)=A(I,J)/MAX
220   B(I,J)=B(I,J)/MAX
      DO 230 J=1,N
      IF(J.EQ.I)GOTO 230
      RATIO=A(J,I)
      DO 240 K=1,N
      A(J,K)=A(J,K)-RATIO*A(I,K)
240   B(J,K)=B(J,K)-RATIO*B(I,K)
230   CONTINUE
1000  CONTINUE
      GOTO 3000
2000  WRITE(*,11)
11    FORMAT(' INVERSE NOT POSSIBLE')
3000  RETURN
      END
```

Sample inputs and outputs

The twelve outputs on the following pages are examples of file 'heat.r' for each of the twelve cases in sequence from damage type 1 to 12. The parameters for the members have been kept as consistent as possible so that a contrast of the heat-straightening repair for the different cases is possible. The outputs include *input echoes* for easy reference. The final output is a sample output of the 'INDET' program for a girder with two intermediate diaphragms.

The outputs of the 'HEAT' program are for a beam with a flange 9" X 0.6" and a web 24" X 0.4", with a 36 ksi yield stress. The remaining data is clearly indicated in the input echoes given in the outputs.

The outputs are given in a sequential order on the following pages for quick reference. The input will vary depending on the damaged member and the site conditions.

```
                #####  H. E. A. T.  #####
              ==============================

 A State-of-Art Software for Heat Straightening Repair
 Dept. of Civil Engineering, Louisiana St. Univ., 1992


 This program generates:
 1. The degree of damage of the damaged girder.
 2. The number of heating cycles required for repair.
 3. The repair methodology and heat pattern details.
 4. The magnitude of the external jacking forces.

 I.]  DAMAGE TYPES OF THE DAMAGED MEMBER
 Available number codes for Damage types are:
 Indeterminate Composite W-shape                    .. 1
 Determinate Composite W-shape                      .. 2
 Determinate Category S W-shape                     .. 3
 Determinate Category W W-shape                     .. 4
 Axially-loaded Determinate Category S W-shape      .. 5
 Axially-loaded Determinate Category W W-shape      .. 6
 Determinate Category S Channel                     .. 7
 Determinate Category W Channel                     .. 8
 Determinate Category S Angle                       .. 9
 Determinate Category W Angle                       .. 10
 Determinate Category S Plate                       .. 11
 Determinate Non-composite W-shape                  .. 12

 The number code entered for member type is :            1


  II.]  MEMBER GEOMETRY AND PROPERTIES:
 Values entered for Flange width, Flange thickness, Web
 depth, Web thickness (in) and Yield Stress (ksi) are
  9.000        .600     24.000       .400
 36.000


  III.]  EXTERNAL LOAD RATIO
 The Load Ratio selected for repair is :
   .125

 Do you wish to calculate the Number of Heats required
 to heat-straighten the damaged girder? (Y/N):   Y
IV.]  METHODOLOGY OF REPAIR
 i) Degree of Damage of member:
 The distance of Four Reference Stations from the
 left end of unsupported span:
  2.00       6.00      14.00      18.00

 Values input for the Damage Measurements along the
 bottom flange at the Four reference stations (in):
   3.000        6.000        7.000        4.000

 ## OUTPUT:  Degree of damage (rad) is :
   .1248
 ## OUPUT:   Degree of damage (deg) is :
    7.15
```

```
ii)  Heating Pattern Details:
The Heating Temperature selected is (deg F):
         1200
Vee Depth selected is (in):
  9.00
## OUTPUT:   Vee Angle (deg) is:
 30
## OUTPUT:    Vee Width (in) is:
   4.82

NOTE: The Users manual illustrates the recommended
repair methodology for the member type selected.


V.]  NUMBER OF HEATING CYCLES REQUIRED FOR REPAIR
## OUTPUT: The No. of Heating Cycles required for
           repair is:          26


Do you wish to find the Jacking Force (Y/N)?:   Y


VI.]  MAGNITUDE OF EXTERNAL APPLIED JACKING FORCE

Is there Strong Axis Damage in the Web? (Y/N):   N

Jack Distance from near end of Simple Span is (ft):
   9.00


NOTE :   Stiffness Modification Factor is :
  1.538

Value of Residual Moment input is (k-ft):
   635.00


## OUTPUT: Required external Jacking Force is (kips):
  3.06


              [ End of file: heat.r ]

#########################################################
```

```
          #####  H. E. A. T.  #####
        ==============================

A State-of-Art Software for Heat Straightening Repair

Dept. of Civil Engineering, Louisiana St. Univ., 1992


This program generates:
1. The degree of damage of the damaged girder.
2. The number of heating cycles required for repair.
3. The repair methodology and heat pattern details.
4. The magnitude of the external jacking forces.



I.]  DAMAGE TYPES OF THE DAMAGED MEMBER
Available number codes for Damage types are:
Indeterminate Composite W-shape                .. 1
Determinate Composite W-shape                  .. 2
Determinate Category S W-shape                 .. 3
Determinate Category W W-shape                 .. 4
Axially-loaded Determinate Category S W-shape  .. 5
Axially-loaded Determinate Category W W-shape  .. 6
Determinate Category S Channel                 .. 7
Determinate Category W Channel                 .. 8
Determinate Category S Angle                   .. 9
Determinate Category W Angle                   .. 10
Determinate Category S Plate                   .. 11
Determinate Non-composite W-shape              .. 12

The number code entered for member type is :            2


II.]  MEMBER GEOMETRY AND PROPERTIES:
Values entered for Flange width, Flange thickness, Web
depth, Web thickness (in) and Yield Stress (ksi) are
 9.000        .600     24.000       .400
36.000



III.]  EXTERNAL LOAD RATIO
The Load Ratio selected for repair is :
  .125


Do you wish to calculate the Number of Heats required
to heat-straighten the damaged girder? (Y/N):   Y

IV.]  METHODOLOGY OF REPAIR
i) Degree of Damage of member:
The distance of Four Reference Stations from the
left end of unsupported span:
 2.00       6.00      14.00      18.00
```

```
Values input for the Damage Measurements along the
bottom flange at the Four reference stations (in):
  3.000        6.000        7.000        4.000

## OUTPUT:  Degree of damage (rad) is :
  .1248
## OUPUT:   Degree of damage (deg) is :
   7.15


ii)  Heating Pattern Details:
The Heating Temperature selected is (deg F):
         1200
Vee Depth selected is (in):
  9.00
## OUTPUT:   Vee Angle (deg) is:
 30
## OUTPUT:    Vee Width (in) is:
   4.82

NOTE: The Users manual illustrates the recommended
repair methodology for the member type selected.


V.]  NUMBER OF HEATING CYCLES REQUIRED FOR REPAIR
## OUTPUT: The No. of Heating Cycles required for
           repair is:          26


Do you wish to find the Jacking Force (Y/N)?:   Y


VI.]  MAGNITUDE OF EXTERNAL APPLIED JACKING FORCE

Is there Strong Axis Damage in the Web? (Y/N):   N

Jack Distance from near end of Simple Span is (ft):
   9.00

NOTE :   Stiffness Modification Factor is :
     1.54


## OUTPUT: Required external Jacking Force is (kips):
  1.56


               [ End of file: heat.r ]

#########################################################
```

```
          #####  H. E. A. T.  #####
        ==============================

A State-of-Art Software for Heat Straightening Repair

Dept. of Civil Engineering, Louisiana St. Univ., 1992


This program generates:
1. The degree of damage of the damaged girder.
2. The number of heating cycles required for repair.
3. The repair methodology and heat pattern details.
4. The magnitude of the external jacking forces.



I.]  DAMAGE TYPES OF THE DAMAGED MEMBER
Available number codes for Damage types are:
Indeterminate Composite W-shape                .. 1
Determinate Composite W-shape                  .. 2
Determinate Category S W-shape                 .. 3
Determinate Category W W-shape                 .. 4
Axially-loaded Determinate Category S W-shape .. 5
Axially-loaded Determinate Category W W-shape .. 6
Determinate Category S Channel                 .. 7
Determinate Category W Channel                 .. 8
Determinate Category S Angle                   .. 9
Determinate Category W Angle                   .. 10
Determinate Category S Plate                   .. 11
Determinate Non-composite W-shape              .. 12

The number code entered for member type is :            3


II.]  MEMBER GEOMETRY AND PROPERTIES:
Values entered for Flange width, Flange thickness, Web
depth, Web thickness (in) and Yield Stress (ksi) are
 9.000        .600     24.000       .400
36.000



III.]  EXTERNAL LOAD RATIO
The Load Ratio selected for repair is :
  .330


Do you wish to calculate the Number of Heats required
to heat-straighten the damaged girder? (Y/N):   Y

IV.]  METHODOLOGY OF REPAIR
i) Degree of Damage of member:
The distance of Four Reference Stations from the
left end of unsupported span:
 2.00       6.00      14.00      18.00
```

```
Values input for the Damage Measurements along the
bottom flange at the Four reference stations (in):
  3.000        6.000        7.000        4.000

## OUTPUT:  Degree of damage (rad) is :
  .1248
## OUPUT:   Degree of damage (deg) is :
   7.15


ii)  Heating Pattern Details:
The Heating Temperature selected is (deg F):
         1200
Vee Depth selected is (in):
 24.00
## OUTPUT:   Vee Angle (deg) is:
 10
## OUTPUT:    Vee Width (in) is:
   4.20

NOTE: The Users manual illustrates the recommended
repair methodology for the member type selected.


V.]  NUMBER OF HEATING CYCLES REQUIRED FOR REPAIR
## OUTPUT: The No. of Heating Cycles required for
           repair is:          113


Do you wish to find the Jacking Force (Y/N)?:   Y


VI.]  MAGNITUDE OF EXTERNAL APPLIED JACKING FORCE

Is there Strong Axis Damage in the Web? (Y/N):   Y

Jack Distance from near end of Simple Span is (ft):
   9.00


## OUTPUT: Required external Jacking Force is (kips):
 12.67


              [ End of file: heat.r ]

#########################################################
```

```
          #####  H. E. A. T.  #####
        ==============================

A State-of-Art Software for Heat Straightening Repair

Dept. of Civil Engineering, Louisiana St. Univ., 1992


This program generates:
1. The degree of damage of the damaged girder.
2. The number of heating cycles required for repair.
3. The repair methodology and heat pattern details.
4. The magnitude of the external jacking forces.



I.]  DAMAGE TYPES OF THE DAMAGED MEMBER
Available number codes for Damage types are:
Indeterminate Composite W-shape                    .. 1
Determinate Composite W-shape                      .. 2
Determinate Category S W-shape                     .. 3
Determinate Category W W-shape                     .. 4
Axially-loaded Determinate Category S W-shape      .. 5
Axially-loaded Determinate Category W W-shape      .. 6
Determinate Category S Channel                     .. 7
Determinate Category W Channel                     .. 8
Determinate Category S Angle                       .. 9
Determinate Category W Angle                       .. 10
Determinate Category S Plate                       .. 11
Determinate Non-composite W-shape                  .. 12

The number code entered for member type is :            4


II.]  MEMBER GEOMETRY AND PROPERTIES:
Values entered for Flange width, Flange thickness, Web
depth, Web thickness (in) and Yield Stress (ksi) are
 9.000        .600     24.000        .400
36.000



III.]  EXTERNAL LOAD RATIO
The Load Ratio selected for repair is :
  .330


Do you wish to calculate the Number of Heats required
to heat-straighten the damaged girder? (Y/N):   Y

IV.]  METHODOLOGY OF REPAIR
i) Degree of Damage of member:
The distance of Four Reference Stations from the
left end of unsupported span:
 2.00       6.00      14.00      18.00
```

```
Values input for the Damage Measurements along the
bottom flange at the Four reference stations (in):
  3.000        6.000        7.000        4.000

## OUTPUT:  Degree of damage (rad) is :
  .1248
## OUPUT:   Degree of damage (deg) is :
   7.15


ii)  Heating Pattern Details:
The Heating Temperature selected is (deg F):
         1200
Vee Depth selected is (in):
  9.00
## OUTPUT:   Vee Angle (deg) is:
 30
## OUTPUT:    Vee Width (in) is:
   4.82

NOTE: The Users manual illustrates the recommended
repair methodology for the member type selected.


V.]  NUMBER OF HEATING CYCLES REQUIRED FOR REPAIR
## OUTPUT: The No. of Heating Cycles required for
           repair is:          34


Do you wish to find the Jacking Force (Y/N)?:   Y


VI.]  MAGNITUDE OF EXTERNAL APPLIED JACKING FORCE

Is there Strong Axis Damage in the Web? (Y/N):   N

Jack Distance from near end of Simple Span is (ft):
   9.00


## OUTPUT: Required external Jacking Force is (kips):
  5.35


              [ End of file: heat.r ]

#######################################################
```

```
          #####  H. E. A. T.  #####
        ==============================

A State-of-Art Software for Heat Straightening Repair

Dept. of Civil Engineering, Louisiana St. Univ., 1992


This program generates:
1. The degree of damage of the damaged girder.
2. The number of heating cycles required for repair.
3. The repair methodology and heat pattern details.
4. The magnitude of the external jacking forces.



I.]  DAMAGE TYPES OF THE DAMAGED MEMBER
Available number codes for Damage types are:
Indeterminate Composite W-shape                    .. 1
Determinate Composite W-shape                      .. 2
Determinate Category S W-shape                     .. 3
Determinate Category W W-shape                     .. 4
Axially-loaded Determinate Category S W-shape      .. 5
Axially-loaded Determinate Category W W-shape      .. 6
Determinate Category S Channel                     .. 7
Determinate Category W Channel                     .. 8
Determinate Category S Angle                       .. 9
Determinate Category W Angle                       .. 10
Determinate Category S Plate                       .. 11
Determinate Non-composite W-shape                  .. 12

The number code entered for member type is :            6


II.]  MEMBER GEOMETRY AND PROPERTIES:
Values entered for Flange width, Flange thickness, Web
depth, Web thickness (in) and Yield Stress (ksi) are
 9.000        .600     24.000       .400
36.000



III.]  EXTERNAL LOAD RATIO
The Load Ratio selected for repair is :
  .330


Do you wish to calculate the Number of Heats required
to heat-straighten the damaged girder? (Y/N):   Y

IV.]  METHODOLOGY OF REPAIR
i) Degree of Damage of member:
The distance of Four Reference Stations from the
left end of unsupported span:
 2.00       6.00      14.00      18.00
```

```
Values input for the Damage Measurements along the
bottom flange at the Four reference stations (in):
  3.000        6.000        7.000        4.000

## OUTPUT:  Degree of damage (rad) is :
  .1248
## OUPUT:   Degree of damage (deg) is :
   7.15


ii)  Heating Pattern Details:
The Heating Temperature selected is (deg F):
         1200
Vee Depth selected is (in):
  9.00
## OUTPUT:   Vee Angle (deg) is:
 30
## OUTPUT:    Vee Width (in) is:
   4.82

NOTE: The Users manual illustrates the recommended
repair methodology for the member type selected.


V.]  NUMBER OF HEATING CYCLES REQUIRED FOR REPAIR
Value of Axial Load ratio entered is:
    .350
Distance from Apex of vee to Stiffening leg (in) is :
   4.50
## OUTPUT: The No. of Heating Cycles required for
           repair is:          33


Do you wish to find the Jacking Force (Y/N)?:   Y

VI.]  MAGNITUDE OF EXTERNAL APPLIED JACKING FORCE

Is there Strong Axis Damage in the Web? (Y/N):   N

Jack Distance from near end of Simple Span is (ft):
   9.00

Axial Load (kips) and Current Deflection at the
center of damage (in) are:
  25.00          8.00


## OUTPUT: Required external Jacking Force is (kips):
  9.05


              [ End of file: heat.r ]

#########################################################
```

```
          #####  H. E. A. T.  #####
        ==============================

A State-of-Art Software for Heat Straightening Repair

Dept. of Civil Engineering, Louisiana St. Univ., 1992


This program generates:
1. The degree of damage of the damaged girder.
2. The number of heating cycles required for repair.
3. The repair methodology and heat pattern details.
4. The magnitude of the external jacking forces.



I.]  DAMAGE TYPES OF THE DAMAGED MEMBER
Available number codes for Damage types are:
Indeterminate Composite W-shape                    .. 1
Determinate Composite W-shape                      .. 2
Determinate Category S W-shape                     .. 3
Determinate Category W W-shape                     .. 4
Axially-loaded Determinate Category S W-shape      .. 5
Axially-loaded Determinate Category W W-shape      .. 6
Determinate Category S Channel                     .. 7
Determinate Category W Channel                     .. 8
Determinate Category S Angle                       .. 9
Determinate Category W Angle                       .. 10
Determinate Category S Plate                       .. 11
Determinate Non-composite W-shape                  .. 12

The number code entered for member type is :            7


II.]  MEMBER GEOMETRY AND PROPERTIES:
Values entered for Flange width, Flange thickness, Web
depth, Web thickness (in) and Yield Stress (ksi) are
 9.000        .600     24.000       .400
36.000



III.]  EXTERNAL LOAD RATIO
The Load Ratio selected for repair is :
  .330


Do you wish to calculate the Number of Heats required
to heat-straighten the damaged girder? (Y/N):   Y

IV.]  METHODOLOGY OF REPAIR
i) Degree of Damage of member:
The distance of Four Reference Stations from the
left end of unsupported span:
 2.00       6.00      14.00      18.00
```

```
Values input for the Damage Measurements along the
bottom flange at the Four reference stations (in):
  3.000        6.000        7.000        4.000

## OUTPUT:  Degree of damage (rad) is :
  .1248
## OUPUT:   Degree of damage (deg) is :
   7.15


ii)  Heating Pattern Details:
The Heating Temperature selected is (deg F):
         1200
Vee Depth selected is (in):
 24.00
## OUTPUT:   Vee Angle (deg) is:
 10
## OUTPUT:    Vee Width (in) is:
   4.20

NOTE: The Users manual illustrates the recommended
repair methodology for the member type selected.


V.]  NUMBER OF HEATING CYCLES REQUIRED FOR REPAIR
Distance from Apex of vee to Stiffening leg (in) is :
  24.00
## OUTPUT: The No. of Heating Cycles required for
           repair is:          113


Do you wish to find the Jacking Force (Y/N)?:   Y
 VI.]  MAGNITUDE OF EXTERNAL APPLIED JACKING FORCE

Is there Strong Axis Damage in the Web? (Y/N):   Y

Jack Distance from near end of Simple Span is (ft):
   9.00


## OUTPUT: Required external Jacking Force is (kips):
 12.67


              [ End of file: heat.r ]

#####################################################
```

```
          #####  H. E. A. T.  #####
        ==============================

A State-of-Art Software for Heat Straightening Repair

Dept. of Civil Engineering, Louisiana St. Univ., 1992


This program generates:
1. The degree of damage of the damaged girder.
2. The number of heating cycles required for repair.
3. The repair methodology and heat pattern details.
4. The magnitude of the external jacking forces.



I.]  DAMAGE TYPES OF THE DAMAGED MEMBER
Available number codes for Damage types are:
Indeterminate Composite W-shape                 .. 1
Determinate Composite W-shape                   .. 2
Determinate Category S W-shape                  .. 3
Determinate Category W W-shape                  .. 4
Axially-loaded Determinate Category S W-shape .. 5
Axially-loaded Determinate Category W W-shape .. 6
Determinate Category S Channel                  .. 7
Determinate Category W Channel                  .. 8
Determinate Category S Angle                    .. 9
Determinate Category W Angle                    .. 10
Determinate Category S Plate                    .. 11
Determinate Non-composite W-shape               .. 12

The number code entered for member type is :            8


II.]  MEMBER GEOMETRY AND PROPERTIES:
Values entered for Flange width, Flange thickness, Web
depth, Web thickness (in) and Yield Stress (ksi) are
 9.000        .600     24.000       .400
36.000



III.]  EXTERNAL LOAD RATIO
 The Load Ratio selected for repair is :
   .330


 Do you wish to calculate the Number of Heats required
 to heat-straighten the damaged girder? (Y/N):   Y

 IV.]  METHODOLOGY OF REPAIR
 i) Degree of Damage of member:
 The distance of Four Reference Stations from the
 left end of unsupported span:
  2.00       6.00      14.00      18.00
```

```
Values input for the Damage Measurements along the
bottom flange at the Four reference stations (in):
  3.000        6.000        7.000        4.000

## OUTPUT:  Degree of damage (rad) is :
  .1248
## OUPUT:   Degree of damage (deg) is :
   7.15


ii)  Heating Pattern Details:
The Heating Temperature selected is (deg F):
         1200
Vee Depth selected is (in):
  9.00
## OUTPUT:   Vee Angle (deg) is:
 30
## OUTPUT:    Vee Width (in) is:
   4.82

NOTE: The Users manual illustrates the recommended
repair methodology for the member type selected.


V.]  NUMBER OF HEATING CYCLES REQUIRED FOR REPAIR
Distance from Apex of vee to Stiffening leg (in) is :
    .00
## OUTPUT: The No. of Heating Cycles required for
           repair is:          45


Do you wish to find the Jacking Force (Y/N)?:   Y

VI.]  MAGNITUDE OF EXTERNAL APPLIED JACKING FORCE

Is there Strong Axis Damage in the Web? (Y/N):   N

Jack Distance from near end of Simple Span is (ft):
   9.00


## OUTPUT: Required external Jacking Force is (kips):
  5.35


              [ End of file: heat.r ]

#######################################################
```

```
      #####  H. E. A. T.  #####
     ==============================

A State-of-Art Software for Heat Straightening Repair

Dept. of Civil Engineering, Louisiana St. Univ., 1992


This program generates:
1. The degree of damage of the damaged girder.
2. The number of heating cycles required for repair.
3. The repair methodology and heat pattern details.
4. The magnitude of the external jacking forces.



I.]  DAMAGE TYPES OF THE DAMAGED MEMBER
Available number codes for Damage types are:
Indeterminate Composite W-shape
Determinate Composite W-shape                          .. 1
Determinate Category S W-shape                         .. 2
Determinate Category W W-shape                         .. 3
Axially-loaded Determinate Category S W-shape          .. 4
Axially-loaded Determinate Category W W-shape          .. 5
Determinate Category S Channel                         .. 6
Determinate Category W Channel                         .. 7
Determinate Category S Angle                           .. 8
Determinate Category W Angle                           .. 9
Determinate Category S Plate                           .. 10
Determinate Non-composite W-shape                      .. 11
                                                       .. 12
The number code entered for member type is :                    9

II.]  MEMBER GEOMETRY AND PROPERTIES:
Values entered for Flange width, Flange thickness, Web
depth, Web thickness (in) and Yield Stress (ksi) are
 9.000          .600     24.000          .400
36.000

III.]  EXTERNAL LOAD RATIO
The Load Ratio selected for repair is :
  .330


Do you wish to calculate the Number of Heats required
to heat-straighten the damaged girder? (Y/N):   Y

IV.]  METHODOLOGY OF REPAIR
i) Degree of Damage of member:
The distance of Four Reference Stations from the
left end of unsupported span:
 2.00        6.00        14.00        18.00
```

```
Values input for the Damage Measurements along the
bottom flange at the Four reference stations (in):
  3.000         6.000         7.000         4.000

## OUTPUT:  Degree of damage (rad) is :
  .1248
## OUPUT:   Degree of damage (deg) is :
   7.15


ii)  Heating Pattern Details:
The Heating Temperature selected is (deg F):
         1200
Vee Depth selected is (in):
 24.00
## OUTPUT:   Vee Angle (deg) is:
 10
## OUTPUT:    Vee Width (in) is:
   4.20

NOTE: The Users manual illustrates the recommended
repair methodology for the member type selected.


V.]  NUMBER OF HEATING CYCLES REQUIRED FOR REPAIR
Distance from Apex of vee to Stiffening leg (in) is :
  24.00
## OUTPUT: The No. of Heating Cycles required for
           repair is:          68


Do you wish to find the Jacking Force (Y/N)?:   Y

VI.]  MAGNITUDE OF EXTERNAL APPLIED JACKING FORCE

Is there Strong Axis Damage in the Web? (Y/N):   Y

Jack Distance from near end of Simple Span is (ft):
   9.00


## OUTPUT: Required external Jacking Force is (kips):
 12.67


                [ End of file: heat.r ]

#########################################################
```

```
          #####  H. E. A. T.  #####
        ==============================

A State-of-Art Software for Heat Straightening Repair

Dept. of Civil Engineering, Louisiana St. Univ., 1992


This program generates:
1. The degree of damage of the damaged girder.
2. The number of heating cycles required for repair.
3. The repair methodology and heat pattern details.
4. The magnitude of the external jacking forces.



I.]  DAMAGE TYPES OF THE DAMAGED MEMBER
Available number codes for Damage types are:
Indeterminate Composite W-shape                    .. 1
Determinate Composite W-shape                      .. 2
Determinate Category S W-shape                     .. 3
Determinate Category W W-shape                     .. 4
Axially-loaded Determinate Category S W-shape      .. 5
Axially-loaded Determinate Category W W-shape      .. 6
Determinate Category S Channel                     .. 7
Determinate Category W Channel                     .. 8
Determinate Category S Angle                       .. 9
Determinate Category W Angle                       .. 10
Determinate Category S Plate                       .. 11
Determinate Non-composite W-shape                  .. 12

The number code entered for member type is :          10


II.]  MEMBER GEOMETRY AND PROPERTIES:
Values entered for Flange width, Flange thickness, Web
depth, Web thickness (in) and Yield Stress (ksi) are
 9.000        .600     24.000       .400
36.000


III.]  EXTERNAL LOAD RATIO
The Load Ratio selected for repair is :
  .330


Do you wish to calculate the Number of Heats required
to heat-straighten the damaged girder? (Y/N):   Y

IV.]  METHODOLOGY OF REPAIR
i) Degree of Damage of member:
The distance of Four Reference Stations from the
left end of unsupported span:
 2.00       6.00       14.00      18.00
```

```
              3                          -635.00
              6                          -154.45
 Member End Actions for Span Number: 3
    End Action no.              Residual moment(k-in)
              3                          154.45
              6                            .00

              [ End of File: indet.r ]
###############  End of Program  ###################
```

This public document is published at a total cost of $ 4,697.08. Three Hundred Fifty (350) copies of this public document were published in this first printing at a cost of $ 3,437.08 . The total cost of all printings of this document including reprints is $ 4,697.08 . This document was published by Louisiana State University, Graphic Services, 3555 River Road, Baton Rouge, Louisiana 70802, to report and publish research findings of the Louisiana Transportation Research Center as required in R.S.48:105. This material was printed in accordance with standards for printing by State Agencies established pursuant to R.S.43:31. Printing of this material was purchased in accordance with the provisions of Title 43 of the Louisiana Revised Statutes.